Imperial College London
Department of Life Sciences

Investigating Behavioural Correlates of Sleep States in *Drosophila*

Laurence Andrew Blackhurst

Supervisor: Dr Giorgio Gilestro

A thesis presented for the degree of
Doctor of Philosophy in Life Sciences
October 2024

Abstract

Sleep is a universal yet diverse phenomenon across the animal kingdom. Despite its evolutionary conservation, sleep varies significantly among mammals and even more so when compared to birds, reptiles, fish, cephalopods, and insects. Recent studies have bridged the understanding of sleep across different animal classes, revealing that multiphasic sleep, characterised by distinct stages like REM and NREM in mammals, may be present across a wider range of species, though not necessarily in a structurally or functionally equivalent manner. To generate a general theory of sleep, it is essential to accurately identify and classify sleep types across species to facilitate meaningful comparisons.

In the past two decades, *Drosophila melanogaster* has emerged as a leading model for studying sleep. However, most research has treated *Drosophila* sleep as monophasic, typically defined by the cessation of movement for five minutes or more. These metrics have become outdated, as recent studies have uncovered evidence of multiphasic sleep patterns in *Drosophila*, including brain activity indicative of different sleep phases, behavioural markers of deeper sleep, and shorter sleep latencies. To understand sleep in *Drosophila*, it need to integrate these new findings into our analysis toolbox without compromising the high-throughput nature of *Drosophila* research.

This study investigates behavioural markers of sleep, utilising both high-throughput, low-resolution machine vision tracking data and individual, high-resolution limb tracking to identify behavioural correlates of sleep states. Our findings reveal that low-resolution data cannot currently classify sleep states or depth more accurately than the traditional five-minute inactivity rule. However, it does allow for more detailed analysis of sleep patterns, particularly when characterising sleep in new *Drosophila* species or mutants. High-resolution tracking, while capturing sleep postures, has limited applicability for standard sleep research due to experimental setup constraints. This work aims to be a foundation for developing more refined metrics for understanding sleep in *Drosophila*.

Declaration

I declare that this thesis was created by myself, that the work is my own except where explicitly reported in the text, and no part has been submitted for another degree or qualification.

The copyright of this thesis rests with the author. Unless otherwise indicated, its contents are licensed under a Creative Commons Attribution-Non Commercial 4.0 International Licence (CC BY-NC). Under this licence, you may copy and redistribute the material in any medium or format. You may also create and distribute modified versions of the work. This is on the condition that: you credit the author and do not use it, or any derivative works, for a commercial purpose. When reusing or sharing this work, ensure you make the licence terms clear to others by naming the licence and linking to the licence text. Where a work has been adapted, you should indicate that the work has been changed and describe those changes. Please seek permission from the copyright holder for uses of this work that are not included in this licence or permitted under UK Copyright Law.

Acknowledgements

Undertaking the PhD has been a long process and was followed by writing the thesis that has felt both rapid and an eternity. I came into the PhD slightly lost with the direction in my life, but through the process of work and the people I've met I've begun to understand what makes me tick and what brings joy into my life.

Firstly, I would like to express my gratitude and love to all the members of the Gilestro lab group over the years for fostering a great environment to be in. From the original core of Alice, Hannah, and Michaela who helped welcome me into the fold. Michaela especially was always on hand to be distracted by me upstairs. To Federica who joined alongside me who introduced me to all things Italian, including modern Roman slang. Also. to Lei who arrived late but has amazed me with his ability to dive into all aspects of British culture, sharing in my passion for Brentford FC. Special mention must also go to the Southall lab group who moved in late into our space, bringing a whole new energy and fun into the office.

I'd also like to thank Giorgio, my supervisor, for all his help along the way. His leadership style is always inclusive, making you feel an equal to him from day 1. His efforts to make and keep a socially cohesive lab group has borne fruit for us all.

Secondly, I'd like to thank my friends throughout this period, The great group of people I met on my masters course have suffered alongside me in their PhDs at Imperial or work elsewhere, providing support, scientific discussion, and gallows humour. My myriad of friends from school and university scattered across London who I've now shared what feels like an eternity with. Special thanks must go to Miles, Tim, Amy, and Josh, my housemates throughout the years in London. Miles, Tim, and Amy spent the COVID lockdown with me, a time we'll never forget. All four helped make a house I was happy to go home to every evening, calming me when I was stressed and tired from work. Some of the events from the house in Ealing will be forever in my memory as times of joy.

Thanks must go to my parents. They have set me up for this future by their dedication to my education. Of note was their help in getting me to my masters course in Sheffield after a last minute decision the week it started. Without their safety net I wouldn't be where I am now. Also, thanks to my siblings Louise and Alastair for always keeping me grounded.

Lastly, my deepest thanks and love must go to my partner, Naima. We met when my PhD began and hers followed not long after. Our lives have become entangled as the PhDs unwound us. She provided support, love and understanding for the whole time, helping to soothe all woes as they arose. Her dedication to her work and others has inspired me this whole time and keeps me going on. We now look forward to our lives together as we take the next step beyond the PhDs.

Contents

Abstract **i**

Declaration **i**

Acknowledgements **v**

1 General Introduction **3**

1.1 Behaviour as a tool of Neuroscience 3

1.2 Overview of Sleep 4

1.2.1 Historical Context 4

1.2.2 Definitions of Sleep 4

1.2.3 Regulators of Sleep 6

1.2.4 Consequences of Sleep Loss 12

1.2.5 Differences in Animal Sleep 14

1.2.6 Evolution and Theories of Sleep 17

1.2.7 Evolution and diversity of Sleep States 21

1.3 Behaviour and Neuroscience 26

1.3.1 Context . . . 26
1.3.2 Defining Behaviour . . . 26
1.3.3 Behaviour to understand Neurobiology . . . 26
1.3.4 Behavioural States . . . 28
1.4 *Drosophila*: Background and behaviour . . . 29
1.4.1 Context . . . 29
1.4.2 *Drosophila* Behaviours and their paradigms . . . 30
1.5 Sleep In *Drosophila* . . . 33
1.5.1 Methods to Study Sleep and their findings . . . 33
1.5.2 Mechanisms of Sleep . . . 37
1.5.3 Determinants of Sleep . . . 39
1.6 Summary and Aims of this Work . . . 41
1.6.1 Aims and Objectives . . . 42

2 Material and Methods 43

2.1 Animals . . . 43
2.1.1 Fly Maintenance and Handling . . . 43
2.1.2 Species Stock . . . 43
2.2 Ethoscope . . . 45
2.2.1 Ethoscope Data Generation . . . 45
2.3 Hidden Markov Model . . . 46
2.3.1 Data Curation . . . 46

2.3.2 Training 49
2.3.3 Scoring Models 49
2.3.4 Decoding Datasets 50
2.4 Odour Response Experiments 50
2.5 Sleep Deprivation Experiments 51
2.6 Time Series Analysis 52
2.7 Machine Learning 52
2.7.1 Dynamic Time Warping 53
2.7.2 Catch-22 53
2.8 High definition videos 57
2.8.1 Video capture 57
2.8.2 Video Curation 58
2.8.3 Manual Behaviour Categorisation 58
2.8.4 SLEAP and keypoint analysis 59
2.9 Statistics, data collection and visualisation 61

3 Ethoscopy: An open-source behavioural analysis toolbox 63

3.1 Rationale 63
3.2 Improving accessibility 65
3.2.1 Dockers 65
3.2.2 Jupyter notebooks and Tutorials 66
3.3 Design Philosophy and Structure 68

3.4 User Workflow 69
3.4.1 Loading Data 71
3.4.2 Augmenting Data 72
3.4.3 Visualisation 73
3.5 Specific behavioural tools 75
3.5.1 Circadian Analysis 76
3.5.2 Hidden Markov Models 81
3.6 Integrating Machine Learning 84
3.7 Summary 85

4 Modelling sleep stages with hidden Markov models 86

4.1 Is Drosophila sleep phasic? 86
4.2 Modelling Sleep 88
4.2.1 Previous Attempts to Model Sleep 88
4.3 The fundamentals of hidden Markov models 90
4.3.1 Structure of hidden Markov models 91
4.3.2 Solving the fundamental problems of hidden Markov models 91
4.4 Exploring and validating the hidden Markov models 93
4.4.1 Deciding the model architecture 93
4.4.2 Training and Scoring the Model 94
4.4.3 Describing the decoded model 99
4.4.4 Validating the models predictions 102

4.5 Discussion . . . 107

4.6 Applying the hidden Markov model to multiple *Drosophilids* . . . 108

4.6.1 Species background . . . 109

4.6.2 HMM derived sleep for Drosophilids . . . 111

4.6.3 Interpreting Sleep Rebound with HMMs . . . 118

4.7 Discussion . . . 120

5 Classifying sleep beyond movement **122**

5.1 Rationale . . . 122

5.2 Background . . . 123

5.2.1 Behavioural Criteria for sleep across species . . . 123

5.2.2 Behavioral indicators of sleep in insects and *Drosophila* . . . 124

5.3 Exploring the ethoscope trackers' variables . . . 125

5.3.1 Additional variables from the ethoscope . . . 126

5.3.2 Variables over time . . . 127

5.3.3 Distribution of variables . . . 130

5.3.4 Do variables change over immobile bouts? . . . 133

5.3.5 Are responses dependent on the variable value? . . . 135

5.4 Predicting sleep with machine learning . . . 136

5.4.1 Dynamic time warping classification . . . 140

5.4.2 Catch22 Classification . . . 142

5.5 Discussion 145

6 Identifying sleep hallmarks with high-resolution videos recordings and analysis 148

6.1 Rationale 148

6.2 Behaviour identification through keypoint tracking 149

6.3 Capturing high resolution videos 150

6.3.1 Setup 150

6.3.2 Curation 152

6.4 Applying keypoint tracking 152

6.4.1 Model training 152

6.4.2 Model accuracy 153

6.5 Manual behaviour segmentation 154

6.5.1 Description of postures 154

6.5.2 Do the angles at keypoints describe the behaviours? 155

6.5.3 Does the centroid describe the behaviours? 158

6.5.4 Does the distance between keypoints describe the behaviours? 158

6.5.5 Do changes in the y-coordinate of keypoints describe the behaviours? . . 160

6.6 Time-series analysis of postural keypoints 162

6.7 Behavioural observations 164

6.8 Discussion 166

6.9 Further work 168

7 General discussion **170**

7.1 Summary 170

7.2 Findings 171

7.2.1 Probabilistic modeling Vs Inferential analysis 171

7.2.2 Should the Five-Minute Assumption Remain? 175

7.2.3 Behavioural Identifiers 177

7.3 Conclusion 179

A Appendix **181**

Bibliography **181**

List of Tables

2.1 The *Drosophila* species and their collection sites. 44

2.2 The variables generated in real time by the ethoscope. As used in *Chapter 5*. . . 47

2.3 The variables generated post experiment in ethoscopy. As used to label movement and behaviours. 48

2.4 Catch-22 features and their descriptions. 56

2.5 Parameters and the arguments used when calling the video function *libcamera-vid* to capture HD videos. 57

4.1 A breakdown of the architecture of the hidden Markov models presented in *Figure 4.1* 95

A.1 HMM transition probabilities 182

A.2 HMM emission probabilities 183

List of Figures

1.1 Description of the sleep and wake stages of humans 7

1.2 The two-process model of sleep regulation 9

1.3 The conservation of neurotransmitters that regulate sleep and wake. 11

1.4 REM sleep total versus core body temperature in the homotherm order 16

1.5 Phylogenetic tree showing the distribution of sleep states across the animal kingdom 25

1.6 The ethoscope: an automated video behavioural tracking system and its modules 31

1.7 Circadian activity peaks and daily sleep in *Drosophila* 38

2.1 Visual representation of the variables tracked by the ethoscope 46

2.2 Diagram of the keypoint label locations and subsequent calculations 59

3.1 Diagram of the *ethoscopy* ecosystem and its architecture 70

3.2 An example of the loading functions in *ethoscopy* 72

3.3 An example of some of the methods available in *ethoscopy* 74

3.4 Visualisation methods available in *ethoscopy* 76

3.5 Visualisation of the circadian analysis tools available in *ethoscopy* 80

3.6 Visualisation of the output of hidden Markov models in *ethoscopy* 83

4.1 A modified version of the Wiggin four state model scores the best 97

4.2 The new model HMM architecture with two observables is the best representative of the data when decoded 98

4.3 HMM predicted sleep states have unique characteristics and vary over the day . 101

4.4 Each predicted HMM state has a unique arousal threshold 105

4.5 Manually segmenting light sleep classification reproduces an uptick in response rate at the end 106

4.6 A partial pylogenetic tree of the selection of *Drosophila* used in this study . . . 110

4.7 Each Drosophilid has a unique HMM profile and sleep pattern 114

4.8 Distribution of the lengths of HMM states per Drosophilid 117

4.9 Only *D. melanogaster* exhibits homeostatic sleep rebound after mechanical sleep deprivation 119

5.1 Depiction of the variables tracked by the ethoscope 127

5.2 The tracked variables follow a circadian rhythm over the 24-hour day 129

5.3 The distribution of each tracked variable per HMM state 132

5.4 Tracked variables change over the bout with no difference between non-responding and responding bouts 134

5.5 The response rate changes for different values of X, W, Area, and mean velocity 138

5.6 An example of how variables change over an inactive bout 139

5.7 k-NN classification with DTW fails to predict response or HMM sleep state . . . 141

5.8 Time series features from Catch22 can marginally predict responses better than random 144

6.1 The new high-definition video capture setup 151

6.2 Videos of inactive bouts were labelled on the head, body, and abdomen 153

6.3 Three observable sleep postures were manually identified 154

6.4 The angle at each keypoint does not distinguish the postures 157

6.5 Changes in length between the head and abdomen identify *full prone* in female flies 159

6.6 Changes in the y-coordinate of keypoints identify postures 161

6.7 Time series analysis of keypoint locations reveals no differences 163

6.8 The sleep identifier the 'haltere switch' and terminalia protrusion were observed 165

List of Abbreviations

ACV apple cider vinegar.

AIC Akaike Information Criterion.

BIC Bayesian Information Criterion.

Catch22 CAnonical Time-series CHaracteristics.

CI confidence interval.

CS canton-S.

DAM *Drosophila* Activity Monitoring.

DTW Dynamic Time Warping.

EEG electroencephalogram.

HCTSA High-Content Time-Series Analysis.

HD high definition.

HMM hidden Markov model.

ID unique identifier.

IR infrared.

k-NN k-nearest neighbour.

ML machine learning.

NREM non-rapid eye movement.

REM rapid eye movement.

ROI region of interest.

ROS reactive oxygen species.

SD sleep deprivation.

SWA slow wave activity.

t-SNE t-distributed stochastic neighbor embedding.

ZT zeitgebers.

Chapter 1

General Introduction

1.1 Behaviour as a tool of Neuroscience

Behaviour, whether conscious or unconscious, encompasses the entirety of our daily interactions—from the simple, such as rhythmic breathing, to the intricate, such as social relationships. Similarly, as the lungs extract oxygen from the air, the nervous system governs and maintains these behaviors, allowing an organism to engage with its environment [1].

The core ambition of neuroscience is to decipher how the brain orchestrates these behaviours in response to the world. Despite increasingly sophisticated tools and a better understanding of the mechanical dynamics of the brain, a comprehensive theory of brain function remains elusive. Even in the well-mapped neuronal circuitry of *Caenorhabditis elegans*, which consists of only 302 neurons, our ability to predict behaviour is limited [2]. Clearly, understanding neural circuitry alone is insufficient; it must be coupled with detailed insights into behaviours and their contexts [3, 1].

Sleep is a particularly complex behaviour, occupying a significant portion of our lives and widely regarded as essential across species. Yet, from an external perspective, sleep offers little visible information beyond what is indicative of internal electrophysiological states. Nevertheless, its quality, quantity, and drive are shaped by our behaviours over days and even years. To develop

a general theory of sleep, we must examine how it adapts to varying conditions both within and across species.

1.2 Overview of Sleep

1.2.1 Historical Context

Sleep has fascinated humans for millennia and is intertwined with ideas and mythologies surrounding death. This connection is evident in ancient texts and mythologies, as far back as the Epic of Gilgamesh, where Gilgamesh slays Humbaba, a giant that never sleeps, and in ancient Egyptian culture, where death is referred to as the "eternal sleep", a euphemism still in use today [4]. This association likely stems from the observable similarities between sleep and death: both states involve immobility, a prone position, and a lack of consciousness. Aristotle, the pioneering scientist of ancient Greece, regarded sleep as a form of affliction (pathos) in his treatise ***On Sleep and Sleeplessness*** [5], a sentiment that persists in modern attitudes where sleep is often viewed as a limitation of the body.

This philosophical, and often emotive, discourse on sleep has been the only outlet for scientists limited to observations alone. For all one could tell the mind and person ceased to observe the world, becoming motionless, leading to its label as a unitary off-period [5, 6]. Sleep, however, was known to be different to death. Most poignantly by the fact that it is reversible. It was from this key behavioural identifier that modern sleep studies grew out.

1.2.2 Definitions of Sleep

Behavioural Classification

Despite its ubiquity in life, systematic studies of sleep did not emerge until the late 19th century. Kohlschütter was among the first to approach sleep scientifically by applying mathematical theories of sensory stimulation and perception. By exposing subjects to graduated sounds, he

demonstrated that the depth of sleep varies over time, producing the first sleep depth curve [7] —an experiment that remains replicable today [8]. J. S. Szymanski further explored sleep's relationship to wakefulness through continuous measurements of activity and rest in animals and infants over 24-hour periods (1914-1922). His work quantified monophasic and polyphasic activity patterns, and diurnal and nocturnal species [5].

These early studies led to the development of behavioural criteria for defining sleep that could be extrapolated to all animals. In 1913, Henri Piéron proposed the following criteria [9]: (1) the adoption of a stereotypic or species-specific posture, (2) sustained behavioural quiescence beyond a minimum duration, (3) an elevated arousal threshold, and (4) rapid reversibility upon significant stimulation. These criteria have proven robust, with Campbell and Tobler [10] later using them to review sleep duration across a broad range of species. Their review highlighted the predominance of mammalian sleep studies and, to a lesser extent, avian studies, while showing that sleep-like states are present in most animals, including invertebrates—previously overlooked in sleep research.

The behavioural criteria were further refined when *Hendricks et al.* added two additional conditions: (5) altered sensory information processing, and (6) regulation by homeostatic and circadian controls, key controllers of sleep that will be explored later[11].

Behavioural sleep research remains focused on measuring and contextualising sleep within these six criteria, investigating the length and location of quiescence across the animal kingdom [12, 13, 14, 15].

Electrophysiological Classification

While behavioural criteria are useful for identifying sleep across species, the invention of the electroencephalogram (EEG) by Hans Berger in 1928 allowed for direct measurement of brain activity during sleep. Soon after, Alfred Loomis published research differentiating wakefulness, sleep, and hypnosis purely through EEG recordings [16]. Loomis and colleagues further categorised sleep into five stages, laying the groundwork for modern sleep scoring [17].

In the 1950s, the idea of sleep as a uniform state was challenged when EEG data revealed periods of brain activity similar to wakefulness, accompanied by rapid eye movements [18, 19]. This discovery led to the classification of sleep into two distinct categories: rapid eye movement (REM) sleep and non-REM (NREM) sleep. In 1968, Allan Rechtschaffen and Anthony Kales formalised this classification with their manual of EEG-based sleep scoring, defining sleep as an alternating cycle of REM and NREM stages [20]. Each cycle typically includes one REM stage—characterised by eye movements, a low-amplitude, mixed-frequency EEG, and reduced muscle tone—and four NREM stages—marked by K-complexes, sleep spindles, and slow-wave activity (SWA) (0.5-4 Hz) in the later stages. In all adult mammals studied to date, SWA sleep is the predominant sleep state, usually occupying 75% of total sleep time [21]. REM and NREM sleep are sometimes referred to as "active sleep" and "restful sleep," respectively, although this rule has been known to be broken with the finding of myoclonic twitches during REM in older infants [22] and distal muscle twitching in adults [23], so should not be used as definitive proof.

In humans, a full sleep cycle typically repeats four or five times per night. Figure 1.1 provides a breakdown of these stages.

Since their discovery, EEG-defined sleep stages combined with electromyograms —to distinguish REM from wake— have become the gold standard for sleep classification. However, this sleep architecture classification has only been conclusively demonstrated in mammals and birds, with limited evidence of similar electrophysiological patterns in other animal groups [24, 25, 14].

1.2.3 Regulators of Sleep

Our earliest understanding of sleep recognised its periodic nature, reflecting the Earth's natural rhythms. Both modern human societies and hunter-gatherer societies have robust activity patterns, that follow the 24-hour cycle. Sleep onset and wake may differ, but the totals remain similar [29]. Deviating from this pattern, such as staying awake beyond the usual bedtime, leads to an increasing internal urge to sleep. The ancient Greek physician Galen attributed this to "pneuma" being depleted during wakefulness—what we now refer to as sleep pressure [5]. These

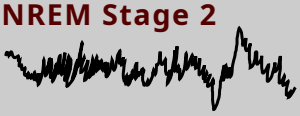
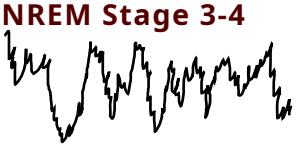
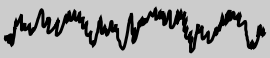
Human Sleep Stages and EEG signal	Description adapted from Pan et al., 2012, 2021	Siginal generation / origin adapted from Joiner., 2016
Wake 	In a closed eye subject: - >50% consists of alpha (3-13 Hz) activity or low-voltage, mixed (3-7 Hz) frequency activity	Cholinergic and monoaminergic brainstem nuclei generate cortex wide excitement through both the ventral and dorsal excitatory pathways. Priming the cortex for sensory signal processing.
NREM Stage 1 	The transitional state from wakefullness Low-voltage mixed (3-7 Hz) activity, theta waves Low arousal thresholds Some evidence of eye rolling	
NREM Stage 2 	Lengthens with each progressive cycle Appearance of sleep spindles and/or K complexes < 20% of the state may contain high voltage (> 75 µV, <2 Hz) activity Higher arousal thresholds than state 1	Cholinergic and monoaminergic signalling are both reduced. Leading to dampened cortex excitement and increased filterering of sensory information
NREM Stage 3-4 	Mostly occurs in the first third of the night Synchronised large amplitude, low-frequency SWA 20%-50% consists of high voltage and low-frequency (>75 µV, <2 Hz) activity, delta waves Highest arousal thresholds	
REM 	Similar EEG to wake Relatively low-voltage mixed frequency activity Episodic rapid eye movement Reduced chin EMG activity Lengthens progressively each cycle Arousal thresholds similar to stage 2	Cholinergic activity from the brain stem, akin to wake is produced. However, monoaminergic signalling is reduced, resulting in altered firing of the thalamic neurons. This filters out sensory signalling in the cortex

Figure 1.1: **Description of the sleep and wake stages of humans**.
Sleep cycles through from wake to NREM to REM with representative EEG recordings and description. Transition from stage to stage is sequential from top to bottom. REM will cycle back into NREM-1 is no awakening occurs. Description of signal adapted from *Pan et al. 2012, 2021* [26, 27]. Description of signal origin adapted from *Joiner 2016* [28].

two well-established phenomena, sleep debt and daily rhythm, were later formalised into the widely accepted "two-process model": homeostatic control (Process S) and circadian control (Process C). Together, these processes synchronise our sleep-wake cycle with both internal physiological needs and external environmental cues (Fig. 1.2) [30].

Homeostatic Control – Process S

Process S represents the build-up of sleep pressure, which increases steadily during wakefulness. The longer we stay awake, the greater the pressure, driving the need for sleep. Sleep relieves this pressure, bringing it back to baseline levels [30]. The key regulators include melatonin [31], which promotes sleep onset in the evening, and orexin [32], which maintains wakefulness during the day. The primary function of Process S is to ensure adequate daily sleep

When sleep is insufficient or disrupted, the body compensates with sleep rebound, characterised by deeper, more intense sleep to recover lost rest. Sleep rebound typically involves increased SWA and a higher threshold for arousal [33, 34, 35]. Recovery sleep typically takes less time than sleep lost, indicative that sleep quantity is not a fixed process that may be related to sleep type.

Circadian Control – Process C

Process C operates on a 24-hour cycle, governed by the internal biological clock located in the suprachiasmatic nuclei of the hypothalamus [36, 37]. Additionally, evidence suggests localised rhythms within other tissues [38]. Unlike Process S, Process C is self-sustaining and continues even in the absence of external cues like light and darkness. However, without alignment with external signals—known as zeitgebers (ZT), such as light, temperature, and social interactions—the circadian rhythm can drift over time [36].

Process C not only regulates sleep but also orchestrates daily physiological rhythms, ensuring that bodily functions occur at optimal times based on an organism's needs. For humans, morning light and evening meals are the most powerful zeitgeber [39].

Interaction Between Process S and C

Although distinct, Process S and Process C interact to regulate sleep-wake cycles. Their interplay aligns the physiological need for sleep with optimal sleep times. Recent revisions to the two-process model suggest that these processes influence each other in more complex ways than initially understood [40].

The framework remains central to understanding sleep regulation, emphasizing the dynamic interplay between biological need and environmental adaptation.

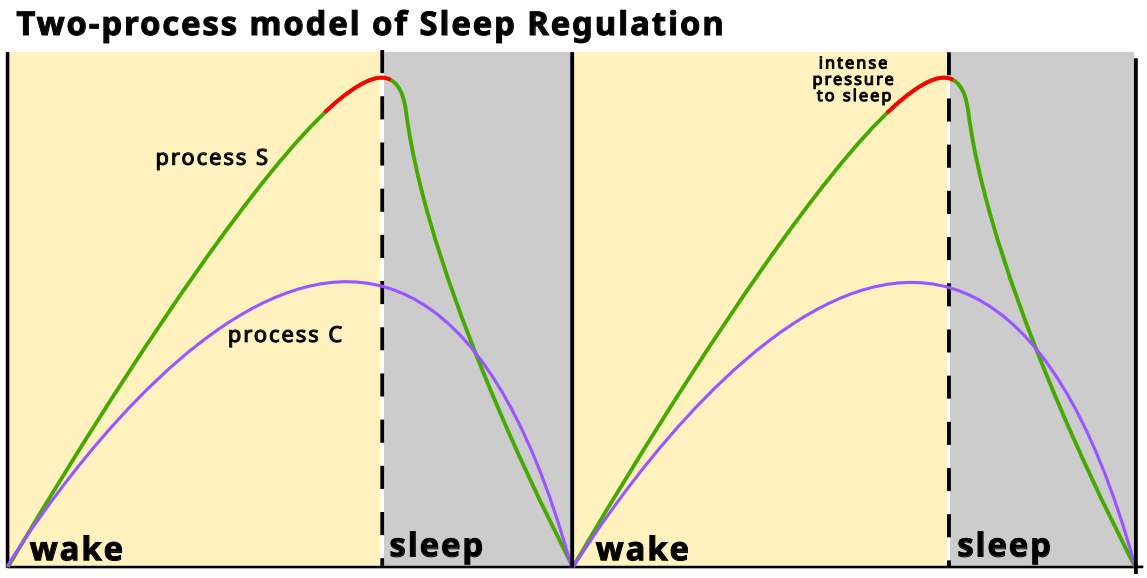


Figure 1.2: **The two-process model of sleep regulation**.
Sleep propensity grows during periods of wakefulness and abates during sleeping periods. The homeostatic process-S (green line) generates an increasing pressure to sleep upon consecutive time awake until it becomes intense enough to initiate sleep (red line). The circadian process-C (purple line) follows a daily rhythm, peaking at differing times for different animals.

Conserved neurotransmitters of sleep

The neuromolecular regulators of sleep are remarkably conserved across species (Fig. 1.3). In mammals, zebrafish, and fruit flies, the activation of aminergic and cholinergic neurons plays a key role in promoting wakefulness [28]. Pharmacological interventions further underscore this conservation: antihistamines and GABAergic agonists consistently promote sleep, while caffeine induces wakefulness by antagonising adenosine receptors. Histological studies confirm that in zebrafish, the spatial distribution of aminergic, cholinergic, and GABAergic neurons closely mirrors that found in mammals [41]. Moreover, both pharmacological and genetic manipulations of neurotransmitter systems in zebrafish reveal striking similarities to mammalian responses [28]. However, this high degree of similarity is only partially observed in Drosophila. Notably, orexin has not been identified in invertebrates, and in Drosophila, both serotonergic [42] and glutamatergic [43] neurons have been found to promote sleep, contrasting with their wake-promoting roles in mammals and zebrafish. It is clear that the regulators of sleep are strongly conserved throughout the animal kingdom, indicating that the basic arousal and sleep promoting circuits were defined molecularly very early on. Later evolution may have seen the

loss or adaption of some circuits in invertebrates

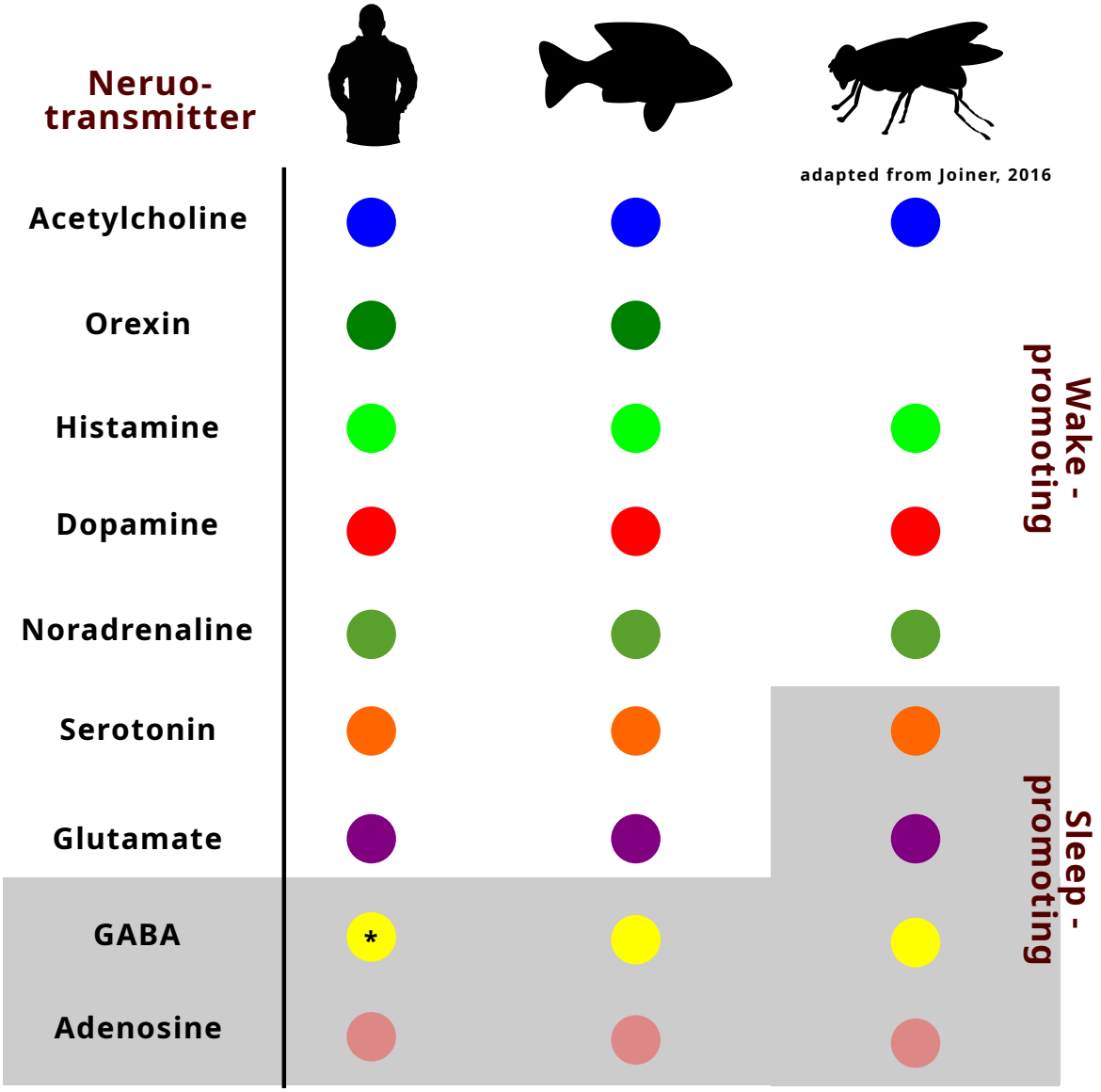


Figure 1.3: **The conservation of neurotransmitters that regulate sleep and wake.** Colored circles represent pharmacological, histological or genetic confirmation of the existence of neurotransmitter systems in mammals, zebrafish and flies. Where the background is white the neurotransmitters and known to promote wake when activated. Where the background is grey the neurotransmitters are known to promote sleep. The invertebrate neurotransmitter equivalent of norepinephrine is octopamine. * Some sub-populations of GABAergic neurons promote wake in mammals. Adapted and updated from *Joiner, 2016* [28]

1.2.4 Consequences of Sleep Loss

Is it lethal?

The common discourse surrounding sleep is the worry of not getting enough and the potential consequences effects. Early studies on chronic sleep deprivation (reviewed in Bentivoglio & Grassi-Zucconi, 1997 [44]) indicated that chronic sleep loss could be fatal, based on experiments conducted in dogs [45, 46, 47] and rats [48, 49]. This belief is still supported by some researchers, with recent studies in *Drosophila* [50, 51] and cockroaches [52] reporting similar findings. However, the methods used in these studies often involve highly stressful conditions, such as forcing animals to stay constantly active or in a state of fear, irrespective of their sleep state. In contrast, experiments using more targeted and less intrusive sleep deprivation techniques [53], or similar methods applied to other species like pigeons [54], have shown that sleep deprivation is not lethal. Notably, no human has ever died from voluntary chronic sleep deprivation [55, 56]. Although pathogenetic sleep loss from fatal familial insomnia, a prior protein based neurogenerative disease, will lead to death within 8-72 months [57]. Fatal familial insomnia is characterised by increasing inability to fall asleep or refreshment from sleep, that coincides with motor impairment, decreasing intellectual abilities, and emaciation.

Physical adverse effects?

While sleep deprivation may not be fatal, numerous clinical and experimental studies have linked abnormal sleep with health issues [58, 59, 60], such as weight gain leading to obesity and diabetes [61], as well as impairments to the immune system [62]. Both too much and too little sleep correlate with a greater risk of death [60]. Research into sleep loss suggests that these health deficits might be associated with increased levels of toxins in the brain that are cleared more effectively during sleep [63, 64, 65] and that by bolstering stress response genes the effects can be mitigated [50]. However, this brings us back to the debate on lethality—are these outcomes driven by sleep loss or by the stress induced during sleep deprivation, and can the two ever be fully disentangled? Unpublished findings from the Gilestro lab suggest that the

build-up of reactive oxygen species (ROS), previously thought to cause death in sleep deprived *Drosophila* [51], is a result of mechanical stress rather than sleep loss. Additionally, *Miao et al.* work challenges the notion that sleep promotes clearance of brain toxins, instead observing a decrease [66]. These examples show the conflicting discourse about the restorative affects of sleep. All theories must first answer the question of why these processes can not be achieved during wake before they can be accepted.

Cognitive effects?

Sleep deprivation has long been linked to declines in cognitive function [67]. Studies have shown that participants are less likely to learn new tasks if their sleep is disrupted [68], and their performance improves if they are allowed to nap [69]. Similar findings have been observed in *Drosophila*, short-sleep mutants [70] and sleep-deprived flies [71] exhibit impairments in learning and memory, consistent with effects seen in humans [72, 73].

Some researchers attribute these cognitive deficits specifically to disrupted REM sleep. Individuals with REM sleep disorders are at a much higher risk of developing neurodegenerative diseases [74, 75], and those with naturally low REM sleep and high NREM-stage 1 sleep show a greater risk of cognitive decline [76]. This evidence aligns with the observation that REM sleep is most prominent during developmental stages [77, 78], with chemical disruption of REM sleep affecting brain maturation in both rats [79] and flies [80]. However, the emphasis on REM sleep's role in cognition is challenged by findings that sleep rebound tends to prioritise NREM sleep and SWA [81]. Any disruption of REM sleep is likely to have wide ranging effects, independent of REM sleep's function.

The evidence surrounding the effects of sleep loss remains complex and often contradictory. One of the main challenges in sleep research is effectively controlling confounding factors like stress. Among the various findings, the most convincing link is between sleep and memory or learning processes. Even during Randy Gardner's famous 1963 experiment, where he stayed awake for 11 days, significant cognitive decline only appeared near the end, while his motor skills remained remarkably intact [82]. Interestingly, humans sleep the least among primates,

albeit with the highest proportion of REM sleep [83]. If sleep is not directly tied to cognitive ability, then the regulation of sleep quantity and quality must be influenced by other factors—an idea best explored through a broader examination of sleep across different species.

1.2.5 Differences in Animal Sleep

As previously mentioned, using behavioural criteria pioneered by Henri Piéron, sleep can be observed across the animal kingdom [84, 24, 85]. Many researchers view sleep as a universal phenomenon, deeply conserved throughout evolution [86, 87, 88, 12]. This section focuses on the differences and variations found in sleep across species, as a mode to explore its function.

Variation in length

While sleep is ubiquitous, it is far from uniform. There is significant variation both within and across species [89]. In humans, sleep duration changes across developmental stages, ranging from 12-15 hours in infancy to 6-8 hours in adulthood [90], and the proportion of REM sleep decreasing over time [77]. Even within these averages, sleep duration varies widely among a population [91], a distribution also observed in birds [92] and fruit flies (*Drosophila melanogaster*) [53]. Some of this variation can be attributed to genetics [93], but environmental flexibility plays a significant role as well [94]. Hunter-gatherer societies sleep about an hour more during the winter as nights grow colder [29], and pre-industrial Northern Europeans exhibited biphasic sleep patterns during the long winter months [95]. The three-toed sloth changes its sleep total from the wild (10 hours) to captivity (16 hours) [96].

Understanding sleep function requires considering why some animals sleep much more than others. Among 22 studied primates, humans sleep the least, while the grey mouse lemur (*Microcebus murinus*) sleeps the most—up to 16 hours [83]. The brown bat (*Myotis lucifugus*) takes the crown for the longest sleeping mammal at 20 hours a day [97], which dwarfs the sleep of giraffes (*Giraffa camelopardalis*) [98] and elephants (*Elephas maximus*) [99] who will only sleep 4-5 hours. One of the few correlations of sleep total in mammals is weight in

herbivores, and to a lesser extent omnivores, where larger animals sleep the least on average. This correlation is not seen in carnivores [13]. But this is not an exact predictor; for instance, the golden-mantled ground squirrel (*Callospermophilus lateralis*) and the degu (*Octodon degus*), despite being similarly sized rodents (200-300 g), sleep 15.9 hours and 7.7 hours respectively [100]. Differences in sleep in animals of the same size could be due to differing basal metabolic rate, which is shown to negatively correlate with total sleep time and the amount of SWA sleep [101]. Clearly, sleep duration is influenced by multiple factors, and no single variable model can fully explain this variation.

Variation in type

Sleep duration is the simplest metric to compare, but EEG data allows us to explore differences in sleep type, primarily in mammals and birds. Some animals, such as *cetaceans* (an infraorder of aquatic mammals), exhibit unihemispheric sleep, where one cerebral hemisphere sleeps while the other remains awake [102]. This has been observed in species like bottlenose dolphins (*Tursiops truncatus*) [103, 104] and beluga whales (*Delphinapterus leucas*) [105]. During unihemispheric sleep, cetaceans can continue swimming in circles [106, 103] or will rhythmically surface and submerge [105]. Interestingly, bottle nose dolphins maintain sensory awareness during sleep and exhibit no REM sleep [107, 108].

Semi-aquatic mammals, such as fur seals (*Callorhinus ursinus*) and sea lions (*Otaria flavescens*), switch between bilateral sleep on land and unihemispheric sleep when in the water for extended periods. While in the water, they may spin in water or rest on the floor [85, 109]. Like cetaceans, these mammals lack REM sleep while in water, although it is present on land, and have unaffected cognition after sleep deprivation [110, 111]).

Unihemispheric sleep is not exclusive to marine mammals, it is also apparent in birds, typically during long migratory flights [112]. Initially, this was thought to be necessary for maintaining flight and navigation, but recent studies on great frigatebirds (*Fregata minor*) reveal that they can sleep both unilaterally and bilaterally while soaring [113, 114]. Unihemispheric sleep could function as a defense mechanism; mallards (*Anas platyrhynchos*) on the periphery of a group

tend to sleep with one eye open, while those in the center sleep bilaterally [115].

The architecture and origins of sleep states can also differ across species. *Monotremes*, such as echidnas (*Tachyglossus aculeatus*) [116, 117] and platypuses (*Ornithorhynchus anatinus*) [118], exhibit bursts of REM-like sleep activity confined to the brainstem, while the rest of the brain remains in a typical NREM state. Interestingly, *monotremes* have the highest proportion of REM sleep (if it can be called REM sleep) among all mammals, a feature linked to their low core body temperature, which is inversely correlated with total REM sleep across mammals (Fig. 1.4) [119].

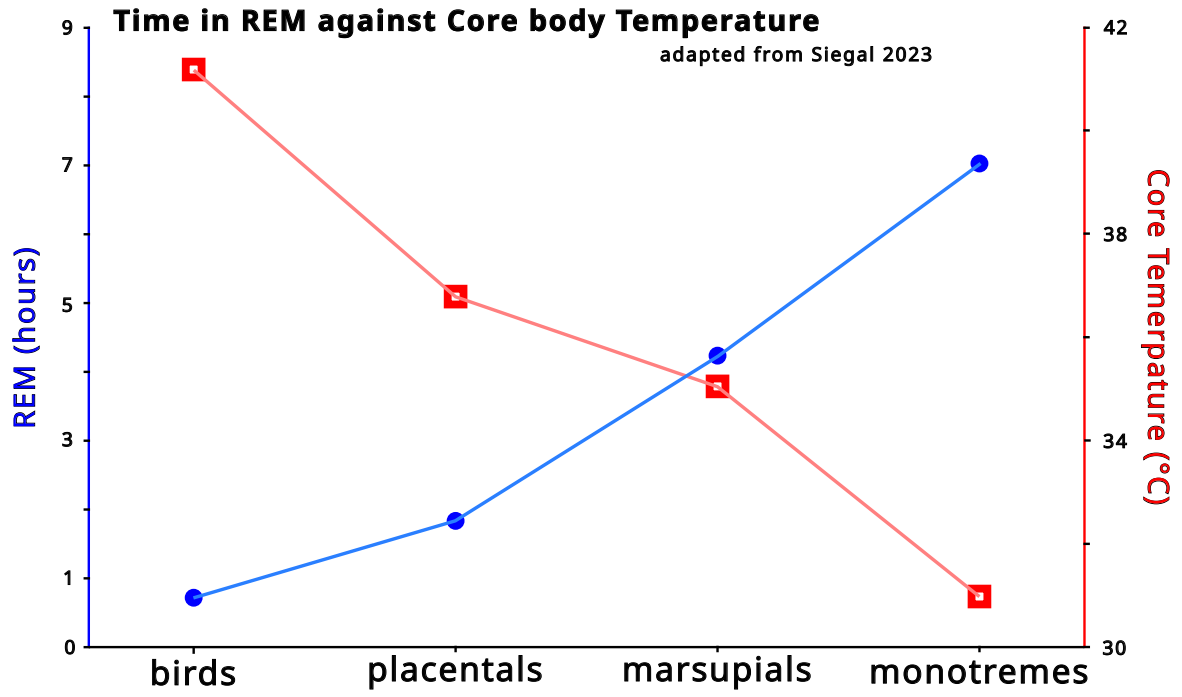


Figure 1.4: **REM sleep total versus core body temperature in the homotherm order**. Homotherms with the lowest body temperature (red line), monotremes, have the highest total REM sleep (blue line). The inverse relationship is true across birds, placentals, and marsupials. Adapted from *Siegel 2022* [12]

Forgoing sleep

Some animals are capable of temporarily abandoning sleep in response to environmental changes. Dolphins and seals can go without sleep for up to five days without noticeable deficits [107, 111], and white-crowned sparrows (*Zonotrichia leucophrys*) reduce sleep by 63% during migration [120]. Breeding and rearing activities are also strong modifiers of sleep. Walruses (*Odobenus*

rosmarus) forego sleep during breeding season [121] and sleep deprived male *Drosophila* will forgo rebound sleep in the presence of female pheromones [122].

Short Sleepers

Parental duties also influence sleep patterns. Incubating chinstrap penguins (*Pygoscelis antarcticus*) experience extremely short bouts of SWA sleep (4 seconds) but in greater quantities compared to non-incubating individuals, mirroring behaviours seen in birds at the edges of colonies [123]. In both cases, sleep is thought to adapt to mitigate predation risk. In *Drosophila*, 6% of wild-type females sleep for less than 5% of the day, while 50% sleep less than 20% [53]. This is attributed to females' need to find suitable egg-laying sites or meet higher caloric demands. Notably, virgin fruit fly females exhibit sleep patterns similar to males [124].

Cavefish populations provide an intriguing model for studying the evolutionary pressures on sleep. In Mexico (*Astyanax mexicanus*) [125, 126] and Southeast Asia (*Balitoridae*) [127], cave-dwelling fish populations have evolved away from their surface-dwelling ancestors. These populations show common adaptations to life in darkness, including reduced pigmentation, eye degeneration [128], and a dramatic reduction in sleep duration—up to 80% less in A. mexicanus [125]. The cavefish model offers a unique perspective on how sleep can evolve in response to environmental pressures.

1.2.6 Evolution and Theories of Sleep

The evidence is for sleep as a universal behaviour across the animal kingdom, despite its variability in duration and structure. Its widespread presence in nature has driven many to consider sleep essential with evolutionally conserved physical biological functions [129, 130, 86]. However, while we have deep insights into sleep mechanisms and its physiological impacts, general theories about the purpose of sleep struggle to account for all species' behaviours. Broadly, sleep theories can be categorised into adaptive and restorative perspectives, with cognitive functions sometimes considered a subset of the restorative view.

Sleep as an Adaptive Response

The adaptive theory of sleep suggests that animals evolved sleep as a strategy to conserve energy, avoid danger, and wait for more favorable environmental conditions [131, 132, 133, 134]. This idea aligns with how species adapt to specific temporal niches, becoming active during either diurnal or nocturnal periods based on when they are most efficient at crucial survival activities, like hunting and mating. During unfavorable periods, animals enter a low-energy state which could be an optimal strategy to avoid engaging in activities when conditions are less favorable.

However, the adaptive theory faces challenges, especially when considering why animals would increase their vulnerability by reducing sensitivity to their surroundings during sleep [135]. For instance, why not simply remain in a state of quiet wakefulness rather than fully "switching off"? While some species take precautions—such as chinstap penguins micro sleep [123]—the risk associated with reduced vigilance remains. Additionally, animals with a high basal metabolic rate have less sleep when logically they would stand to gain the most energy conservation from sleeping [101].

One extension of the adaptive theory posits that sleep evolved as a safeguard against niche expansion. This theory suggests that by entering a reduced-sensitivity state during unfavorable conditions, animals prevent gradual adaptation toward an alternate niche. This aligns with cases like the cavefish, which have drastically reduced sleep in the absence of niche changes in light [125], or large herbivores like elephants and giraffes that sleep very little who live in relatively stable environments and require a lot of energy [99, 98]. However, this view does not account for why animals with adaptations for both day and night still engage in sleep or why animals will sleep in the day in the absence of something to do.

Some argue that sleep may have initially evolved as an adaptation against unfavorable niches, and over time, sleep architecture evolved to take advantage of this period for restorative purposes [134, 130]. This perspective might explain why sleep persists even in the most consistent niches: as the recuperative benefits of sleep became integral, they became tightly interwoven with the sleep process, making its eradication unlikely despite environmental stability.

Sleep as a Restorative Process

The restorative theory posits that the physiological and metabolic demands of daily activity necessitate a recovery period, with sleep being the optimal state for this restoration [136]. Sleep is thought to allow for cellular repair, metabolic regulation, and the clearing of metabolic waste products, particularly in the brain [65], although these theories are contested as discussed in the Consequences of Sleep Loss section. Increased synthesis of growth and repair proteins during sleep do support this notion [136], and studies across species—from rats to flies to humans—show a link between sleep and recovery from wounds and infections [137, 138, 139]. Opposing this, a study claims a protective role in sleep deprivation in humans [140].

However, this theory is complicated by examples of animals, like migratory birds or dolphins, that can forgo sleep for extended periods without apparent detriment [102, 112]. Or by short sleeping animals such as the chin strap penguin [123]. If sleep is only lasting a few seconds, can the body be shifting that rapidly into the healing processes. It is more likely many of these functions are occurring during all hours.

Sleep and Cognitive Restoration

While the robustness of the clearance and healing theory may be shaky, there is a universal agreement upon the association of sleep and cognitive processes. Sleep deprivation is known to impair cognitive functions, such as decision-making, attention, and memory [141, 142].

The synaptic homeostasis hypothesis offers one explanation, proposing that sleep allows the brain to downscale synaptic connections strengthened during wakefulness, refining and pruning those connections that are less critical [143, 33, 144, 145]. Studies have shown that dendritic connections are more numerous from wake to sleep [146, 147], and in flies protein levels of pre- and postsynaptic components are higher during wake declining in sleep [148]. This synaptic downscaling improves signal-to-noise ratios, helping with memory consolidation. As a caveat to the restorative theory, this pause in neuronal activity may also be a time when the neuron can rest and recover, preplacing damaged proteins and lipids [149], or repaired neuronal DNA

[150].

The active system consolidation model builds on this, suggesting that specific patterns of neural activity during sleep, particularly SWA in NREM sleep, are crucial for transferring memories from short-term to long-term storage [151, 144, 152]. Region-specific consolidation has been observed, where brain areas involved in tasks during wakefulness show elevated activity during sleep [153, 71].

However, this theory does not explain the lack of correlation between sleep duration and cognitive complexity across species. For example, elephants, which have sophisticated social systems, sleep far less than other complex animals like primates [154, 84, 86]. The tripartite model proposed by Dr. Giorgio Gilestro seeks to address the failures of both theories by combining them. The model suggests that time asleep can be placed in three broad categories: vital; which is immutable with a core function that is necessary for a healthy life, useful; which help an animal thrive but can be lost without too much short term recompense, and accessory; which can scale to as short and long as evolution requires. The first two parts of the model would encompass the restorative / memory and learning theories of sleep, both conserved functions of sleep and species-specific. The last part, accessory, would fulfill the adaptive theory and possibly be the largest amount of time proportionally. Here, sleep time will increase to counter selectivity against a favoured niche when other drivers, such as eating and mating, are sated or impossible. With the tripartite model we can begin to unify all animal sleep under a single theory that allows for variation in sleep metrics from species to species.

The Evolutionary Balancing Act

The ubiquity of sleep, contrasted with the wide variation in its duration and structure, complicates the alignment of any single theory. This is especially true when considering that restful, quiet wakefulness might seem a safer alternative for recuperation. To examine this idea, Lima and Rattenborg modeled the brain as a network of neural units, where the number of active units is proportional to the likelihood of detecting danger, while inactive units undergo maintenance [155]. Interestingly, the model found that the optimal strategy was for all units to

go offline simultaneously rather than partially. If the model's core assumption holds—that maintenance (restoration) is indispensable—this could explain why sleep evolved as a universal state instead of simple resting.

There may not be a singular primary function of sleep; rather, the functions and theories proposed could hold varying significance across different species, influenced by their ecological histories [101]. The relative importance of a specific function within a species' niche may dictate the total amount of sleep and the subsequent architecture of their sleep states.

1.2.7 Evolution and diversity of Sleep States

The restorative effects of sleep in mammals seem to have been compartmentalised into distinct functions attributed to NREM and REM sleep. As mentioned earlier, SWA during late-stage NREM sleep is implicated in cortical memory consolidation (Stickgold 2013), while REM sleep is involved in other types of learning, such as pruning and sensorimotor skills [25]. The ratio of NREM to REM varies significantly across mammals [119] and changes over developmental stages, with REM sleep peaking in infancy in humans [156]. Historically, distinct sleep states were considered unique to mammals and later to birds [114]. However, increasing interest in the evolution of sleep states has revealed evidence of two-stage sleep in a wide range of species, from reptiles and fish to arthropods and cephalopods (Fig. 1.5). This section will explore these similarities and differences as we move away from mammals on the phylogenetic tree. A more comprehensive review of this topic can be found in *Rattenborg & Ungurean, 2023* [14], *Yamazaki et al., 2020*[25], and *Joiner, 2016* [88], *Lesku et al., 2006, 2009* [101, 87].

NREM and REM sleep signals have been detected in birds [114, 157, 158], despite fundamental differences in cytoarchitecture [159]. In pigeons (*Columba livia*), 1-5 Hz SWA activity occurs in the hyperpallium, transitioning into wake-like brain activity or REM sleep, which can be predicted by pupillary constriction and reduced muscle tone [160, 161, 162]. Similar to mammals, birds will prioritises SWA sleep during rebound [157] and their REM sleep reverses the cooling of the brain that occurs during NREM sleep [161]. Wehr theorised that this warming function might be the primary purpose of REM sleep [163], enhancing performance upon

waking or increasing vigilance. However, this theory is contested, as REM sleep decreases in animals at higher risk of predation [135, 164, 165], suggesting that the warming might be a costly side effect of REM activity rather than its primary function [161]. Avian sleep is not entirely identical to mammalian sleep—REM sleep in birds is very brief (less than 10 seconds), more frequent [165], and lacks the repeated cycles typical of mammals [166].

The similarities between avian and mammalian sleep raise questions about whether their sleep states evolved independently or share a common ancestor. Since birds belong to the clade Dinosauria, sharing a more recent common ancestor with reptiles than with mammals [167], we would expect similar sleep states in reptiles if there were a shared chordate sleep ancestor.

Studying sleep in reptiles is challenging due to their cortical EEG, which complicates unambiguous identification of sleep states [168]. Additionally, as ectotherms, reptiles engage in quiescence or basking which has similar behavioural indicators [25]. Nevertheless, reptiles exhibit sleep-specific postures, and advancements in electrophysiological recordings have provided new evidence of distinct sleep states [168, 169]. The central bearded dragon (*Pogona vitticeps*) exhibits low-frequency (0.5-4 Hz) sleep characterised by numerous negative high-amplitude sharp waves [169]. Similar sharp waves, though not identical, are seen in the Argentine Tegu (*Salvator merianae*) [170] and in two crocodile species [171, 172]. The homology to NREM sleep is supported by how the waves propagate across the brain and can be used as markers of homeostatic sleep pressure [168, 173], though evidence supporting functional similarity is currently limited.

A second sleep state has been identified in both the Argentine tegu [170] and bearded dragons [169], characterised by beta waves of 10-40 Hz that are distinct from wake states and accompanied by eye movements. This sleep state can be reduced using the REM-suppressing drug fluoxetine [170]. Commonalities in neuropeptides involved in sleep regulation, such as orexin [174] and melanin producing neurons [175], also point to a shared mechanism between reptiles and mammals. Although the exact mechanisms driving sleep state transitions in reptiles remain unclear [25]. The presence of these states supports the idea that the clade *Amniota*, which includes mammals, birds, and reptiles [176], shares a common sleep state ancestor.

The evidence for sleep states in amphibians and fish is less definitive [14]. Research on amphibian sleep is sparse, with a study of tree frogs (*Hyla*) noting changes in brain activity during sleep-like behaviours, but failing to identify distinct sleep stages [177].

However, more recent studies in zebrafish (*Danio rerio*), have identified two sleep states resembling NREM and REM [178]. Analysis of brain activity, eye movement, and muscle activity revealed distinct sleep stages, with the REM-analogous state characterized by trunk muscle contractions absent during NREM sleep. These contractions propagate from the base to the cortex, similar to the onset of REM sleep in mammals. Interestingly, zebrafish exhibit suppressed brain activity for 20 minutes after REM-like sleep, a phenomenon not observed in mammals or birds. *Leung et al.'s* findings provide a potential foundation for the theory that NREM/REM sleep stages are a conserved feature of chordate animals.

Beyond the chordate phylum, direct comparisons to NREM and REM sleep become more challenging, although evidence of two-state sleep exists across various model organisms, including many insects [14].

In forager honeybees' (*Apis mellifera*) spontaneous activity in the optic lobes decreases during periods of rest [179]. The bees exhibit a relaxed thorax, head, and antennae during sleep. By analysing correlations between arousal thresholds and behavioural posture changes, researchers identified three distinct sleep states and sleep rebound [180, 181, 182]. This relaxed posture has been observed in multiple insect species including flour moths [183], cockroaches [184], as well as fruit flies [185]. However, electrophysiological evidence is limited to only honeybees and fruit flies, with both having evidence for regulation of sleep originating in the mushroom bodies, with rhythmic activity correlated with higher arousal thresholds [186, 187].

Drosophila, like honeybees, have evidence of two-phase sleep based on further electrophysiology studies [188, 189, 190] and arousal thresholds experiments [35, 189]. As the focus of this study, the evidence and background for multi-staged sleep in *Drosophila* is discussed in more detail in the introduction section of *Chapter 4*.

Other arthropods, like spiders and crayfish, also provide additional insights. *Rößler et al.* de-

scribed a potential nocturnal sleep posture in jumping spiders (*Evarcha arcuata*), characterised by leg twitching and curling, which they suggest is analogous to REM sleep [191, 192]. However, this claim lacks support from arousal threshold or electrophysiological data. Crayfish (*Procambarus clarkii*), on the other hand, show reduced brain activity during sleep accompanied by increased arousal thresholds [193, 194]. Bursts of high-frequency activity in crayfish could be indicative of a REM-like state, although this requires further investigation [193].

Sleep has also been observed in several mollusks, including the great pond snail (*Lymnaea stagnalis*) [195], California sea hare (*Aplysia californica*) (Vorster 2014), common European cuttlefish (*Sepia officinalis*) [196, 197], and octopuses (*Octopus insularis*) [198]. Although electrophysiological evidence for different sleep states is currently lacking in these mollusks, both cuttlefish and octopuses display dynamic active sleep phases featuring eye movements, twitching, and, most notably, skin pattern changes and darkening [197, 198]. These skin texture changes occur after a period of sleep-like activity and have no correlation with environmental dangers, suggesting that, like REM twitches in mammals, they might be unintended byproducts of brain restoration functions.

In summary, the presence of multiphasic sleep outside the chordate phylum suggests that sleep states are evolutionarily conserved across diverse taxa. Comparative studies seeking similarities often encounter challenges due to differing classifications, particularly as sleep in non-chordates deviates from the REM and NREM EEG distinctions. However, given the substantial differences in brain structure and physiology across species, it is improbable that the descriptive characteristics of sleep will be identical. Even within mammals, EEG data reflecting sleep states can vary significantly [13]. It is important to recognise that the EEG signals associated with sleep are mere correlates and are unlikely to be evolutionarily conserved. Thus, it may be more appropriate to shift from classifying sleep based on electrophysiological criteria to an approach centered on understanding the sleep patterns and behaviours exhibited by different animals.

To further dissect the functions of these sleep states, we must examine their behavioural contexts—how they change under different conditions and how restriction impacts an animal's

fitness. To contribute to this understanding, this study will expand how sleep in the model organism *Drosophila melanogaster* is analysed, integrating free-living quantification of multiphasic sleep in flies while retaining high-throughput experimental approaches. The next section will introduce how behaviour can be used as a tool to understand the brain, and its applications with *Drosophila* to understand cognition and sleep.

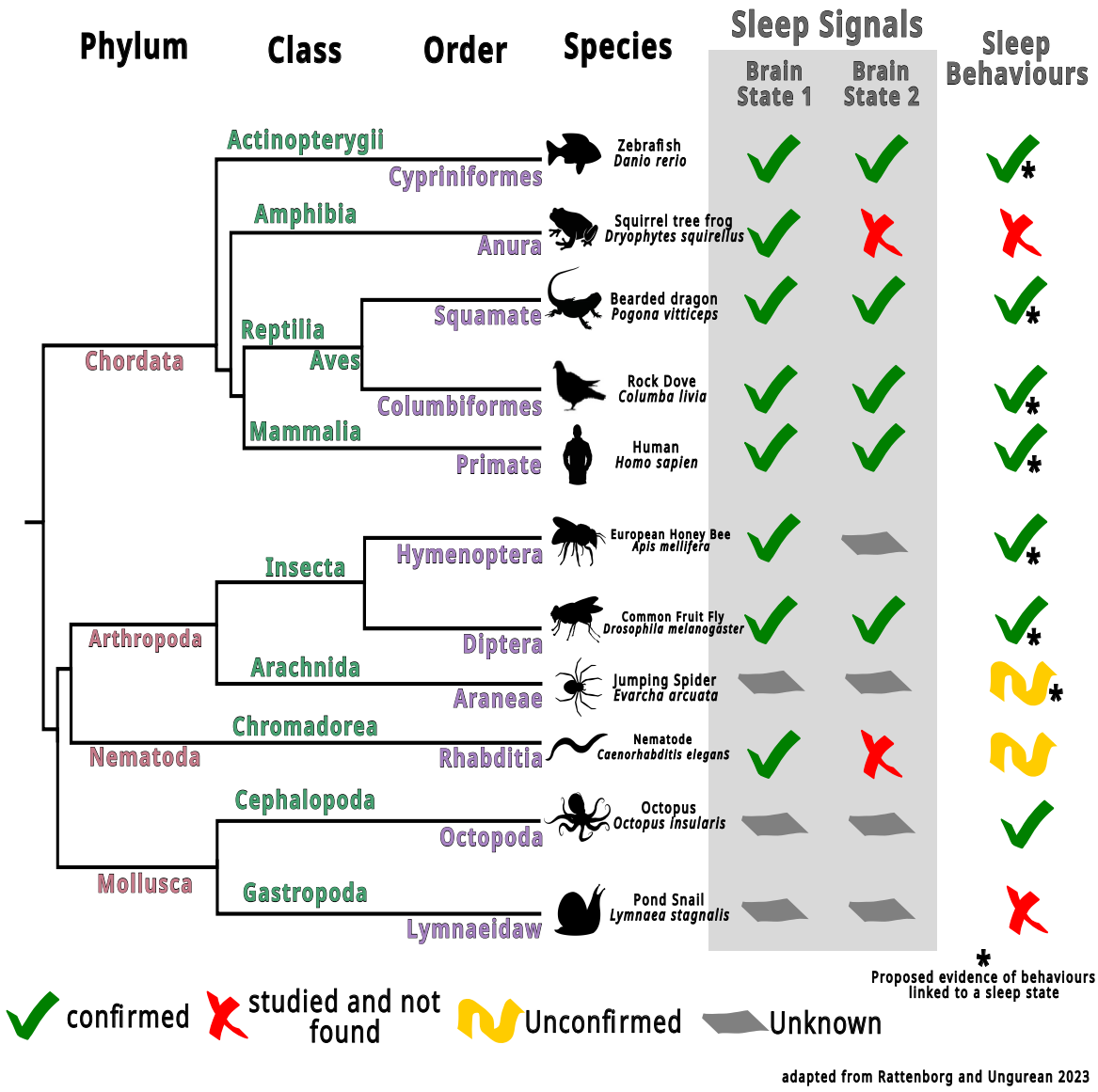


Figure 1.5: **Phylogenetic tree showing the distribution of sleep states across the animal kingdom.**
Sleep signals were classed as present if confirmed by brain activity monitoring. Where studied and not found the author of the study has declared the sleep signatures are not present. Sleep behaviours include twitches of the appendages, rapid eye movement, antennal dropping, changes in skin colour, ect. For well studied taxonomic groups, such as mammals and birds, a representative species was chosen. Adapted from *Rattenborg & Ungurean 2023.* [14]

1.3 Behaviour and Neuroscience

1.3.1 Context

Drosophila have a rich repertoire of behaviours that they use to navigate their natural environment that include, but not limited to flying, walking, mating, fighting, and feeding. Whilst not the most socially complex compared to mammalian models or bees [199], these behaviours are core mechanisms for many organisms in the world and can be explored to understand how the brain and its circuitry control them [1].

1.3.2 Defining Behaviour

The definition of behaviour is a point of contention and varies by field [200, 201]. Debates often arise around passive versus active interactions, cognitive extensions, and even comparisons to computer programmes. For the purpose of this work, I will adhere to the definition of behaviour as "an internally coordinated response of the whole organism to internal or external stimuli" [200]. Behaviours can range from higher-order behaviours, such as courtship or feeding, which may last for extended periods and repeat throughout the organism's life, to sub-behaviours like wing vibrations in courtship or leg movements during walking. Depending on the level of resolution, these behavioural sequences may represent entire motifs of higher-order actions or smaller-scale motifs. Regardless, they will be treated equivalently in context.

1.3.3 Behaviour to understand Neurobiology

Using the above definition of behaviour, we can begin to appreciate its importance in understanding neurobiology. Behaviour is the culmination of neural processing, translating and combining incoming information with the internal state into observable actions. Despite advances in techniques to measure brain activity down to single neurons, we are still not much closer to understanding how the brain generates behaviour [3, 202, 203]. A key reason for this

is the brain's inherent degeneracy, the ability for the same behaviour to arise from different neural configurations [204] or for the same circuit to produce various behaviours [205, 206]. Application of neuroscientific ananlysis to microprocessors, such as generating a connectome or lesion studies of causal effect, revealed they lacked any ability to describe the hierarchy of information processing [207]. It therefore stands that observation alone, with no known ground truth, may be severely limited.

Brain activity data is most informative when combined with well understood or simple behaviours. One example is flight; work by the Maimon lab has shown how neurons in the central complex calculate heading and goal angles in *Drosophila* flight, where protocerebral bridge and fan-shaped body neurons perform vector arithmetic to steer the fly [208, 209, 210]. These series of papers demonstrate the power of utilising stereotyped behaviour to understand computation. Rather than only identify the circuitry that activates during the behaviour, they sought to understand how it processed sensory input, how they organised behaviour.

Nevertheless, understanding brain function via behavioural observation alone remains powerful. *Maimon et al.'s* experiments are effective for studying reactive behaviours such as flight. However, for these to work, the fly must be restrained, with a screen simulating flight direction [211]. In doing so, they manipulate the fly's entire *umwelt*, its unique sensory world capable of influencing behaviour [212]. Yet, this approach compromises naturalistic behaviours and their sequential patterns (Miller 2022). Some of the most significant breakthroughs in understanding brain computations have come from free-living observational studies [3].

For example, Packard and McGaugh devised a T-maze for rats, allowing them to learn which arm contained food (the right). After several days of learning, they reversed the maze [213]. Initially, the rats continued to turn right but eventually adjusted to turn left, illustrating a shift in decision-making strategies from egocentric to allocentric. This experiment laid the foundation for computational models that explore how animals process and learn from various types of information, as well as how they transition between strategies [214].

Every run of the trial the rat was presented with the same *umwelt*, but its behavioural outcome changed with time. What changed was its internal model of the world and how this processed

the incoming information.

1.3.4 Behavioural States

The brain is in constant flux, and its hidden dynamics can often be captured through the concept of internal states [215, 216]. Internal states act as a context within which the brain processes stimuli, modulating the relationship between stimulus and behaviour [217, 218].

Internal states can be applied to all situations where the outcome is not a singular output. *Drosophila* have varying valence to odours at different times or states, attracted to strong CO_2 odours when in a state of flying and foraging [219, 220], and preferentially waking to food based odours when asleep [221]. The act of walking or flying will also change the receptive gain of neurons in the visual system, becoming more responsive and able to process higher image speeds [211, 222]. Internal states, however, are not always overt; they may be inferred from transitions between behavioural motifs, where an animal's response is shaped by its previous actions.

Calhoun et al. utilised unsupervised learning to identify internal states that could model the changing behaviours during male courtship [223]. Their model uncovered three latent states, which were able to predict moment-to-moment variations in song-patterning decisions. Further investigation revealed two neurons that acted as state-switchers, governing transitions between these internal states.

Sleep states, such as light sleep, deep sleep, REM, and NREM, are typically not classified as internal states due to their specific and identifiable nature. However, they share similarities with internal states in that they involve fluid transitions of states that alter the brain's processing of external stimuli, which are often reflected in the animal's behavioural patterns. Building on these similarities, this study aims to characterise internal states to predict sleep states through two approaches: (1) by employing analytical methods similar to *Calhoun et al.*, uncovering latent internal states that predict sleep states based on sequential behaviour, and (2) by identifying specific behavioural poses that may serve as hallmarks of distinct sleep states.

1.4 *Drosophila*: Background and behaviour

1.4.1 Context

Drosophila melanogaster has been a cornerstone of biological research since the pioneering work of William Castle in 1901 [224] and his student Thomas Hunt Morgan, who first identified sex-linked genetic inheritance [225]. *D. melanogaster* has been instrumental in advancing our understanding of genetics, neurocircuitry, and behaviour. Many developmental genes initially characterised in *D. melanogaster* have since been shown to be critical for all animal development, including humans [226]. Whole genome sequencing of *D. melanogaster* in 2007, revealed that approximately 60% of its genes are shared with mammals [227]. Although the final architecture of a fly and human differ greatly at a cursory glance, our understanding of both creatures genetics, building blocks, and engineering processes show they bear striking resemblance, evidence of a conservation throughout evolution.

Ecology and life cycle

D. melanogaster are small flies, typically 2-3 mm in length, with females being slightly larger than males [228]. Commonly referred to as "fruit flies" or "vinegar flies," they are attracted to fermented foods, such as rotting fruit, where they feed and lay eggs. As generalist feeders and cosmopolitans, *D. melanogaster* thrive in a variety of environments, including urban settings [229]. Originally native to sub-Saharan Africa, they have spread across the globe over the last 10,000 to 15,000 years [230, 231].

Like other dipterans, *Drosophila* undergo complete metamorphosis, passing through four distinct life stages. A female fly can lay up to 100 eggs per day, with the egg stage lasting about one day [226, 232]. The larvae hatch and go through three instar stages over a five-day period (at 25°C), during which they feed and grow [233]. After reaching maturity, the larvae pupate and undergo metamorphosis over four days, culminating in the sexually active adult fly. The entire developmental process is controlled by pulses of the steroid hormone 20-hydroxyecdysone [234].

While the larval stage focuses on growth and development in nutrient-rich environments, the primary drive of the adult fly is reproduction. In laboratory conditions, the adult *Drosophila* can live for up to 90 days, although this lifespan is shorter in the wild [235].

This rapid development, combined with the ease and low cost of maintaining *Drosophila* colonies, has made it an invaluable model organism in biological research.

1.4.2 *Drosophila* Behaviours and their paradigms

Activity

One of the earliest behaviours measured in *Drosophila* was general activity, initially scored manually and later automated using infrared (IR) beams. Each time a fly crossed an IR) beam, the movement was recorded, eventually leading to the development of the *Drosophila* Activity Monitoring (DAM) system [236]. DAM has been foundational in many significant studies on circadian rhythms and sleep, which will be discussed further later [237].

With the advent of computational vision, more refined tools for measuring activity and capturing detailed movements have emerged. Over the past 20 years, numerous machine vision hardware and software packages have been developed to automatically quantify activity [238, 239, 240, 241, 242, 35, 243]. These tools typically employ variations of background subtraction to identify the fly's centre of mass or utilise machine learning to recognise the fly's outline.

In this study, most of the work will be conducted using the ethoscope, a hardware/software combination developed by the Gilestro group (Fig. 1.6.a) [244]. The ethoscope is a self-contained behavioural tracker capable of housing up to 20 individual flies. Ground-truth experiments have shown that its velocity resolution is sensitive enough to differentiate three behavioural states: inactivity, micro-movements, and walking (*see Methods*). Furthermore, accessory modules have been developed to investigate sleep deprivation and arousal, which will also be employed in this study (Fig. 1.6.b&c).

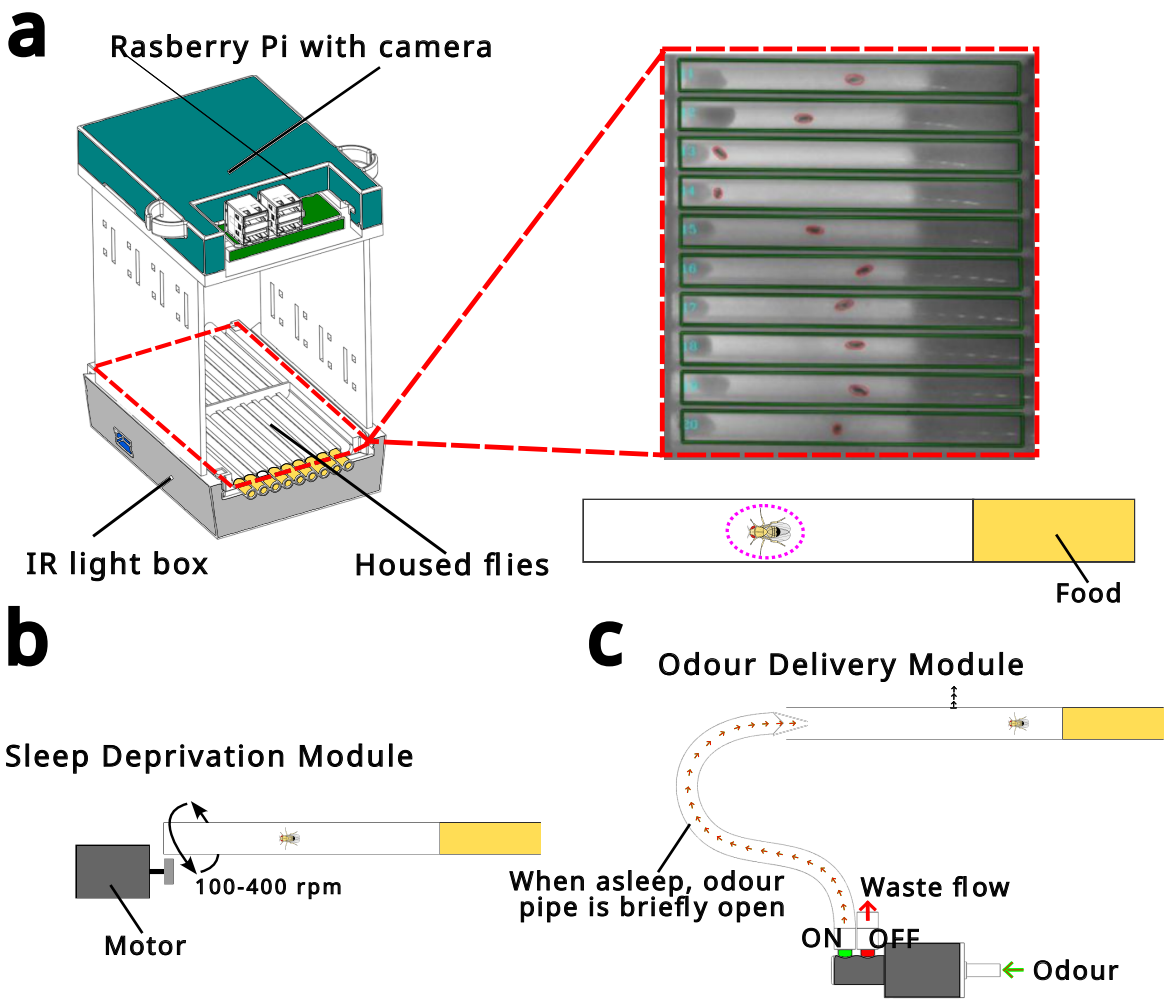


Figure 1.6: **The ethoscope: an automated video behavioural tracking system and its modules**.
(a) The ethoscope is a Raspberry Pi powered automated fly tracker that can track in real-time the movement behaviours of up to 20 flies. Flies are housed in individual tubes and illuminated by IR light. **(b)** A schematic of the SD attachment module. Taking real-time input from the ethoscope, the motors will spin the tube housing the fly when it is immobile for a user given time. **(c)** A schematic of the odour delivery attachment module. Like the SD module the valve is triggered in real time in response to an immobility criteria. Odours can be mixed with air to deliver a puff that may awaken the fly. See the *Methods* for more details or these publications for the ethoscope [244], SD module [53], and odour module [221]

Activity tracking has advanced to the point where multiple flies or animals can be monitored in group-housed settings to explore social interactions and hierarchy [240, 245, 246]. Some systems can even reconstruct the flies' trajectories in 3D space [247] or create 3D reconstructions of their limbs as they move through time [248, 249]. However, these more detailed setups are often unique to specific laboratories. Over the past six years, user-friendly KeyPoint trackers such as DeepLabCut [250], (S)LEAP [251, 252], and DeepPoseKit [253] have become more popular.

These tools provide packaged software that allows researchers without computational expertise to rapidly quantify fine behaviours such as limb movements.

Social Behaviours

Before automated tracking, social behaviours in *Drosophila* were manually scored. The two primary social interactions are courtship and mating, and fighting.

Male flies initiate courtship with females by performing an elaborate ritual that involves stereotyped movements and wing vibrations [240]. If successful, copulation follows. Courtship behaviour has been widely used to study memory and learning [254, 255], behavioural transitions [256, 223], and the underlying neuronal circuitry [257, 258]. Male flies also engage in aggressive interactions with other males to establish dominance, which influences access to food, shelter, and mates [259]. Larger males are more likely to initiate and win fights, leading to higher reproductive success [260]. Aggression assays have been pivotal in identifying genetic factors that influence aggression, such as the role of octopamine in reducing aggressive behaviour when silenced [261, 240].

Feeding

Drosophila feed by extending their proboscis into food, exhibiting a proboscis extension reflex in response to attractive stimuli [262]. This reflex has been key in studying the neural circuits controlling feeding [262, 263]. Rapid proboscis extensions have also been observed during sleep bouts, though their function remains unclear [264]. Automated tracking of feeding [265, 266] has shown that neural circuits regulate food intake by modulating the likelihood and duration of feeding bouts [267, 220, 265]. Differing responses to food under varying conditions has been utilised to gain insight into internal states. Researchers have identified the neuronal circuitry responsible for directing food choices based on factors such as satiety, mating status, and food composition [268].

Grooming

Drosophila groom themselves frequently, and can often be observed cleaning various parts of their body while stationary. Grooming behaviour can be broken down into discrete cleaning movements [269], which vary depending on the stimulus and cleanliness of the fly [270]. When fully covered in dust, flies engage in a full cleaning sequence [271]. *Seeds et al.* utilised this behaviour to develop a hierarchical model of motor movements, demonstrating how each motor process suppresses or promotes the next in sequence. This is an excellent example of how observable behaviours can be used to infer computational hierarchies in the brain. This hierarchical control is surprisingly well conserved with no variation between sub-populations [202].

1.5 Sleep In *Drosophila*

Sleep is widely studied in *Drosophila* following seminal papers by *Hendricks et al.* and *Shaw et al.*, which established it as a model organism for sleep research. Much of what we know about circadian and homeostatic sleep control has been uncovered in *Drosophila*, shedding light on the neural circuits, neuromodulators, and environmental factors that influence sleep [272, 273].

1.5.1 Methods to Study Sleep and their findings

Activity monitoring

Hendricks et al. and *Shaw et al.* first identified long periods of immobility in fruit flies, postulated as sleep, IR and ultrasound systems. They demonstrated that these bouts of inactivity were governed by circadian and homeostatic factors, along with increased arousal thresholds and rebound from sleep deprivation [274, 275]. Impressively, ultrasound recordings were matched to IR activity with only a 2.35% false negative for capturing motion.

The packaged hardware IR system, DAM, is the main device used in fruit fly circadian and

sleep studies due to its ease of use and historical prevalence [236]. DAM can log the movements of up to 32 animals over long durations. Early models relied on just one IR beam with the norm now four, although this has now increased to up to 17 in some cases. However, advances in tracking have revealed that the beam cross systems were severely underestimating sleep due to missed micro-movements or small bouts of walking [239, 244]. Newer tools like the ethoscope have refined sleep measurements, showing variability across sex, age, mutants, and time of day.

Arousal

Early studies by Shaw and Hendricks found that flies inactive for five minutes or more were less likely to respond to mechanical disturbances [275, 274, 190]. This led to the widespread adoption of the "five-minute rule" in sleep studies, which was later corroborated [71]. However, this rule is not without limitations. Studies have shown that arousal likelihood decreases gradually over time rather than being a binary response at the five-minute mark. The rate at which flies fall asleep and their arousal thresholds can also vary in mutants and short-sleep populations [35, 189, 264, 185]. Despite its limitations, the simplicity and scalability of the five-minute rule have kept it in use.

Arousal is also used to assess how flies process sensory stimuli during sleep. Responses to mechanical stimuli depend on both the intensity of the stimulus and the fly's internal state [122]. For example, food odours or aversive smells are more likely to wake a fly than neutral ones, with starved flies being especially responsive to food-based odours [221]. An extension of food choice internal state modulation observed in *Munch et al.* [268].

Sleep deprivation

Sleep deprivation (SD) refers to any reduction in sleep below an animal's baseline level and can be categorized into perturbation or suppression methods. SD studies mainly explore the homeostatic response and the consequences of sleep loss.

Perturbation

Sleep perturbation incorporates any method that induces sleep loss through unnatural means, such as through mechanical, chemical, and genetic means.

Mechanical

Mechanical stimulation is often used due to its simplicity and effectiveness. Traditionally, non-targeted systems, such as random shaking of the platform [276, 51], rotating and dropping tubes [275, 274, 277], or vibration [278, 35] have been employed. However, these methods face criticism for potential habituation or damage at higher speeds [244]. Targeted systems, such as the ethoscope, apply stimuli only when individual flies stop moving. These methods have shown that some observed consequences of sleep loss, like increased ROS accumulation [279] or death [53], may stem from mechanical stress rather than sleep deprivation itself.

Despite these concerns, mechanical SD studies have demonstrated that flies exhibit a homeostatic response, sleeping more deeply and for longer durations after the perturbation ends [35].

Chemically

SD can also be achieved through pharmacological activation of wake-promoting circuits. Drugs like caffeine [280, 281] and methamphetamine are used to induce wakefulness, increasing movement and reducing sleep during both day and night. Caffeine, for example, affects dopamine signaling by targeting a cluster of dopaminergic neurons [280]. This results in a rebound effect similar to that seen with mechanical SD [282, 283, 284].

However, as with untargeted mechanical SD, the analysis of drug-induced sleep loss is complicated by the broad and varied effects of these drugs.

Genetic Activation

Wake-promoting circuits, such as dopaminergic neurons, can be activated using thermo- and opto-genetic mutants [285, 51, 274]. This allows for highly targeted SD. Conversely, activating inhibitory circuits, such as GABAergic neurons [43], can induce a deeper sleep.

However, the degeneracy of neural circuits and potential off-target effects means that genetic activation studies must be interpreted carefully to distinguish if the effects are due to SD or from perturbing the whole system.

Suppression

Suppressive SD aims to prevent sleep through natural methods, with the goal of revealing behavioural changes rooted in sleep's evolutionary context.

Social

Social SD can be induced in two ways: (1) male-male interaction and (2) male-female interaction. Introducing a male intruder reduces total sleep but does not eliminate it [148, 122]. This sleep loss typically results in a rebound once the intruder is removed. In contrast, sleep rebound is not observed in male-female interactions or when a sleep-deprived male is introduced to a new female partner [122].

Starvation

Starved flies prioritise foraging over sleep, overriding both homeostatic and circadian drivers [286, 287]. Sleep rebound is likely absent in starved flies [288, 281], although one unpublished study suggests otherwise [286]. *Brown et al.* observed that, while total sleep remains unchanged, starved flies show more consolidated sleep and longer bouts the following day, potentially indicating a rebound effect [281].

Temperature and Light

High light intensity or temperatures reduce total sleep in flies [289]. However, since both are strong zeitgebers of circadian rhythms, they are infrequently used in SD studies [272].

Brain activity

While insects lack the complex brain structures found in mammals, birds, and reptiles that produce EEG signatures of sleep [14], they possess a neuro-electrical cortex whose activity can be measured. In quiescent flies, localised brain activity is reduced compared to wakefulness [190, 290]. Emerging evidence also suggests the presence of sub-sleep states based on brain activity [189, 278]. These aspects will be explored further in *Chapter 4*.

1.5.2 Mechanisms of Sleep

The mechanisms underlying sleep in *Drosophila melanogaster* exhibit striking similarities to those in mammals. This section explores the specific drivers and regulators of sleep in fruit flies.

Circadian

D. melanogaster, like many animals, have daily rhythms that occur approximately every 24 hours. In the lab this is typically entrained to a 12:12 hour light:dark rhythm that is characterised by increased activity around the light transitions (Fig. 1.7). In the absence of light, their activity patterns persist but may drift over time. *D. melanogaster* sleeps during the day and night, with the most consolidated sleep occurring between ZT12-15 [291] (Fig.1.7.b).

The molecular basis of the circadian rhythm was largely elucidated through studies in fruit flies. Key genes involved in the circadian clock include *period* [292], *timeless* [293], *Clock* [294], and *cycle* [295]. The circadian clock operates via a transcriptional feedback loop that aligns with the animal's circadian rhythm.

PERIOD and TIMELESS proteins accumulate during the day and inhibit their own mRNA production, creating an autoregulatory loop. TIMELESS facilitates the delayed entry of these proteins into the nucleus, where they interact with CLOCK and CYCLE to regulate their

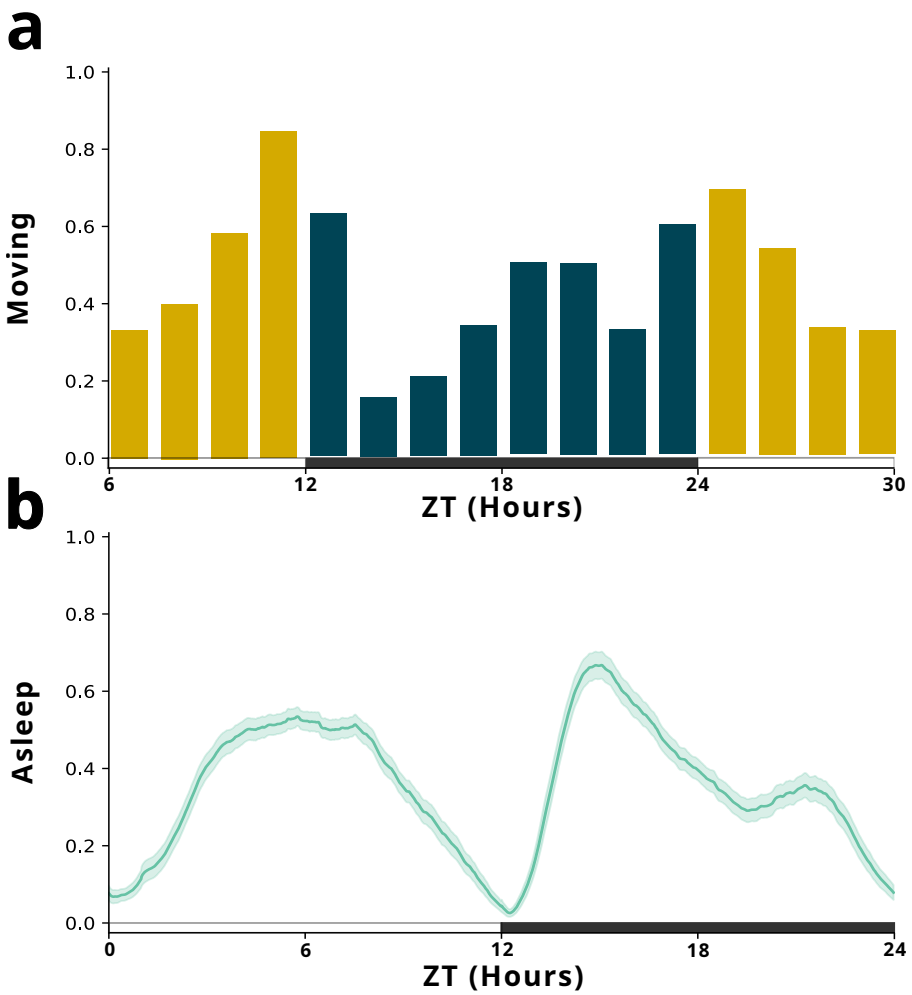


Figure 1.7: **Circadian activity peaks and daily sleep in *Drosophila*.**
(a) Representation of *D. melanogaster* daily activity in 1.5-hour bins with the evening and morning anticipatory peaks. **(b)** Sleep profile of a male *D.melanogaster* over a 24 hour day with 12:12 light:dark conditions. Flies preferentially sleep during the midday siesta and during the early night, ZT13-16. *D.melanogaster* are diurnal animals that preferentially sleep more during the night than the day.

own mRNA levels [296, 297, 298]. This delayed interaction is crucial for maintaining the approximately 24-hour cycle [291].

In the fly brain, approximately 150 neurons house the core molecular clock, analogous to the mammalian suprachiasmatic nuclei . These neurons are divided into dorsal and lateral groups, each with sub-groups, and their core molecular clocks remain synchronised [299, 300].

Homeostatic

Homeostatic control of sleep in Drosophila melanogaster is well established, but as demonstrated in SD experiments, compensatory mechanisms are context-dependent and likely involve different circuitry [122]. Chronic activation of three wake-promoting neurotransmitter systems only induced sleep rebound in the cholinergic neurons, suggesting that sleep loss and sleep drive are not inherently linked and require specific pathways for sleep rebound [285]. The evolutionary rationale for this context-dependent recovery remains unclear, with no current explanation for the variability in functional responses to sleep deprivation.

While the two-process model of sleep regulation is often studied independently, integrated models using *Drosophila* sleep data reveal a strong coupling between these processes [301]. Modelling both processes together allows for a more comprehensive understanding of how changes in one process affect the overall sleep pattern. For example, the model remained unaffected by sleep loss of less than 30 minutes, indicating that longer sleep bouts drive the patterning and rigidity of sleep, which may be linked to different sleep states.

1.5.3 Determinants of Sleep

Sleep in *D. melanogaster*, like in mammals, is influenced by a complex interplay between genetics and environmental factors. Key determinants include:

Age

In *Drosophila*, sleep patterns change throughout the lifespan. Young flies exhibit greater sleep depth and total sleep, which diminishes with age, leading to more fragmented sleep bouts [302, 303]. Juvenile sleep occurs primarily in the first 3 days before transitioning to adult sleep patterns, coinciding with sexual maturation. Early differences in sleep patterns are though to be linked to developmental and learning processes [303, 80].

Sex

Virgin males and females show similar sleep amounts and structures [304]. However, mated females shift their behaviours to optimise egg laying, such as dietary changes and increased exploration, resulting in a significant decrease in sleep driven by the male sex peptide, without a corresponding loss in fitness [305, 306, 124]. Mated females may also experience shortened lifespans [307].

Diet

Food availability and composition impact sleep. Starvation reduces sleep without recovery [281, 288]. High-protein diets promote deeper sleep post-feeding, a phenomenon observed across various species [308, 309]. Conversely, increased dietary yeast and sucrose decrease sleep in males [310].

Genetics

D.melanogaster has a high variance in sleep total amongst the wild type population [53]. This is likely internally driven by uncontrolled genetic variation and stochastic development. Selective breeding for short- and long-sleeping lines can result in a 10 hour difference in average sleep without affecting fitness or lifespan [311].

Mutagenesis screens have identified several mutants with abnormal sleep patterns, including, but not exclusively, the following. Shaker: A point mutation in a potassium channel gene results in only 3-4 hours of sleep and no rebound after sleep deprivation [312]. While it has no fitness loss, it does have a shortened lifespan. Sleepless: This mutant lacks the SLEEPLESS protein, leading to an 80% reduction in sleep and a shortened lifespan, but it does show rebound after sleep deprivation [302]. Fumin: Hyperactive due to lesions in the dopamine transporter gene, this mutant shows reduced sleep rebound [313].

These mutants highlight the variability and complexity of sleep regulation in *Drosophila*, reflecting the intricate balance between wake-promoting and sleep-promoting mechanisms.

1.6 Summary and Aims of this Work

The current literature on sleep presents a complex and often contradictory picture, with some sources emphasising its critical importance while others downplay it, depending on their perspective.

To gain a comprehensive understanding of sleep, it is essential to examine it across a range of animal species. From the elephant, which sleeps only two hours a day [99], to small insects that sleep intermittently throughout the day [314], it is evident that sleep is a widespread phenomenon with evolutionary significance. However, its precise nature remains elusive across the animal kingdom.

Emerging evidence suggests that multiphasic sleep, previously thought to be exclusive to mammals and birds, is likely present across many animal species. Investigating these phases could provide insights into the fundamental functions of sleep, if such phases indeed exist.

D. melanogaster has become a key model organism in sleep research. However, findings from *D. melanogaster* studies have sometimes struggled to translate to human sleep due to a lack of detailed understanding of the internal sleep architecture. Recent literature suggests that there are substructures in fly sleep that may be analogous to mammalian sleep [189, 278, 301].

Obtaining sleep data from fruit flies is an invasive and time-consuming process, as it often requires restraining the flies and limiting their normal behaviour. Despite this, *Drosophila* remains a valuable model due to its ease of use and high-throughput capabilities. To make the latest findings from fruit fly research more accessible and impactful, we need to address two key challenges: first, developing methods to approximate different sleep stages similar to the 5-minute rule to facilitate broader adoption; and second, creating self-contained analysis systems to assist users in generating meaningful and impactful results.

This study aims to address both of these challenges.

1.6.1 Aims and Objectives

- Generate a software framework to aid and expand the analytical toolbox that *Drosophila* sleep researchers can use
- Find behavioural correlates of sleep using non-invasive, free living methods
- Further investigate if multiphasic sleep can be inferred from behavioural correlates

Chapter 2

Material and Methods

2.1 Animals

2.1.1 Fly Maintenance and Handling

Flies were reared in grouped housed vials on standard yeast-based media (As a percentage of H_2O: 10% brewer's yeast – Whole Foods Market, 8% fructose – Whole Foods Market, 2% polenta – Whole Foods Market, 0.75% - proprionic acid – Sigma Aldrich, & 0.5% of 15% nipagin in EtOH – Sigma Aldrich). All flies were kept at $25°C$ in an incubator (LMS Cooled Incubator – Model 400NP) with a 12:12 light:dark, 24 hour light cycle.

For all experiments flies were mildly anaesthetised with CO_2 before being placed in their arena. In both the ethoscope and high definition (HD) arena the space also contained food that is the same as the housed food.

2.1.2 Species Stock

The *Drosophila* species used in this study were primarily obtained from the National *Drosophila* Species Stock Center (NDSSC, Cornell University, USA) and were kindly provided to us by Lucia Prieto-Godino (Francis Crick Institute, UK). The *D. melanogaster* lab strains used were

Canton-S CS (originally from Ralf Stanewsky - Münster University, Germany). Wild-caught *D. melanogaster* strains were a gift to the Gilestro laboratory from Darren Obbard (University of Edinburgh, UK). The non-*melanogaster* fly strains included: *D. simulans*, *D. sechellia*, *D. erecta*, *D. yakuba*, *D. willistoni*, and *D. virilis*. Information regarding the wild-type flies and their original collection regions is available in *Table 2.1*.

***Drosophila* Species**	**Code**	**Source**	**Collection Region**
D.melanogaster lab strain	Canton-S	Ralf Stanewsky	Canton, USA
D.melanogaster wild strain	Wild caught #4	Darren Obbard	Edinburgh, UK
D.simulans	14021-0251.254 #60	NDSSC	Cape Town, South Africa
D.sechellia	14021-0251.254 #60	NDSSC	Cousin island, Seychelles
D.erecta	14021-0224.01 #11	NDSSC	Unknown
D.yakuba	14021-0261.01 #5	NDSSC	Liberia
D.willistoni	14030-0811.24 #1	NDSSC	Guadalupe Island, Caribbean
D.virilis	15010-1051.87 #9	NDSSC	Unknown

Table 2.1: The *Drosophila* species and their collection sites.

2.2 Ethoscope

All data used in *Chapters 3-5* was generated using the ethoscope, an automated video tracking system developed in the Gilestro Laboratory at Imperial College London [244]. The ethoscope monitors fly movement in real-time and consists of two main components: an upper compartment housing a Raspberry Pi computer and an infrared camera, and a lower compartment where experiments take place. The upper compartment's camera tracks the flies' movements, while the lower section, equipped with infrared light for dark-phase tracking, can be customised with different arenas depending on experimental requirements. These compartments are separated by laser-cut acrylic walls, approximately 10 cm high (Fig. 1.5.a).

The ethoscope system is entirely open source, with both the software and hardware running on a version of the GNU/Linux operating system. Since its inception, the system has undergone numerous iterative upgrades to improve functionality and ease of use.

It's worth noting that the historical dataset used to train the HMM from *Geissmann et al.* [53] utilised a Raspberry Pi 2 and a PiNoIR V1 camera, whereas the apple cider vinegar (ACV) and Air datasets employed the more advanced Raspberry Pi 3 B and PiNoIR V2 camera.

The ethoscope APIs were implemented using the Python programming language. Further technical details can be found in the original publication [244] or the lab website (https://lab.gilest.ro/) or on GitHub (https://github.com/gilestrolab/ethoscope - dev branch).

2.2.1 Ethoscope Data Generation

resolution of The ethoscope captures images as a resolution of up to 1,920 x 1,080 pixels, at 30 frames per second. From these images, in real-time, machine vision software generates an ellipse around multiple fruit flies housed in the machine, see ethoscope paper for more details [244]. The tracked ellipse metrics are tracked and stored at approximately 1-4 Hz. Data is later retrieved post experimentation and processed using the software ethoscopy (Python) [315]. Variables such as t, x, y, w, h, phi, and distance (mm) are generated in real time (Fig.

2.1). Additional metrics like velocity and behavioural states (immobile, micro-movements, and walking) are computed when the data is retrieved. For more details, refer to *Chapter 5* or *Table 2.2*, which provides a breakdown of each variable and its calculation method.

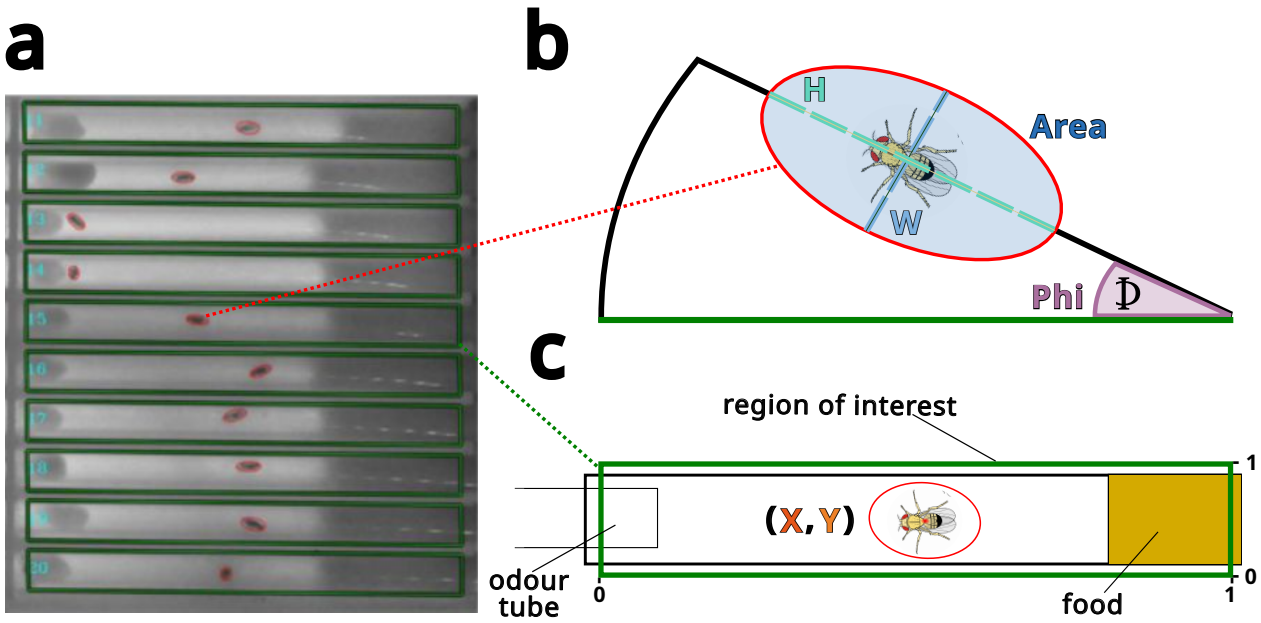


Figure 2.1: **Visual representation of the variables tracked by the ethoscope.** **(a)** A still image from the ethoscope as it tracks in real-time. The green boxes are the regions of interest (ROI) in which the fly can be tracked with boundaries of 0-1 in both the width and height per fly. **(b)** The fly is tracked via a red ellipse around the fly. Of this ellipse the width (W - blue) and height (H - teal) are recorded, as well as the angle of H to the lower ROI boundary (phi - purple). **c** A schematic of the ROI and the tube housing the fly. X (red) and Y (orange) are the coordinates of the centroid of the ellipse in relation of its space in the ROI.

2.3 Hidden Markov Model

2.3.1 Data Curation

Fly movement data used for model training was sourced from historical datasets recorded in the Gilestro lab group, specifically using CS male flies under 12:12 light-dark conditions. The data primarily consisted of baseline sleep information from *Geissmann et al., 2019* [53].

The dataset was processed with each row representing 60 seconds of recordings. Maximum velocity per 60 seconds was used to label whether the fly was immobile or moving. The dataset was

Variable	Description	Generation
t	The time in seconds post first lights on	Generated in real time to the microsecond
x	The location on the x-axis of the centroid of the ellipse that was generated around the fly	Generated in real time on a scale of 0 – 1 based on the ROI. For *Chapter 5*, per fly, outliers are removed and forward filled, and values rescaled to between 0 and 1
w	The width of the ellipse that is generated around the fly	Generated in real time as a value of the width (pixels) of the ellipse. For *Chapter 5*, per fly, outliers are removed and forward filled, and values are rescaled to between 0 and 1
h	The height of the ellipse that is generated around the fly	Same as above
phi	The angle of the center of the ellipse to the bottom (lower x-axis) of the tracked region	Generated in real-time as a value between 0 – 180 that indicates the angle of w against the lower boundary of the ROI. For *Chapter 5* values are restructured to 0-90 to reflect either horizontal or vertical position
distance	The difference (millimeters) in the coordinates of the centroid each time stamp, measured in millimeters	Generated by subtracting the sub-pixel centers of mass which are used to define the position of each animal

Table 2.2: The variables generated in real time by the ethoscope. As used in *Chapter 5*.

Variable	Description	Generation
velocity	A modified velocity value at each time point. The max velocity per time period is used to label the below behavioural movements as per *Geissmann et al.* ground truth experiments [244]	Velocity is calculated as distance / time ($mm.s^{-1}$). It is subsequently modified by a correction coefficient to maintain consistent values across varying FPS [316]. The velocity correction coefficient varies per tube / region size. Short tube (20) experiments = 0.003, and long tube (10) experiments = 0.0015. As such, velocity values are given as augmented units (a.u.)
inactive	The values of the corrected velocity that correspond to the fly being still with no micro-movements	$0 \leq$ velocity < 1
micro movements	The values of the corrected velocity that correspond to the fly performing micro-movements, e.g. grooming, egg laying	$1 \leq$ velocity < 2.5
walking	The values of the corrected velocity that correspond to the fly walking	velocity ≥ 2.5

Table 2.3: The variables generated post experiment in ethoscopy. As used to label movement and behaviours.

then trimmed to include only movement data prior to any experimental manipulations and limited to the first day. Dead flies were identified and excluded using the ***curate_dead_animals*** method in *ethoscopy*, which detects extended periods of immobility. Additionally, any flies with fewer than 3.5 days (≈5000 data points) of movement data were excluded. For model training, behavioural values were encoded as follows: in the two-state model, immobile = 0 and moving = 1; in the three-state model, immobile = 0, micro-movements = 1, and walking = 2.

2.3.2 Training

The training process utilised an *ethoscopy* method that wraps a categorical HMM object from the *hmmlearn* Python package [317]. Each model presented in Chapter 2 was divided into a 90% training set and a 10% test set. The training data were used to train a new HMM instance 100 times per model architecture. Transition probabilities not fixed at 0 (indicating impossible transitions) were randomised in each instance to avoid the model converging on a local minimum (Winters-Hilt 2006). During training, the start, transition, and emission probabilities were iteratively updated until the tolerance dropped below 5, or the model completed 100 iterations. This iterative process was conducted using the Baum-Welch variant of the Expectation-Maximisation algorithm [318] in *hmmlearn*. Once the model had converged or reached 100 iterations, the score method from *hmmlearn* was used to generate a log-likelihood probability on the test dataset. If this score surpassed the previous best model, it replaced the older model. For full transition and emission probabilities, refer to Appendices *Table A.1-2*.

2.3.3 Scoring Models

Where the architecture was labelled "Wiggin," it directly replicated the HMM architecture from *Wiggin et al.* [319]. The architecture referred to as "Tainton-Heap" was designed to reflect sleep states described in *Tainton-Heap et al.* [278]. Other models followed no prior literature.

Models were scored using internal methods from hmmlearn, including log-likelihood [320], Akaike Information Criterion [321], and Bayesian Information Criterion [322].

2.3.4 Decoding Datasets

All datasets were decoded using trained models specific to the species and sex of the fly. Decoding into states was performed using the Viterbi algorithm [323] in hmmlearn. For a four-state model, the hidden states were encoded as follows: "deep sleep" = 0, "light sleep" = 1, "quiet awake" = 2, "active awake" = 3.

2.4 Odour Response Experiments

Odour response experiments utilised an additional module called the Air Gas Odour Delivery Module (AGO), solenoid variant. The AGO consists of 10 solenoid valves controlled by an Arduino Nano board, which receives real-time input from the Ethoscope's Raspberry Pi.

For these experiments, two odours were used: 10% ACV – Aspall Organic Cider Vinegar (diluted in milliQ H2O), and air (control) – milliQ H2O. The odourants were stored in glass bubblers during the experiment. Air was pumped through the bubblers by a Tetra aqaurium pump, with the incoming air first passing through an activated charcoal filter to deodorise it. Airflow was regulated using a Brooks Instrument MR3000 variable area flow meter at a rate of 1.6 L/min before being passed through the odourant. Plastic tubing connected the glass bubbler to a 10-way splitter inside the AGO, which then directed air through solenoid valves. Smaller plastic tubing linked each valve to a metal tube (35 mm long, 4 mm diameter) that was partially inserted into the glass tube housing the fly. A small amount of cotton wool was inserted between the metal tube and the fly to prevent direct interaction.

All experiments were conducted in an incubator (LMS Cooled Incubator – Model 240NP) at 25°C, with 50-70% humidity, under a 12:12 light-dark cycle. Flies aged 4-7 days were used. The arousal threshold, or response rate, was assessed after one day of baseline activity recording. The ethoscopes were programmed to deliver the odour puff after a predefined period of inactivity (ST) and with a predefined probability factor (P). In the experiments validating the HMM in *Chapter 2*, both 10% ACV and air were tested with conditions set to $ST = 30$ seconds and P

= 10%. For the experiments involving *Drosophilids*, conditions were set to either $ST = 30$ or 150 seconds, and $P = 10\%$ or 50%. Both combinations were used to cover a full spectrum of responses per minute per HMM state, allowing efficient data collection when fewer experiments could be run.

Responses were calculated automatically using the *stimulus_response* function when loading the dataset. A positive response to a puff was recorded if the fly moved within 10 seconds after the puff, including micro-movements. When inactivity triggers a chance for puff deployment but the probability factor denied it, the event was logged as a mock stimulus, and the same analysis was applied. This generated the "spontaneous movement" group. For response plots involving the HMM, movement data was binned into 60-second intervals and decoded. The decoded dataset was then matched with the response dataset using timestamps and ID. Since any positive response would change the predicted state to an "awake" state, the preceding minute's state was used as the label for the analysis.

2.5 Sleep Deprivation Experiments

Sleep deprivation was achieved by manually rotating the tube housing the fly within the ethoscope using the optomotor module [244]. The optomotor module is an accessory to the ethoscope, containing 10 motor devices positioned beneath half of the 20 tubes, allowing targeted sleep deprivation based on real-time tracking. When a fly remained immobile for more than 30 seconds, the motor for that tube was triggered by the ethoscope software. The motor rotated the tube at approximately 400 rpm for 3 seconds, causing it to spin several times and wake the fly, as demonstrated in *Geissmann et al., 2019* [53].

Flies were given one baseline day of normal sleep before undergoing sleep deprivation from ZT0 to ZT24 (24 hours). Following the deprivation period, the activity sequence between ZT0-3 was used to quantify sleep, with data decoded using the appropriate HMM.

2.6 Time Series Analysis

For each dataset used in *Chapter 5*, data was summarised at 10-second intervals. When multiple timestamps occurred within 60 seconds, the mean was calculated for each variable, except for velocity, where both the mean and maximum values were determined. Data was filtered to include only time points during light periods (12 hours per day) due to variations in ellipse recordings when tracking switched to infrared light.

For *Figure 5.4*, bouts of immobility were identified by counting runs of inactivity lasting between 5 and 20 minutes. Bouts with fewer than 31 datapoints (for a 5-minute duration) were excluded. The first and second-to-last datapoints in each bout were used to calculate start and end values for each variable, to avoid responses changing the values. For *Figure 5.5*, the datapoint immediately before a puff was used to calculate responses for each variable.

2.7 Machine Learning

Two curated datasets were used for machine learning: one for predicting the response to a puff (ACV dataset) and another for HMM state classification (*Geissmann et al. 2019* dataset). For the puff response dataset, runs of immobility lasting 5–9 minutes were isolated, and low-data-point series were removed. Only the last 4 minutes of each bout was retained to ensure uniformity across time series. For HMM prediction, bouts of 8 minutes of predicted deep sleep and light sleep were used. This length was chosen to balance sample size with consistency, as variations in bout length were found to bias the Catch22 analysis.

The null model scores were generated by running the model 100 times with different test-train splits. Accuracy scores were recorded, and the same split labels were shuffled to train and score new instances of the model with identical parameters.

2.7.1 Dynamic Time Warping

Dynamic Time Warping (DTW) was implemented using the Python package sequentia [324]. The DTW algorithm acted as the distance metric for a K-nearest neighbour classifier. For each plot, the number of neighbours was set to $\frac{\sqrt{N}}{2}$, where N is the total number of time series in the training subset. Various combinations of variables were tested, with the best-performing models presented in Chapter 5. When multiple variables were used, the DTW distance was calculated separately for each variable.

To reduce label bias, the dataset was curated to include an equal number of time series for each label, based on the smallest group. The data was split 80% for training and 20% for testing, with stratified sampling to ensure equal label distribution.

2.7.2 Catch-22

The Catch-22 algorithm suite was applied to three variables: mean velocity, area of the ellipse, and phi. This generated 66 features (3 x 22) per 8-minute time series. The name and description of each feature can be seen in *Table 2.3* which was reproduced from *Table 1 of Lubba et al.* [325]. Equal numbers of each label were analysed, and features with more than 5% missing (NaN) values were removed. Likewise, any time series with more than 5% missing values were excluded.

For classification, the dataset was split 70% for training and 30% for testing. The ***MinMax-Scaler*** from sklearn [326] was applied to normalise the data. A range of classifiers (random forest, support vector machines, and gradient boosting) was used, and the best-performing model was selected for *Figures 5.7-8*. A parameter grid search was conducted to find the optimal settings for each classifier, and these were used to generate the null model plots.

Feature Name	Description	Category
DN_HistogramMode_5	Mode of z-scored distribution (5-bin histogram)	Distribution
DN_HistogramMode_10	Mode of z-scored distribution (10-bin histogram)	Distribution
SB_BinaryStats_ mean_longstretch1	Longest period of consecutive values above the mean	Simple temporal statistics
DN_OutlierInclude_ p_001_mdrmd	Time intervals between successive extreme events above the mean	Simple temporal statistics
DN_OutlierInclude_ n_001_mdrmd	Time intervals between successive extreme events above the mean	Simple temporal statistics
CO_f1ecac	First 1 / e crossing of autocorrelation function	Linear autocorrelation
CO_FirstMin_ac	First minimum of autocorrelation function	Linear autocorrelation
SP_Summaries_welch_ rect_area_5_1	Total power in lowest fifth of frequencies in the Fourier power spectrum	Linear autocorrelation
SP_Summaries_welch_ rect_centroid	Centroid of the Fourier power spectrum	Linear autocorrelation

Continued on next page

Table 2.4 – continued from previous page

Feature Name	Description	Category
FC_LocalSimple_ mean3_stderr	Mean error from a rolling 3-sample mean forecasting	Linear autocorrelation
CO_trev_1_num	Time-reversibility statistic $((x_{t+1} - x_t)^3)t$	Nonlinear autocorrelation
CO_HistogramAMI_ even_2_5	Automutual information: $m = 2, \tau = 5$	Nonlinear autocorrelation
IN_AutoMutual InfoStats_40_gaussian _fmmi	First minimum of the automutual information function	Nonlinear autocorrelation
MD_hrv_classic_pnn40	Proportion of successive differences exceeding 0.04σ [327]	Successive differences
SB_BinaryStats_ diff_longstretch0	Longest period of successive incremental decreases	Successive differences
SB_MotifThree_ quantile_hh	Shannon entropy of two successive letters in equiprobable 3-letter symbolization	Successive differences
FC_LocalSimple_ mean1_tauresrat	Change in correlation length after iterative differencing	Successive differences

Continued on next page

Table 2.4 – continued from previous page

Feature Name	Description	Category
CO_Embed2_Dist_ tau_d_expfit_meandiff	Exponential fit to successive distances in 2-d embedding space	Successive differences
SC_FluctAnal_2_ dfa_50_1_2 _logi_prop_r1	Proportion of slower timescale fluctuations that scale with DFA (50% sampling)	Fluctuation Analysis
SC_FluctAnal_2_ rsrangefit_50_1 _logi_prop_r1	Proportion of slower timescale fluctuations that scale with linearly rescaled range fits	Fluctuation Analysis
SB_TransitionMatrix_ 3ac_sumdiagcov	Trace of covariance of transition matrix between symbols in 3-letter alphabet	Others
PD_PeriodicityWang_ th0_01	Periodicity measure of *Wang et al. 2007* [328]	Others

Table 2.4: Catch-22 features and their descriptions.

2.8 High definition videos

2.8.1 Video capture

HD videos were captured using a Raspberry Pi 3 model B+ combined with a Raspberry Pi High Quality Camera (12.3-megapixel Sony IMX477 sensor) equipped with a 16mm telephoto lens. The camera's pre-installed infrared (IR) filter was manually removed to allow exclusive capture in IR light. An IR bandpass filter was applied to the lens, ensuring only IR light was recorded. Both the front and back of the arena housing the fly were illuminated by IR light strips (see *Figure 6.1* for the setup).

Custom-designed 3D-printed PLA structures were used to hold the camera, lens, and fly arena. The arena space measured 11 mm (width) x 1.8 mm (height) x 2.5 mm (depth) on both floors, and was sealed with a 1 mm thick glass slip. The rear wall, approximately 0.38 mm thick, allowed IR light to pass through. 3D models of the setup are available upon request.

Videos were recorded using the *libcamera-vid* software provided with Raspbian (Raspberry Pi OS), captured continuously over a 24-hour period. Specifications can be found in *Table 2.4*.

libcamera-vid parameter	**Argument**
framerate	38
mode (resolution)	2028:1520
bitrate	20 000 000
contrast	2
tuning-file	imx477_noir (compensates for no IR filter)

Table 2.5: Parameters and the arguments used when calling the video function *libcamera-vid* to capture HD videos.

2.8.2 Video Curation

Each 24-hour recording was split into 1-hour segments. Videos recorded after the fly had either died or become trapped were manually excluded. The remaining videos were automatically segmented into shorter clips based on periods of immobility or activity. Bouts of inactivity less than 3 minutes were discarded.

This segmentation was performed using Python and the OpenCV library [329]. For each fly, batches of frames totaling 5 seconds (570 frames at 38 fps) were processed. Frames were converted to grayscale and smoothed using Gaussian blur. The absolute difference between consecutive frames was calculated and areas with changes above a threshold of 30 were set to a maximum value of 255 (white). The image was then dilated, and contours of movement were detected. If more than 105 contours (7 per second) exceeded a score of 1500 (arbitrary unit of difference in contours), the batch was labeled as moving. Consecutive immobile batches were combined until movement occurred, and the same process applied to activity sequences.

Threshold values from above were chosen after analysing multiple behaviours to exclude small movements, such as grooming, while retaining significant postural changes, proboscis extension, and anal extension. Despite this, some videos contained minor movements and were manually reviewed and edited to remove wake activities.

2.8.3 Manual Behaviour Categorisation

Selected videos were manually categorised into four behavioural groups based upon the following visual observation (Fig. 2.2):

- **Full Prone**: The fly's abdomen, thorax, and head were lowered to the surface
- **Part Prone**: Only the abdomen was lowered, while the thorax and head remained relatively still
- **Rise**: The fly extended its legs, increasing the distance between its body and the surface, often accompanied by a lowered abdomen

- **No change**: No visible movement and the fly was not already in one of the previously described postures

2.8.4 SLEAP and keypoint analysis

Model training

SLEAP software [252] was installed and executed on a remote virtual machine running Ubuntu, equipped with an NVIDIA T4 GPU. Individual models were trained for each fly, with the head, body, and abdomen labeled on 40 to 60 frames (Fig. 6.2). Training was conducted using the multi-animal bottom-up pipeline, with a maximum of one instance per frame. The default model parameters were employed, allowing for iteration until no significant improvement was observed or 100 epochs had been completed.

Once trained, the model was prompted to predict 20 frames in an unlabeled video. Predictions were manually inspected for obvious errors, which were corrected and used for re-training. When the desired accuracy was achieved, the model was applied to predict all frames across all videos, and the resulting predictions were saved as HDF5 files and exported to a local machine.

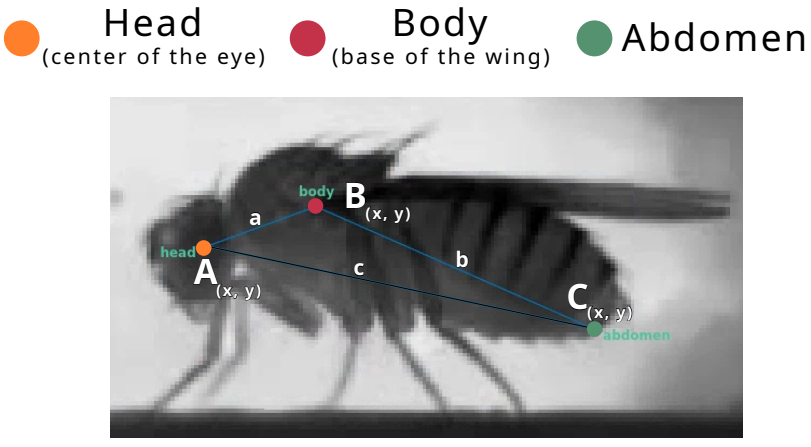


Figure 2.2: **Diagram of the keypoint label locations and subsequent calculations.** Labelling guide for the three keypoints. The head (orange) keypoint was placed in the center of the eye. The body (red) keypoint was placed at the base of the wing. The abdomen (green) was placed at the center of the end of the abdomen (terminalia). In white are the notation labels for the calculated metrics such as length of sides. See the section below: *Keypoint curataion and analysis*

Keypoint curataion and analysis

SLEAP predicts keypoints locations giving the user (x, y) coordinates given the size of the image (fig. 2.2). As videos were setup in a uniform manner, it assumed that differences in keypoint locations values are comparable. The predicted keypoint locations were augmented to fit the ethoscopy data format. During loading a rolling mean (76) was applied to each (x, y) coordinate per keypoint, per individual. Only the first 70% of the tracking was retained to standardise ensure the end of the time series was during the sleep bout.

Several metrics were calculated using the keypoint (x, y) coordinates. Their descriptions and equations are as so:

Size of angle at each keypoint (*Figure 6.4*):

- Distance between points (also used in *Figure 6.5.b*:

$$A = \sqrt{(A_x - B_x)^2 + (A_y - B_y)^2}$$

- Length of sides:

$$a = \sqrt{(B_x - C_x)^2 + (B_y - C_y)^2}$$

$$b = \sqrt{(A_x - C_x)^2 + (A_y - C_y)^2}$$

$$c = \sqrt{(A_x - B_x)^2 + (A_y - B_y)^2}$$

- Angle calculation:

$$B_{angle} = \arccos \frac{a^2 + c^2 - b^2}{2ac}$$

- Convert to degrees:

$$B^\circ = B_{angle} \frac{180}{\pi}$$

Centroid of the fly (*Figure 6.5.a*):

- Centroid calculation:

$$centroid_x = \frac{A_x + B_x + C_x}{3}$$

$$centroid_y = \frac{A_y + B_y + C_y}{3}$$

Changes in Y-coordinate (*Figure 6.6*):

- Absolute difference to t0:

$$y_n = [y_1 - y_1, y_2 - y_1, y_3 - y_1, ..., y_n - y_1]$$

2.9 Statistics, data collection and visualisation

All ethoscope data were analysed using *ethoscopy*, which utilises Python. Additionally, keypoint data from SLEAP analysis were augmented to fit the *ethoscopy* structure. *Ethoscopy* over time and quantification plots (e.g. Fig. 4.4.a&b, Fig. 5.5, and Fig. 6.4) display the mean and 95% confidence intervals (CI), which were bootstrapped using 1,000 resamples. Visualisations in *ethoscopy* were generated using a combination of *plotly* [330], *seaborn* [331], and *matplotlib* [332], with the latter two used for non-*ethoscopy* plots, such as distributions, t-SNE, and histograms.

Statistical comparisons are indicated in the figures as follows: * = p-value $\leq$ 0.05, ** = p-value $\leq$ 0.01, and *** = p-value $\leq$ 0.001 for comparisons between two groups. For multiple groups, significance was indicated with letters to denote significance levels. The Kruskal-Wallis nonparametric test was employed, with Dunn's post hoc testing for inter-group comparisons.

In Figures 4.4.c and 5.5, significance testing was supplemented with DABEST estimation statistics [333]. Bootstrapped distributions of the effect size difference are plotted against a chosen control or average.

Data for training the HMM were collected by Dr Quentin Geissmann, as previously indicated. All subsequent data were collected solely by the author, except for the Drosophila species data

in Figures 4.7 and 4.8, which were gathered in collaboration with Dr Michaela Joyce and are also found in *Joyce et al.* [334]. All analyses were conducted by the author.

Chapter 3

Ethoscopy: An open-source behavioural analysis toolbox

3.1 Rationale

Activity monitoring systems like the ethoscope enable researchers to continuously track model organisms over long periods, often generating large and multidimensional datasets that span days or even weeks [244, 335, 239, 241]. This transition from conventional behavioural studies to ethomics, a term coined for the analysis of large-scale behavioural data [336], can pose challenges for traditional biologists seeking to extract meaningful insights from their data. In response, open-source analysis tools have been developed alongside these platforms to help researchers unlock the full potential of their data [337].

One such tool, developed specifically for the ethoscope, is *rethomics*—a suite of R packages designed to facilitate the analysis of behavioural time series data. *Rethomics* functions as a 'bottom-up' toolbox that builds upon existing R packages, tailoring them for the analysis and visualisation of activity data. With its well-documented tutorial, *rethomics* guides users from data extraction to advanced plotting with tools like *ggplot2* [335, 338]. However, like many open-source projects, *rethomics* has suffered from a decline in active development as its creators have moved on, resulting in a tool that struggles to keep pace with the rapid changes

in software ecosystems and emerging scientific needs.

While *R* boasts a vast repository of packages catering to the diverse needs of data scientists, its strength is somewhat marred by a lack of conceptual coherence. Its amalgamation of syntax and data structure designs, stemming from its origin as a statistical playground rather than a software development language, often perplexes beginners transitioning between different packages. Despite these challenges, *R* has retained its status as a powerful language for those experienced enough to navigate its complexities, thanks to its flexibility and the depth of its resources.

Python contrasts sharply with *R* in that it was designed as a software development language from the ground up, featuring a cohesive syntax and intuitive data structures. While this strong foundation gives Python significant advantages in flexibility and ease of use, its early adoption in data science and research lagged due to the lack of a dynamic environment for live data exploration. Early tools like *IPython* (which eventually evolved into *Jupyter*) were still underdeveloped, and visualisation options were largely limited to *matplotlib*, which fell short in many areas when compared to *R*'s *ggplot*.

However, over the last decade, *Python's* popularity has surged, particularly among beginners, thanks to its intuitive syntax and growing ecosystem. This growth was fueled by the development of robust data science libraries such as *numpy* [339] and *pandas* [340] for data manipulation, *SciPy* for scientific computing [326], and *seaborn* [331] and *plotly* [330] for visualization, which adopted principles from the "Grammar of Graphics," similar to *ggplot* in *R* [338, 341]. The rise of machine learning as a dominant force in research and industry has further cemented Python's status, with powerful libraries like *tensorflow* [342], *pytorch* [343], and *scikit-learn* [326] offering seamless integration for both academic and applied projects. As a result, *Python* has become the go-to tool for behavioral scientists and ethomics researchers alike, providing a versatile environment that can easily accommodate the demands of modern data science.

In this section, I will introduce *ethoscopy*, an advanced data analysis toolbox developed in *Python*. *Ethoscopy* is more than just a *rethomics* equivalent in a more accessible language; it represents an evolution, incorporating novel functionalities and methodologies aligned with cur-

rent advances in sleep and circadian rhythm research. Furthermore, *ethoscopy* serves as an entry point into the expansive machine learning ecosystem. This section will begin by examining how *ethoscopy* improves upon the accessibility challenges faced by *rethomics*. I will then provide an overview of *ethoscopy's* structure and key features, before diving into behavior-specific analysis tools designed for circadian rhythm and hidden Markov models (HMM) investigations. Finally, I will showcase how *ethoscopy* bridges the gap between conventional analysis and machine learning applications, empowering researchers with cutting-edge tools for behavioural study.

3.2 Improving accessibility

Researchers can often be reluctant to share their code, concerned that it may be poorly written or only superficially understood, pieced together from scripts they have gathered online [344]. These were certainly my own concerns. However, as computational methods and algorithms become increasingly embedded in all facets of research, it is crucial to recognise the challenges this trend poses for reproducibility. While algorithms should, in theory, enhance the consistency and repeatability of data pipelines, the use of unpublished or overly complex scripts often introduces barriers to replicating results, even when identical datasets are available [345]. Reproducibility lies at the heart of scientific inquiry, allowing others to refine and build upon existing methods, while also testing the validity of findings through alternative approaches. Yet, we face a situation where simply installing the software used by the original research team can be a frustratingly difficult and time-consuming endeavour, creating obstacles before the work can even begin.

3.2.1 Dockers

A remedy to the issue of scattered code and the need for multiple installations lies in Docker containers. Docker, an open-source platform widely embraced by developers, facilitates the building, deployment, execution, updating, and management of containers. These containers represent a standardised software unit that encapsulates not only the code but also all

its dependencies into a single application. Within the container image, the entire environment—including code, system tools, libraries, and more—is stored. When executed, the container runs in isolation on the user's computer, leveraging a Linux kernel akin to a virtual machine [346, 345, 347].

In essence, Docker ensures consistent execution regardless of the underlying infrastructure, alleviating concerns regarding dependency resolution and system compatibility. With broader adoption, this approach holds the promise of accelerating and encouraging researchers to delve into research data independently, using a unified environment to replicate and further explore findings [345].

Ethoscopy-lab, available on DockerHub, serves as the Docker container for *ethoscopy*, offering users seamless access to the latest version of *ethoscopy* within a *Jupyter* instance. Comprehensive installation instructions for *ethoscopy-lab* across all systems are provided in the online tutorial for *ethoscopy*. Links to this tutorial, as well as to DockerHub, GitHub, and PyPi, can be accessed at https://lab.gilest.ro/ethoscopy.

The introduction of a Docker container is expected to streamline the adoption of *ethoscopy* as the successor to *rethomics*, reducing the complexities associated with setting up Python environments and *Jupyter* notebooks. However, while Docker containers effectively address software reproducibility, they do not inherently simplify the use or understanding of the software itself.

3.2.2 Jupyter notebooks and Tutorials

Ethoscopy was designed to be used in an interactive environment, namely *Jupyter* notebooks. *Jupyter* notebooks provide a dynamic environment where code execution, narrative documentation, and visualisations integrate seamlessly. As a free and open-source tool, it is widely adopted by students, educators, and researchers alike [348]. For data science and research, *Jupyter* notebooks empower users to iteratively explore datasets, experiment with analysis, and visualise results in real time, encouraging an exploratory approach to data analysis. Users can note

insights and document processes, much like a traditional lab notebook. Upon completing an analysis, the notebook can be refined, annotated, and presented as a clear, interactive narrative that demonstrates how the data was processed to produce the final figures [348, 349, 350].

Ethoscopy and *ethoscopy-lab* harness this potential in two key ways. Firstly, its functions and methods, which will be discussed in detail later, are designed to condense common and complex analyses into single, easily comprehensible commands. This aligns with the *Jupyter* ethos, allowing users to clearly signpost their choice of analysis, making it accessible even to those unfamiliar with Python. Readers can then focus on the narrative being conveyed, without getting bogged down by intricate code details [349]. Secondly, the *ethoscopy* tutorial includes several instructional *Jupyter* notebooks that demonstrate practical applications using real-world data. These notebooks help to lower the learning curve for students and researchers new to *ethoscopy*, whether they are joining a lab or adopting the tool for the first time. They serve as both educational resources and templates, enabling users to explore *ethoscopy's* capabilities with provided datasets before applying them to their own projects. This approach enhances engagement and eases the transition to integrating *ethoscopy* into research workflows [348].

By reducing the barriers to entry through comprehensive instructional resources, *ethoscopy* aims to become a widely adopted tool across labs utilising the ethoscope or similar behavioural monitoring systems. In line with this, *ethoscopy-lab* is packaged with a stable release of JupyterHub, a multiuser, web-based notebook platform [350]. The vision is for labs to maintain a shared, high-performance workstation hosting JupyterHub, where *ethoscopy* is readily available. This setup would allow users to connect remotely from any device and access the software, eliminating the need for multiple powerful computers and repeated setup processes. This centralised approach requires only one technically proficient user to set up and maintain the system, freeing up others to focus on their analysis.

3.3 Design Philosophy and Structure

Behavpy is the core class in *ethoscopy*, modeled after *behavr* from *rethomics*. It is designed to seamlessly manage large multi-specimen behavioural datasets that include varied individual information such as genotype, sex, and treatment groups—collectively referred to as metavariables [335]. *Behavpy* achieves this by semantically linking two tabular structures: the main behavioural data and the metadata (Fig. 3.1). The design philosophy behind *behavpy* simplifies the process of handling complex datasets by enabling direct manipulation of the data via metadata without requiring extensive knowledge of *pandas* data frame operations.

The metadata holds metavariables that describe all experimental conditions, with each row representing a specimen which has been assigned a unique identifier (ID) that corresponds to its behavioural data (Fig. 3.1.b). This linkage allows the user to filter or sort the data with simple commands. For example, filtering by sex and calculating the average velocity per specimen can be accomplished in just two lines of code, dramatically reducing the complexity of such operations (Fig. 3.3).

While *ethoscopy* is optimised for analysing data from ethoscope devices, it adheres to general scientific standards for quantifying locomotor activity, making it adaptable to a wide range of behavioural data [351]. The core requirement is that the data must include three descriptors: (1) an ID for each specimen, (2) a time series, and (3) a behavioural trait—typically whether the organism is moving or stationary (Fig. 3.1.b). This data is usually stored in tabular formats, such as CSV files, spreadsheets, or database files, all of which can be read into a *pandas* data frame. If the data can be loaded into *pandas*, *ethoscopy* can process it. *Pandas* [340], a powerful Python library for data analysis, serves as the foundation of *behavpy*. By sub-classing *pandas* data frames, *behavpy* inherits all existing *pandas* methods while introducing additional functions specific to behavioural analysis. These new methods are applied to the individual specimens rather than the whole group, making it easier to conduct behaviour-specific analysis with minimal coding.

A significant deviation from *rethomics'* design lies in the approach to visualisation. *Rethomics*

relies heavily on *ggplot2*, an *R*-based library [338]. While this provides flexibility, it also requires a high-level understanding of *ggplot2* syntax, making it less accessible to new or transient lab members, particularly undergraduates. *Ethoscopy*, on the other hand, favours simplicity by offering single-callable methods for generating common plots. In Figure 3.4 all the plots are generated by one line of code with several arguments to augment the output. This trade-off sacrifices some flexibility but dramatically lowers the learning curve, making it easier for non-experts to produce publication-quality figures. Advanced users, however, retain the option to build custom visualisation functions due to the underlying *pandas* compatibility.

For plotting, users can choose between *plotly* and *seaborn*, each with distinct advantages (Fig. 3.1.c). *Plotly*, which outputs interactive plots by default, allows users to zoom, filter, and explore data directly within the visualisation—ideal for interactive presentations and exploring complex datasets. For instance, a user can dynamically focus on specific experimental groups and remove visual clutter without altering the code [330]. On the other hand, *seaborn*, built on top of *matplotlib*, provides static plots that are lightweight and better suited for embedding in *Jupyter* notebooks. While interactive, *plotly* plots can consume significant memory and slow down notebooks, making *seaborn* the more efficient choice [331].

This integrated and intuitive approach reflects the ethos behind *ethoscopy*: providing a versatile yet accessible toolbox for behavioural researchers that reduces the steep learning curve traditionally associated with behavioural data analysis.

3.4 User Workflow

In this section, I will guide you through a typical workflow using *ethoscopy*, from loading the data to manipulating and analysing it, and finally visualising the results.

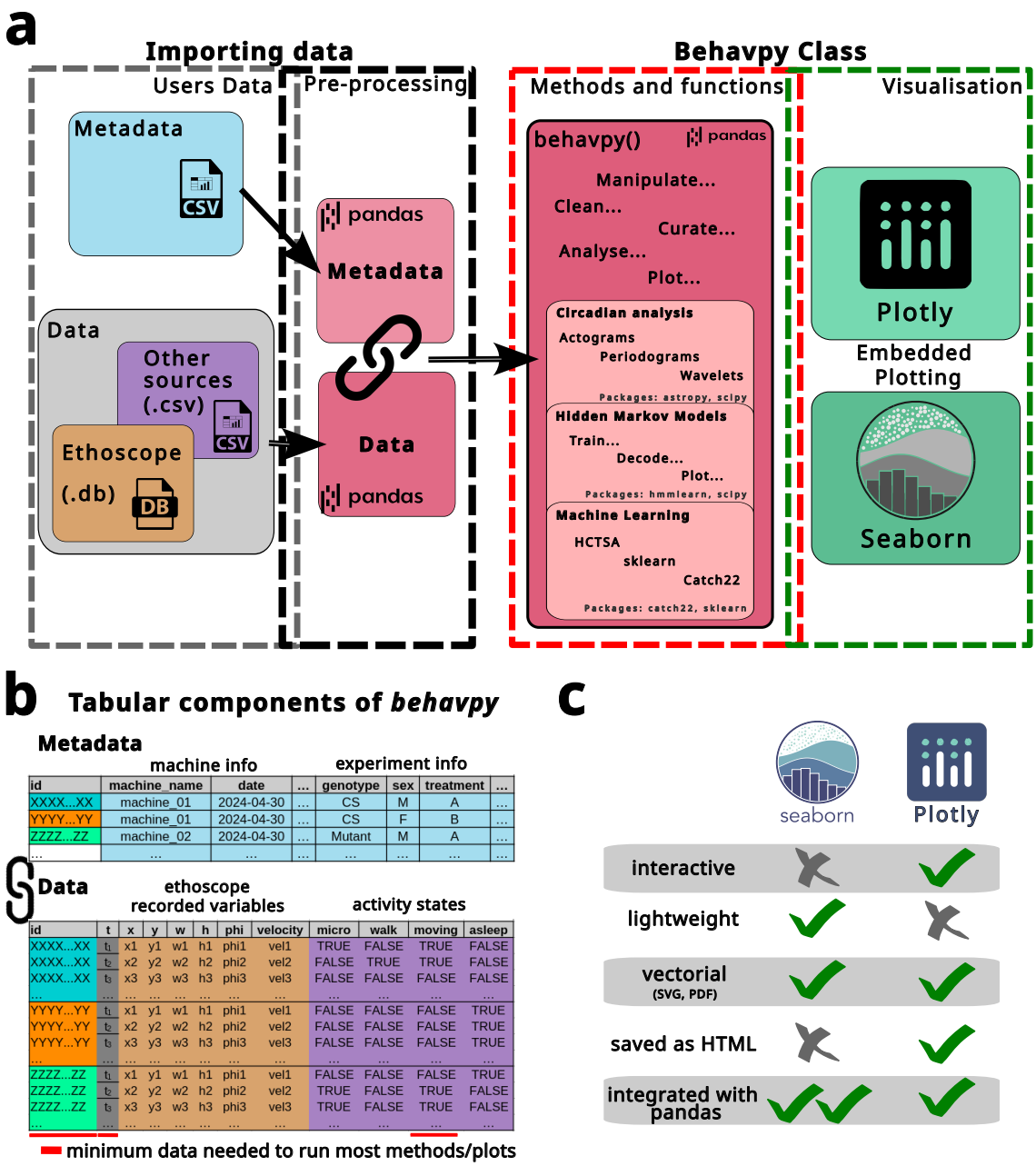


Figure 3.1: **Diagram of the *ethoscopy* ecosystem and its architecture.**
(a) Overview of the pipeline to bring data into the *ethoscopy* framework. Importing the data can be simply achieved by linking a metadata and data file through *behavpy* if formatted as in (b). Within *behavpy* the data can have several methods applied to it to filter, curate, and analyse the dataset. The data can then be visualised using built-in methods that utilise *plotly* or *seabron*, depending on the users choice. **(b)** Representation of the format needed for the metadata and data to be accepted in *ethoscopy*. Key data types are a unique ID, time stamps, and a behaviour. **(c)** The pros and cons of *plotly* and *seabron*. *Plotly* excels at data exploration in a notebook, whereas *seaborn* is more lightweight

3.4.1 Loading Data

When using your own data, simply initialise the *behavpy* class (Fig. 3.2.b). The only required inputs are a metadata table and a dataset, both structured as *pandas* data frames (Fig. 3.1.b). When working outside the ethoscope ecosystem, users would need to curate, organise, and format their own data to fit the structure. However, for ethoscope users, key tasks such as generating and formatting IDs, along with other essential steps, can be automated programmatically, significantly reducing the workload.

The data loading process is built around a standardised metadata file and a directory structure for database storage. The function ***'link_meta_index'*** (Fig. 3.2.a) connects the metadata to the corresponding database file, guiding the entire loading process. The metadata CSV file contains key information such as the machine name, experiment name, and date (Fig. 3.1.b). This information is used to automatically search the specified directory for a matching database file. Once found, the function augments the metadata with details about the database's location, making it ready for loading.

Data can be loaded in two main ways: without an analysing function or with one. Loading without an analysing function simply reads the raw data from the database into a *pandas* data frame, applying only minimal processing, such as converting time into seconds relative to the reference hour (lights-on time, set as t=0) and generating an ID column that links to the metadata.

Loading with an analysing function allows for the automatic application of common processing tasks during data import, reducing the need for repeated computation on large datasets (Fig. 3.2.a). For example, functions like ***'sleep_annotation'***, which calculates sleep episodes based on movement data, or ***'stimulus_response'***, which evaluates activity following a stimulus, can be applied during the loading process. Given that datasets often contain thousands of rows, applying these functions as the data is imported significantly improves efficiency. Users are also encouraged to develop their own analysing functions tailored to their specific research needs.

This linked loading approach offers several benefits. The standardisation ensures consistency in data storage across a lab, allowing any researcher to share their metadata file with a colleague, enabling instant access to the data without additional setup. This system also facilitates inter-lab collaboration by maintaining a uniform format. Moreover, it simplifies the process of concatenating data across multiple experiments. By merging metadata files from individual replicates into a master document, researchers can easily assess covariates and perform aggregated analyses across different datasets.

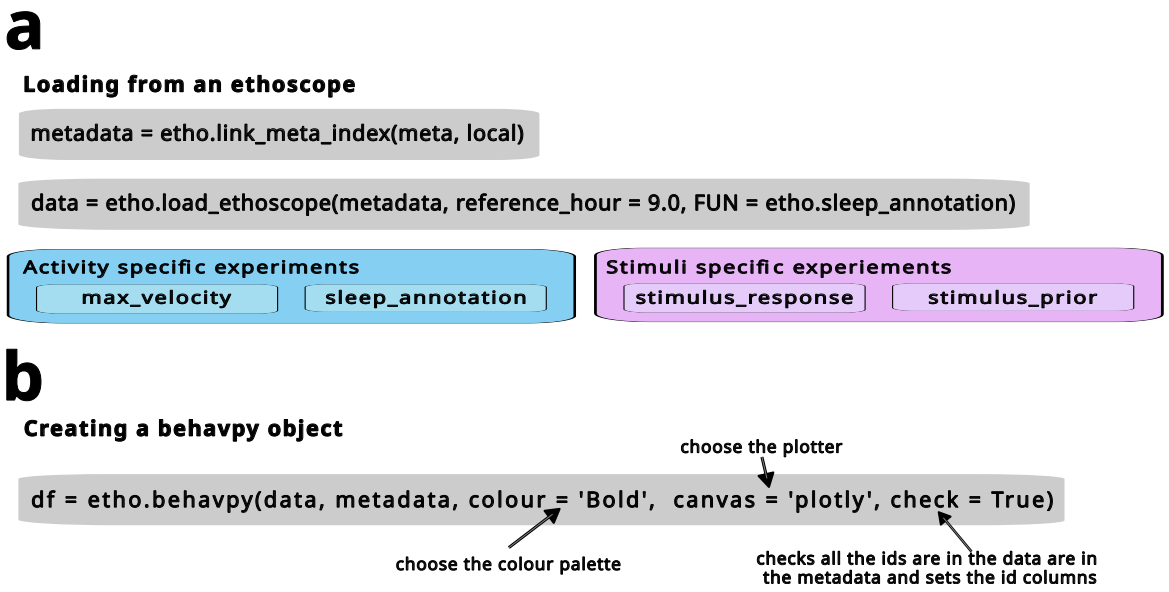


Figure 3.2: **An example of the loading functions in *ethoscopy*.**
(a) Loading the data from an ethoscope needs no prior user curation. Simply link your metadata file with the location of your ethoscope database files. Calling ***etho.load_ethoscope*** with the augmented metadata will load and augment the data to have standardised time points of equal time difference and normalised to the first lights on. **(b)** Data loaded from (a) or created by the user is then linked to the metadata by calling ***etho.behavpy***. Users can choose the colour palette from within *plotly* and *seaborn*, depending on their canvas choice.

3.4.2 Augmenting Data

While this section is not intended as a tutorial, I will briefly outline the backbone of *behavpy* and its enhancements to the *pandas* library (Fig. 3.3). *Behavpy*, a subclass of *pandas*, enables users to perform typical data manipulation tasks such as applying functions to individual columns, generating new columns by combining existing ones, and filtering rows based on specified conditions [340]. However, these standard operations usually apply to the entire

dataset, which is not always desirable when working with behavioural data. Often, one needs to execute these operations on a per-specimen or per-group basis, which is where *behavpy's* tailored approach shines.

Behavpy's core methods are designed to handle common data cleaning tasks at the level of individual specimens or metavariables (Fig. 3.3.a). For example, users can easily filter by treatment group, time intervals, or exclude specimens with insufficient data points. These foundational tools are intuitive for behavioural scientists who often need to clean and organise datasets based on specific experimental conditions.

Beyond basic cleaning, *behavpy* offers several behaviour-specific methods (Fig. 3.3.b). These include calculating metrics like sleep bout length and frequency, excluding deceased or inadequately sleep-deprived specimens, and estimating feeding times—features particularly suited for data derived from ethoscope. These functions are designed for one-line invocation, streamlining analysis and allowing users to focus on interpreting results rather than on managing complex code.

The goal of these methods is to simplify the user's workflow. By providing clear, single-line commands, *behavpy* allows for swift chaining of multiple analytical techniques while maintaining the cleanliness and readability of *Jupyter* notebooks. This structure is particularly valuable for collaborative work, as it makes it easier for others to follow and annotate the analysis process.

3.4.3 Visualisation

Visualisation is essential for behavioural research; it helps researchers assess data quality, summarise population trends, and refine or generate new hypotheses. *Ethoscopy* supports this through a range of graphical representations, including ethograms, heatmaps, and interactive visualisations (Fig. 3.4).

Given the typically large datasets in behavioural studies—often comprising multiple specimens per experimental group pre-processing is crucial before plotting. Both *plotly* (*plotly express*) and *seaborn* offer automatic plotting functions that can handle some level of preprocessing, such

as calculating averages and standard errors [330, 331]. However, these tools are not inherently designed to work with a linked metadata but to operate on a data frame where each row has a single label. This can result in a loss of per-specimen resolution. *Ethoscopy* resolves this by integrating the metadata and IDs into the analysis pipeline.

Depending on the plotting method, the executed code will apply a combination of smoothing averages, z-score analysis, and bootstrapping resampling for confidence intervals before feeding the data into the chosen plotting package. The specific approach can vary between plotting tools: *plotly* often employs more custom analysis to tailor visualisations to specific needs, while *seaborn* leverages its built-in functions for standard statistical plots and simpler analysis.

Quantification plots produced by *ethoscopy* also return a *pandas* data frame containing plot

a **Basic Filtering / Formatting**

method	description
df.xmv()	Filter the data by descriptive variables in the metadata. i.e. sex, experimental group
df.curate()	Remove individuals from the dataset that have too few data points
df.t_filter()	Filter the data by time to remove baseline days or isolate experimental days. i.e. between 24 - 48 hours
df.concat()	Add seperate datasets together, including the metadata.
df.bin_time()	Increase the time each row desribes. i.e. rows summarise from 10 seconds to 60
df.wrap_time()	Change time values (in seconds) from being sequential to representative of the time of day

b **Behaviour / Sleep specific**

method	description
df.add_day_phase()	Add a new column with the lighting- light, dark- and the day of the experiment. For use with filtering.
df.sleep_bout_analysis()	Calculate and count the length of sleep bouts per individual. Can also be automatically plotted for visual analysis.
df.curate_dead_animals()	Remove animals that may be dead. Calculated by animals with long runs of not moving.
df.remove_sleep_deprived()	Calculate the effectiveness of sleep deprivation methods and remove those that weren't sleep deprived enough.

Figure 3.3: **An example of some of the methods available in *ethoscopy*.**
(a) Basic augmentation methods are useful for trimming the dataset to only include animals you might want to plot or to remove animals that are not needed or wrong. **(b)** Behaviour specific methods often require a non-essential data type, such as whether the animal is asleep or not.

points per group. These data arrays can be further tested for significance using statistical packages such as *SciPy* [326] and *DABEST* [333]. *DABEST* is utlises estimation statistics to focuses on the effect size difference of two populations (experimental groups) and the bootstrapped confidence intervals of said averages. Within *DABEST* the user sets an experimental group as the control. Each other groups effect size difference is calculated, generating a distribution plot of the difference using the bootstrap resampling method [333]. These distributions can then be used with traditional p-value statistics to calculate significant difference. It is hoped that utilising this method will highlight true differences rather small effect size differences in large, similar populations.*DABEST* estimation plots are used intermittently throughout this study to highlight the differences between two or more groups.

While this approach may limit stylistic and analytical flexibility, it aims to cover most common visualisation needs comprehensively. Users who require different stylistic choices can use post-editing software such as *inkscape*. Additionally, those with advanced needs can leverage *ethoscopy's* core functionalities to prepare data for custom analyses and plots.

3.5 Specific behavioural tools

Building upon the core methods and functions of *ethoscopy*, two specialised toolsets have been developed to address specific behavioural research questions.

The first toolset is designed for exploring, analysing, and visualising circadian rhythms, a fundamental aspect of behavioural research. The second focuses on training, decoding, and visualising HMMs, a technique increasingly utilised in sleep research to uncover hidden behavioural states [319].

Both sets of tools are integrated within the *behavpy* class and are readily accessible. However, specific methods must be executed initially to generate the necessary data for further analysis and visualisation. The following section will outline these steps and their associated visualisation processes.

3.5.1 Circadian Analysis

Circadian rhythms are biological processes that follow a daily cycle, normally 24-hours, typically aligning with the Earth's day-night cycle. These rhythms regulate a variety of physiological functions and manifest in behavioural changes, such as locomotion or activity levels [36]. The tools provided by *ethoscopy* are designed specifically for analysing locomotion, although they can be applied to any behaviour measured in a binary format (True/False, happening/not-happening).

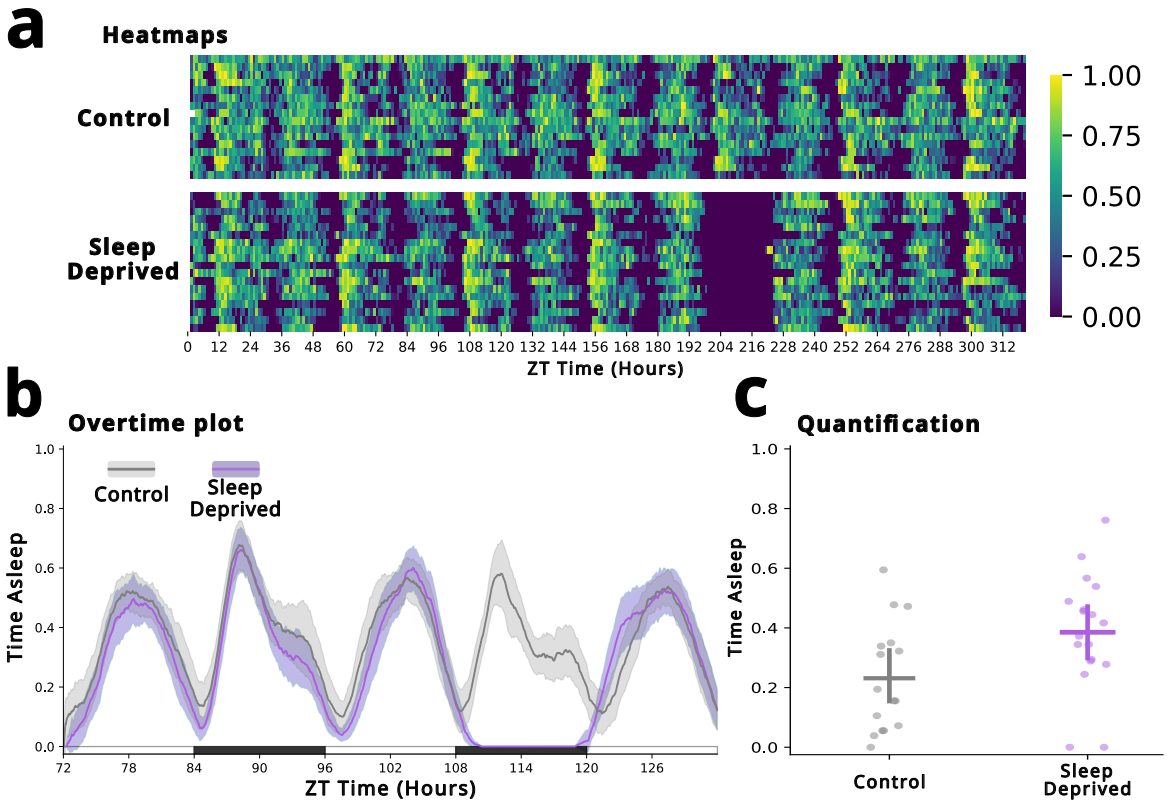


Figure 3.4: **Visualisation methods available in *ethoscopy*.**
(a) Heatmaps can be generated for any numeric behaviour. Heatmaps are best used to identify any issues within experimental groups, e.g. identifying non-SD flies in the SD group. **(b)** Overtime plots best show the temporal changes in a behaviour. *Ethoscopy* generates 95% CIs around the mean. Experimental groups that are labelled 'control' or 'ctrl' will automatically be coloured grey. **(c)** Filter datasets by time to isolate periods you which to quantify and compare behaviours. Here the sleep of the first 3 hours post SD are quantified. Like the overtime plots, the mean is plotted with 95% CIs that are bootstrapped. All plots shown here were generated using *seaborn* as the canvas.

Actograms

Actograms offer a straightforward visual assessment of rhythmic behaviour by double plotting total activity over time. Two days of activity are plotted on one row, this is then shifted forward by one day on the row below (Fig. 3.5.a). When read vertically any shifts in the activity can be quickly observed. As shown in *Figure 3.5.a* an organism that holds its circadian rhythm (wild type) actogram will be strongly vertically aligned. In contrast, those with an atypical short circadian rhythm ($per^{s}hort$) activity will drift to the left diagonally and long circadian rhythm ($per^{l}ong$) will drift to the right diagonally. Within *Ethoscopy*, the user can plot each individual specimens actogram or an average per group.

Periodograms

Whilst actograms offer a quick insight into any circadian drift, they are not quantitative. To attribute quantifiable strength/power to different frequencies periodograms are usually employed. Periodograms estimate the spectral density of a signal, or in other words the distribution of frequencies in a time series [352]. Given a sequence of activity and a band of frequencies to search, periodograms will generate a power score for each frequency. Typically, the strongest frequency (peak) will be the daily circadian rhythm, although it will also identify sub-daily rhythms too.

Within *ethoscopy* the user can apply the periodogram analysis to their dataset on an individual basis, generating a power for each frequency per specimen. Using this new data the user can plot the average power of each frequency per group (Fig. 2.4.b) or the average strongest frequency of each specimen per group (Fig. 2.4.c)

Within *ethoscopy* several methods can be used to compute the amplitude of the frequency spectrum:

- **Chi-Squared Method**: A statistical approach that evaluates periodicity by fitting sine waves of varying frequencies to the data and assessing goodness-of-fit via chi-squared

statistics. Particularly useful for irregularly sampled data, this method does not assume uniform time intervals, making it well-suited for behavioural and physiological time series. [352].

- **Fourier Method**: A classical spectral analysis technique that decomposes a time series into its constituent frequencies using sinusoidal basis functions. Best suited for evenly sampled data, this method efficiently identifies dominant oscillatory components but may require pre-processing, such as interpolation, for datasets with missing points. [353].
- **Lomb-Scargle Method**: An adaptation of the Fourier transform that accommodates unevenly spaced data. It estimates power at different frequencies by projecting the signal onto sinusoidal functions, adjusting for phase shifts. It is also particularly effective for detecting circadian rhythms in fragmented or incomplete datasets. [354].

Whilst some of the methods can handle missing data, *Ethoscopy* automatically applies an interpolation function to ensure a complete time series before conducting spectral analysis, to ensure robustness in the output.

Wavelets

Wavelet analysis differs from traditional frequency methods by decomposing signals into wavelets that are localised in both time and frequency. This technique is particularly useful for analysing signals with transient characteristics, such as circadian mutants transitioning from light-dark to constant dark conditions, which can cause the circadian clock to drift [355]. If this data were to be analysed by a periodogram, the drift in frequency would be difficult to identify as the power would be spread over a range.

The wavelet plot (Fig. 3.5.d) produced in *ethoscopy* is of a wild type fly in dark:dark conditions for 10 days. During which the internal circadian rhythm begins to drift as there is no entrainment from light, one of the strongest zeitgebers [36]. This is identifiable by the decrease in power in the 24 hour frequency as the experiment progresses. Also evident is the loss of sub-daily rhythmns at 12 hours at the beginning of the recording. The user can select from

several wave types available in the *PyWavelets* package [356] to tailor the analysis to their specific needs.

The tools outlined above, while not exhaustive, offer a comprehensive set of methods for circadian analysis, covering a broad range of use cases and providing accessible options for researchers studying rhythmic behaviour.

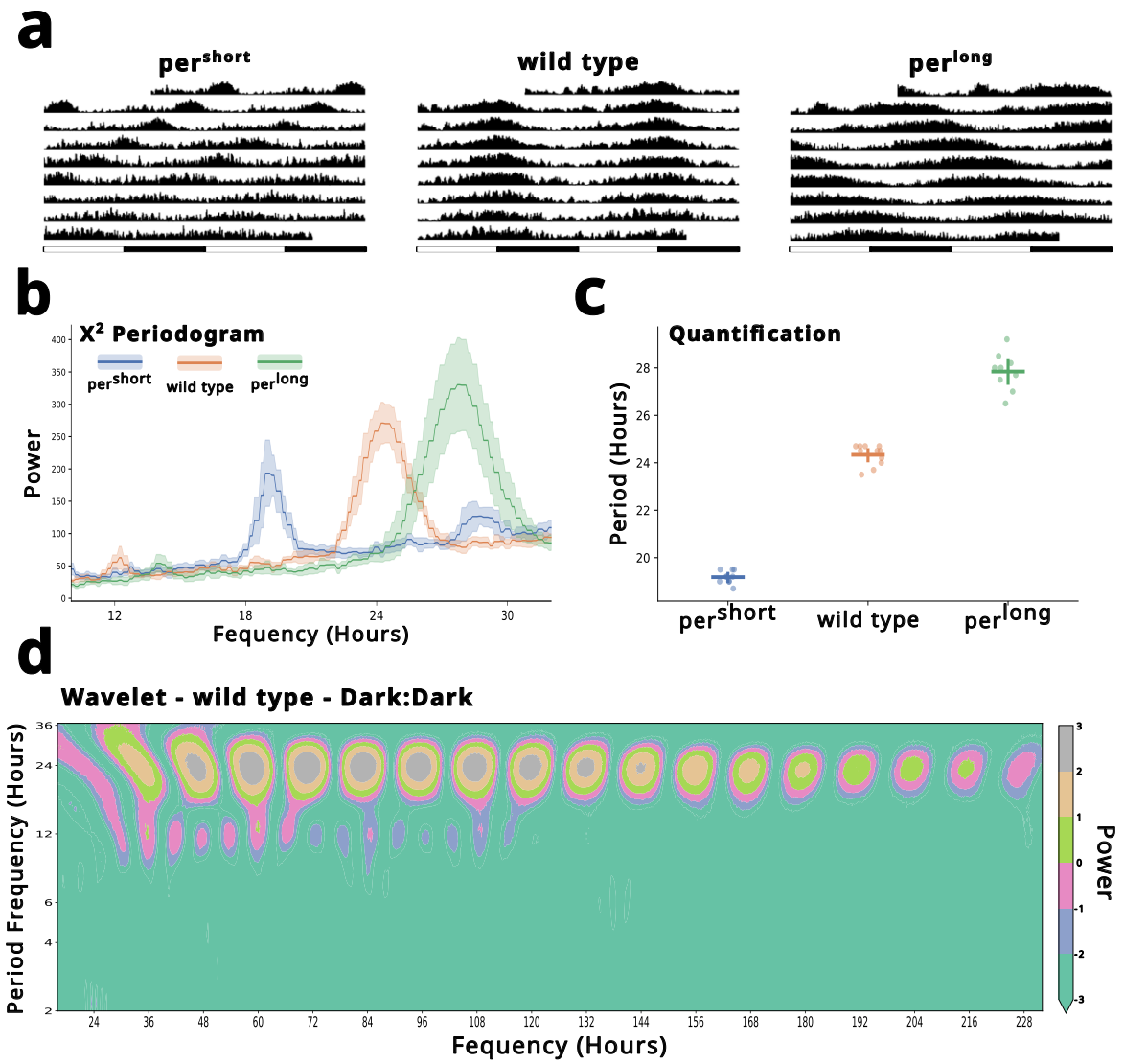


Figure 3.5: **Visualisation of the circadian analysis tools available in *ethoscopy*.** **(a)** Actogram plots for three experimental groups with different circadian backgrounds. Long and short mutants activity can be seen to drift under and over the 24-hour cycle. **(b)** Visualisation of the results from chi-squared periodogram analysis. Peaks in power indicate the frequency that is most dominant in the experimental group. **(c)** Quantification of (b). The frequency with the highest power per individual is found and the mean of the group calculated with 95% CIs. **(d)** A wavelet transformation using a 'morlet' wavelet. Wavelet transformations best visualise the how periodicity changes throughout the experiment, such as in dark:dark experiments, as shown here. Strength of 24 hour frequency is shown to decrease over the course of the recording.

3.5.2 Hidden Markov Models

HMMs originated in signal processing and have since been adopted across various fields, including bioinformatics, ecology, and behavioural research. Recently, their application to sleep research has demonstrated their ability to differentiate between distinct sleep states, such as deep and light sleep [319, 357, 358, 359]. HMMs are particularly useful for decoding latent behavioural states that underlie observable data, revealing complex patterns and transitions in animal behaviour [360]. HMMs will be used in *Chapter 4* of this study, providing greater detail to the background of HMMs.

HMM Components in Ethoscopy

Ethoscopy integrates the Python package *hmmlearn* into the *behavpy* ecosystem. *Hmmlearn* is a well-established HMM repository that offers several types of HMMs. Currently, *ethoscopy* utilises the ***CategoricalHMM*** class from *hmmlearn* [317].

To prepare for HMM training, users must create a categorical data column in *behavpy*, with states encoded numerically starting from 0 (e.g., 0 for immobile and 1 for movement). It is crucial that the dataset is fully populated, as missing time points will not be adjusted for during model training.

Model Training

When training an HMM, users specify the number of hidden states they wish to identify. For instance, a four-state model might include 'deep sleep', 'light sleep', 'quiet awake', and 'active awake'. The training process involves the following steps:

- **Iteration and Optimisation**: The model is trained iteratively over the dataset to optimise performance. By default, the model undergoes ten training iterations. Each iteration involves randomising transition matrices to mitigate the risk of local minima, with the model selecting the configuration that yields the highest log-likelihood score.

- **customisation**: Users can define and restrict specific state transitions by customising the initial transition matrix, allowing for tailored modeling approaches that better fit the experimental design or behavioural hypotheses.

Visualisation and Analysis

Once the model is trained, *ethoscopy* provides a suite of visualisation tools to interpret and quantify the decoded states:

- **Ethograms**: Visualise the probability of different states over time, offering insights into the duration and transitions between states (Fig. 3.6.a).
- **Split Versions**: Compare the probability of the same state over time between experimental groups or differently trained HMMs (Fig. 3.6.c).
- **Quantification Plots**: Assess and quantify state durations, percentage of transitions, and average state bout lengths, providing detailed insights into behavioural dynamics (Fig. 3.6.b).
- **Raw Decoded States**: Plot the predicted state at each time point alongside the observable sequence to get a visual understanding of how they are related (Fig. 3.6.d).

Ethoscopy's integration of HMM training, testing, and visualisation offers researchers a streamlined platform for in-depth behavioural analysis, enhancing the understanding of complex behavioural states and transitions.

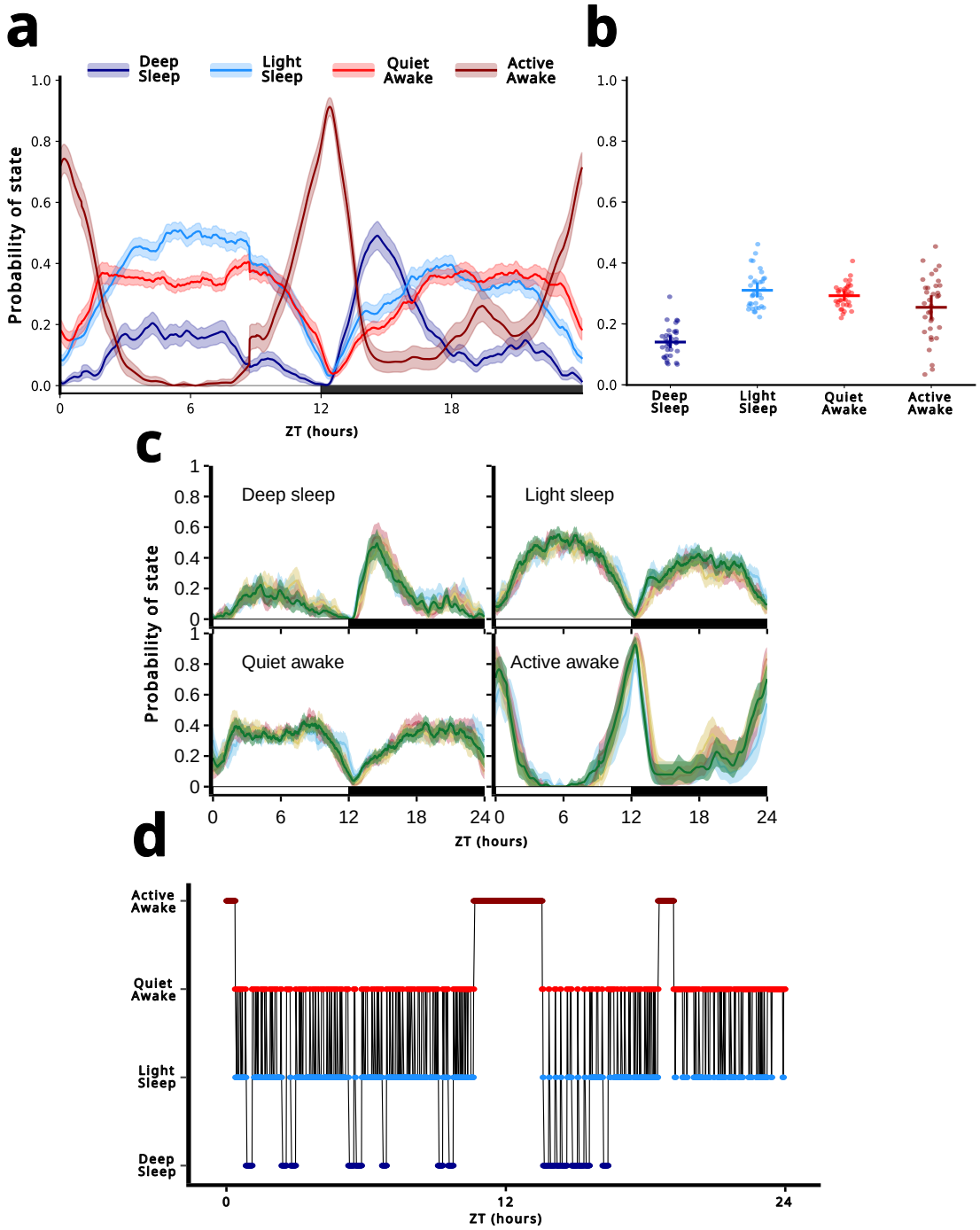


Figure 3.6: **Visualisation of the output of hidden Markov models in *ethoscopy*.** **(a)** An example dataset whose activity data was decoded by a 4-state model to investigate sleep stages. An overtime plot can show when each state is most likely to occur. **(b)** Quantification of (a) with mean and 95% CIs. **(c)** When comparing multiple experimental groups HMM outputs the overtime plots can be split by state to better visualise differences. Colours are unique to each experimental group and not the state. **(d)** An individuals decoded sequence can be plotted to visualise how state sequences interact.

3.6 Integrating Machine Learning

Historically, behavioural analysis has relied heavily on manual classification and hierarchical ordering of behaviours, a process requiring significant human effort and time [361, 362]. The repetitive nature of behavioural patterns makes ethology particularly amenable to machine learning (ML), which excels in pattern recognition and extracting insights from large, complex datasets [363].

Machine learning has become a powerful tool in behavioural research, particularly for supervised classification tasks. Combined with limb tracking software, ML can automate the scoring of behaviours, significantly reducing the time and effort required for manual classification [250, 251, 252, 364]. Furthermore, ML's ability to analyse data across both micro and macro timescales offers an unbiased method for identifying novel behaviours, which can be challenging for humans to conceptualise [365].

To facilitate the integration of machine learning into behavioural research, *ethoscopy* provides guidance on incorporating *HCTSA*/Catch22 [366, 325] and scikit-learn [326]. *HCTSA* (High-Content Time-Series Analysis) is a MATLAB-based software that performs extensive feature extraction, yielding over 7000 features. Catch22 is a Python implementation of *HCTSA*, focusing on 22 of the most descriptive time-series features.

Within the *ethoscopy* Github and tutorial website there are currently six notebooks that run through all the basics discussed so far, including circadian rhythm analysis and HMM creation and plotting. Additionally, there are also two notebooks specifically for *HCTSA/Catch22*. The first details how to augment an *ethoscopy* dataset into the matlab format required by *HCTSA*, expediting the process between the two. The second, using the Pythonic *Catch22*, runs in more detail. Demonstrating how you can combine the time series analysis tool of *Catch22* to generate datapoints that can be utilised by simple ML classification tools. Using a basic out of the box support vector machine classifier I was able to achieve an 80% accuracy in predicting the genetic background of the circadian mutants plotted (Fig. 3.5). The notebook also details a lot of the visualisation tools available in *seaborn* to explore data distribution and correlation.

These notebooks are not intended to be exhaustive guides to ML, but rather examples to show users how they can leverage the *ethoscopy* ecosystem as a starting point for ML exploration.

3.7 Summary

Ethoscopy stands as successor or alternative to *rethomics* the first software toolbox for the ethoscope. Like *rethomics*, *ethoscopy* is a comprehensive Python toolbox designed to streamline the analysis, visualisation, and interpretation of behavioural data, particularly within the context of circadian rhythms and sleep research. However, it expands upon this ecosystem to include machine learning and modelling through HMMs.

It is hoped that *ethoscopy* will reduce the burden on researchers and students in the analysis of data and the subsequent figures, producing high quality visualisations that can be used both for exploration and for publication.

Chapter 4

Modelling sleep stages with hidden Markov models

4.1 Is Drosophila sleep phasic?

Emerging evidence suggests that sleep in *Drosophila melanogaster* is not monophasic, but multiphasic. This observation aligns with a broader trend in sleep research. Studies have uncovered evidence of slow wave activity (SWA) sleep and active sleep in various non-mammalian species, including reptiles, fish, and cephalopods. These phases could be said to be at the least analogous to NREM and REM sleep, if not homologous [169, 178, 194, 88, 14].

Sleep in *Drosophila* can be distinguished from wake and rest by a decrease in brain activity (10-100 Hz) in the medial protocerebrum that corresponded with an increase arousal threshold [190, 367]. *Yap et al.* found SWA (7-10 Hz) in the central brain that induced sleep stage transitions most prominently at the start and end of a sleep bout, both spontaneously and when stimulated (GABA and dorsal fan shaped body activation). This was corroborated in *Raccuglia et al.* which found slower SWA (0.5-1 Hz) would increase in power as sleep pressure increased, dissipating in power when asleep [368]. Differing frequency bands appear to be due to experimental techniques, with the former measuring the dorsal fan shaped body and the latter measuring R5 neurons of the ellipsoid body. *Yap et al.* demonstrated that frequencies changed

in power over a bout of sleep, but they did not tie this to changing arousal thresholds [188]. Although earlier work from the same group showed a correlation between low frequency signals power spikes between 6-12 minutes and increasing arousal thresholds, prompting analogy to SWA (0-4 Hz) in late stage NREM sleep [189, 20]. Flies do have increasing arousal thresholds as time immobile increases [35], possibly indicative of a transition to a deeper sleep [283].

Beyond localised brain activity readings, a novel experimental setup in *Tainton-Heap et al.* measured the activity of 100s of neurons in a fixed fly via fluorescent calcium imaging [278]. Using the 5-minute rule of sleep to define the beginning of sleep, they demarcated five distinct phases: prior (5 minutes before sleep), early (first 5 minutes of sleep), mid (5-10 minutes), late (10 – pre-wake sleep), and pre-wake (5 minutes before wake) sleep. Both prior and late sleep have low total neuronal activity (1-5%), that differs significantly from awake (≈30%) and early (≈5%) activity. It could be argued early sleep activity could just be an awake brain whilst immobile, as it's neuronal overlap is not different when comparing two separate awake bouts. However, late sleep neuronal share is different to both early and prior, 5% and 4% respectively (23% awake-awake control). This difference is compounded by late and awake sharing 60% of neurons. Together, it appears prior and early sleep consists of selected neuronal firing to induce sleep followed by an unknown brain activity function which the author compares to REM sleep or paradoxical sleep, due to the activity spike. Following studies using the same techniques showed differing brain activity when inducing sleep opto-genetically or pharmacologically despite phenotypically similar observations, highlighting the problems with broadly considering all sleep bouts of the similar length the same [369].

Whilst the research provided is not uniform on what the stages could be or exactly when they occur, there is strong evidence to propose a new hypothesis, that *Drosophila* sleep is multiphasic, possibly with homologous architectural functions seen in mammalian sleep, but that is to be determined.

4.2 Modelling Sleep

When modeling sleep in *Drosophila*, it is important to approach the subject with caution, particularly when using mammalian sleep terminology. Terms like "light sleep" and "deep sleep," commonly associated with human sleep stages, are not directly applicable to insect sleep but are often used due to the absence of better alternatives [370]. For simplicity, I use these terms here as a shorthand: "light sleep" refers to states of lower arousal thresholds, and "deep sleep" to states with higher arousal thresholds.

Given these broad categorisations, and assuming that internal sleep processes manifest through observable behaviours, mathematical models offer a powerful tool for predicting sleep states [371]. Direct measurement of sleep states is invasive and often impractical, especially in small organisms like *Drosophila*. However, the rhythmic nature of behaviours such as walking, grooming, and feeding suggests they may provide indirect insights into internal sleep states. These behaviours are governed by circadian rhythms and could reflect homeostatic sleep changes in response to an individual's activity levels [372], similar to how sleep-deprived humans exhibit increased SWA [81].

If these assumptions are correct, there should be repetitive behavioural patterns, motifs, that correlate with specific sleep states.

4.2.1 Previous Attempts to Model Sleep

Numerous efforts have been made to model sleep in order to better understand its intrinsic rhythms and predict how an individual's sleep may respond to varying conditions. In humans, sleep modeling has become a significant endeavour, with wearable trackers integrated into smartwatches and rings to gain better resolution of metrics that are influential or measure sleep. These devices typically monitor heart rate and movement to infer sleep and sleep stages with varying degrees of accuracy [373]. Such tracked metrics are often calibrated against EEG and EOG data obtained in clinical settings, employing large datasets and machine learning

techniques to automatically classify sleep stages [374, 358]. Similar approaches have been successfully applied in mice, enabling automatic sleep scoring during experiments [359]. However, these mathematical models are largely predictive, they indicate which sleep stage is likely to occur at a given time but do not address how environmental factors influence sleep.

Several attempts have also been made to develop physiologically based mathematical models of the sleep–wake cycle, integrating elements such as neuronal population dynamics, homeostatic pressure, and circadian influences [375, 376, 377]. These models aim to define the rates of change and the interplay between multiple sleep–wake circuits that are robust under varying environmental pressures, such as changes in day length or enforced wakefulness. For instance, *Song et al.* extended previous physiological models to incorporate forced wakefulness and forced sleep, thereby predicting drowsiness and alertness in shift workers [378]. By utilising individual sleep patterns obtained from wearable devices and alertness diaries, the researchers identified a novel sleep–wake pattern, termed "adaptive circadian split sleep," which incorporates a late nap to sustain high alertness during unconventional working hours. Such mathematical models hold promise for personalising sleep recommendations tailored to an individual's needs.

In contrast, models of sleep in *Drosophila* are less refined, generally describing the interplay between homeostatic and circadian processes based on the two-process model. *Abhilash and Shafer* adapted earlier work by *Daan et al.* [379] to generate sinusoidal waves that serve as thresholds in their sleep pressure equation—an upper bound for sleep pressure and a lower bound for wake pressure [301]. Their model demonstrated that previously assumed independence between the two processes might be inaccurate; indeed, shortening of the circadian period was accompanied by a more rapid decay of homeostatic sleep pressure. Experimentally validated, this model explained variations in sleep–wake phenotypes through parameter changes in either the homeostatic or circadian components.

Hidden Markov models (HMMs) have also been widely employed in human and mouse studies to aid in the automatic scoring of EEG/EOG data, owing to their capacity to account for transitions between sleep states [26, 374, 358, 357]. In *Drosophila*, however, the inability to easily record brain activity in free-living individuals has led researchers to adapt these models

to translate behavioural observations into inferred sleep states. This approach was first demonstrated by *Wiggins et al.* with notable success, as the model predicted deeper sleep stages that correlated with increased arousal thresholds [319].

This chapter will build on the introductory discussion of HMMs from the previous chapter, further exploring their underlying principles, specific applications in *Drosophila* sleep research, and the insights they can offer.

4.3 The fundamentals of hidden Markov models

The fundamentals of HMMs lie in their ability to represent systems where underlying states are not directly observable but can be inferred through observable data. The key idea is that these hidden states influence the likelihood of certain observations occurring. HMMs have found application across various fields, ranging from speech recognition to bioinformatics, behavioural ecology, and notably, sleep research [380, 381, 360, 26].

HMMs operate on sequences where the process being studied is assumed to follow the Markov property. This property dictates that the probability of transitioning to the next state depends solely on the current state, independent of the sequence of preceding states. In other words, the system "has no memory" beyond the present moment. This property can be formally expressed as:

$$Pr(X_{n+1} = x | X_1 = x_1, X_2 = x_2, ..., X_n = x_n) = Pr(X_{n+1} = x | X_n = x_n)$$

This Markov assumption is applied twice within an HMM: first to the sequence of hidden states and secondly to the sequence of observable data [380]. While real-world data may not strictly follow these assumptions, they can still be used to model systems effectively if the simplifications provide an adequate approximation of the underlying dynamics.

4.3.1 Structure of hidden Markov models

The structure of a Hidden Markov Model (HMM) consists of five fundamental components [380]:

- **States**: These represent the hidden elements of the model and are determined by the user. The number of states, N, corresponds to the possible hidden states that the model seeks to learn.
- **Observations**: These are the measured data points that can be directly measured. For the HMMs applied in this context, the observations are represented as discrete categories corresponding to observable behaviours.
- **Transition Probabilities**: This is a matrix, A, that describes the likelihood of transitioning from one state to another. Each element A_{ij} represents the probability of moving from state i to state j. For any given state, the sum of its outgoing transition probabilities equals 1.
- **Emission Probabilities**: This matrix, B, captures the probability of an observation being generated from a particular state. Each element B_{ij} represents the probability of observing j given that the system is in state i.
- **Initial State Probabilities**: This component represents the probability distribution for the system's starting state. It defines which states are more likely at the beginning of the sequence.

4.3.2 Solving the fundamental problems of hidden Markov models

Rabiner [382] identified three fundamental problems that must be addressed when working with HMMs:

1. **Learning**: Given the sequence O and the set of states in the HMM, learn the HMM parameters A and B.

Learning revolves around adjusting the HMM parameters to maximise the likelihood of the observed data. This involves iteratively adjusting the model's parameters to maximize the likelihood of the observed data. The standard approach for this is the forward-backward or Baum-Welch algorithm, a specialized iterative Expectation-Maximization method [318]. This algorithm estimates the expected number of transitions and emissions for a given model and adjusts the parameters to better match the observed data. The process repeats until the model converges to a set of parameters that optimally explains the data [383, 380]. In *ethoscopy*, this step is executed via the ***hmm_train*** function using the *hmmlearn* package (hmm).

2. **Evaluation**: Given a model λ with matrices (A, B) and a sequence of observations O, what is the likelihood $P(O|\lambda)$.

   Although computing $P(O|\lambda)$ is conceptually straightforward, it is computationally intensive due to the exponential number of possible hidden state sequences. For a HMM with N states and a sequence length T, there are N^T possible paths. To overcome this complexity, the forward algorithm is used. This algorithm employs dynamic programming to efficiently compute the likelihood by combining paths with shared segments, drastically reducing the computational burden [380]. In *ethoscopy*, this likelihood calculation is used to evaluate models and select the best-scoring one during training.

3. **Decoding**: Given the sequence O and the model λ, generate the best sequence of hidden states, Q.

   Finally, if you're interested in the hidden states transition dynamics you will need to calculate the most likely sequence. The Viterbi algorithm is the standard method for this problem. Like the forward algorithm, it leverages dynamic programming but specifically tracks the highest-probability paths to determine the most likely sequence of hidden states. By backtracking through the recorded paths, Viterbi identifies the optimal sequence [323]. Within *ethoscopy*, Viterbi is the algorithm used to decode the hidden states, although alternative decoding methods are available.

These three core problems—learning, evaluation, and decoding—are all addressed in *ethoscopy's*

HMM implementation via the *hmmlearn* library [317]. The primary task remaining involves choosing the architecture of the hidden states to best capture the behavioural dynamics of the system under investigation.

4.4 Exploring and validating the hidden Markov models

4.4.1 Deciding the model architecture

The choice of HMM architecture was initially influenced by the approach of *Wiggin et al.*, who first showed the utility of a four-state model adapted from NREM/REM sleep modeling in mammals [319, 384]. However, given that these structures remain speculative in *Drosophila*, it was important to explore alternative models with varying numbers of states and different transition dynamics to better capture the nuances of fly behavior.

Limitations of Low-State HMMs

In this study, the number of hidden states was deliberately restricted to a small number to generate an easily interpretable model, with the hope that these few states would suffice to capture the dynamics of sleep, analogous to the stages observed in mammalian sleep. However, this restriction introduces several limitations that may affect the model's reliability and its ability to fully represent the underlying biological processes.

A low-state HMM assumes that the system is entirely described by fixed probabilities for state transitions and observations. In biological systems, these probabilities are often subject to variability in response to changing internal and external conditions. In principle, a highly parameterised or even infinite-state HMM could account for this variability by assigning a unique state to each subtle change in the stochastic process, thereby more accurately reflecting the true nature of sleep dynamics. While such a model might improve predictive accuracy by more closely matching the observational sequence, it would do so at the expense of interpretability, as each state could correspond to a minute biological process.

Moreover, the underlying Markov assumption—where the next state depends solely on the current state—implies a memoryless process. This simplification may be inadequate for capturing the temporal dependencies inherent in sleep behavior, such as those influenced by circadian rhythms or accumulated sleep pressure. By limiting the model to a few states, there is a risk of overlooking these longer-range dependencies that can be critical to understanding the complete stochastic properties of sleep.

4.4.2 Training and Scoring the Model

All models were trained using a dataset consisting of male Canton-S (CS) flies, originally used in the ethoscope study by *Geissmann et al.* [53] see *Methods* for details. The dataset was prepared for model training in two ways. First, following the methodology of *Wiggin et al.*, the observable behaviors were categorized into a binary classification: 'immobile' or 'moving'. Second, taking advantage of the ethoscope's enhanced detection capabilities, which can distinguish micro-movements like grooming and feeding, the 'moving' category was further split into two subcategories: 'micro-movements' and 'walking' [244]. This extra capability allows for a model with three observable states.

To determine the optimal HMM architecture, five models were generated for the two sets of observables, ranging from 2 to 6 states, including architectures inspired by *Wiggin et al.*(cite) and *Tainton-Heap et al.* [278] (*Table 4.1*). Each model underwent multiple training runs with randomized initialisations to ensure convergence to a global minimum (Winters-Hilt 2006). The best-performing model was selected based on its log-likelihood score on a 10% test segment (*see Methods for details*). Among all candidates, the four-state models for both the two- and three-emission models performed the best when evaluated using three criteria: log-likelihood score (yellow) [320], Akaike Information Criterion (AIC) (blue) [321], and Bayesian Information Criterion (BIC) (green) [322] (Fig. 4.1.a).

As anticipated, the six-state models scored poorly, as both AIC and BIC heavily penalised the additional complexity. This complexity was not justified by a significant increase in explanatory

power, primarily the length of time immobile. On the other hand, the simpler models with fewer states lacked the necessary complexity to adequately capture the observed data.

These findings validate the conclusions of *Wiggin et al.* that a four-state model best represents sleep from movement data. However, I opted for a slightly modified four-state architecture, despite the models' similar performance scores. In this new model, the two wake states can transition freely between each other, rather than only transitioning from an 'early wake' state to a 'full wake' state, (Fig. 4.1.b). This adjustment better differentiates a mildly active wake state from a highly active one, unlike the *Wiggin et al.* model where 'early wake' served primarily as a transitional state between sleep and 'full wake'.

Closer inspection of the decoded state sequences for the *Wiggin et al.* architecture revealed that 'deep sleep' was never transitioned into (Fig. 4.2). Using the pre-trained transition values from *Wiggin et al.* led to more comparable decoded sequences but yielded less overall 'deep sleep.' This discrepancy is likely due to differences in datasets, as the *Wiggin et al.* model was trained with female CS flies using different HMM training software and DAMS tracking [319]. Since my focus was on using a model trained with ethoscope data, which better captures fly

Number of states	**Sleep states**	**Awake states**	**Reference**
2	1: 'asleep'	1: 'awake'	N/A
3	1: 'deep sleep' 2: 'light sleep'	1: 'awake'	N/A
4	1: 'deep sleep' 2: 'light sleep'	1: 'early wake' 2: 'full wake'	*Wiggin et al.*[319]
4	1: 'deep sleep' 2: 'light sleep'	1: 'quiet wake' 2: 'active wake'	This study
6	1: 'early sleep' 2: 'mid sleep' 3: 'late wake' 4: 'prior-wake'	1: 'prior-sleep' 2: 'wake'	*Tainton-Heap et al.*[278]

Table 4.1: A breakdown of the architecture of the hidden Markov models presented in *Figure 4.1*

movement at all times compared to DAMs [244, 239], the modified architecture was preferred.

It was hypothesized that the three-observable model would offer more informative insights, as micro-movements like grooming or feeding could act as motifs predictive of sleep, akin to nesting behavior seen in mice [385]. However, the top-performing models with three observables failed to effectively predict the active awake state, albeit with predictions of light sleep and deep sleep that were largely similar (Fig. 4.2). Therefore, the decision was made to proceed with the two-observable four-state model. Interestingly, a breakdown of movement profiles for the predicted quiet and active awake states in the two-observable four-state model revealed distinct patterns (Fig. 4.1.c). The quiet awake state consisted of 40% micro-movements and 55% walking, whereas the active awake state comprised 7% micro-movements and 90% walking. Despite being agnostic to the underlying division of activities, the model segmented the behavioral data in a logical and interpretable manner.

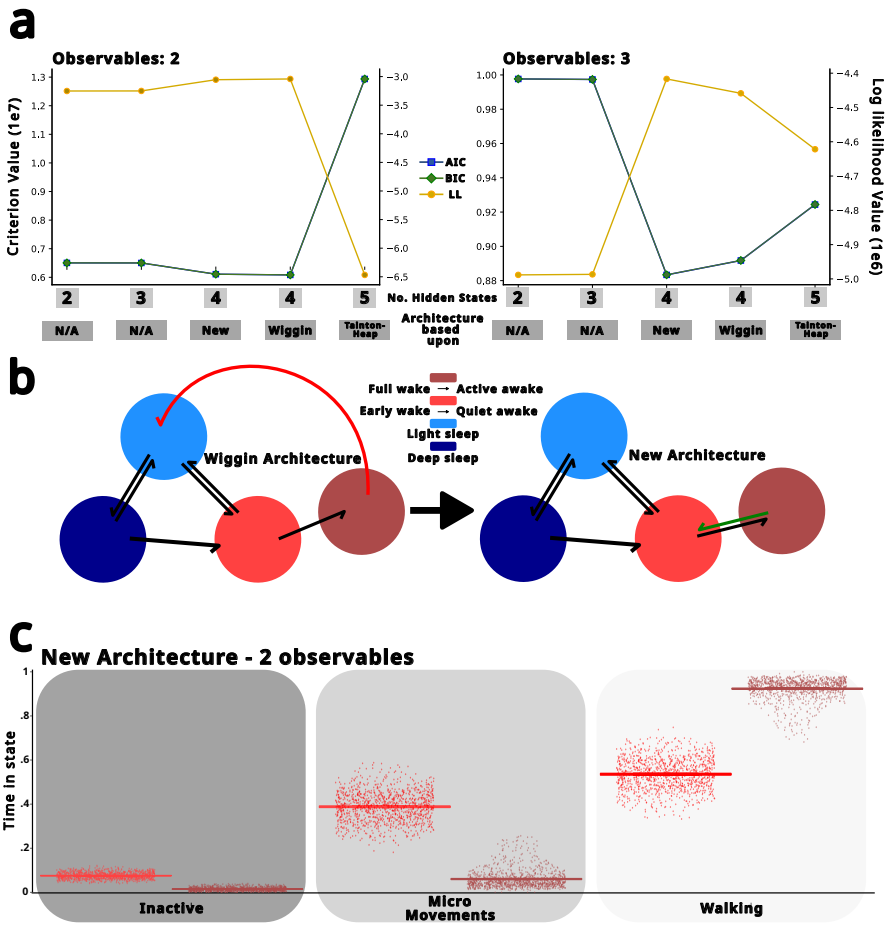


Figure 4.1: **A modified version of the Wiggin four state model scores the best.** **(a)** Scoring the models with architecture from *Table 4.1* with log likelihood (yellow), Akaike Information Criterion (AIC) (blue), and Bayes information criterion (BIC) (green). Log likelihood values closest to 0 have the least error. AIC and BIC scores closest to zero best explain the data. Both AIC and BIC penalise more complex models to prevent overfitting. **(b)** This studies four state model (right) is a modified version of the Wiggin model (left). 'Deep sleep' was prevented from transitioning into 'active awake', which was also allowed to transition into 'quiet awake'. Awake states names were also changed from 'early wake' to quiet awake' and 'full wake' to 'active awake' to better reflect the studies findings. **(c)** Breakdown of the activity of each awake state (quiet and active) for the studies four state model with two observables. 'Quiet awake' has greater proportion of micro-movements and inactivity than 'active awake' despite being agnostic of their differences.

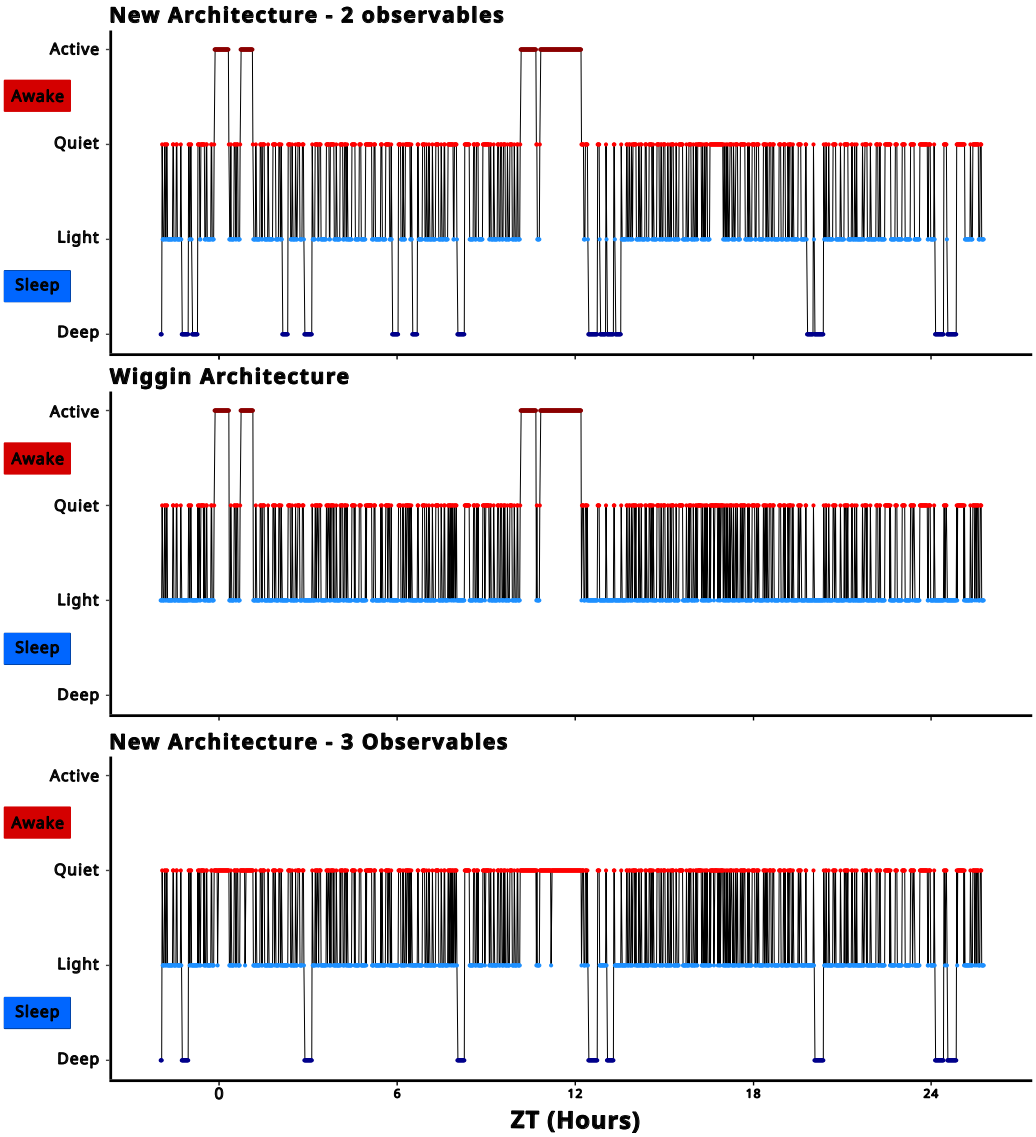


Figure 4.2: **The new model HMM architecture with two observables is the best representative of the data when decoded**.
The new HMM architecture with two and three observables, as well as the Wiggin HMM architecture were decoded into a HMM state sequence. Only in the new architecture with two observables were all states observed.

4.4.3 Describing the decoded model

With the model established, examining the transition and emission probabilities (Fig. 4.3.a) does not provide immediate, tangible insights into the predicted sleep patterns. Instead, decoding the dataset used to train the HMM reveals the posterior probability of each state for each specimen, translating the observable behaviors into a sequence of hidden states (Fig. 4.3.b).

The average probability of each state varies over time with a daily rhythm, with 'deep sleep' increasing above 'light sleep' between ZT13-16 at night (Fig. 4.3.c). A period previously associated with a deeper sleep due to the increased length of sleep bouts and arousal threshold [189, 264, 35, 283]. 'Light sleep' and 'quiet awake' follow a similar pattern, consistently prevalent throughout the day and night, decreasing during the morning and evening peaks when 'active awake' is most prevalent. An activity pattern consistent with *Drosophila*s' crepuscular activity [275, 274, 283]. Interestingly, unlike the findings in *Wiggin et al.* the combined sleep states total exceeds the 5-minute calculation, 15.4% more in total (Fig. 4.3.g&h).

The increased prediction of sleep stems from 'light sleep' bouts being between 1 and 11 minutes long, classifying some bouts of immobility below 5 minutes as sleep that would have previously been excluded (Fig. 4.3.e&f). This discrepancy suggests that the HMM model is more sensitive to sleep patterns, potentially distinguishing less than 5-minute sleep bouts from wake bouts, a hypothesis to be explored in the next section.

Predicted 'deep sleep' and 'light sleep' are segmented by time, albeit with a small crossover window at 11 minutes (Fig. 4.3.e&f). Any bout of immobility that is 11 minutes or longer will be wholly classified as 'deep sleep', any whose total length is shorter will be 'light sleep'. The model does not demonstrate a transitional type of sleep, such as early sleep being 'light sleep' that changes to 'deep sleep' with time. This classification puts it at odd with the mammalian sleep and the aims of the design of the HMM architecture.

Over the whole day 'light sleep' (34%) is the most frequent state, followed by 'quiet awake' (30%), 'deep sleep' (18%), and 'active awake' (17%) (Fig. 4.3.d). The most frequent states, 'light sleep' and 'quiet awake' are the middle states. They have a much lower average bout length

which is made up for by frequent transitions. If correct, this predicted behaviour would suggest that D.melanogaster, when not very active or having consolidated sleep, oscillate between short sleep bouts, 'light sleep', and stationary actions such as grooming, 'quiet awake'.

Whilst the sleep states are segmented approximately by time, the awake states can emit as either 'inactive' or 'active' and have very different bout timing and averages (Fig. 4.3.e&f). Calculating the number of bouts with at least a single period of inactivity (1 minute) reveals that nearly 59% of 'quiet awake' includes a period of inactivity compared to 50% for 'active awake' (Fig. 4.3.f). It seems both active states are interspersed with at least one minute of inactivity, which within 'quiet awake' compliments the increased level of micro-movements.

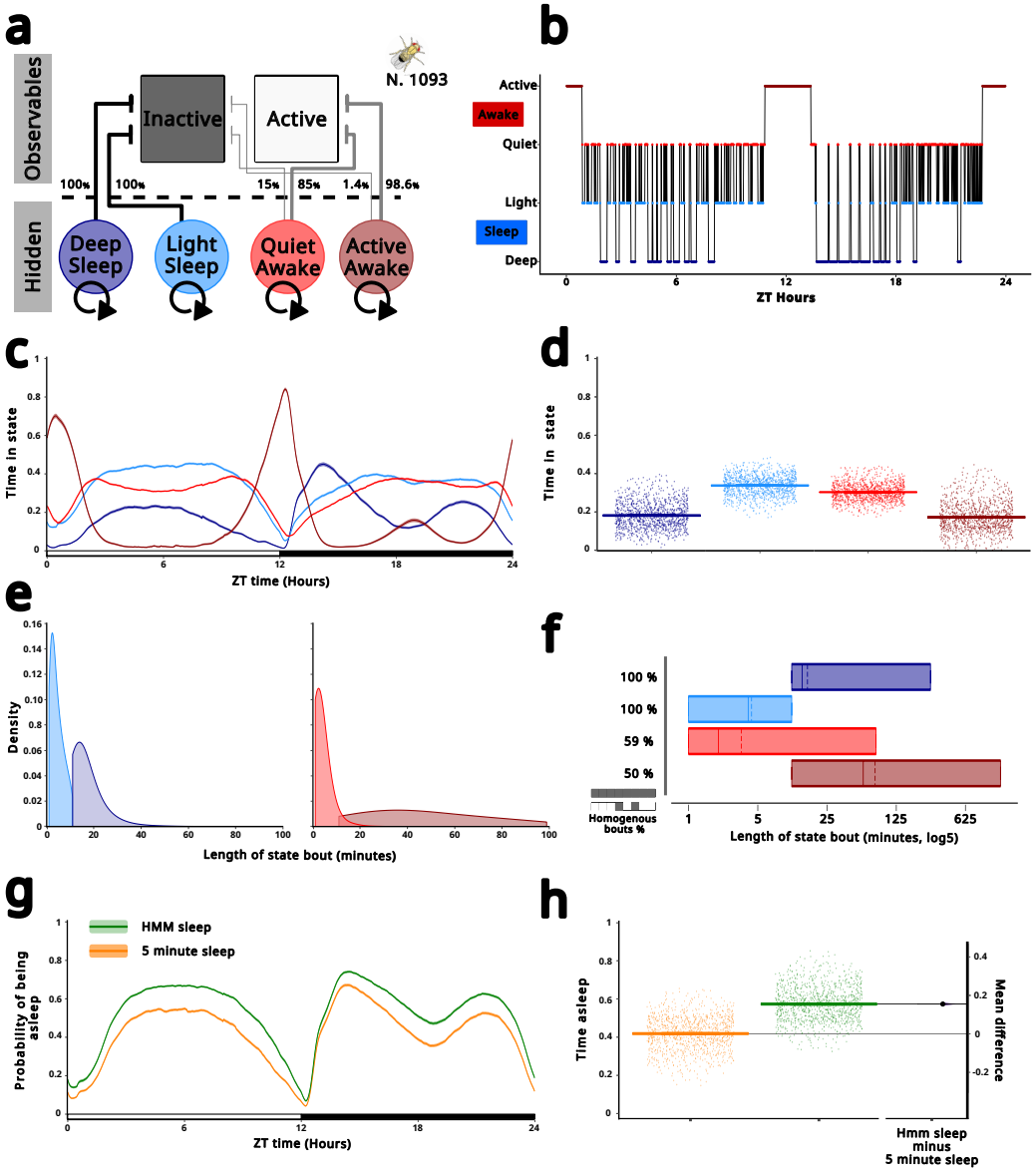


Figure 4.3: **HMM predicted sleep states have unique characteristics and vary over the day**.
(a) A schematic of the new four state HMM. 'Deep sleep' (dark blue) and 'light sleep' (light blue) can only emit as inactivity. 'Quiet awake' (light red) and 'active awake' (dark red) can emit as both inactive and active. 'Quiet awake' is more likely to be inactive (15%) than 'active awake' (1.4%). **(b)** An example behavioural sequence decoded with the HMM from (a). **(c)** The time in each state over a 24 hour day (12:12, light:dark). 'Active awake' if most prevalent during the morning and evening, and 'deep sleep' is dominant in the early night. **(d)** Quantification of (c). Mean and 95% CIs are plotted. **e** A kernel density estimate of the lengths of each states (mins.). **f** Minimum and maximum lengths of each state with their mean (dotted line) and median (solid line), the x-axis increases in increments of log5. 'Deep sleep' and 'light sleep' have little overlap (10-11 mins.). The y-axis indicates the percentage of states that contain at least one inactive observable. **g** The likelihood of being asleep as being predicted by the HMM (green) and the five-minute rule (yellow) (12:12, light:dark). **h** Quantification of (g). HMM predicted sleep is 15.4% more than the five-minute rule.

4.4.4 Validating the models predictions

A model's description is all conjecture unless it can be shown the predicted behavioural states are reflected in how it interacts with real world stimuli. For sleep the most obvious change in interaction is a reduced response to external cues [386], the measure by which sleep was established in D.melanogaster. Typically, by mechanical stimulus [274, 275, 35, 189], although there are examples of light [190] and heat being used as a stimulus [71, 185].

However, perception and response to external stimuli is not linear against magnitude but is discriminative. As shown by sleeping humans response to their own names [387] as well as conceptually similar observations in model mammals [388, 389]. This concept has recently been applied to *D.melanogaster* in *French et al.* where during sleep bouts, the response rate to differing puffs of air borne odours changed depending on the salience and hunger state of the fly [221].

Utilising a solution of apple cider vinegar diluted to 10% strength in water (ACV), which was established as a strongly salient odour in *French et al.*, and a modular extension for the ethoscope (see *Methods*), I probed the activity of male, wildtype flies by delivering a puff of air or ACV after 30 seconds of immobility [221]. The delivery was gated by a randomising function that only allowed the puff to be delivered 10% of the time, so as not to over challenge the flies, whilst providing ample coverage of all states. A wake event was classified if there was any movement within 10 seconds post puff.

Response rate per state for both puffs of air and ACV were significantly different from each other and their respective spontaneous movement, confirming the predicted states are representative of a change in the internal behavioural state *(**Air**: deep sleep = 0.03 std:0.01, light sleep = 0.17 std:0.17, quiet awake = 0.24 std:0.206, active awake = 0.50 std:0.40, **ACV**: deep sleep = 0.045 std:0.04, light sleep = 0.28 std:0.17, quiet awake = 0.40 std:0.19, active awake = 0.64 std:0.26)* (Fig. 4.4.a). Likewise with *French et al.* [221] this work demonstrates the salience of the odour dictates the arousal threshold, with the flies more likely to respond to ACV in all states compared to air (**Air**: avg. = 23.8%, **ACV**: avg. = 34.2%).

Of particular interest is the differing response rates between the earlier parts of 'quiet awake' and 'light sleep', given temporally the states can be thought of as transitory states often only a few minutes apart that transition frequently into each other (Fig. 4.4.b&c). 'Light sleep' bouts from 2-5 minutes have a lower response rate (32.6%) to comparable 'quiet awake' bouts (44.0%), which suggests flies are entering sleep much earlier than 5 minutes, a refutation of the 5-minute rule. If true it means we have been chronically underestimating sleep in *D.melanogaster* as well as possibly under sleep depriving them if assays were only triggering a sleep deprivation routine after 5 minutes.

Comparing the sleep states there is a large difference in response, 'light sleep' (**ACV** = 28.0%), 'deep sleep' (**ACV** = 4.60%) (Fig. 4.4.a). This could potentially be strong evidence that sleep is not monophasic in *D.melanogaster* but more like the multi-phasic mammalian sleep that also has differing arousal thresholds per sleep state [14, 13, 25]. However, as mentioned previously the sleep state predictions are not transitory from 'light sleep' to 'deep sleep' over time immobile, but a block classification given the total length of time that bout is immobile. This is clearly demonstrated in the 0% response rate for 'deep sleep' during the early periods of the bouts (1-10 minutes) as any positive response would fix the total bout length to 10 minutes or less, resulting in a 'light sleep' classification and therefore bringing 'deep sleeps' response rate down (Fig. 4.4.b).

As the criteria for sleep is time immobile, looking at the response rate over minutes inactive we can see a gradual decrease in response rate from minute one (Fig. 4.4.d). There is no large change as seen in earlier studies [71] or what we could expect given the large arousal difference between 'light sleep' and 'deep sleep'.

The aberration in response rate over time for 'light sleep' is evident in the rapid increase in responsiveness after 8 minutes, surpassing the response rate seen during 'quiet awake' and approaching that of 'active awake' (Fig. 4.4.b). It is highly unusual that a fly, having remained immobile for such an extended period, would exhibit a responsiveness comparable to an active fly. This trend is not mirrored in the response rate of inactive flies (Fig. 4.4.d).

When 'light sleep' is manually classified into bouts of maximum lengths of 5, 7, 11, 15, or

20 minutes, the upward trend in response rate persists (Fig. 4.5). This suggests a selection artefact: the closer a bout approaches its upper time limit, the more likely it is that the fly wakes up, which is then recorded as a positive response. Flies that do not respond are more likely to remain asleep for an extended period, transitioning into a state classified as 'deep sleep'. This quirk in classification appears to influence the interpretation of response rates during 'light sleep', as it skews the data towards increased wakefulness near the upper limit of the sleep bout.

To assess whether the state transition probabilities captured the daily dynamics of fruit fly sleep, we generated 1000 simulated runs (see Fig. 4.4). Each simulation was initialized in the 'active awake' state—reflecting the most likely state at the start of the day—and allowed to evolve over two simulated days. However, the resulting sequences failed to reproduce the characteristic daily patterns of fruit fly activity (Fig. 4.3.c). Instead, the state probabilities quickly converged to a narrow range between 20% and 40% for all states. This convergence suggests that the estimated transition probabilities do not inherently incorporate information about the circadian rhythm. It appears that the assumption of stationarity in these probabilities neglects the time-varying influences present in biological systems. These findings are consistent with the work of *Abhilash and Shafer*, who demonstrated that accurate modelling of the two-process model of sleep requires more dynamic descriptive equations [301].

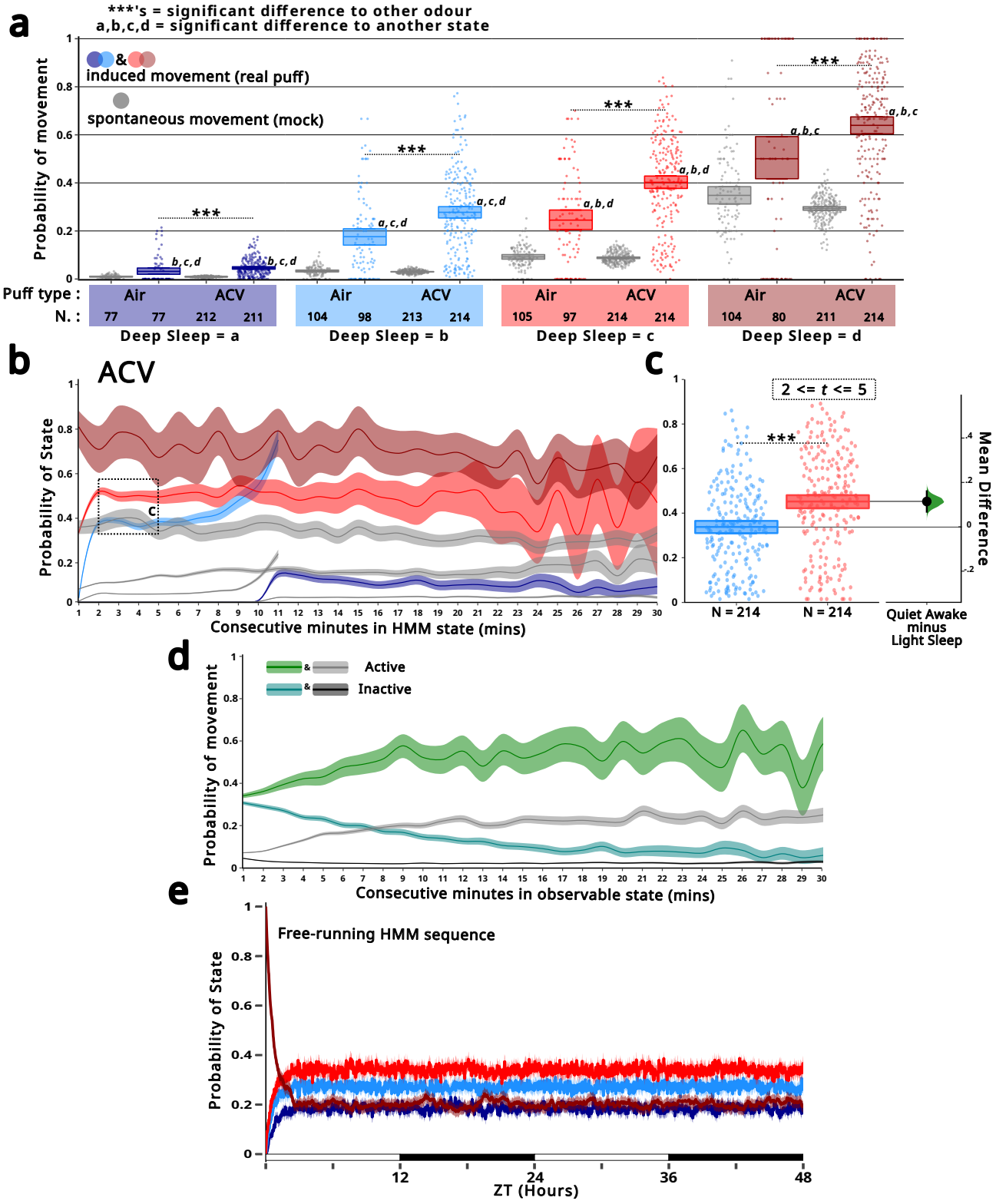


Figure 4.4: **Each predicted HMM state has a unique arousal threshold.**
(a) The likelihood of a fly moving after the delivery of a puff of air or apple cider vinegar (ACV) in each state. Each state's response rate was significantly different compared to each other and the type of stimuli. Spontaneous movement was calculated as the likelihood of moving after a mock puff. The mean and 95% CIs are plotted. Significance between air and ACV is denoted with *'s (*** ≤ 0.001). Significance between states is denoted by the letters *a* (to 'deep sleep'), *b* (to 'light sleep'), *c* (to 'quiet awake'), and *d* (to 'active awake') **(b)** The response rate of each state to ACV at different time points during a bout. The mean and 95% CIs are plotted. For most time points response rates are separate, except for between 10 and 11 minutes for 'light sleep'. **(c)** Quantification of 'light sleep' and 'quiet awake' between 2 and 5 minutes as highlighted by the dotted box in (b). The response rate of 'quiet awake' was 11.4% greater than 'light sleep'. **d** The response rate of a fly as they are consecutively active (green) or inactive

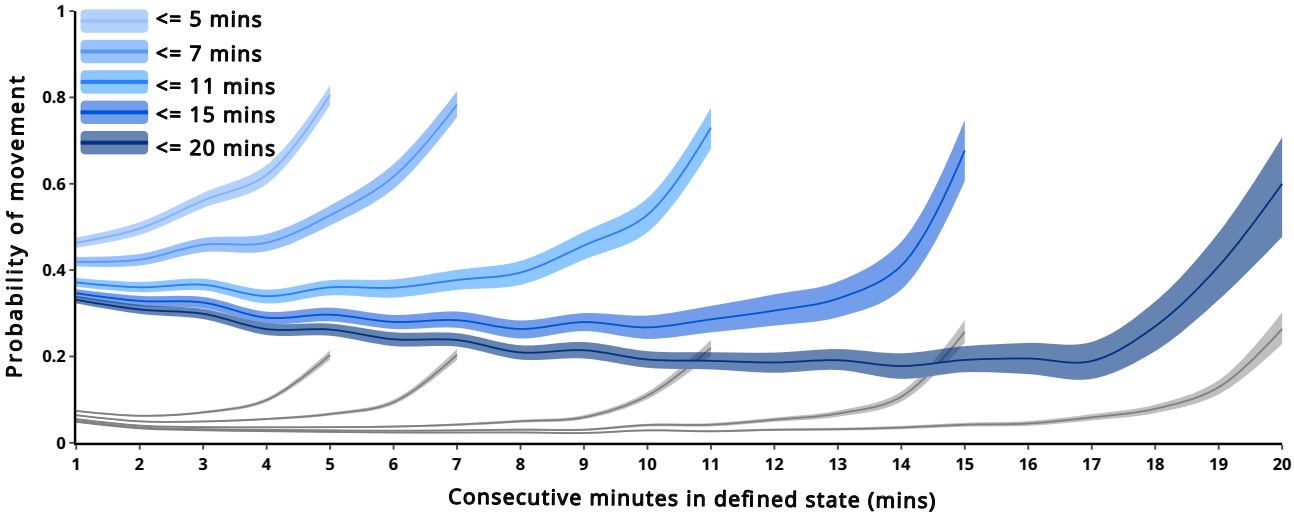


Figure 4.5: **Manually segmenting light sleep classification reproduces an uptick in response rate at the end**.
Sequences of inactivity were manually segmented to be less than 5, 7, 11, 15, and 20 minutes. This segmentation replicated the uptick of response rate at the end of the bout, identifying it as a quirk of the modelling and not a behavioural trait.

4.5 Discussion

The model appears to accurately predict four behavioural stages in *D.melanogaster* as measured by arousal threshold, including two sleep states.

Taken at face value, the model appears to be a strong additional tool in describing *D.melanogaster* sleep. The model can be retroactively applied to flies of the same or similar background to provide more information on the type or quality of sleep the fly is getting in response to the experimenter's conditions. The model can also be trained on mutants or variants to see if there are differences in their baseline sleep. Although not shown here, the same model architecture was used to train a model with wildtype female CS flies, producing a slightly different transition matrices.

The validation of the model can be critiqued as the decoding is applied retroactively to the response dataset. For example, taking a period of immobility of 1.5 minutes. At 1.5 a puff is given, a positive response will generate an observable sequence of ['immobile', 'moving'] and a negative response ['immobile', 'immobile']. The former would likely be classified as 'quiet awake' and the latter as 'light sleep', so the response can be seen as dictating the state and not the other way round. This can be clearly seen for the response rate at 1 minute for 'light sleep' and less than 10 minutes for 'deep sleep' which are both 0%, as any response would change the classification to 'quiet awake' and 'light sleep' respectively (Fig. 4.4.b). However, this is not true of all time points in a state. For example, the differing response rate between 2-5 minutes for 'light sleep' and 'quiet awake' (11.4%) (Fig. 4.4.c). At these given times the response has no bearing on the classification, yet there is a clear difference in average response rate, indicating the model is reflecting something true to reality.

Observing the variance of the sleep states, it can be clearly seen that when responding to ACV 'light sleep' has large variance with some flies continually responding in 'light sleep' and others never responding (Fig. 4.4.a). In comparison 'deep sleep' has some variation but it is considerably smaller for ACV response, with air response being mostly 0%. This could be explained by natural variation within flies, how each fly's arousal threshold changes with sleep

and how salient they find ACV. But when this is viewed in parallel with the gradual decrease in response rate over time inactive (Fig. 4.4.d) it can inform a different view, one that there are no separate sleep states. The HMM segments time inactive into two discrete states that have differing response rates. If you were to artificially segment your own states by time inactive, say every additional 5 minutes inactive is a new sleep state you would still get differing response rates per state as the response rate is always decreasing till roughly 20 minutes.

It could be viewed that the lowest response rate around 2-5% of deep sleep is the baseline response rate for a sleeping fly in general. What we see as a decrease in response rate is an increasing likelihood that a fly is asleep. In other words, during 'light sleep' we see only a fraction of the flies asleep at this time and this fraction causes the overall decrease compared to 'quiet awake'. This would also explain the high variance, as it is a population mix of awake and sleeping flies. The 'deep sleep' state is then just a period when it is most likely all flies are asleep. This logical issue is one that affects the 5-minute rule too, as experiments were just looking to find the first moment in time response rate changed significantly [275].

Overall, the HMM does provide greater insights for describing *D. melanogaster* sleep beyond the traditional framework. The HMM described here demonstrates that flies are sleeping for shorter bouts than previously accounted for and that arousal threshold changes with time inactive. However, as with any measure that relies upon activity data and arousal threshold alone, it can only be used as an informer of the likelihood that a fly is asleep, which in turn can be used in general population statistics. But it is not much closer to classifying sleep on an accurate individual basis in flies, much like the 5-minute rule.

4.6 Applying the hidden Markov model to multiple *Drosophilids*

The power of the insight from HMMs can be explored by how differing sleep backgrounds entrain the model. The *Drosophila* genus has a wide variety of species, many thriving in

highly divergent ecological niches in comparison to the generalist of the genus *D. melanogaster* [232, 230, 390]. These niches require differing behaviours that are reflected in their sleep patterns [391, 392, 334, 393].

4.6.1 Species background

The classification of *Drosophila* species dates back to the seminal work of geneticist Alfred Sturtevant in the 1920's, who organised 242 specimens into subgenera and species [394, 229, 395, 396]. Since then, over 1200 species have been identified, with 90% belonging to either the *Sophophora* or *Drosophila* subgenera. These subgenera are further divided into groups and subgroups [397].

In this study, seven *Drosophila* species were selected from different ecological niches and global regions. To provide a comparative baseline, a wild-caught strain of *D. melanogaster* was included alongside the standard lab strain. Of the selected species, only *D. virilis* belongs to the *Drosophila* subgenus, while the others fall within the *Sophophora* subgenus (Fig. 4.6).

Sophophora **subgenus**

Within the *Sophophora* subgenus, there are three primary clade of the species presented: (1) *D. melanogaster*, *D. simulans*, and *D. sechellia*; (2) *D. erecta* and *D. yakuba*; and (3) *D. willistoni*. *D. melanogaster*r, a global generalist, is thought to have originated in sub-Saharan Africa and spread globally over the last 10,000 to 15,000 years [230, 398, 231].

D. simulans is the closest relative to *D. melanogaster* in this study, diverging between 2-3 million years ago and is also a generalist species. Unlike *D. melanogaster* they prefer more unpopulated areas, specifically those areas in Eastern Africa, Madagascar, Seychelles and Mascarene islands [390]. *D. simulans* is joined in the Seychelles by its nearest relative, the aptly named *D. sechellia*. *D. sechellia* is endemic to the Seychelles and is specialised towards the typically toxic fruit *Morinda citrifolia* (morinda) [390]. The toxin in morinda, octanoic acid, is preferentially sought by *D. sechellia* when it is avoided by others. Demonstrating a preference rather than

an indifference to the toxin. This preference and adaptation were found to be multifactorial genetically [399]. In fact, this adaptation was found to have a negative pleiotropic effect, reducing the number of ovariaoles by 50-60% in comparison to *D. simulans*. This led to egg production rate 60% of their cousins. This reduction could be partially reversed when allowed to oviposit on morinda rather than lab media [400, 401].

Adaption to morinda has also lowered the production rate of L-dopa, the dopamine precursor, as it is supplemented from the fruit. *D. simulans* on non-morinda diets have reduced L-dopa level, but contradictorily elevated levels of dopamine when compared to *D. melanogaster* [402]. As of now, there are no conclusive theories to the contradictory levels both L-dopa and dopamine, although some have suggested that it could be to shield against octanoic acid [402].

The next clade includes *D. erecta* and *D. yakuba*, both native to sub-Saharan Africa. While

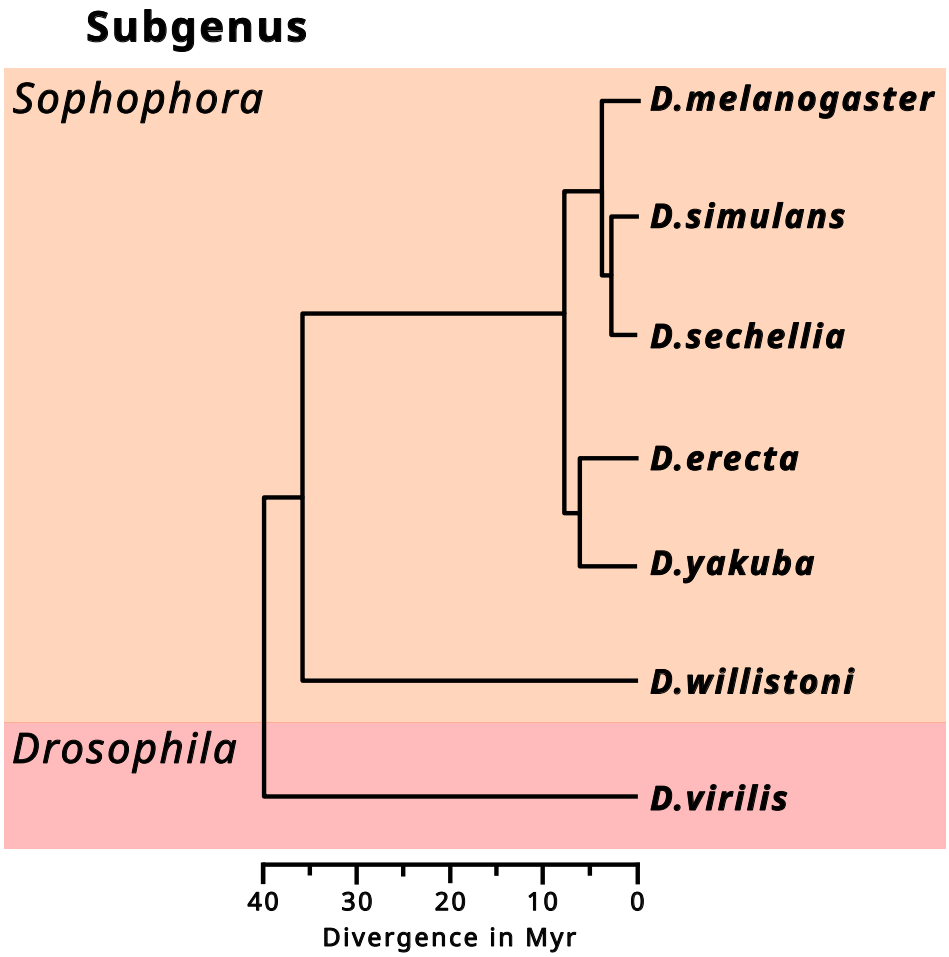


Figure 4.6: **A partial pylogenetic tree of the selection of *Drosophila* used in this study.**

D. yakuba is a generalist, *D. erecta* is restricted to the coastal regions of the Gulf of Guinea, specialising in *Pandanus* fruit. Seasonal availability of *Pandanus* forces *D. erecta* to feed and breed on alternative fruits during off-seasons [390, 403].

D. willistoni, the most distantly related species in this subgenus, inhabits regions stretching from southern Florida to South America and the West Indies [404, 405].

Drosophila **subgenus**

In the *Drosophila* subgenus, *D. virilis* is characterised by its cosmopolitan distribution and evolutionary adaptability. Originally thought to have emerged in the arid regions of Iran/Afghanistan or the forests of China, *D. virilis* is now widespread globally [406, 407, 408]. *D. virilis* have been used as a model in study the evolutionary components of their rapid expansion into novel habitats [408]. Its adaptability is linked to various traits, including weak species discrimination during mating [407], variable male courtship songs [409], and high tolerance for extreme temperatures [410], high altitude [411] and ethanol [412]. Notably, *D. virilis* is approximately 30% larger than the other species in this study, which limited its movements partially in the glass house tubes [393].

4.6.2 HMM derived sleep for Drosophilids

Baseline activity data from all species was utilised to train a four-state HMM, as previously described. Notably, for wild *D. melanogaster*, the pre-trained HMM from the lab strain of *D. melanogaster* was applied due to persistent aberrations observed in the species-specific HMM. Arousal thresholds were assessed through mechanical stimulation using puffs of air, as opposed to ACV, due to varying levels of salience to the odour among species.

All species displayed similar circadian rhythms, with peaks of 'deep sleep' during the midday siesta, except for *D. erecta*, whose midday siesta predominantly consisted of 'light sleep' instead (Fig. 4.7.a). This deviation in *D. erecta* is consistent across the day, with a 'light sleep' to 'deep sleep' ratio of 10.2:1 —almost ten times greater than the average ratio of 1.5:1 observed

in other species. The total amount of 'deep sleep' was relatively consistent across 6 of the 8 species, averaging around 20%. However, *D. erecta* and *D. simulans* were outliers, with 5.0% and 30.0% of total sleep as 'deep sleep,' respectively.

'Deep sleep' generally exhibited a reduced presence during daylight hours compared to 'light sleep,' except during ZT12-15, at the beginning of the night (Fig. 4.7.a). The exception was *D. erecta*, which displayed its highest amount of 'deep sleep' during this period, though it still did not surpass the amount of 'light sleep'. Previous studies have demonstrated that the first three hours of the night typically contain the longest bouts of sleep, aligning with observations of 'deep sleep' prevalence in this window [283].

The findings suggest that while the overall architecture of sleep is conserved across the Drosophilids, the specific patterns and distribution of sleep states can vary significantly, potentially reflecting ecological or evolutionary adaptations specific to each species.

All trained models applied the same criteria for demarcating 'light sleep' from 'deep sleep,' based on the duration of sleep bouts, as discussed previously (Fig. 4.8). For *D. melanogaster*, the threshold at which 'light sleep' was reclassified as 'deep sleep' was set at 11 minutes, the shortest of all species examined. The thresholds for the other species were as follows: *D. simulans* at 12 minutes, *D. sechellia* at 15 minutes, *D. erecta* at 26 minutes, *D. yakuba* at 12 minutes, *D. willistoni* at 23 minutes, and *D. virilis* at 17 minutes. Notably, *D. simulans* exhibited a threshold similar to *D. melanogaster* but displayed a much higher overall time spent in 'deep sleep' (30% compared to 17%), suggesting a higher frequency of entering consolidated sleep (Fig. 4.7.a&b).

D. willistoni, despite having a high threshold for 'deep sleep,' exhibited an average total time spent in this state. This likely indicates that *D. willistoni* achieves its 'deep sleep' through longer, though less frequent, bouts of consolidated sleep.

D. erecta demonstrated the highest threshold at 26 minutes, coupled with the shortest maximum duration and spread of 'deep sleep' (Fig. 4.8). This may explain its low total amount of 'deep sleep,' as the species enters long consolidated sleep bouts infrequently and for shorter peri-

ods. One possible explanation for this could be an overestimation of the 'deep sleep' threshold by the model. This is suggested by the observation that *D. erecta* spends 54% of its time in 'light sleep'—defined as inactivity bouts between 1 and 26 minutes. Interestingly, the median response rate for 'light sleep' in *D. erecta* is 25%, which aligns with other species. If the predicted 'light sleep' included both 'light' and 'deep sleep' states, the response rate would likely be lower than the species average. Furthermore, there is no obvious difference in the response rate over time during inactivity for *D. erecta* compared to other species, as it consistently decreases over time (Fig. 4.7.c).

If long consolidated sleep is crucial for Drosophilids, *D. erecta* might be an outlier, achieving the functions typically associated with 'deep sleep' through shorter sleep bouts, a phenomenon observed in other species across the animal kingdom [123]. This potential adaptation could reflect a unique evolutionary strategy within the species, allowing it to meet its physiological needs through a distinct sleep architecture.

The total amount of 'light sleep' varies significantly among species, with wild *D. melanogaster* exhibiting the least (21%), which is notably lower than that of the lab strain. This reduction in 'light sleep' is compensated by increased time spent in the 'active awake' state (Fig. 4.7.b). This discrepancy highlights the utility of the same HMM for quickly visualising differences between experimental groups, demonstrating that wild *D. melanogaster* tends to sleep less, at the expense of shorter bout sleep, not longer consolidated sleep.

In general, all species tend to spend more time in 'light sleep' than in the 'quiet awake' state, with the exception of wild *D. melanogaster*. Across all species, the response rate during 'light sleep' is significantly higher than during 'deep sleep' (Fig. 4.7.d), indicating that the model consistently differentiates between these sleep states, regardless of arousability. The response rates for 'light sleep' range between 20-40% across most species, except for *D. yakuba*, which exhibits a notably lower response rate of 12%. This lower response rate in *D. yakuba* could suggest that this species enters a deeper sleep more quickly. However, *D. yakubas'* response to air puff stimulation is low across all states except 'active awake' (Fig. 4.7.c&d), which might indicate a greater tolerance to disturbances during restful states.

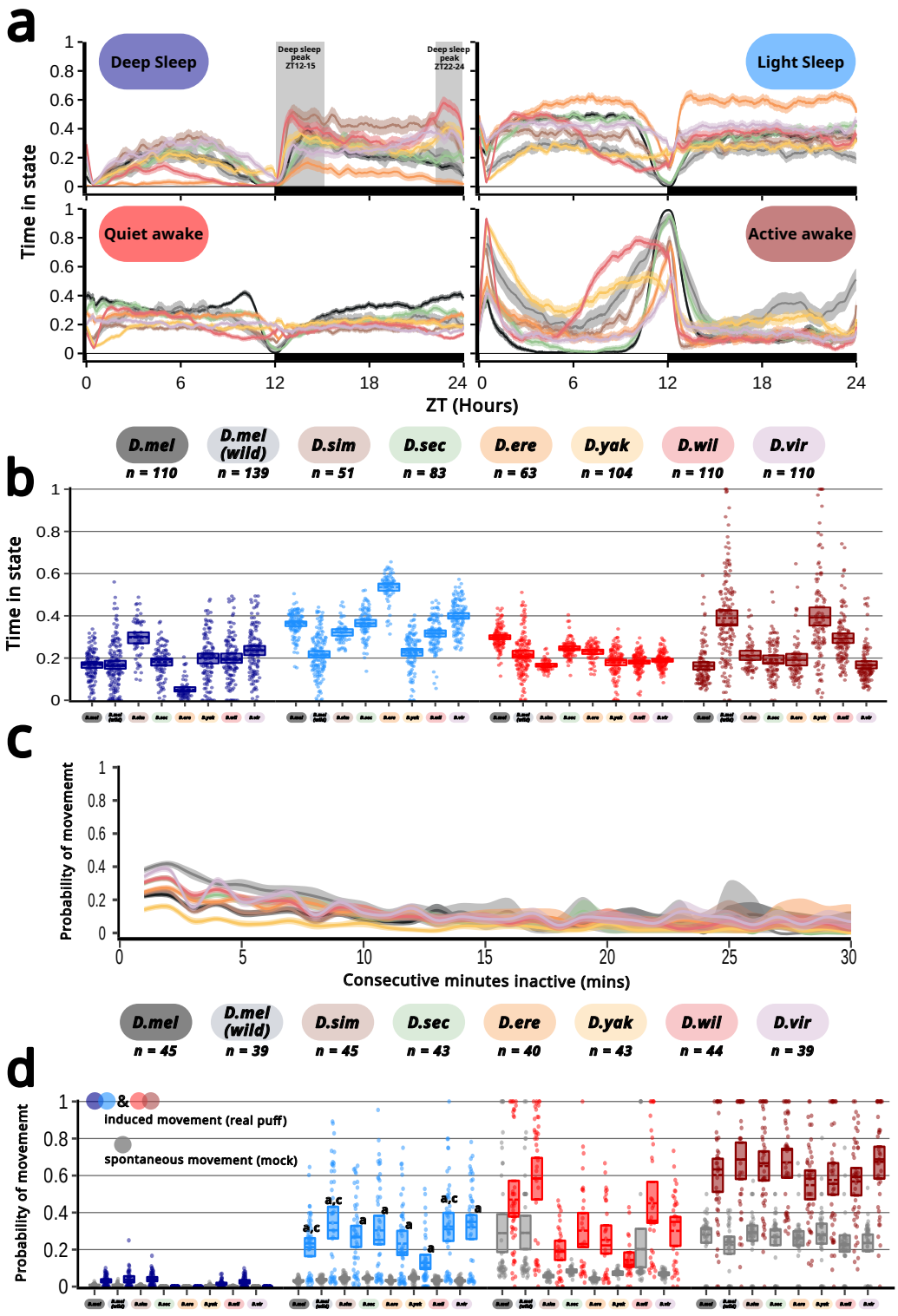


Figure 4.7: **Each Drosophilid HMM has a unique profile and sleep pattern.** **(a)** The time in each state for *D. melanogaster* CS (dark grey), *D. melanogaster* wild caught (light grey), *D. simulans* (brown), *D. sechellia* (green), *D. erecta* (orange), *D. yakuba* (yellow), *D. willistoni* (pink), *D. virilis* (purple). Most of the species have a peak in 'deep sleep' between ZT12-15 & ZT22-24 (grey boxes). **(b)** Quantification of (a). Mean and 95% CI's. **(c)** The response rate per Drosophilid to a puff of air over time inactive. All species have linear decrease in response rate till the approximately 15 minutes. **d** The likelihood of a Drosophilid moving after the delivery of a puff of air in each state. Significant difference in response rate between 'light sleep' and 'deep sleep' is denoted by *a*. Significant difference between 'light sleep' and 'quiet awake' is denoted by *c*.

While all predicted 'light sleep' states showed greater arousability across species, this trend was not observed when comparing 'light sleep' to 'quiet awake' *(**a, b** = significance from 'light sleep' against 'deep sleep' and 'quiet awake'; **a** = significance between 'light sleep' and 'deep sleep')* (Fig. 4.7.c). Interestingly, only *D. melanogaster* and *D. willistoni* displayed arousal thresholds for 'quiet awake' that were significantly higher (40-60%) compared to other species (10-30%). There is no clear explanation for this difference, although both *D. melanogaster* strains exhibit a broader range of 'quiet awake' durations and a lower proportion of time spent in pure movement during wakefulness (Fig. 4.8). However, these trends do not extend to *D. willistoni*.

One notable similarity among the groups with higher 'quiet awake' arousal thresholds is their elevated spontaneous movement, averaging between 20-30%, which is comparable to the spontaneous movement observed in the 'active awake' state. This higher level of spontaneous movement likely reflects a heightened baseline alertness in these flies, as it indicates more frequent micro-movements during 'quiet awake.' On average, 50-70% of 'quiet awake' bouts are homogeneous for movement, similar to the longer bouts observed during 'active awake' (Fig. 4.8). It is therefore surprising that baseline activity is not higher in other species.

Given that a puff of air is delivered after 30 or 150 seconds of immobility, the data is inherently biased toward bouts of 'quiet awake' that are heterogeneous. It is possible that homogeneous 'quiet awake' bouts, which may align with the higher arousal thresholds seen in *D. melanogaster*, are more resistant to arousal, while heterogeneous bouts might include instances where other species quickly transition into sleep. However, this hypothesis is not supported by the response rate over time (Fig. 4.7.d), as all species except *D. yakuba* exhibit a higher response rate at one minute compared to the lab strain of *D. melanogaster*. This inconsistency makes it challenging to definitively conclude whether the 'light sleep' observed in 5 out of 8 species truly represents a distinct sleep state, as their arousability does not change markedly.

For all species, the likelihood of responding to a puff of air diminishes the longer they remain immobile (Fig. 4.7.d). The baseline response to the stimulus at one minute of inactivity varies across species, with wild *D. melanogaster* showing the highest response rate and *D. yakuba*

the lowest. By approximately 15 minutes of inactivity, the response rates among the different species converge and become indistinguishable from one another. At this time point, the HMM would predict a transition into 'deep sleep' for 6 out of 8 species (rounding down *D. virilis'* 17-minute threshold). However, for *D. erecta* and *D. willistoni*, the model would still classify them as being in 'light sleep.'

Given that *D. erecta* and *D. willistoni* both exhibit average to high response rates during 'light sleep,' it is likely that most interactions occurred during shorter sleep bouts, which keeps the average response rate high. This observation suggests that the model might be overestimating the duration of 'light sleep' for these two species since their arousal thresholds do not decrease after 15 minutes of immobility.

As previously discussed, it is challenging to discern whether the decreasing response rate over time indicates a higher likelihood of transitioning into a different sleep state with a higher arousal threshold, as described in *van Alphen et al.* [189], or if it simply reflects a higher proportion of the flies being asleep. If sleep across all species were categorised into 0-10 minutes as 'light sleep' and over 10 minutes as 'deep sleep,' the same differences in response rates would likely be observed. However, the HMM provides valuable insights into the distribution of sleep bouts, such as identifying when long, consolidated bouts of inactivity occur and when sleep is more sporadic and brief.

For instance, the model reveals that *D. erecta* and *D. sechellia* tend to have shorter bouts of long, consolidated sleep, whereas wild-caught *D. melanogaster* have fewer short sleep episodes due to higher energetic activity. This ability to quickly visualise and quantify the patterns of sleep across species highlights the utility of the HMM in comparative sleep studies, despite the challenges in interpreting the nuances of arousal thresholds and sleep state transitions.

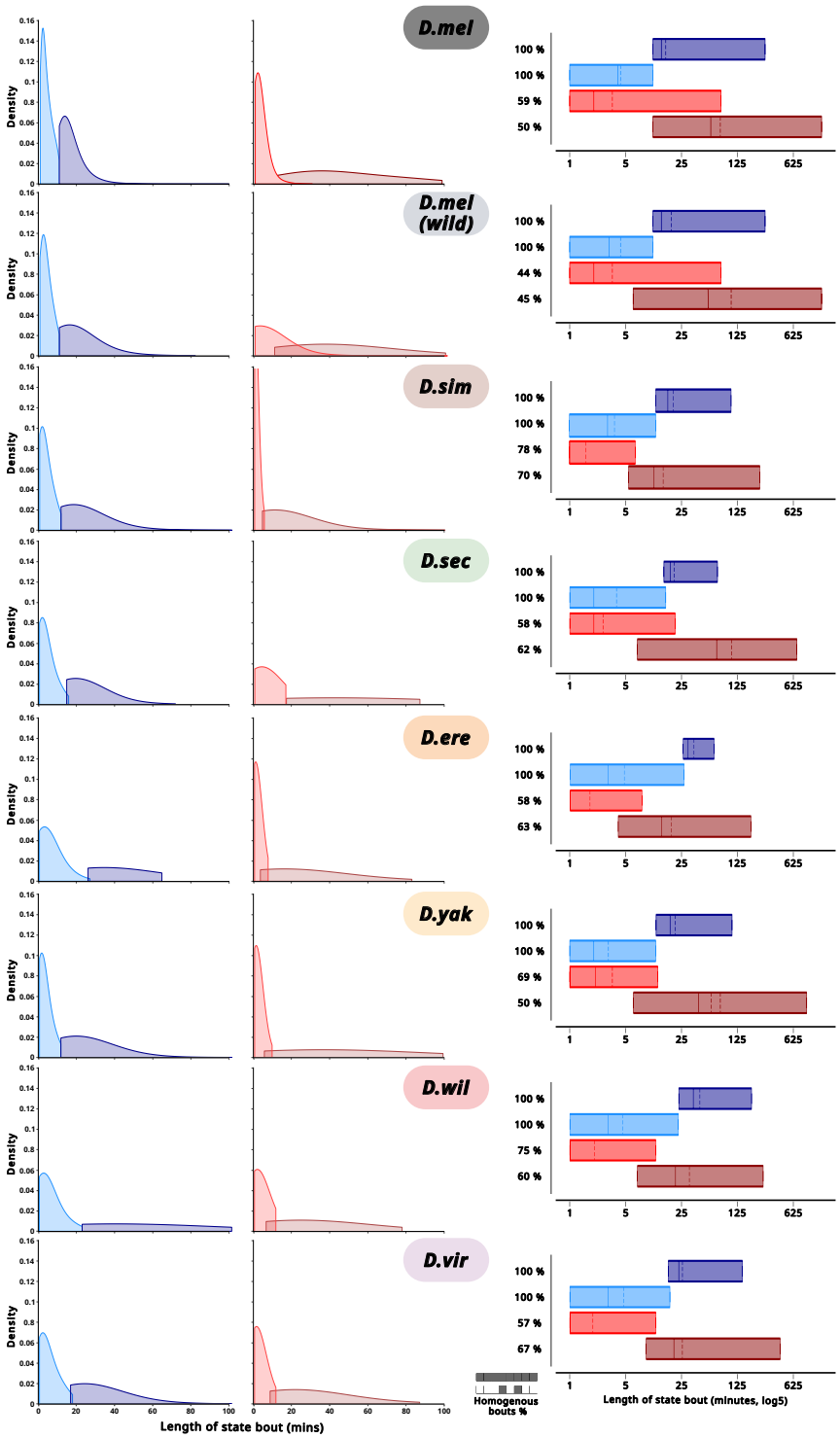


Figure 4.8: **Distribution of the lengths of HMM states per Drosophilid**.
A kernel density estimate of the bout lengths of each HMM state and the minimum and maximum lengths with mean (dashed line) and median (solid line) per Drosophilid. Each species has 'deep sleep' and 'light sleep' segmented by time inactive. The y-axis of the minimum and maximum plots indicates the percentage of states that contain at least one inactive observable.

4.6.3 Interpreting Sleep Rebound with HMMs

Circadian rhythms appear to be tightly regulated across Drosophilids, with all species showing morning and evening peaks in activity and consolidated sleep during the night. In *D. melanogaster*, mechanical sleep deprivation results in longer and more consolidated sleep during recovery, characterised by extended sleep bouts, higher arousal thresholds, and fewer awakenings. A strong homeostatic response to sleep loss [275, 274, 71, 189, 35]. However, not all forms of sleep deprivation produce this rebound effect. Males kept awake through female interaction, for instance, show no sleep rebound [122, 413]) and sleep deprivation via activation of wake-promoting neurons only causes rebound in one of three sub-stypes [285]. This raises the question of whether all forms of sleep deprivation are equally effective and whether the rebound circuitry is conserved across different species.

To investigate sleep rebound across various Drosophilid species, flies were sleep-deprived for a single day (Fig. 4.9.a), and the first three hours of morning activity were quantified using a HMM. Sleep deprivation was achieved through targeted mechanical awakening after 30 seconds of inactivity, using an ethoscope accessory module (see *Methods*).

Surprisingly, a clear sleep rebound was observed only in *D. melanogaster* (Fig. 4.9.b). The lab strain of *D. melanogaster* showed a substantial increase in 'deep sleep' (44%) compared to its non-sleep-deprived control (19%), with a corresponding reduction in 'light sleep' to control levels. In contrast, the wild strain of *D. melanogaster* exhibited an increase in 'light sleep' but no significant increase in 'deep sleep'.

None of the other species studied displayed significant changes in either 'deep sleep' or 'light sleep' following sleep deprivation (Fig. 4.9.b). Counterintuitively, *D. virilis* exhibited an increase in 'active awake' time. Homeostatic rebound is considered one of the defining characteristics of sleep [11, 414, 24]. Based on this criterion, it could be argued that, among the Drosophilids studied, only *D. melanogaster* exhibits true sleep as traditionally defined.

A study by *Joyce et al.*, which includes some of the data presented here, attempted to replicate the sleep deprivation experiments with two modifications: flies were deprived of sleep through

male-male interaction, and the duration of sleep deprivation was extended to seven days [334]. Under these conditions, sleep rebound was observed in *D. simulans*, *D. sechellia*, and *D. yakuba*, in addition to both strains of *D. melanogaster*. All these species are closely related (Fig. 4.6), except for *D. erecta*, which showed no rebound within this clade. More distantly related species, such as *D. willistoni* and *D. virilis*, also showed no sleep rebound.

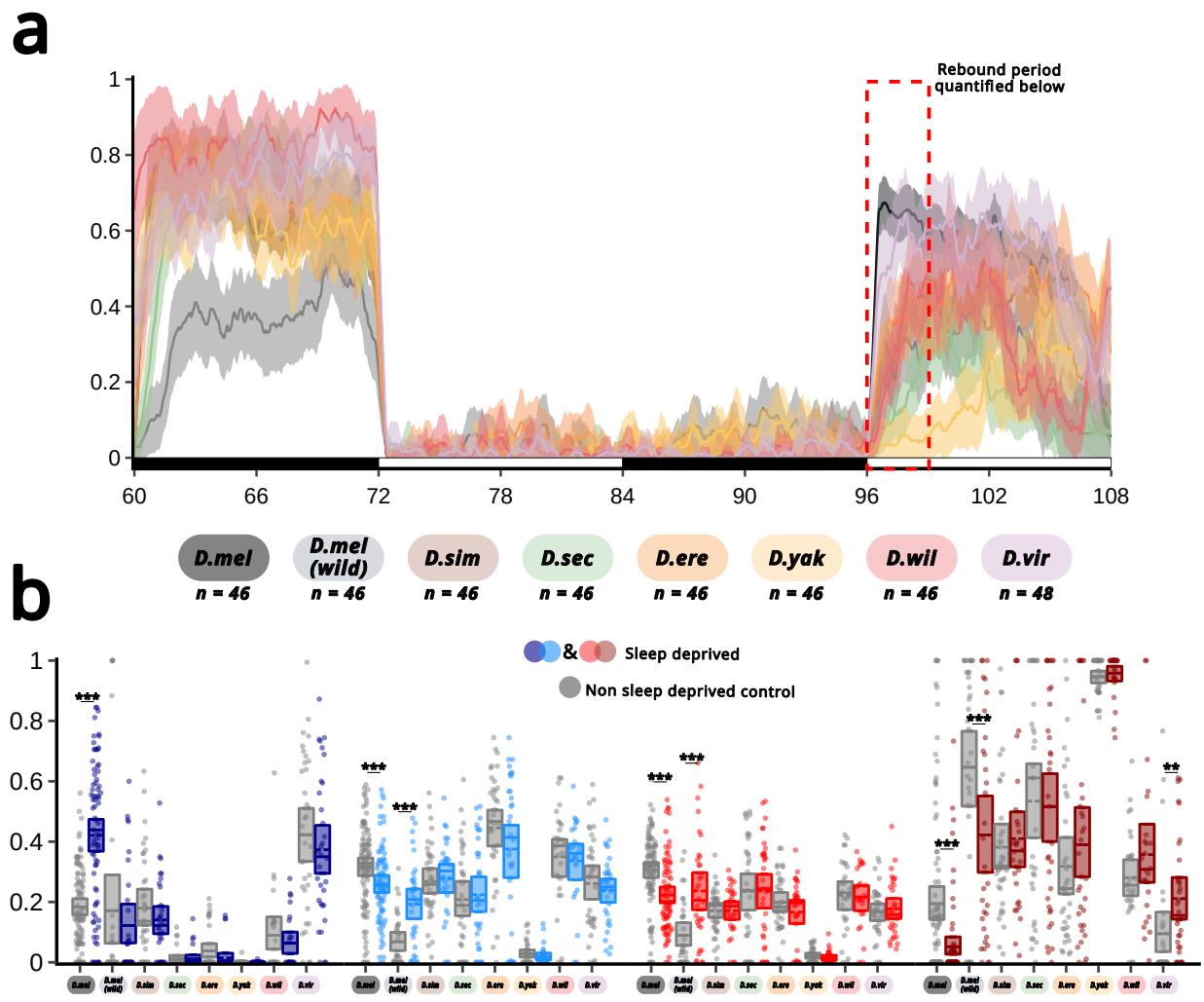


Figure 4.9: **Only *D. melanogaster* exhibits homeostatic sleep rebound after mechanical sleep deprivation.**
(a) Mechanical SD via rotation of the tube housing the fly reduces sleep to a minimum over 24 hours. Homeostatic rebound sleep is measured in the first 3 hours after lights on (red dotted box). *D. melanogaster* CS (dark grey), *D. melanogaster* wild caught (light grey), *D. simulans* (brown), *D. sechellia* (green), *D. erecta* (orange), *D. yakuba* (yellow), *D. willistoni* (pink), *D. virilis* (purple). **(b)** Quantification of the time in each HMM state during the rebound period against non-SD controls (grey). Significant difference to controls is denoted by *'s (** ≤ 0.01, *** ≤ 0.001). Only *D. melanogaster* (CS and wild caught) had an increase in sleep post SD.

4.7 Discussion

The results of this study illuminate the divergent evolutionary pathways in the homeostatic regulation of sleep across *Drosophila* species. Sleep rebound following mechanical perturbation has long been considered a hallmark of *Drosophila* sleep, especially within *D. melanogaster* strains and mutants [71, 129]. However, our findings suggest that this sleep rebound mechanism is predominantly limited to *D. melanogaster*, with notable variation even within the species, particularly between wild and laboratory strains.

The wild *D. melanogaster* strain exhibits shorter, more frequent rebound sleep, likely due to the heightened risk of predation in natural environments, necessitating greater vigilance. In contrast, the laboratory strain, CS, which has been inbred for decades under conditions with minimal predation pressure, has potentially had a drift in its homeostatic sleep regulation. This is consistent with observations in other species, such as cavefish populations, where sleep patterns have adapted in response to environmental pressures like low nutrient availability [125, 127, 126]. Similarly, significant natural variation in locomotion has been documented within CS populations [415]. Indeed, the wild *D. melanogaster* strain used in this study was selected from twelve distinct strains, each with a unique sleep profile, the chosen one being most similar to CS.

The observed differences in sleep rebound suggest that while *D. melanogaster* retains its homeostatic control, albeit altered, this mechanism appears absent in species like *D. erecta*, *D. willistoni*, and *D. virilis*. Furthermore, in *D. simulans*, *D. sechellia*, and *D. yakuba*, sleep rebound was only observed following male-male sleep deprivation. According to the criteria often employed in animal sleep studies [24, 10], the absence of rebound in these species might classify them as non-sleepers. However, this classification conflicts with the evident increase in arousal thresholds accompanying immobility, which is arguably a stronger criterion for defining sleep.

If we accept that these species do sleep, our findings lend support to the adaptive sleep theory, which posits that sleep evolved as a strategy to reduce predation risk and prevent evolutionary drift into alternative ecological niches [131, 132, 133, 134]. The lack of sleep rebound following

chronic sleep deprivation in non-*D. melanogaster* species [334] could indicate that sleep in these species serves no restorative function, existing instead as a circadian-entrained behaviour that minimizes activity during unfavourable conditions. For instance, *D. virilis*, known for its adaptability to extreme conditions without speciation, might be utilizing sleep to evade the most challenging circumstances.

In *Joyce et al.*, we linked sleep rebound after mechanical deprivation with synaptic plasticity, demonstrating a reversal of the phenotype by reducing the expression of genes involved in synaptic plasticity [334]. However, this reversal did not occur with male-male sleep deprivation, implying distinct neural circuits are involved—one related to synaptic strength and the other to overall possibly related to stress. It is unlikely that the other species lack mechanisms to manage increasing synaptic strength or are unaffected by the stress of male-male interactions. These tasks might still occur, perhaps continuously, rather than being restricted to sleep. This suggests a possible divergence in the evolutionary role of sleep, with these functions becoming decoupled from sleep in some species.

The evolutionary benefits of this decoupling warrant further investigation. Both *D. virilis* and *D. willistoni* inhabit extensive ecological ranges and are classified as generalists, much like *D. melanogaster*. If the variation in their sleep regulation imposed a significant cost, we might expect to see it reflected in their adaptability. The absence of such a cost might indicate that the evolution of sleep in these species has conferred an advantage, allowing them to maintain flexibility in their response to environmental challenges.

Chapter 5

Classifying sleep beyond movement

5.1 Rationale

To date, sleep in *Drosophila* has predominantly been classified by the presence or absence of movement [275, 274]. This straightforward measure has long been the foundation of *Drosophila* sleep studies, beginning with the early adoption of the '5-minute rule' of immobility. However, even in its inception, *Hendricks et al.* described additional behavioural markers, noting that, "prior to resting, the flies turned away from the food, walked a few millimetres and then adopted a supported position, usually prone" [275]. The challenges in consistently reproducing such qualitative observations, combined with the ease of simply measuring activity, led to the 5-minute rule becoming the dominant paradigm in *Drosophila* sleep research for the last two decades.

Recent advancements in recording resolution and computational modeling have begun to challenge this simplistic view, raising the question of whether sleep in *Drosophila* can, and should, be inferred from more than just a lack of movement [283]. This shift necessitates a deeper re-examination of the criteria used to classify sleep, particularly in light of these technological developments.

5.2 Background

Sleep, in one form or another, is now understood to be a universal phenomenon across the animal kingdom, with well-established behavioural and physiological markers in both laboratory and wild animals [100, 10, 84]. Historically, the gold standard for identifying sleep relied on synchronised changes in electromyography, electroencephalography , and electrooculography —standards first proven in mammals and birds [11]. These techniques, while invaluable, are impractical for many species and are based on the assumption that the markers of sleep in mammals and birds are universal.

To address these constraints, a set of behavioural criteria for sleep has been proposed that can be applied more broadly across taxa, such as sleep posture and site, quiescence, and homeostatic rebound. See the *Introduction* for more details. These criteria helped identify sleep in various fish, reptiles, amphibians, and invertebrates such as cockroaches, bees, and octopuses.

5.2.1 Behavioural Criteria for sleep across species

While seemingly more simplistic than electrical recordings, behavioural hallmarks of sleep can reveal much about its underlying purpose. Humans, for instance, seek shelter and arrange their sleeping environments to maximise safety, wearing night clothes and using bedding to promote sleep through localised skin warming [416, 417]. Similar behaviours are observed in other species: mice construct nests that balance heat conservation with safety [385], and birds tuck their heads into their bodies for warmth, despite this reducing their capacity for external detection [418]. These actions provide quick visual cues for classifying sleep and lend insight into generalised theories of sleep, such as those relating to energy conservation, discussed earlier.

Describing sleep qualitatively is more straightforward in mammals due to their anatomical and behavioural similarity to humans. Yet, similar observations have been made in smaller, distantly related species. European jumping spiders, for instance, suspend themselves from silk threads at night, curling their legs inward and reducing their responsiveness to visual stimuli, instead relying on vibrations through the thread [191]. During these supposed sleep bouts,

retinal movements and limb twitching have been observed, suggesting a REM-like state. If confirmed, this would represent the first documented case of REM-like sleep in invertebrates [192].

In standard laboratory model organisms, such as *Danio rerio* (zebrafish), sleep is characterised by a clear preference for specific locations, either near the surface or at the bottom of the tank, accompanied by a drooping caudal fin [419, 420]. Similarly, in *C. elegans*, during the lethargus stage, distinct postures correspond with reduced arousability, suggesting a sleep-like state that may shed light on the early evolution of sleep [421]. These postural changes are the standard method for classifying sleep in these organisms, which, like insects, are difficult to quantify via electrophysiology.

5.2.2 Behavioral indicators of sleep in insects and *Drosophila*

Observations in various insect species reveal similar postures during presumed sleep. Flour moths [183], cockroaches [184], and honeybees [179, 422], for example, relax their bodies, move closer to the ground, and tuck or lower their antennae. In the case of flour moths, the antennae are tucked under the wings, while in honeybees, such behavioural changes are accompanied by electrophysiological shifts, reinforcing the link between posture and sleep. These descriptions align with *Hendricks et al.'s* findings [275].

Improvements in video recording technology have renewed interest in studying sleep postures and behaviours in *Drosophila*, offering the potential for more accurate sleep classification. Investigations into deep sleep in *Drosophila* have uncovered rhythmic proboscis pumping which occurs in short bouts throughout sleep. Some have suggested that this behaviour may play a role in toxin clearance, echoing a contested theory in mammalian sleep research [264, 66]. Although *Hendricks et al.* also noted this sporadic protrusion and retraction of the proboscis, similar behaviour has been observed during grooming, walking, and flight, indicating that it cannot be used as a definitive sleep marker [423, 424, 185].

Earlier studies relied on tethered flies, likely inducing stress and limiting the natural expression

of sleep behaviour. High-resolution imaging of freely moving flies, viewed in profile and combined with keypoint tracking, has since revealed several distinct micro-behaviours associated with sleep. *Keles et al.* confirmed the prone position described by *Hendricks et al.*, and further identified antennal drooping and a downward (dorsal) shift in the angle of the haltere ("haltere switch") during extended immobility. Interestingly, the haltere switch consistently preceded or coincided with antennal drooping and reversed just prior to arousal triggered by heat or mechanical stimulation. If validated, the haltere switch could be a reliable indicator of a sleeping fly. However, elevated arousal thresholds were sometimes observed without the haltere switch, suggesting it may represent a sub-sleep state rather than a universal sleep marker [185].

Like mammals [13, 425], birds [158], and, zebrafish [419, 420], flies exhibit preferences for particular sleeping locations, often choosing areas near, but not directly on, food sources. This behaviour, however, varies both within and between individuals [244, 185, 35].

The evidence is increasingly clear: *Drosophila*, like other insects and animals, display distinct behavioural and postural shifts during sleep. These include a prone position, antennal drooping, and the unique haltere switch, all of which suggest that sleep in *Drosophila* is more than just a state of immobility.

This chapter will explore if the additional data recorded by the ethoscope can be used to enhance the accuracy of sleep predictions in *Drosophila*, with the hope that the aforementioned behavioural markers of sleep are present in low resolution tracking of flies.

5.3 Exploring the ethoscope trackers' variables

Previous studies using the ethoscope have primarily relied on a single variable output: maximal velocity. Velocity is calculated as $\frac{distance(mm)}{time(s)}$, modified by a correction coefficient that maintains consistency in the metric with variable FPS [316], see *Methods*. As such, units of velocity are augmented. Ground truth annotation has demonstrated that maximal velocity was the most reliable predictor of three distinct behavioural states: 'walking', 'micro-movements' (such as grooming, eating, or egg-laying), and 'immobility' [244]. These three states have formed the

basis for calculating sleep, activity, and general well being [426] within the Gilestro lab group. However, the tracking software provides more information than just the centroid data.

5.3.1 Additional variables from the ethoscope

When tracking a fly, the machine vision software generates an ellipse that outlines the fly's discernible body mass (Fig. 5.1.a). The (x, y) coordinates are then derived from the centroid of this ellipse, scaled from 0 to 1, with 1 representing the rightmost and topmost edges of the region of interest (ROI) box (Fig. 5.1.c). In addition to the centroid data, three other variables are computed from the ellipse, and a fourth variable is calculated post hoc (Fig. 5.1.b):

- **H**: The length of the longest diameter of the ellipse, representing the distance from the abdomen to the head (measured in pixels and rescaled to between 0 - 1).
- **W**: The shortest diameter of the ellipse, representing the width from one side of the body mass to the other (measured in pixels and rescaled to between 0 - 1).
- **Area**: The area of the ellipse, calculated using the formula:

$$area = \frac{H}{2} \cdot \frac{W}{2} \cdot \pi$$

- **Phi**: The angle between the longest diameter (**H**) and the lower line of the ROI rectangle (measured in degrees).

Additionally, velocity per period of time can also be represented as the mean speed or the standard maximal speed used typically in *ethoscopy*. This section will investigate whether these additional variables, either individually or in combination, can serve as predictors of sleep.

5.3.2 Variables over time

Due to incomplete tracking and errors whilst the tracking is being established, outliers (outside 3 standard deviations from the mean) were removed and forward filled. After the data was rescaled to between 0 and 1, to standardise values to an individual's size and space, *see Methods*. Except for Phi and velocity (omitting Figure 5.2), as their values have meaning beyond their individual variance, such as the angle they were facing in the tube or their top speed.

As shown in *Figure 5.2* most variables in the dataset from *Geissmann et al. 2019* have much larger changes in each variables over day and night compared to their counterparts in the ACV arousal dataset. The cause of this discrepancy is uncertain, as both sets of flies were housed in similarly sized tubes at the same temperature, using the same wildtype strain (CS). Nonetheless, significant upgrades to the ethoscope have been made since 2017, including updated software and a newer version of the PiNoir camera which may contribute to the differences, see *Methods*. Additionally, lighting conditions can strongly affect tracking accuracy, which fur-

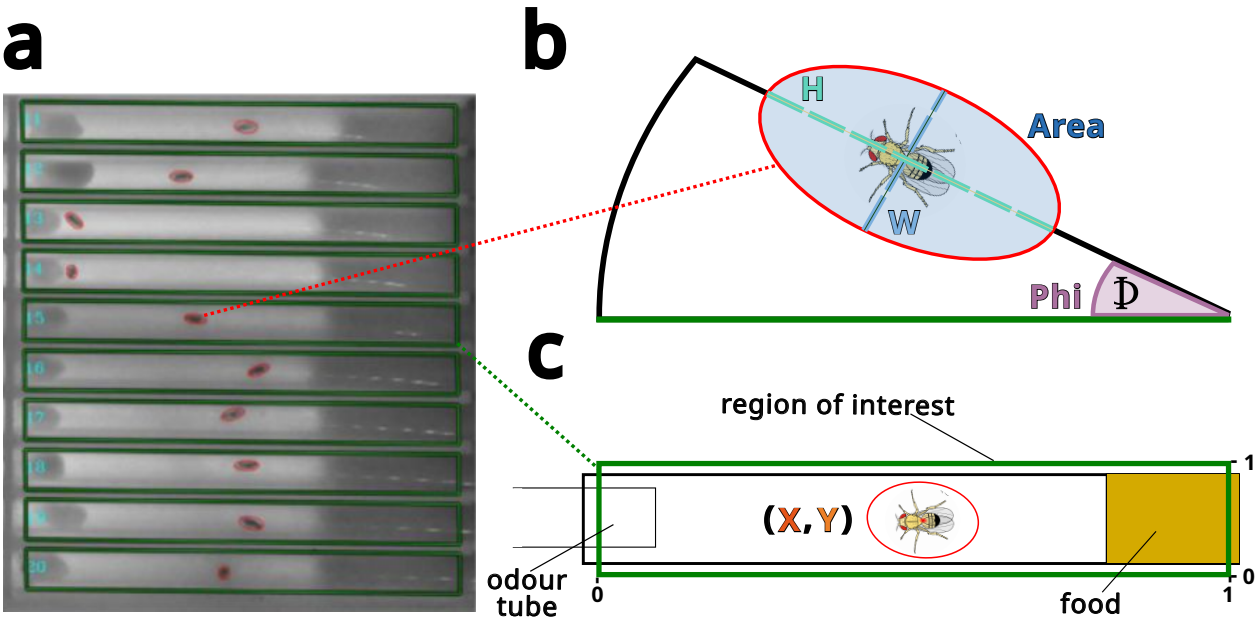


Figure 5.1: **Depiction of the variables tracked by the ethoscope.**
(a) A still image from the ethoscope as it tracks in real-time. The green boxes are the ROI's per fly (circled in red) in which it can be tracked. **(b)** The fly is tracked via a red ellipse around the fly. Of this ellipse the width (W - blue) and height (H - teal) are recorded, as well as the angle of H to the lower ROI boundary (phi - purple). **c** A schematic of the ROI and the tube housing the fly. X (red) and Y (orange) are the coordinates of the centroid of the ellipse in relation of its space in the ROI.

ther complicates direct comparisons. Moving forward, the ACV dataset will be primarily used, except in one section focused on predicting HMM states.

In the Geissmann dataset, both H (the longest diameter of the ellipse) and W (the shortest diameter) decrease during periods of immobility, leading to a corresponding reduction in the area of the ellipse. However, in the ACV dataset, this pattern differs: H decreases, but W increases, and both show much smaller overall changes. Consequently, the area remains relatively stable in the ACV dataset compared to the Geissmann data. At ZT12, when the lights are turned off, both datasets show shifts in H and W values. In the ACV dataset, both H and W decrease sharply, whereas in the Geissmann dataset, H decreases gradually, while W increases abruptly.

It is likely that changes in the tracking software, intended to improve the speed of tracking during transitions, are responsible for the differences observed at ZT12. However, the complete reversal in W between the datasets is particularly troubling for comparisons over time, suggesting potential inconsistencies in the way tracking algorithms have processed fly behaviour.

Given the substantial day-night differences observed in the data, from this point onward, only daytime data will be analysed. This decision is based on the assumption that natural light provides clearer imagery for tracking than infrared lighting used at night, thereby reducing potential biases that could influence classification outcomes.

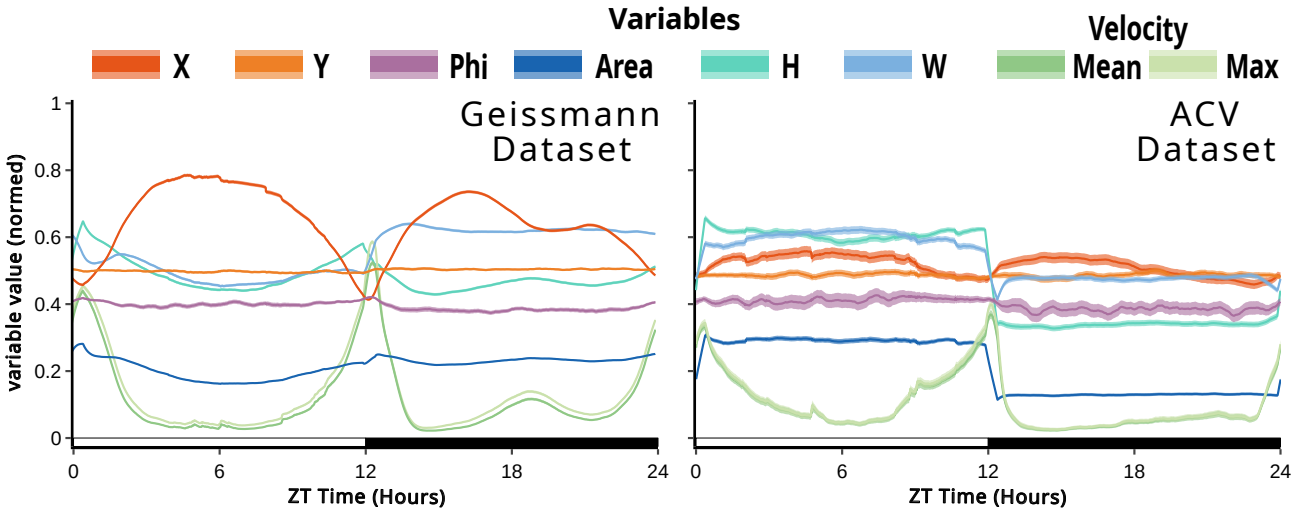


Figure 5.2: **The tracked variables follow a circadian rhythm over the 24-hour day.** All variables were re-scaled to fit between 0 and 1, with 0 being the minimum value found and 1 the maximal value found per individual. The Geissmann dataset [53] (left) has greater variation over the day than the ACV dataset (right). Both datasets have changes in the ellipse variables as the lights turn off (ZT12). The Geissmann dataset was collected in 2018-2019 using an earlier version of the ethoscope. The ACV dataset was collected in 2022-2023 using an updated version of the ethoscope with newer cameras and tracking software (*see Methods*.

5.3.3 Distribution of variables

Often, differences between behavioural states can be observed just by examining the distribution of variables. To aid in visualisation, the dataset was first decoded using the previous HMM into four states. The model is considered robust in distinguishing long and short bouts of immobility, as well as providing a clear separation between the two awake states. In addition, the plotted variables were restricted to periods where the maximal velocity was less than 1, indicating immobility.

The Y values have a bell-shaped distribution centered around 0.5 for all states. Since there is little variation in the Y variable across states or over the day, it will be excluded from further analysis (Fig. 5.3.b). As shown in Figure 5.2, the X values in the ACV dataset do not shift towards the food (1) as much as they do in the Geissmann dataset. This is reflected in the current analysis, where both sleep states are distributed around 0.5 (Fig. 5.3.a). The awake states are distributed closer to the food source, likely during feeding events, with the active awake state occupying all regions of the tube.

The ellipse variables (H, W, Area) show similar distributions across states, with W and Area in the awake states having trailing tails towards 0 compared to the sleep states (Fig. 5.3.d-f). This results in the awake states having lower averages for W and Area. These differences may arise because a moving fly's ellipse appears smaller due to its changing orientation and profile relative to the camera, although this is not confirmed.

Phi shows the most distinct difference between states. Both sleep states, and to a lesser extent quiet awake, tend to remain more horizontal in the tube (closer to 0 degrees), while active awake states are more vertical (closer to 90 degrees) (Fig. 5.3.c). This likely reflects active flies walking up and down the tube, frequently turning. These turning events likely contribute to the higher density of Phi values around 90 degrees.

Ground truth experiments from *Geissmann et al.* [244] demonstrated that mean velocity values below 1 indicated immobile flies with no behavioural micro-movements. Interestingly, in the ACV dataset, there is a bimodal distribution of all states where the mean velocity is less than

1. The sleep states have a tighter distribution, whereas the awake states are more spread out (Fig. 4.3.g). This contrasts with the Geissmann dataset, which shows a uniform distribution for both sleep states, with the awake states evenly distributed across the scale. The appearance of this bimodal distribution in other newer datasets, which also use the updated PiNoir camera and tracking software, suggests that the higher resolution may be detecting smaller changes in the centroid over time. Interestingly, the asleep states have few values of mean velocity between 0.7 and 0.75, whilst the awake states have many.

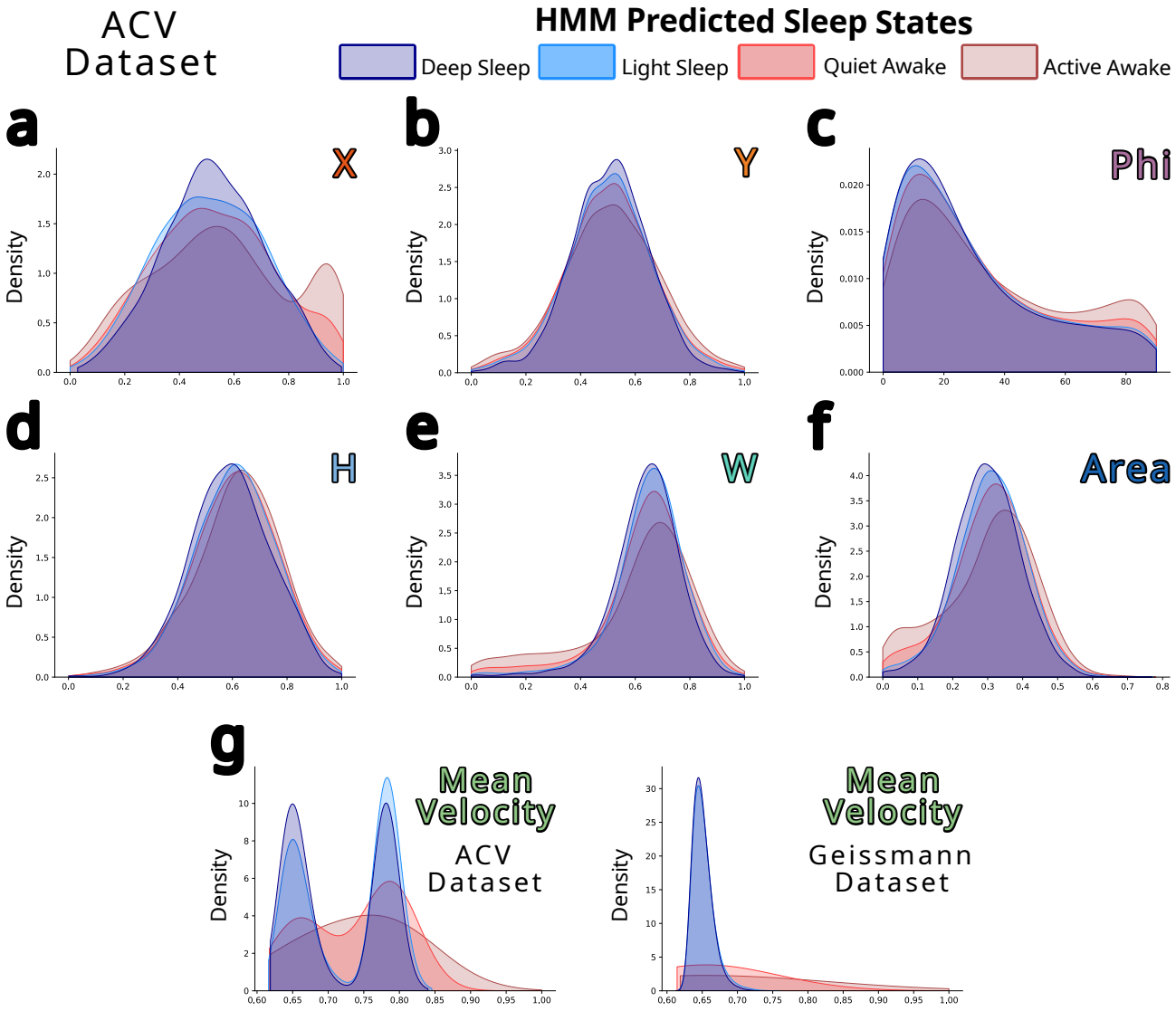


Figure 5.3: **The distribution of each tracked variable per HMM state.** **(a-f)** The distribution of each ACV dataset variable per HMM states shown in *Chapter 4*. For all distributions only instances when the fly was inactive (max velocity < 1) was plotted. **(g)** The distribution of mean velocity for both the ACV and Geissmann dataset for inactive flies. The ACV dataset, which was recorded with newer cameras and has a bimodal distribution of the HMM sleep states. X, Y, H, W, and Area values are arbitrary values re-scaled to between 0 - 1. Phi values are augmented from 0 - 180 to 0 - 90. Velocity values are modified values of $\frac{mm}{s}$.

5.3.4 Do variables change over immobile bouts?

If posture changes when a fly enters sleep, this might be reflected in shifts in variables from the start to the end of an immobile bout, potentially indicating the onset of sleep or arousal in response to an odour. Immobility bouts lasting between 5 and 20 minutes were segmented into those that ended with a response to an odour puff and those that remained immobile.

Counterintuitively, the X-coordinate significantly increased in both groups from the beginning to the end of the bout (Fig. 5.4.a). However, the average increase of 0.000175 is exceedingly small and likely represents noise in the tracking. With a relatively large dataset (8199 bouts), even small shifts in averages can be deemed statistically significant. Interestingly, non-responding bouts occurred closer to the food (1) than responding bouts, although this expectation was not strongly supported by the distribution of X in the sleep states (Fig. 5.3.a).

Phi exhibited no significant change across bouts or between the groups, as expected, (Fig. 5.4.b). The error bars suggest some noise of approximately ±1 degree across bouts. The non-responding group was on average 2 degrees larger, likely due to a small number of values clustering closer to 90 degrees.

The ellipse variables (W, H, and Area) showed no difference in distribution or change between the response groups (Fig. 5.4.c-e). Both groups exhibited a small decrease in these values towards the end of the bout, with a typical change of about –0.003. However, the magnitude of this change is minimal, and its biological relevance remains unclear.

Mean velocity is split into the two distributions (Fig. 5.3.g). Both groups experienced a slight reduction in velocity over time (≈–0.002), though as with the ellipse variables, this change is small (Fig. 5.4.f). There was no difference between the groups for velocities in the higher distribution (≈0.7835), with both decreasing by a similar amount. In the lower distribution (≈0.657), only the non-responding group exhibited a reduction in velocity, while the responding group maintained a consistent low velocity throughout the bout.

Given the small scale of these changes, it is challenging to determine whether they truly reflect behavioural differences or are artifacts of the tracking software's increased accuracy as the fly

remains immobile.

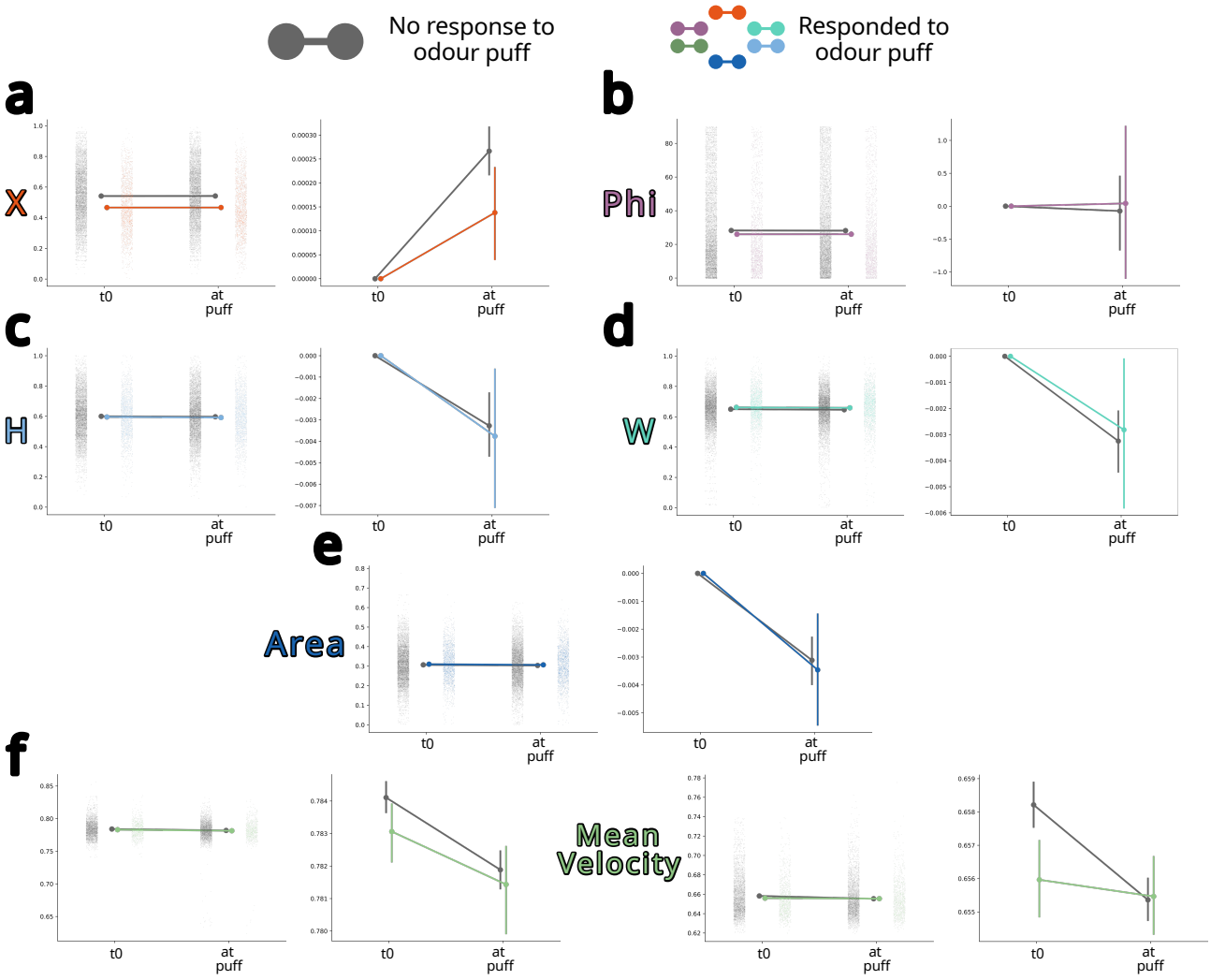


Figure 5.4: **Tracked variables change over the bout with no difference between non-responding and responding bouts.**
(a-e) The value of a variable at the start of a bout of inactivity (t0) compared to the value 10 seconds before a puff of apple cider vinegar is delivered. Inactive bouts that ended with a response (coloured) were not different to bouts with no response (grey). All bouts of inactivity were between 5 and 20 minutes long. **f** Same as in (a-e), except the plots are split between the two distributions of mean velocity seen in *Figure. 4.3.g.* X, Y, H, W, and Area values are arbitrary values re-scaled to between 0 - 1. Phi values are augmented from 0 - 180 to 0 - 90. Velocity values are modified values of $\frac{mm}{s}$.

5.3.5 Are responses dependent on the variable value?

The distribution and changes in the variables do not appear to differ significantly between groups. However, not all predictions of sleep may hold true. It is possible that some flies are simply resting, which could blur the groupings. A better indicator of the relationship between variables and behaviour might be the arousal threshold at different variable values.

The largest difference in the mean between populations is observed in the X variable, where flies that do not respond are, on average, closer to the food (1) (Fig. 5.5.a). This is driven by a consistent decrease in response rate as X increases from 0 to 1. Immobile flies responded to the odour puff approximately 80% of the time when positioned between $0-0.1$, but only around 1% of the time when near 0.9–1. As discussed earlier, flies tend to sleep near their food source, and bouts occurring between $0.6-1$ all have roughly similar response rates. However, it is important to note that the odour delivery tube was positioned at $X = 0$, meaning the mechanical effect of the puff would be strongest near the tube (Fig. 5.1.c). This makes it challenging to separate the mechanical influence from the effect of X position on response behaviour.

Neither Phi nor H seem to affect the response rate as these variables change, which is expected given their minimal variation throughout the bouts (Fig 5.5.b&c). While awake flies are more likely to be perpendicular in the tube (with higher Phi values) and tend to prefer a horizontal orientation when immobile (Fig. 5.3.c) they are not strictly constrained by this and can sleep in a perpendicular position.

W shows more variation in response rate (Fig. 5.5.d). Focusing on the range of W between $0.4 - 0.8$, which accounts for 82% of the predicted sleep bouts, there is a gradual increase in response rate as W increases from 0.5 to 0.8, with an effect size difference of around 20%. However, there is some overlap in bootstrapped estimates of mean distribution. Since no distribution differences were observed between long and short bouts of sleep for W (Fig. 5.3.e) it is unlikely that these changes are due to longer sleep bouts causing a smaller W. It is possible that W reflects some aspect of the sleep state, although the relationship is not robust, given the variation between groups and the gradual nature of the effect size difference. As H remains

relatively constant, Area follows the same pattern as W, with an increase in response rate from $.2 - 0.5$ (Fig. 5.5.e).

Interestingly, the largest effect size difference is observed in the $0.7 - 0.75$ group, which was previously shown to be primarily the values for awake states rather than sleep (Fig. 5.3.g & Fig. 5.5.f). Flies with a mean velocity of 0.75 response rate is approximately 12% higher than those at 0.65. Velocities only 0.5 smaller or larger, 0.65 and 0.75, both have lower response rates, as well as 0.60. Both 0.7 and 0.8 contain files that always responded or never responded, creating a bimodal distribution compared to the bell-shaped distribution of the others. Given response to an odour is not a given in awake flies (Fig. 4.4) but more likely, 0.7 and 0.8 could be an immobile velocity of an awake fly. 0.7 had the lowest n. of all the groups, but this was not much lower than the others *(**0.6**: n. = 87, **0.65**: n. = 90, **0.7**: n. = 60, **0.75**: n. = 125, **0.8**: n. = 108)*, and unlikely to be the explanation for the difference.

In contrast, maximum velocity provides little information about sleep, as the response rate changes minimally across the range, except near 0.95, which likely corresponds to its closeness to the threshold for micro-movements (Fig. 5.5.g). This reinforces the idea that velocity decreases and increases even in immobile flies, possibly a measurement of even smaller posture changes or rhythmicity.

5.4 Predicting sleep with machine learning

The previous analysis examined each variable in a static manner, comparing the sample mean at individual time points. However, biological observations are inherently dynamic and subject to change over time, often making the static approach inadequate for capturing the true nature of these processes. The ethoscope captures high-resolution data continuously, which is well-suited for time series analysis and classification.

Behavioural datasets are typically complex, high-dimensional, and exhibit nonlinear dependencies. Time series analysis can parse and characterise large signal datasets to provide unique fingerprints for each class, which can then be fed into machine learning (ML) classification

algorithms [363, 427]. ML techniques have demonstrated high accuracy in classifying and predicting behaviours such as grooming and courtship [428, 429].

In human sleep classification, ML tools like random forest classifiers achieve approximately 96% accuracy in categorising sleep states from EEG signals. However, EEG recordings require complex setups that restrict the users' movements and environment, leading to a push for sleep classification from more easily capturable markers such as movement and heartrate. This is the basis for modern sleep trackers using smart watches [430, 431, 432].

Although there have been no highly successful ML applications for classifying *Drosophila* sleep based on behaviour, random forest classifiers have been used to classify sleep states from multichannel local field potential data with 99% accuracy, distinguishing early, mid, and late sleep stages despite no obvious differences in simple statistical measures [433]. This study underscores the challenge of interpreting ML classifiers, particularly the "black box" nature of random forest classifiers, which lack clear biological interpretation of the classified states [430, 363].

Plots of the raw time series for the given variables are variable, oscillating higher and lower around the mean (Fig. 5.6). Notably, changes in Phi are the most pronounced. Although the fly's direction is stationary, changes in the ellipse angle (Phi) may reflect alterations in fly posture. However, these changes could also be inherent noise in the tracking system affecting Phi, Area, and mean velocity.

To test the null hypothesis of noise, the variables Velocity, Area, and Phi will be labelled in two ways. First, using the ACV dataset, data will be labelled based on the fly's response to an odour puff. Each time series will consist of immobility bouts lasting 5-9 minutes, truncated to the last four minutes to ensure uniform length. Second, using the HMM training dataset, time series will be labelled according to their HMM-derived states of 'deep sleep' and 'light sleep', with each series lasting 8 minutes. The training dataset was used rather than decoding the ACV dataset due to worries the odour puffs will have affected some of the variables.

Since X rarely changes over time and there is a strong likelihood proximity to the odour delivery tube affects response rate (Fig. 5.5.a), X was omitted from the analysis.

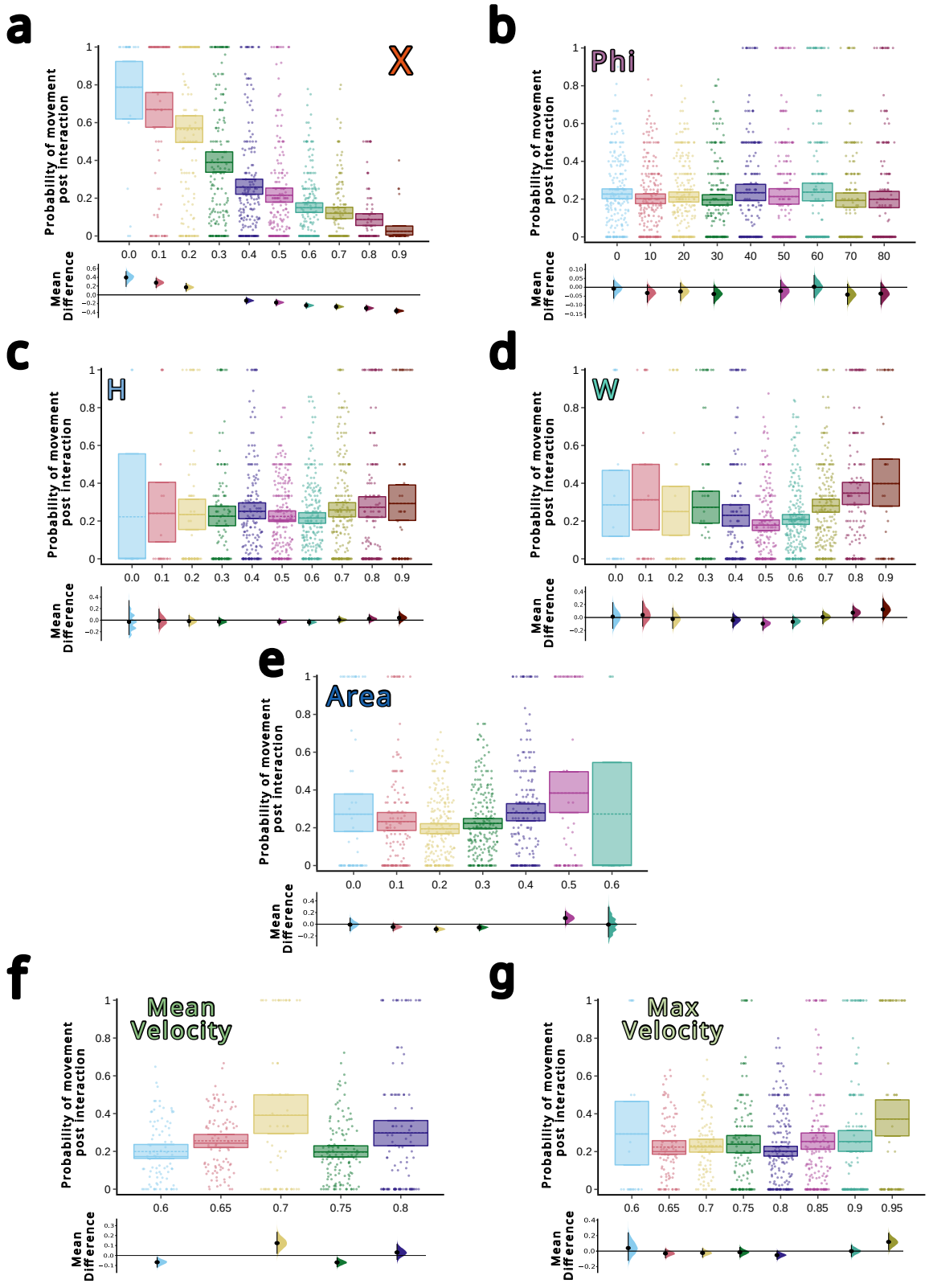


Figure 5.5: **The response rate changes for different values of X, W, Area, and mean velocity.**
(a-g) The value of each variable prior to a puff of apple cider vinegar and its average response rate. The effect size difference of each group was calculated against the median group of each variable using the DABEST statistical package.

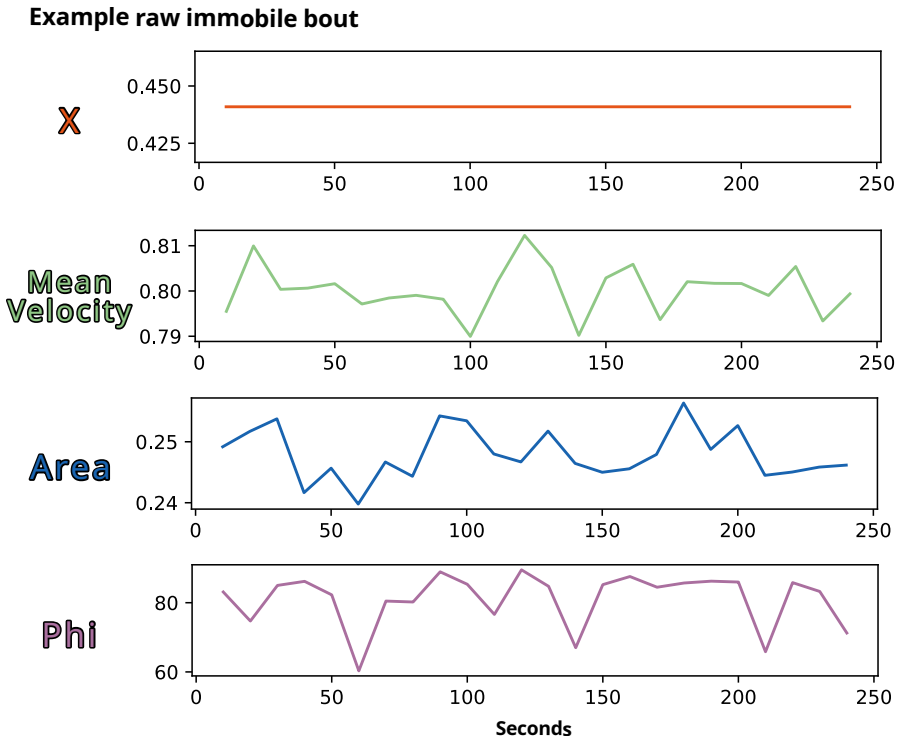


Figure 5.6: **An example of how variables change over an inactive bout.**

5.4.1 Dynamic time warping classification

Dynamic Time Warping (DTW) assesses the similarity between two time series signals by computing the distance between them. Instead of using the Euclidean distance, DTW calculates a warped path that aligns the time series to minimise the loss between corresponding points in the series. This approach allows DTW to effectively match similar signals even when they are shifted along the X or Y axes (Fig. 5.7.a). For example, similarities in walking could be detected even if one person is walking more quickly or slower than the other [434, 435]. Each signal is comapared to one other at a time, generating a distance metric with a lower score indicating greater similarity. The adaptability and simplicity of DTW have made it a robust time series distance measure, and with advances in optimisation, it has become feasible to apply DTW to larger datasets that were previously too computationally-consuming to process [436].

DTW was computed for a multidimensional dataset using an independent strategy. In this approach, each time series in a multidimensional grouping is treated as independent, with the DTW distance calculated between groups summed accordingly [436]. In contrast, the dependent strategy assumes that warping is shared across dimensions.

The DTW distance was employed as the distance metric for a k-nearest neighbour (k-NN) algorithm, a non-parametric supervised classifier [437]. k-NNs relies upon the concept that proximately equals similarity. When applied with DTW, the distance according to DTW between a new times series and the bank of training, labeled, time series is calculated. Given a parameter of 50 neighbours, the labels of the closest 50 banked time series to the new one are counted. The largest label count determines the classification.

For the ACV response dataset, DTW-based classification achieved an average accuracy of 55% in predicting the action at the end of a bout (Fig. 5.7.b&c). While this result was significantly different from the null model, which has randomly shuffled labels, it is only slightly above chance levels. The classifier was most accurate at predicting true responses, with a precision of 63% (Fig. 5.7.b). However, it only recalled between 54-56% of the correct predictions and had a precision of less than 50% for correctly predicting non-responding bouts.

Classifying HMM-generated sleep states yielded accuracy no better than random (Fig. 5.7.d&e). The classifier's accuracy matched the null model, indicating an inability to distinguish between the two sleep states.

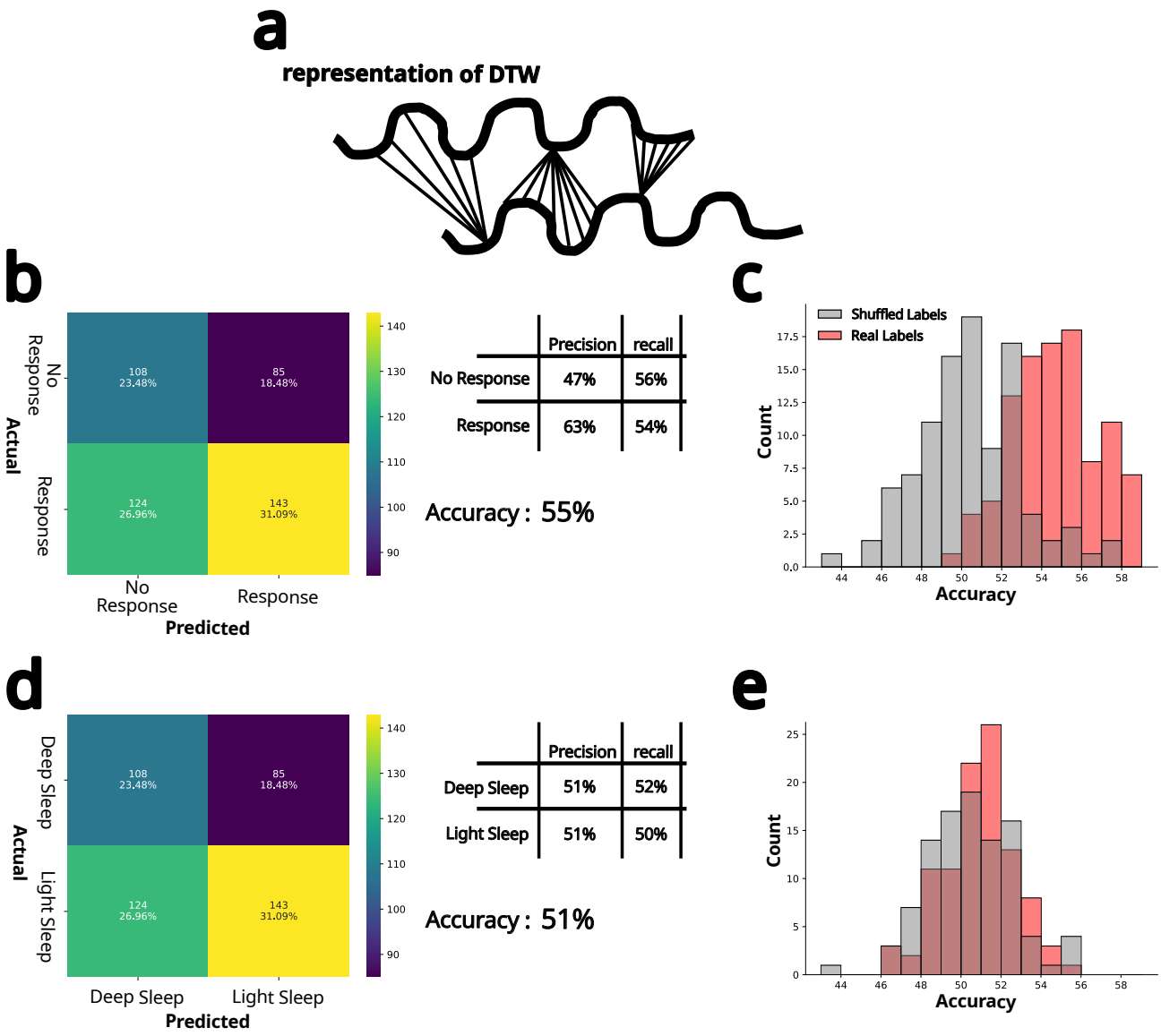


Figure 5.7: **k-NN classification with DTW fails to predict response or HMM sleep state.**
(a) Dynamic time warping (DTW) calculates the optimal match between two given sequences. **(b&d)** An example confusion matrix of a k-NN's predictions using DTW as the distance metric for whether an inactive bout will end with a response or not (b) or if the bout will be classified as 'deep sleep' or 'light sleep' (d) as per a HMM. **(c&e)** Distribution of the accuracy of the model against the null model. The datasets were randomly split into test/train segments 100 times and used to train and test the model (red). Each iteration the labels were shuffled to create a null model (grey).

5.4.2 Catch22 Classification

Canonical Time-series Characteristics (Catch22) refers to a software that generates 22 descriptive statistics per time series [325]. Catch22 is a streamlined version of HCTSA [366], which comprises 4791 features for time series analysis. Many of the descriptive statistics in HCTSA were found to be repetitive or inadequately explanatory of dataset variations [325]. To reduce computing time and complexity the power of each statistic was measured, allowing the creators to reduce the total down to 22. Catch22 captures a diverse and interpretable signature of time series in terms of their properties, including linear and non-linear autocorrelation, successive differences, value distributions and outliers, and fluctuation scaling properties. For a detailed description of each feature see *Methods*.

For each time series instance, the variables (Velocity, Area, and Phi) were processed to generate 22 features per variable, resulting in a total of 66 features. Instances or columns with less than 95% non-special values were excluded (see *Methods*). These features were used to train a random forest classifier.

The random forest classifier achieved an average accuracy of 59% in predicting the correct response to an odour puff, which was significantly better than the null model (Fig. 5.8.a&b). When predicting positive responses, the classifier demonstrated a 67% accuracy. However, it had a lower recall percentage of 58%, which affected its precision in discerning non-responding bouts from responding bouts, achieving only 51% precision. This indicates that while the classifier shows some promise, it struggles to consistently differentiate between the two groups, although certain underlying features are indicative of the action.

A t-SNE plot of the test dataset, labelled with the quality of the prediction, reveals no obvious grouping (Fig. 5.8.c). There is possibly a noticeable concentration of response predictions in the center, contrasting with the more dispersed distribution of non-response predictions.

When replicating the analysis with sleep states generated by the HMM, the results were less promising. The random forest classifier achieved an average accuracy of 52%, which was not significantly different from the null model (Fig. 5.8.e). The classifier had an equal prediction

rate for all classes, indicating randomness (Fig. 5.8.d).

The t-SNE plot shows a slight clustering of time series in the top left quadrant. However, this clustering does not correlate with any specific predictions and likely reflects the distribution of mean velocity (Fig. 5.3.g).

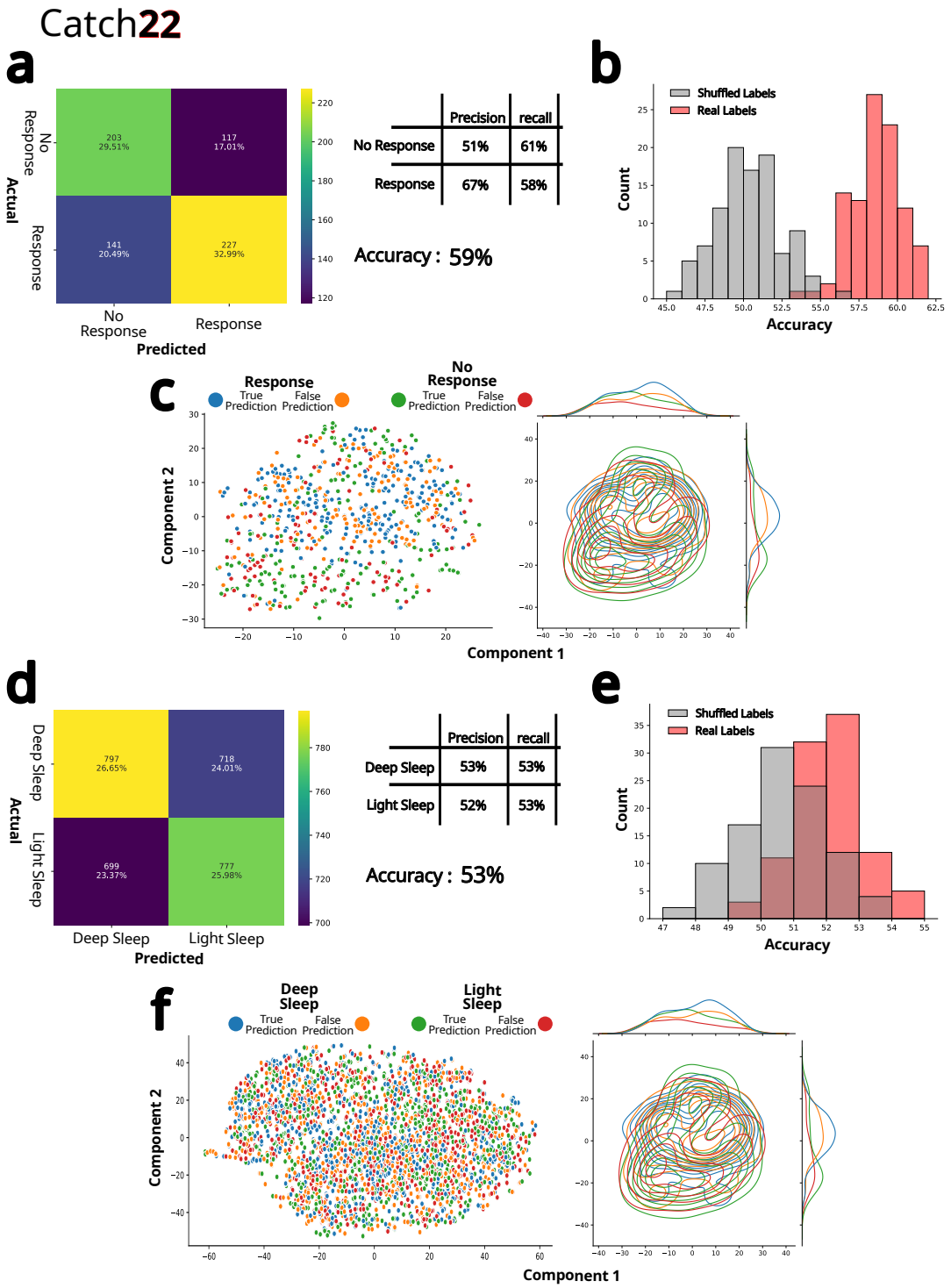


Figure 5.8: **Time series features from Catch22 can marginally predict responses better than random.**
(a&d) An example confusion matrix of a random forest classifiers predictions using the time series features generated by Catch22 [325]. **(b&e)** As in *Figure 5.8* null models (grey) were generated against true models (red). **(c&f)** A two-dimensional t-SNE plot of the predictions and their confusion matrix designation from (a) or (d). Neither, (c) or (f) displayed any obvious clustering.

5.5 Discussion

This section explored whether the variables already tracked by the ethoscope can explain when a fly is sleeping or merely resting, inferring from the animal pose or morphology rather than its time being inactive. The findings offer both promising insights and notable challenges in adapting ethoscope data for a task it was not originally designed for.

The behavioural indicators of sleep described in previous research have typically relied on high-definition cameras or human observation to identify and describe postures during sleep [185, 275] In contrast, the ethoscope's recordings are zoomed out, tracking multiple flies simultaneously. Its primary purpose is to distinguish between walking, micro-movements, and immobility, aiming to improve upon traditional sleep studies that rely on the 5-minute rule [244]. However, as shown in the classification of micro-movements via velocity, the ethoscope can capture small movements imperceptible to the naked eye. Notably, the same velocity data outperformed more detailed keypoint tracking in classifying insecticide effects on *Drosophila* mobility [426]. This suggests that small changes in tracking data could indeed represent sleep behaviours.

A simple exploration of the additional variables showed that apart from W (and Area) and Mean Velocity, the other variables do not appear to reflect meaningful behavioural changes in the fly. Further analysis of Mean Velocity revealed interesting differences between immobile but awake flies, and those immobile for longer periods and presumed to be asleep (Fig. 5.3.g). Sleep velocity falls within two distinct distributions centred around 0.67 and 0.78, a pattern less pronounced in quiet awake flies and absent in active ones. Flies predicted to be asleep with velocities around these two distributions exhibited a higher arousal threshold in response to an odour stimulus than those with velocities around $0.7 - 0.75$. This suggests that sub-one velocity may help to discriminate between behaviours, although the precise biological signal being tracked is still unknown. *Drosophila* sleep may involve rhythmic whole-body movements or postures that are reflected in these velocity values. To identify which movements correspond to these distributions, further research combining high-definition cameras with ethoscope tracking is warranted.

Both the DTW (55%) and Catch22 (59%) models performed better than random in predicting responses to an odour puff (Fig. 5.7-8). Given the dataset was equally split between the two groups, and considering the natural variation in both sleep and awake states, this indicates some degree of difference in the time series features for Phi, Area, and Mean Velocity. Interestingly, using only one variable in the Catch22 classification achieved similar results, with Mean Velocity again proving to be the best predictor, reaching the same average accuracy (59%) as the three-variable classifier. Phi and Area also outperformed the null model, suggesting they contain information related to the response state *(**Phi** = 56%, **Area** = 58%)*. However, a breakdown of each Catch22 feature's distribution revealed no obvious differences between labelled groups. It is likely that small edge-case differences in individual features were enough to enable classification, but only up to a maximum accuracy of 59%. This raises the question of whether the findings are biologically meaningful or merely the result of statistical segmentation. Without further evidence confirming whether the response labels correspond to sleep or wakefulness, the current conclusion must be that the variables are unable to reliably differentiate sleep from wake.

Some elements of the study were flawed from the outset. While the decision to use only daytime data to minimise bias in the response was appropriate, it also limits the study's relevance to daytime sleep, which is less prevalent and generally considered lighter than nocturnal sleep [35, 189, 283]. Future iterations of this work should incorporate infrared filters to standardise tracking across both day and night conditions.

Furthermore, discrepancies in the ellipse values between day and night, as well as between datasets, raise concerns about the ability to derive behavioural insights from the tracking data (Fig. 5.2). If the ellipse can be altered by changes in software or hardware, it casts doubt on its consistency as a behavioural measure and raises the possibility that any patterns observed might be artifacts of the machine. This issue complicates comparisons of data across different machines and time periods, significantly limiting the broader applicability of the findings.

In conclusion, while the ethoscope data has potential, it appears that it cannot yet be used to predict sleep states beyond the conventional 5-minute rule. Further investigation into sub-one velocity data may reveal a more precise rule, but given the significant overlap in distributions,

consistently differentiating between immobile bouts is likely to remain a challenge.

Chapter 6

Identifying sleep hallmarks with high-resolution videos recordings and analysis

6.1 Rationale

The ethoscope was designed to accurately quantify sleep while maintaining high throughput, enabling real-time tracking of *Drosophila* movements for experimental manipulation [244]. However, its purpose was not to capture fine-grained details of every action or body part but rather to differentiate active movements from periods of immobility. As demonstrated in the previous chapter, this tracking method has limited ability to distinguish between flies that are merely inactive or resting and those that are truly asleep. This limitation may stem from the ethoscope's low-resolution, zoomed-out, top-down camera setup, which likely overlooks crucial details that could correlate with known literature on *Drosophila* sleep posture [185].

Given these constraints, it becomes clear that a more detailed experimental setup is required to detect and analyse the subtle changes in posture and behaviour during sleep bouts. High-definition video recording presents the opportunity to capture these nuances, offering a clearer

and more comprehensive picture of sleep in fruit flies. With this enhanced resolution, I aim to identify specific hallmarks of sleep that may have previously been overlooked, thus bridging the gap between behavioural observation and the physiological understanding of sleep in *Drosophila*.

6.2 Behaviour identification through keypoint tracking

Behavioural analysis involves describing and characterising the wide range of responses exhibited by an organism, triggered by internal or external stimuli. This study of behaviour, or ethology, has its roots in the work of early ethologists like Niko Tinbergen, who meticulously documented behaviours to create ethograms with hierarchical structures that reveal how natural behaviours are organised [362, 438, 200].

Ethograms have been instrumental in developing theories about brain function and the evolutionary significance of behaviours, supporting concepts like fixed action patterns and reward-based learning [439, 440, 441]. However, the field has evolved towards greater granularity in analysing behavioural motifs. Today, behaviours once considered as singular actions are dissected into finer sub-components, enhancing our understanding of their neural underpinnings (Brown, 2018). For example, in *Drosophila*, behaviours such as aggression, courtship, and grooming are now broken down into specific sub-components, each with distinct patterns and triggers [259, 223, 202].

This shift towards detailed behavioural analysis has been facilitated by advanced observation tools and recording technologies [336]. However, it has also amplified challenges related to the repeatability and accuracy of manual behaviour quantification [442, 443].

To overcome these challenges, many researchers now employ machine learning algorithms for automated behaviour identification and tracking. These tools have been adapted for various experimental setups, including wildlife video analysis, unsupervised behavioural clustering, and multi-animal tracking in arenas [443, 444, 202]. Such automation has led to the discovery of complex behaviours, especially those involving social interactions, that were previously too

intricate to score manually [245, 240]. Although manual verification and explanation is still an integral part of the process.

User-friendly software interfaces have been developed to democratise access to machine vision tracking, building on robust, generalisable neural networks. Notable examples include SLEAP [252] and DeepLabCut [250], among others [253, 248, 445, 243]. These tools allow researchers to label specific body parts, such as limbs and antennae, within video frames, training convolutional neural networks to recognise these features across frames.

While these tools enable detailed limb tracking without the need for specialised hardware, they are not without limitations. Optimal performance requires videos with consistent lighting and clear feature visibility. It is also important to note that the software does not identify behaviours on its own. Instead, it produces a multi-point time series that tracks the dynamics of labelled body parts, providing the data needed to segment and match these dynamics to specific behavioural motifs [364, 446].

6.3 Capturing high resolution videos

6.3.1 Setup

To achieve high-fidelity recordings of *Drosophila* sleep, a new video capture setup was developed, prioritising resolution over throughput. This setup, while reducing the number of flies recorded simultaneously, offers detailed, high-resolution video of individual subjects. Staying true to the ethoscope's principle of accessibility, the new high-defintion (HD setup continues to utilise a Raspberry Pi microcomputer for video processing and power, paired with its standard 12 MP HD camera and an additional 16mm telescopic lens, see Methods. All components are readily available and cost-effective.

Custom 3D-printed mounts were designed to securely hold the Raspberry Pi, camera, and lens (Fig. 6.1.a). The lens mount also incorporates a filter that allows only infrared light to

pass through, ensuring consistent lighting across all time points, independent of visible light conditions.

The camera mount is attached to a secondary structure that houses the fly arena. To better capture behaviours such as becoming more prone, antennal oscillation, and proboscis extension, actions that are partially obscured in a top-down view, the arena was designed to keep the fly in a profile orientation when not actively turning around (Fig. 6.1.b). This was accomplished by limiting the arena's depth. Due to size differences, female arenas were made slightly deeper than those for males, see *Methods*. Additionally, a second level was introduced to provide the fly with more space to explore and rest, after it was observed that smaller arenas were inducing hyperactive behaviour.

The videos were illuminated using two infrared light sources: one directed onto the glass front and another positioned behind a thin plastic wall at the back of the arena. This dual lighting setup enhanced both the silhouette and profile features of the fly (Fig. 6.1.a).

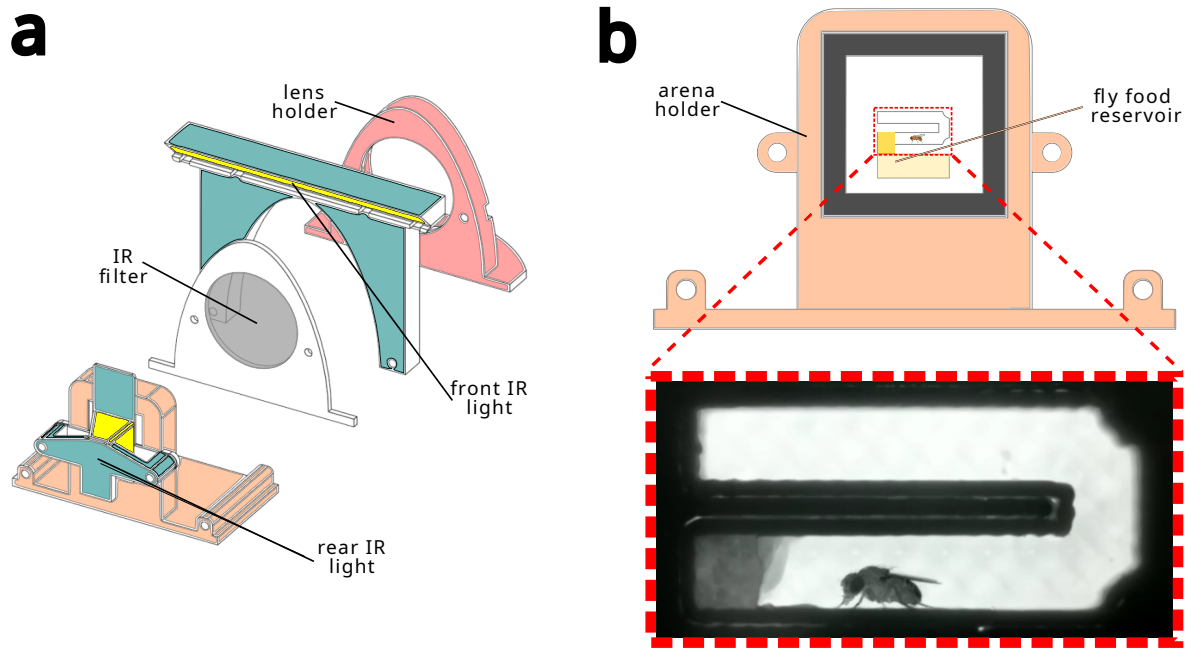


Figure 6.1: **The new high-definition video capture setup.**
(a) Custom 3D printed frames were designed to support the camera and lens (red) , the IR-only filter (white / grey), and the IR lights (green / yellow). **(b)** A custom 3D printed arena was designed to house the fly that kept it in profile view, see *Methods* for the specifications. The arena contains diluted standard media in the base.

6.3.2 Curation

Each individual fly was recorded over a period of 1-2 days, resulting in several large video files capturing a variety of behaviours. Since the primary focus was on identifying behaviours associated with sleep, sequences in which the fly was walking, grooming, or feeding were excluded. To facilitate this, hour-long videos were automatically segmented into shorter clips based on movement detected from frame to frame, determined by a pre-set threshold, see Methods. This segmentation, followed by manual curation, produced a dataset of 157 videos from four male and four female CS flies, with video lengths ranging from 4 to 50 minutes.

6.4 Applying keypoint tracking

6.4.1 Model training

The SLEAP software [252] was selected for its rapid model training capabilities and iterative labelling workflow (Fig. 6.2.b). Individual models were trained for each fly to minimise errors. For each model, three keypoints were labelled across a selection of frames from at least 10 videos. The chosen keypoints were: the head, labelled at the centre of the eye; the body, marked at the junction of the wing and body; and the abdomen, labelled at the centre end (Fig. 6.2.a). Typically, 40-60 labelled frames were used to train the model, which was then tested on a new video. If the model's predictions were visually accurate, it was applied across all frames of all videos. If inaccuracies were found, corrections were made, the new labels were added to the training set, and the model was retrained until satisfactory results were achieved.

Initial attempts were made to label additional keypoints, such as the proboscis and the halteres, to replicate findings from *Keles et al.* [185]. However, due to video quality issues and occasional visual obstructions, tracking accuracy for these keypoints was consistently poor. Consequently, the keypoint skeleton was simplified to the three described above.

6.4.2 Model accuracy

SLEAP provides built-in statistics to assess the accuracy of trained models, using the labelled frames as ground truth [251, 252]. The localisation error across all models generally clustered between 1-2 pixels, with a maximum error reaching up to 5 pixels (Fig. 6.3.a). This level of error is typically considered very good. The greatest inaccuracies were observed in the abdomen labelling, likely due to challenges in maintaining consistent labelling across frames.

Another metric used to evaluate model performance is Object Keypoint Similarity (OKS), which takes into account landmark visibility, animal size, and the difficulty of keypoint localisation [447]. Most models achieved high average OKS scores above 0.8 (Fig. 6.3.b). However, it is worth noting that the model for Female1 displayed a wider distribution of scores, with some clustering around 0.5, while Male1 had a few scores as low as 0.2, indicating poor performance. Female1 had the largest number of videos, 33, which may account for the greater variance in scores.

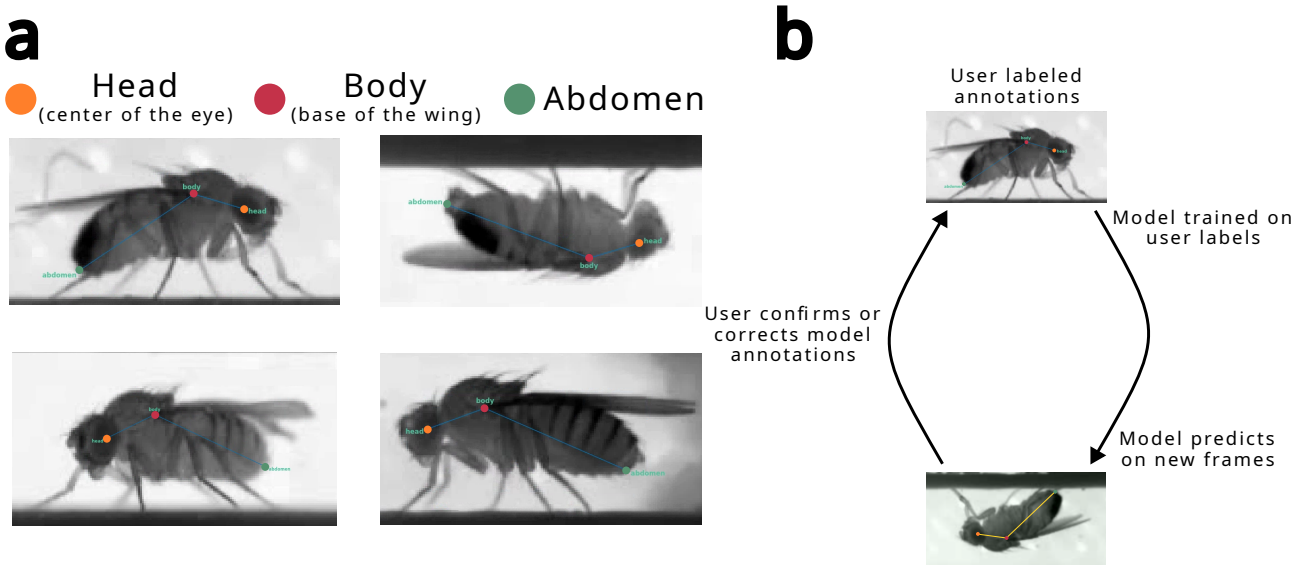


Figure 6.2: **Videos of inactive bouts were labelled on the head, body, and abdomen.** **(a)** Labelling guide for the three keypoints. The head (orange) keypoint was placed in the center of the eye. The body (red) keypoint was placed at the base of the wing. The abdomen (green) was placed at the center of the end of the abdomen (terminalia). **(b)** The SLEAP workflow [252] entails the user labelling a random selection of frames which are used to train and label further frames. The user confirms or corrects the new labels to add to the training dataset.

6.5 Manual behaviour segmentation

6.5.1 Description of postures

During video curation, three distinct posture changes were identified, allowing the majority of videos to be categorised accordingly. These postures have been labelled as *full prone*, *part prone*, and rise (Fig. 6.3.c). Although some videos displayed a combination of these postures, key traits were used to make judgement calls on their categorisation.

In the *full prone* posture *(**female** = 17, **male** = 4)*, the fly lowers its entire body towards the surface, typically, but not always, in alignment with gravity, nearly touching the surface while remaining prone. This posture has been previously described [275, 185]. Notably, this posture

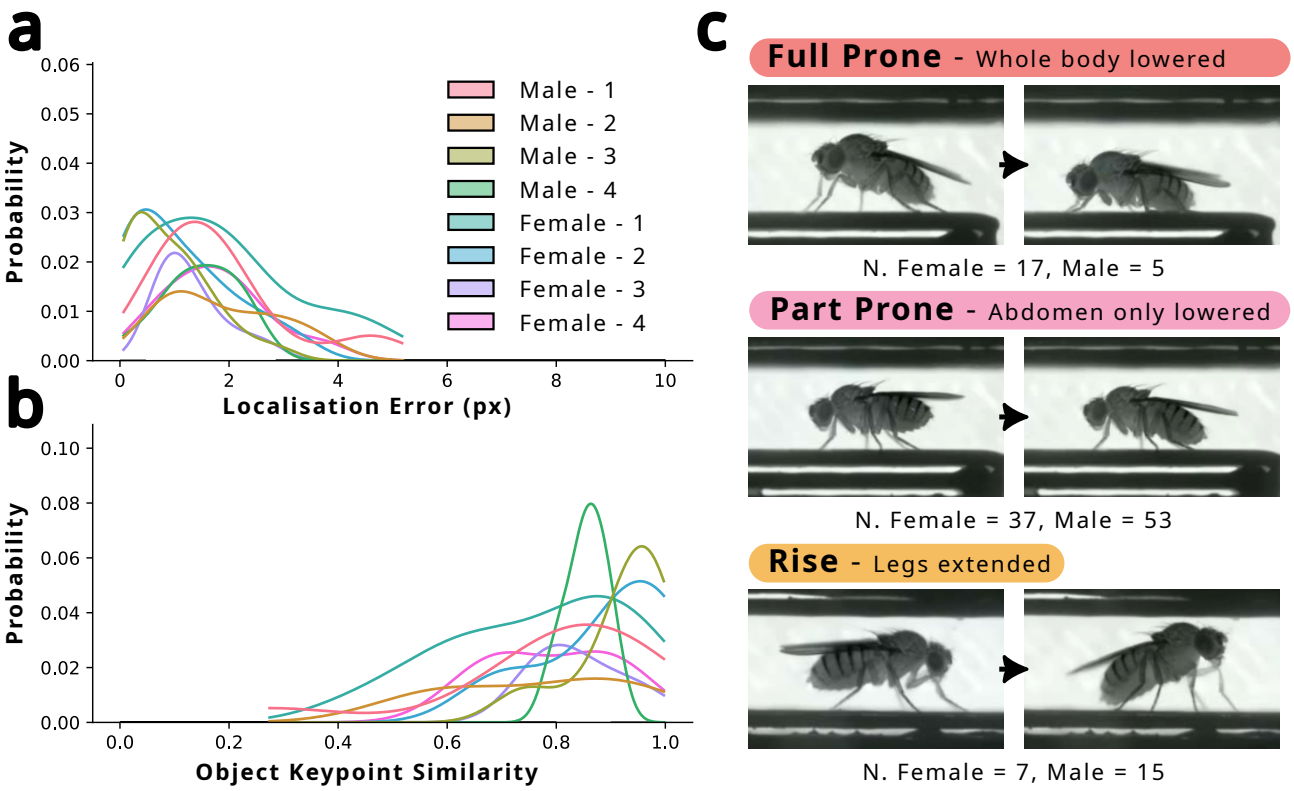


Figure 6.3: **Three observable sleep postures were manually identified.** **(a)** The majority of localisation error from new predictions was less than 2 pixels for all models. **(b)** Most models object keypoint similarity score was greater than 0.8 which is considered good. Some of the frame predictions scored lower, but were infrequent. **(c)** Examples of the observed changes in posture. During ***full prone*** (peach) the fly lowers the its whole body to the surface. During ***part prone*** (pink) only the abdomen is lowered to the surface. Often this pose was already assumed by the fly before coming inactive. During **rise** (yellow) the fly extends their legs, raising the head/body. It is often accompanied by a lowering of the abdomen.

was observed three times more frequently in females than in males, with 11 out of 17 (65%) instances occurring in a single female, marking it as the most disproportionate category.

The *part prone* posture *(**female** = 37, **male** = 53)* represents a variation of the *full prone* where only the abdomen is lowered, while the head and body remain relatively stationary, distinguishing it from the *full prone*. Both *part prone* and rise involve a transition from one posture to another, and they are defined by these movements. However, in the case of *part prone*, the fly's abdomen may already be lowered, suggesting that the automatic video segmentation might be truncating the beginning of these bouts. Often, flies engage in grooming in this position, which could indicate that it is a typical resting posture. The *part prone* is the most common posture, accounting for 57% of observations.

The rise posture *(**female** = 7, **male** = 15)* shares characteristics with the *part prone*, where the abdomen lowers towards the ground. However, the key distinction is that the head and body appear to rise as the legs extend. The extension of the legs was the decisive factor in classifying a bout as rise.

A fourth category, no change *(**female** = 12, **male** = 12)*, was assigned to videos where no postural change was observed, and the fly's abdomen remained elevated.

6.5.2 Do the angles at keypoints describe the behaviours?

To validate these categorised postures, several metrics were explored as hallmarks of each category. For Figures 6.4-6, the first 70% of each video was used to capture the initial pose and the subsequent sleep pose before awakening.

Given that *full prone* and rise involve active changes over time, it was suspected that there might be changes in the angles from the beginning to the end of the sleep posture. To assess this, the mean difference of each angle at the end minus the average angle at the beginning was calculated. In both male and female flies, no significant changes were observed in the head or abdomen angles from beginning to end (Fig. 6.4.a&c). The only change detected was an increase of $\approx 4.5^\circ$ in the body angle in female flies within the rise category (Fig. 6.4.b).

No changes were observed in the *part prone* or *full prone* categories, and none in male flies. This lack of change in *part prone* was expected, as many flies were already in position, thereby excluding them from change. However, in *full prone*, it appears that the action of flattening the fly to the surface maintains the relative positions of each keypoint. It was anticipated that the rise posture would result in a decrease in the body angle due to the lowering and forward movement of the abdomen; however, this change may not be as pronounced as expected or may be offset by the rising of the head.

It was hypothesized that differences in the angles formed by the head, body, and abdomen would be observed between the *part prone* and rise postures, given the lowering of the abdomen and the apparent raising of the head and body in rise (Fig. 6.3.c). However, quantifying the average size of these angles over the bout revealed no significant differences between the three categories in both male and female flies (Fig. 6.4). While differences between the sexes were observed, these were expected due to morphological differences.

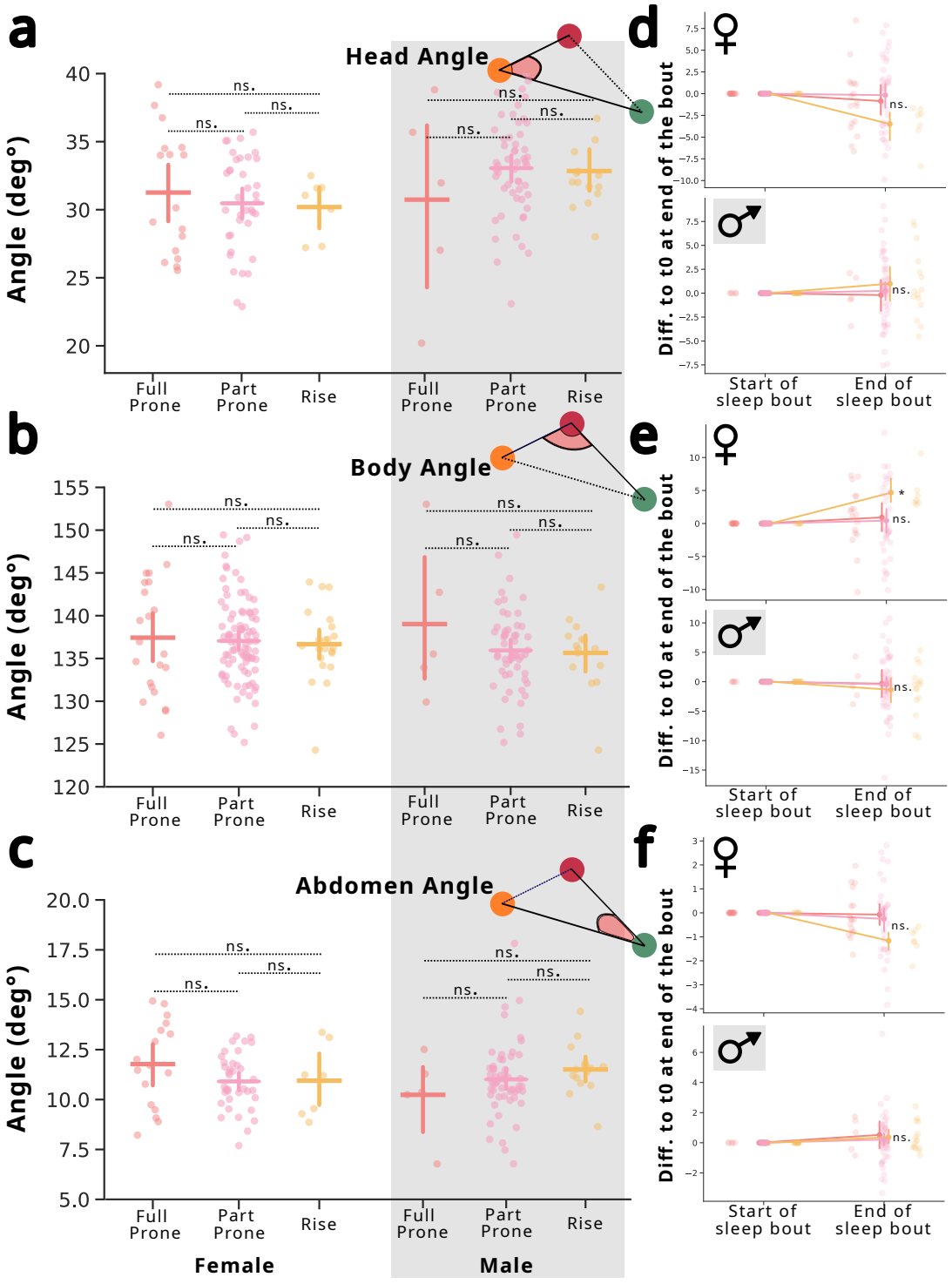


Figure 6.4: **The angle at each keypoint does not distinguish the postures.** **(a-c)** The average angle at the head, body, and abdomen for the first 70% of the inactive bout. Mean and 95% CIs. **(d-f)** Changes in the angle from the beginning of the video (first five seconds) to the angle after 70% of the inactive bout (final five seconds). Ns. denotes no significant difference between groups, $* \leq 0.05$. Grey shading indicates quantification of male fly posture. Mean and 95% CIs.

6.5.3 Does the centroid describe the behaviours?

To identify a metric quantifying the *full prone* posture, the y-coordinate of the centroid was calculated, hypothesizing that it might indicate a lowering of the fly's entire mass. The centroid was standardized at each timestamp as the absolute difference in x and y coordinates relative to t = 0 (t0), see Methods. Surprisingly, there was no significant difference in the average difference to t0 between all categories for both male and female flies (Fig. 6.5.a). Across the sleep bout, all groups exhibited a difference of 2.5 - 5 pixels from the initial position *(**Female**: full prone = 4.2 +- 1.6, part prone = 3.1 +- 1.0, rise = 1.7 +- 0.58, **Male**: full prone = 3.2 +- 1.0, part prone = 2.3 +- 0.8, rise = 3.1 +- 1.3).*

This pattern persisted in the difference between t0 and the end of the bout, with all categories in both male and female flies showing an increase compared to t0, indicating an active change in posture over time for all categories.

6.5.4 Does the distance between keypoints describe the behaviours?

The distance between the head and abdomen was the only metric that differentiated the categories (Fig. 6.5.b). As previously observed, the female fly group exhibited significant change, with the average distance in the *full prone* group being shorter than in the other categories *(**Female**: full prone = 97 ± 1.2, part prone = 101 ± 1.3, rise = 102 ± 0.98).* This suggests that the horizontal alignment of the body in *full prone* shortens the distance between the abdomen and head, while a lengthening occurs when the abdomen is lowered with a raised head. No differences were observed in any keypoint distances from the start to the end of the bout.

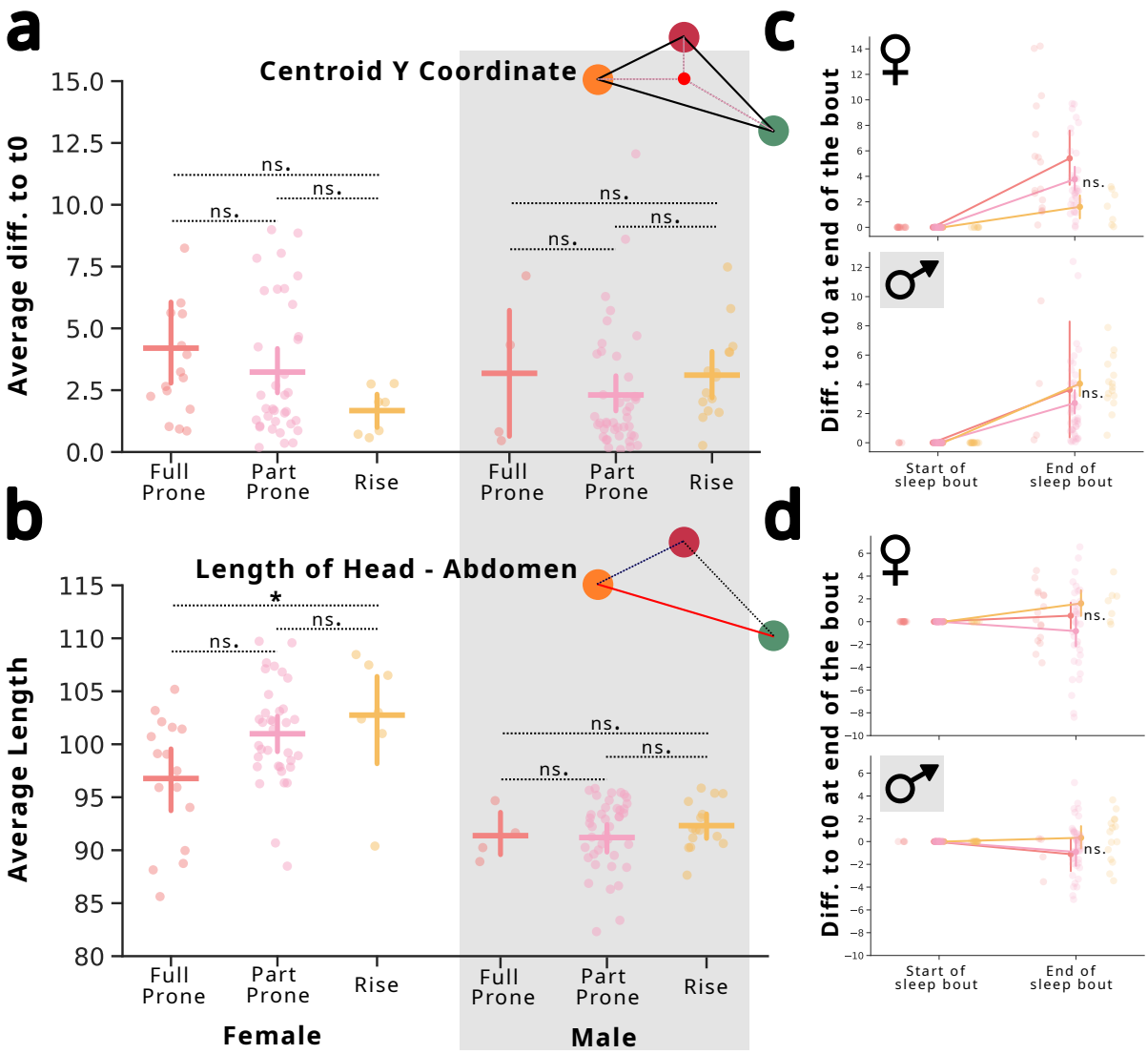


Figure 6.5: **Changes in length between the head and abdomen identify *full prone* in female flies.**
(a) The average absolute difference in the y-coordinate to its value at t0 reveals no difference in postural groups. Mean and 95% CIs. **(b)** The average length from the head to the abdomen over an inactive bout. Mean and 95% CIs. The *full prone* posture in female flies has a decreased length compared to the rise posture. **(c-d)** Changes in values from (a) and (b) from the beginning of the video (first five seconds) to after 70% of the inactive bout (final five seconds). Ns. denotes no significant difference between groups. Grey shading indicates quantification of male fly posture. Mean and 95% CIs.

6.5.5 Do changes in the y-coordinate of keypoints describe the behaviours?

To explore unique changes, the absolute difference of each keypoint to t0 was calculated (Fig. 6.6).

Female flies showed no significant difference in the average absolute difference of the head's y-coordinate over the video or in the difference between the start and end. However, all categories exhibited an absolute change in the y-coordinate from start to finish (Fig. 6.6.a). In male flies, the rise posture showed a greater average change in the head y-coordinate compared to the *part prone*, but not *full prone (**Male**: full prone = 4.9 ± 1.69, part prone = 2.4 ± 1.1, rise = 4.5 ± 1.9)*. This reflects the observable change in head position relative to the fly's center mass (Fig. 6.3.c). This difference is also evident in the change from the start to the end of the bout, indicating that it is a persistent change.

A similar change was observed in the body y-coordinate, suggesting a linked postural change between the head and body, but not the abdomen (Fig. 6.6.b). This was only seen in the male flies *(**Male**: full prone = 3.0 ± 1.0, part prone = 2.1 ± 0.8, rise = 4.1 ± 1.6)*. Again, this difference is reflected in the change from start to the end of the bout.

In female flies, the *part prone* posture showed the largest increase in the abdomen's y-coordinate, both on average and in the difference from start to end *(**Female**: full prone = 3.1 ± 1.32, part prone = 8.1 ± 2.1, rise = 3.3 ± 1.6)* (Fig. 6.6.c). It is interesting that only *part prone* showed a significant change in the abdomen's y-coordinate compared to rise, even though both *full prone* and *part prone* visually involve lowering the abdomen. It is possible that maintaining an upright body and head posture in *part prone* increases the distance the abdomen must travel to be lowered.

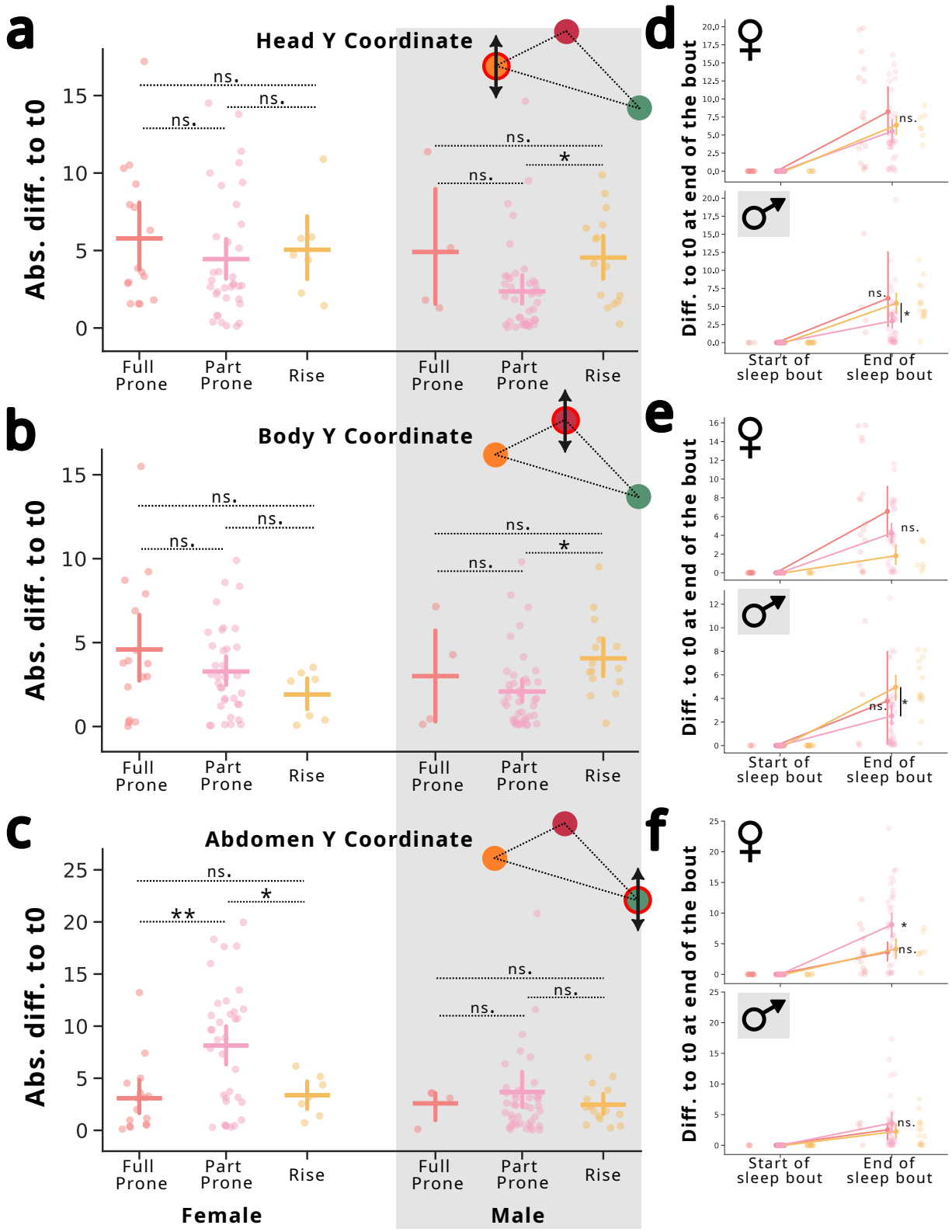


Figure 6.6: **Changes in the y-coordinate of keypoints identify postures.** **(a-c)** The average absolute difference in the value of the y-coordinate from t0 identifies differences in male and female postures. Mean and 95% CIs. **(d-f)** Changes in values from (a-c) from the beginning of the video (first five seconds) to after 70% of the inactive bout (final five seconds). Ns. denotes no significant difference between groups, $* \leq 0.05$, $** \leq 0.01$. Grey shading indicates quantification of male fly posture. Mean and 95% CIs.

6.6 Time-series analysis of postural keypoints

Postural changes, as represented by keypoint coordinate changes over time, can be broken down into separate one-dimensional time series. Many supervised machine learning tools for keypoint behavioural analysis utilize this approach to identify motifs and metrics that characterize user-labelled behaviours [364, 446]. To this end, the individual x- and y-coordinates of each keypoint, as well as the centroid, were analyzed using the catch22 time series analysis suite described in *Chapter 5* [325]. The data were first standardized by subtracting the value at t0 from each value to account for differing coordinates.

Generation of t-SNE plots for both female and male groups revealed no obvious clustering that aligned with the study's generated categories or any that the embedding could identify (Fig. 6.7.a&b). Further analysis of t-SNE plots for each keypoint's time series also revealed no grouping at any level, indicating that the 176 different variables generated were not causing excessive complexity in the dataset (data not shown).

Catch22 includes frequency analysis (*Methods*), but given that antennal oscillation is a well-documented sleep indicator [185, 422, 179, 181], and considering the observed minor movements of the abdomen during immobility bouts, frequency power was investigated independently of Catch22 (Fig. 6.7.c). Frequency analysis using Fourier, Welch, Lomb-Scargle, and chi-squared algorithms revealed no significant power peaks at any frequency. As shown in the sample plot for the abdomen x-coordinate using the Fourier transformation, only noise was detected at frequencies between 0-1.

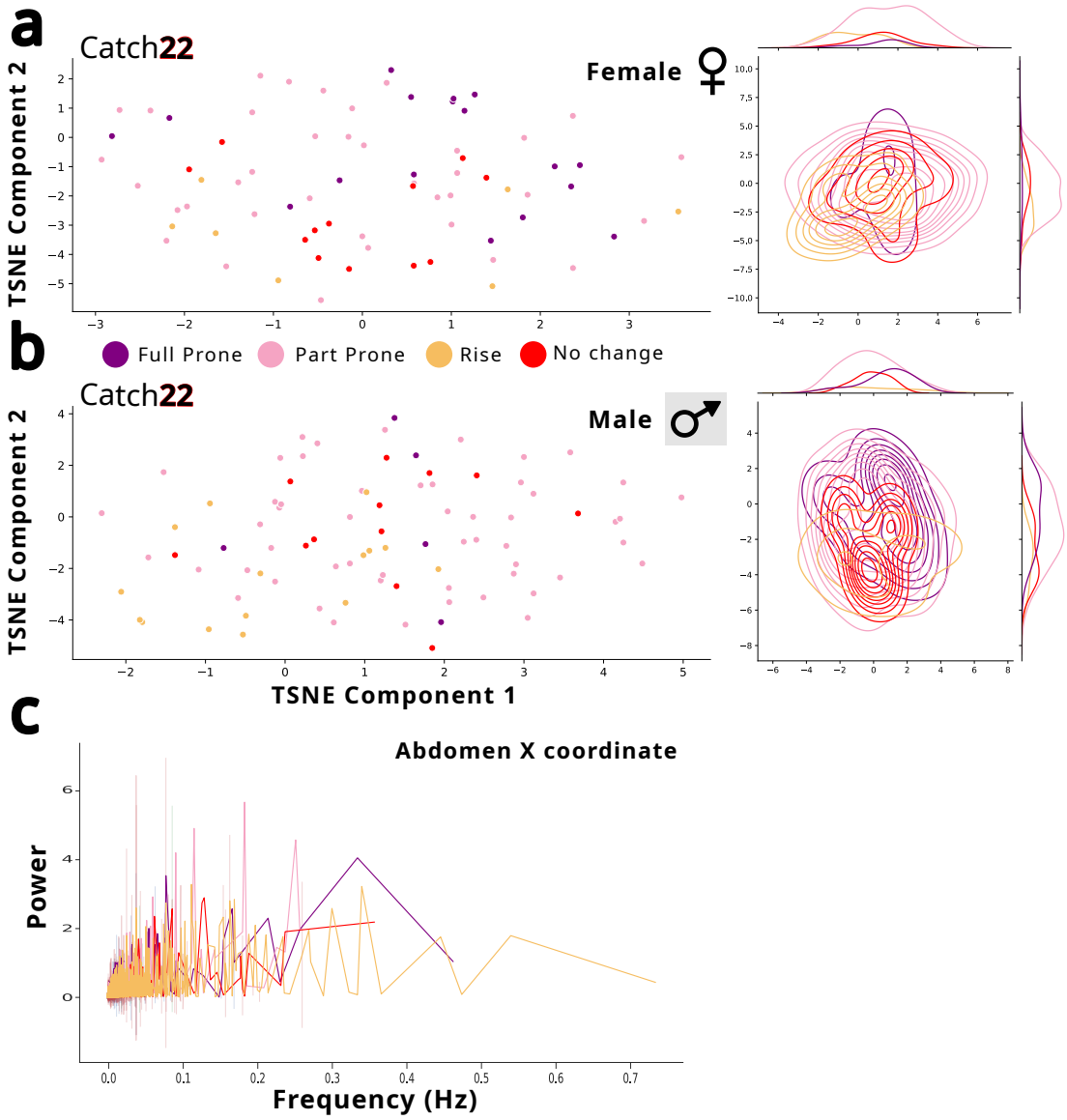


Figure 6.7: **Time series analysis of keypoint locations reveals no differences.** **(a&b)** Catch22 time series analysis was applied to each variables x and y coordinates. A two dimensional t-SNE component analysis showed no obvious clustering. **(c)** An example fast fourier transformation to test for rhythmicity. No coordinate time series had any identifiable peaks in frequency power.

6.7 Behavioural observations

A novel sleep posture in *D. melanogaster* is the 'haltere switch' described by *Keles et al.*, where the haltere moves ventrally, persisting for approximately 2-20 minutes [185]. While this study's hardware limitations precluded consistent tracking of the haltere, manual observations confirmed the occurrence of the switch (Fig. 6.8.a). In the two cases illustrated, the switch was noted near the end of a 3:50 minute bout and at 1 minute into a 4:20 minute bout. As previously described by *Keles et al.*, the switch persisted through the remainder of the bout, accompanied by oscillations. However, due to obstructions and poor focus in some videos, it was not possible to reliably quantify this phenomenon across all observations. Notably, in several immobility bouts lasting over 10 minutes, no haltere switch was observed.

In approximately 13% of all videos, a previously undocumented behaviour was noted: a protrusion of the distal region of the abdomen that contains the genitalia and hindgut, the terminalia [448] (Fig. 6.8.b). This protrusion did not follow a consistent timing, occurring at various points—beginning, middle, or end—of the immobility bouts. It remains unclear whether this behaviour is sleep-related or occurs during wakefulness immediately before or after sleep, or during mid-sleep arousals'. Speculatively, this behaviour may be analogous to the proboscis extension observed during sleep, albeit infrequently in this study's videos. The proboscis extension does not occur in all sleep bouts and varies in duration, having been tentatively linked to waste clearance [264], although evidence is sparse. It could also be indicative of a muscle twitch, akin to those observed in REM sleep [20]. If this were the case, the terminalia protrusion might represent a similar muscular response. However, the absence of this behaviour in the broader literature casts doubt on its significance as a definitive sleep hallmark.

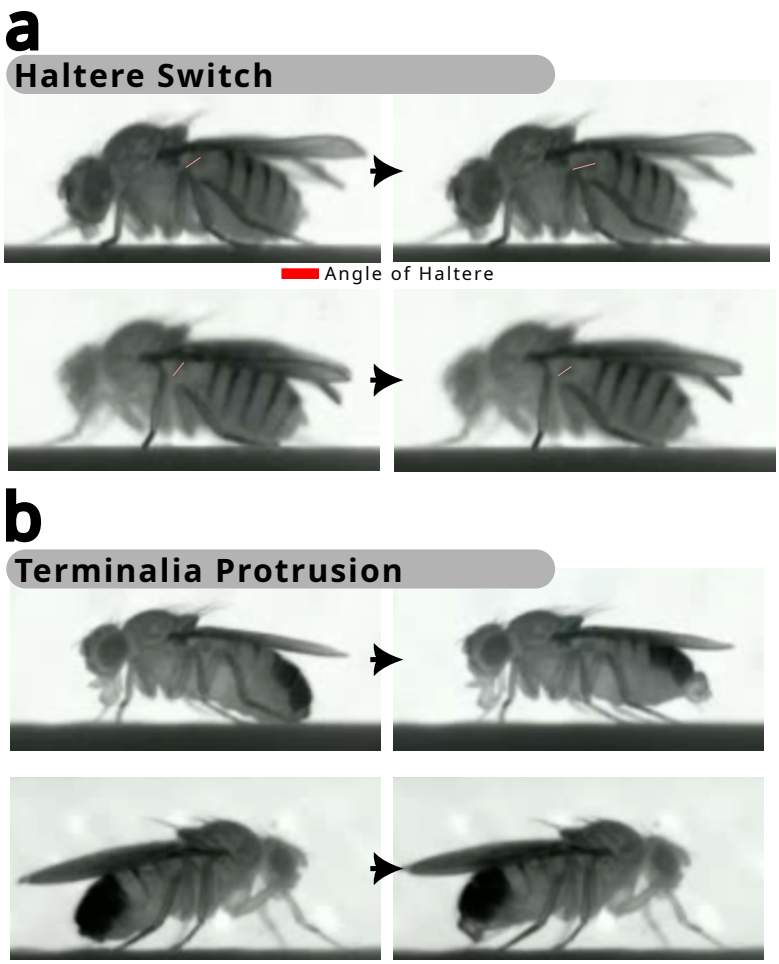


Figure 6.8: **The sleep identifier the 'haltere switch' and terminalia protrusion were observed.**
(a) The lowering of the angle of the haltere as described in *Keles et al.* was observed infrequently in this study. **(b)** Episodic extension of the terminalia is observed in both male and female flies during bouts of inactivity.

6.8 Discussion

The findings of this study aimed to expand the current understanding of sleep posture in *D. melanogaster*. However, due to hardware and time constraints, the study primarily succeeded in re-describing known postures and generating new metrics for their classification.

The relaxation of the body during sleep has been previously documented. The illustration by *Hendricks et al.* aligns with the *full prone* posture described here, where both the abdomen and thorax of the fly lower to the surface [275]. Similarly, *Keles et al.* quantified this behaviour as a lowering of the thorax, a metric that was replicated in this study [185]. Among both male and female flies classified as exhibiting the *full prone* posture, 17 out of 21 (81%) showed an average change in thorax position, ranging from 2.3 to 17 pixels (Fig. 6.6.b). The remaining four flies were already in the prone posture at the start of the observation. This behaviour, where the fly appears fully relaxed and ceases other activities such as grooming, superficially seems to be a clear indicator of sleep. Yet, out of 157 periods of immobility observed over eight days, only 21 (13%) exhibited this behaviour, amounting to approximately 320 minutes of sleep across seven out of the eight flies. Given its infrequency, both within individual flies and across the entire sample, it is unlikely that *full prone* is the sole sleep posture, especially when considering conventional estimates that males sleep for $\approx$ 10 hours and mated females for $\approx$ 5 hours [53].

Keles et al. did state that postural relaxation did not always precede prolonged periods of behavioural quiescence [185]. Nevertheless, they demonstrated that the arousal threshold increased, on average, in flies that remained inactive for more than three minutes, which could suggest that sleep may be present in most quiescent periods. However, they did not specifically compare the arousal threshold of flies exhibiting postural relaxation to those in quiescence without relaxation, which would be necessary to confirm this hypothesis.

Extrapolating from these observations, it is likely that all the behavioural postures described in this study include instances of sleep, though the precise distribution of sleeping versus merely resting flies remains unknown. Unfortunately, this study was unable to conduct arousal

threshold experiments that would have allowed for a more definitive understanding of these differences.

The haltere switch, as described by *Keles et al.* [185], is considered not just a marker of sleep, but specifically of deeper sleep, characterised by a higher arousal threshold compared to quiescent sleep. While this study could not reliably track and quantify the haltere switch, it was potentially observed in several videos (Fig. 6.8.a). The switch typically occurred several minutes after a postural change and was not limited to fully prone flies; it was also observed in part prone flies and those in a rise posture. However, video limitations—such as occlusion of the haltere by wings or legs, especially in the more compact male flies—prevented a full analysis of haltere switch occurrences. While not definitively quantifiable, these observations suggest that all described behaviours may include sleep states capable of deeper sleep, challenging any notion that these postures might represent different types of sleep. Further research is required to confirm this.

If taken at face value, these findings suggest that the description of sleep posture should be revised to include only a relaxation of the abdomen.

Although these behavioural states have not been confirmed through arousal threshold tests, they can be categorised by quantifiable metrics. For instance, *full prone* is marked by a reduced distance between the head and abdomen, *part prone* by a greater change in the y-position of the abdomen, and rise by a greater change in the y-position of the head and thorax. However, these metrics were only confirmed within either male or female populations, not both. The unequal distribution of bouts, with *part prone* comprising 57% of cases, posed difficulties in generating statistically significant demarcations for the other categories. This limitation could be addressed with additional video data.

Furthermore, the automatic segmentation of videos to exclude movement often resulted in the capture of postures that were already present, particularly in *part prone* bouts, though this was also seen in some *full prone* videos but never in rise videos. Standardising the keypoint location time series by subtracting the value at t0 meant that many videos lacked any dynamic change, potentially obscuring useful classifiers of posture transitions. This likely contributed

to the failure of t-SNE plots to generate any meaningful clustering post-time series analysis.

Capturing these transitions is not simply a matter of fine-tuning the movement threshold in the sorting software. Abdominal relaxation is also observed during grooming, which often precedes bouts of quiescence. Therefore, abdominal relaxation should perhaps be considered a general rest posture, rather than exclusively indicative of sleep. Distinguishing between quiescence and sleep during this posture, particularly before a haltere switch to deeper sleep, remains a challenge, and one that is necessary to address given the frequency of abdominal only relaxation sleep.

6.9 Further work

Future research should prioritise the increased capture of fly sleep in both males and females to enhance the robustness of the statistical analyses distinguishing and identifying sleep postures. A larger dataset would enable more accurate and reliable identification of the subtle postural changes associated with sleep.

In parallel, the arousal threshold associated with each posture should be quantified to confirm the presence of sleep definitively. Of particular interest would be the potential separation of the *part prone* posture into two distinct groups: one with a high arousal threshold indicative of sleep, and another with an arousal threshold comparable to wakefulness. To achieve this, an escalating stimulus, such as gradually increasing heat, could be applied to the flies, allowing for the identification of behavioural hallmarks that distinguish these groups. Given the difficulty in visually detecting consistent differences within the *part prone* group, machine learning could be employed to assist in this analysis. Convolutional neural network image classifiers, trained on labelled video data, could be used to predict whether there are subtle visual distinctions between these groups in new video sets.

Should the CNN classifiers demonstrate high accuracy, the next step would be to utilise higher resolution videos, annotated with a greater number of keypoints, to pinpoint specific differences or their dynamic changes over time. This approach would not only refine our understanding

of sleep postures but also potentially uncover previously unrecognised behavioural markers associated with different sleep states in *D. melanogaster*.

Chapter 7

General discussion

7.1 Summary

This study aimed to characterise *Drosophila* sleep through observational markers, with the goal of broadening the metrics we use to understand sleep in fruit flies. The intention was to achieve this without compromising the high-throughput nature and ease of use that are fundamental to *Drosophila* research. This study utilised hidden Markov models, machine vision tracking and learning, and high-definition (HD) video analysis to achieve these goals.

Exploration of HMM-predicted sleep states- 'deep sleep' and 'light sleep'- revealed some uncertainty regarding the biological validity of these predicted states. While they appear to offer a more nuanced and enriched version of the traditional 5-minute rule, which categorises sleep based on movement cessation, the results were ambiguous. These new states provided a more accessible overview of sleep bout lengths and activity patterns over time but did not conclusively establish themselves as true biological sleep states.

This work attempted to move beyond simple movement-based definitions of sleep by incorporating advanced tracking methods. Using both ethoscope data and HD keypoint tracking, this work aimed to capture more intricate behavioural nuances that could be correlated with sleep and sleep stages. While the observations from the videos aligned with established literat-

ure, the limitations of my experimental approach meant that the findings remained qualitative rather than quantitative. Furthermore, the study provided limited insight into the complex phenomenon of multiphasic sleep, which warrants further investigation.

The majority of the above was achieved in ethoscopy, a Python-based behavioural analysis toolbox, created during this study. The aims of ethoscopy were to expand the analysis suite of rethomics and to maintain the accessibility of complex analytical methods for all skill levels. This included the integration of training, decoding, and visualisation of HMMs. It is hoped this new toolbox will help new users generate tailored HMMs for all the animals, mutants, and variants in their experiments.

7.2 Findings

7.2.1 Probabilistic modeling Vs Inferential analysis

The five-minute rule for defining sleep in *Drosophila* is rooted in early work that used inferential statistics to identify the approximate moment when the arousal threshold of resting flies became significantly different from earlier moments. While this method effectively highlights population-level differences, it inherently discards information related to the individuals' probabilistic events of sleep, which are essential for understanding behaviour in its context.

Given that circadian rhythms and behavioural hierarchies exhibit a highly probabilistic nature, it stands to reason that probabilistic models offer a more comprehensive framework for understanding the interplay of these elements, especially under conditions of perturbation [301]. This growing recognition has driven a shift towards quantifying sleep with probabilistic analyses. For instance, *Wiggin et al.* explored the probabilities of transitioning into an inactive state, P(Doze), and transitioning from inactivity to waking, P(Wake), as a means of mapping the shifting pressures of sleep and wake throughout the day. The varying ratios of these transitions can represent environmental changes or mutant phenotypes in a two-dimensional space [319]. Building on this, the framework was adapted into a HMM that assigns probabil-

istic transitions to a hidden layer comprising of four states. My study, though modifying the transition freedom between wake states, corroborates *Wiggin et al.'s* findings, supporting the idea that a four-state model provides more robust and interpretable results, with each state characterised by distinct arousal thresholds.

The study by *Wiggin et al.* did not provide a detailed breakdown of the decoded states, making it challenging to directly compare their findings to the critiques raised here. Assuming the decoded outputs are similar, the HMM's limitation lies in its rigid classification of sleep states. All periods of inactivity longer than 11 minutes are categorised as 'deep sleep', which seems biologically inconsistent with our understanding of multiphasic sleep in other animals [14] and within *Drosophila* itself. Behavioural studies suggest different arousal thresholds following a change in angle of the haltere (haltere switch)[185], while brain activity recordings indicate shifts in activity during extended periods of inactivity, corresponding to increased arousal thresholds [189, 278, 369].

Attempts to distinguish HMM-determined 'deep sleep' and 'light sleep' states using ethoscope-tracked variables bore no results better than random (Fig. 5.7-8). This suggests that the tracked flies in each state exhibited no underlying behavioural differences. However, given the difficulty in distinguishing between active immobile states and sleep immobile states, aside from differences in mean velocity, this observation is not particularly strong.

Analytically, the block classification of inactive bouts as one, not a mix, of the sleep states introduces further bias into the measurement of arousal thresholds. Lengthy inactivity that will be classified as 'deep sleep' post-hoc will have a 0% response rate between 0-10 minutes (Fig. 4.4.b) as any response reclassifies it to 'light 'sleep'. Evidence from response rate over time inactive (Fig. 4.4.d) does demonstrate that flies that are immobile for longer are less likely to respond, indicative of a deeper sleep. However, the earlier sleep would be more responsive, or a lighter sleep. Manually segmenting immobile bouts before 25 minutes by any point in time would always produce a significant difference in population arousal thresholds.

The inability of the HMM to segment bouts of inactivity into more than one state may stem from the mathematical constraints of the model. Both 'deep sleep' and 'light sleep' emit the same

observable state, 'inactive', which forces the model to choose between them. Since each state has a high probability of transitioning into itself, the most likely sequence will always consist of a single state. Short periods of inactivity will be classified as 'light sleep' until the number of inactive instances is sufficient that a transition to 'deep sleep' would have likely occurred, retroactively flipping the entire sequence. This post-hoc decoding is a major limitation of the HMM in this context. For example, probing a fly at 10 minutes of inactivity: if it responds, it is classified as 'light sleep'; if it does not, the sequence is reclassified as 'deep sleep'. Here, the response determines the state, rather than the state predicting the response.

HMMs are memory less, relying solely on the previous state and the observable behaviour, which prevents them from considering the duration of the bout. This restriction has always leveled criticism of HMMs to model sleep, as our understanding is that it is influenced by our previous actions. For example, the homeostatic response is fundamentally controlled by the amount of sleep the animal has prior, increasing the pressure to sleep the longer it is absent [30, 40]. It is also known that the latency to sleep shortens after SD and depth increases [129]. These changes would not be reflected in the HMM decoding, as it will regard the latency and threshold the same at all times due to fixed transition probabilities.

Investigation into the frequency statistics of immobile bouts reveal that they follow a power law relationship. This can be described as having decreasing linear relationship on a log-log scale of time immobile. In short, having a power law relationship indicates that likelihood of leaving the state (inactivity) is proportional to the time in the state [449, 450, 451]. In comparison, activity bouts do not, suggesting they adhere to a different governing rule [451]. Power law distribution of locomotion activity has been shown to correlate with the Ellipsoid-Body in *Drosophila* [450], which is now strongly linked as a driver of sleep [452]. Work by *Xu et al.* applied these techniques as a method to identify sleep onset in individual flies, showing that on average immobility of < 5 minutes follows a power-law decay, changing to exponential after 5 minutes [453]. They theorised this change is indicative of an approximate time point sleep is entered into, changing from a proportional likelihood of leaving immobility (with memory) to a constant chance of exit (memory-less).

This evidence would suggest the mechanics of the HMM are sufficient for modeling most classically defined sleep bouts, but not the shorter bouts, which it may be over or under estimating with a constant exit transition. However, a notable finding from this study was the rapid decrease in response rate observed when transitioning from 'quiet awake' to 'light sleep' states (Fig. 4.4.b). Specifically, flies that had been inactive for just 2 minutes were significantly less likely to respond than those that exhibited intermittent periods of activity and inactivity during the same time frame. This observation suggests that a portion of the population enters a sleep-like state relatively quickly, reinforcing the idea that *Drosophila* can display sleep transitions over short timescales.

Both HMMs and temporal decay analysis offer the ability to apply analytical modelling of sleep to different fly populations, including mutants, species, and environmental settings. All that is needed is sufficient baseline dataset of activity data. Together, these methods each provide unique insights into the structure and regulation of sleep in *Drosophila* beyond the traditional 5-minutes rule and traditional statistics.

The HMM, for example, allows for user-defined architectures that can be customised to explore the distribution of short and long bouts of sleep across the circadian cycle, as well as the breakdown of different types of activity. As shown in the application to other Drosophilid species, the HMM delivers fast, interpretable insights into how sleep patterns vary between groups. For instance, it can reveal whether long or short sleep bouts dominate a species' sleep architecture (Fig. 4.7-8). Furthermore, the HMM decoded sleep data provided a more detailed understanding of the homeostatic response across species, showing how non-*D. melanogaster* species have no rebound after mechanical sleep deprivation in either long or short bout sleep (Fig. 4.9). It also revealed that wild-caught *D. melanogaster* recover sleep through more frequent but shorter bouts. These insights would have been overlooked using traditional statistical approaches.

Likewise, temporal decay analysis can generate individual based metrics, such as sleep latency, activity index, sleep duration, and bout number, which can be used to compare sleep patterns across different populations or under varying environmental conditions, such as constant darkness or during homeostatic rebound [453]. This approach allows for a more detailed char-

acterisation of sleep behaviour at both group and individual levels, offering valuable insights into how sleep is modulated under different circumstances.

Together, these two analytical approaches represent a significant improvement over traditional methods. They excel at generating nuanced information that allows for more accurate comparisons between populations. This study advances the field by introducing ethoscopy, a software platform that enables non-computational researchers to apply HMMs to their *Drosophila* sleep data. By doing so, it bridges the gap for new users, allowing them to move beyond the simplistic five-minute rule and embrace more sophisticated, probabilistic analysis of sleep behaviour.

7.2.2 Should the Five-Minute Assumption Remain?

As discussed, the five-minute rule is a non-tractable operational rule based upon early data in the field. Neither in *Hendricks et al.* or in *Shaw et al.* did the authors show the relationship between time immobile and arousability, simply stating that it was different at this point in time [275, 274]. In fact, Hendricks and colleagues observed that typical sleep posture often occurred after around nine minutes [275]. *Huber et al.*, using a tapping stimulus, provided some evidence for this rule, showing a near-linear decrease in response rate until five minutes, after which it plateaued [71]. Despite the large error margins in these studies, the five-minute rule became a widely accepted standard for measuring sleep in *Drosophila*.

The decreasing response rate, interpreted as an increase in the percentage of flies falling asleep, positioned the five-minute rule as a practical, albeit simplified, assumption of when most flies are asleep. However, with advancements in methodology and deeper insights into sleep dynamics, does this rule still hold?

Several studies, including this one, have demonstrated varying relationships between immobility duration and response rate. In this study, for example, the response rate does not plateau at five minutes but continues to decrease until around 20 minutes, at which point it levels off (Fig. 4.4.d). Similar trends have been observed in *van Alphen et al.* and *Faville et al.*, who both used mechanical vibration to probe flies arousability. *Faville et al.* reported a continuous decrease

in response rate up to the maximum recorded sleep bout of 40 minutes [35]. *Van Alphen et al.* on the other hand, observed a response rate decrease to a low point at 10 minutes, followed by a slight increase and then another drop, reaching a nadir at 30 minutes [189]. This cyclical pattern was interpreted in the study as the transiting between sleep states of differing arousal. An interesting observation, but one that has not been replicated here or in other literature.

If we were to just synthesise the findings from above into a new rule for determining when most flies are asleep, the threshold would need to be raised to 10–15 minutes. Given that sleep bout durations tend to be heavily skewed towards shorter bouts [283], the field would be overestimating sleep under the five-minute assumption.

However, evidence from brain activity data suggests that sleep can occur much earlier than five minutes. Multiple studies report changes in electrical activity, including frequency power and total brain activity, after just two minutes of inactivity [188, 189, 278, 433]. This is corroborated in this study by the observed decrease in response rate after only two minutes of inactivity (Fig. 4.4.c). In both this study and brain activity studies evidence of early reduced arousal or brain activity has high variance, with many in the population responding frequently or having high brain activity in comparison to mid to late sleep [188, 278, 433]. Thus, while sleep can occur early, it is not a consistent phenomenon and will often be interspersed with quiescent but awake flies. This does align with our broader understanding of variability in sleep latency.

Not all evidence challenges the five-minute rule. *Xu et al.*'s analysis of immobile flies defined sleep onset as the point at which immobility transitions from a linear to an exponential decay on a double logarithmic scale for bout length probability, the former section being power law decay. Their data showed that daytime sleep onset averaged around five minutes, with error bars of ± 1 minute for both male and female flies [453]. Interestingly, nighttime sleep had a shorter onset of around three minutes, which mirrors findings that the night is a preferential time for sleep [189, 129, 283, 274]. Additional work is needed to test the trackability of power law analysis. The study did apply it to changing conditions and mutants, but they did not test if changes in sleep latency were reflected in differing arousal thresholds.

Neuronal activity measurements in *Tainton-Heap et al.* also support a general change in activity

at 5 minutes. Their definition of mid-sleep (5-10 minutes) saw activity drop significantly during this time [278]. In their study, 0–5 minutes was still classified as sleep, although with higher activity compared to mid-sleep or prior wakefulness.

Given the variability of findings, it does appear that five minutes holds up as a general marker of sleep, encompassing a time when a significant majority of flies will be asleep. However, as with many rules it is an estimate that will be often incorrect for an individual. The rule does lack credibility when applied to different species, mutants, or even environmental background —such as diet, temperature, or mating status. Given these limitations, it would be more appropriate to apply HMMs or power-law analysis in novel experimental setups to assess whether underlying patterns still hold.

7.2.3 Behavioural Identifiers

To accurately measure sleep in *Drosophila* on an individual basis without invasive brain activity measurements, we must rely on behavioural indicators. As previously discussed, a repertoire of sleep postures has been identified to classify sleep stages. For sleep initiation, a fly typically lowers itself onto the substrate, as observed in multiple studies [275, 185]. This study builds upon that definition, suggesting that simply lowering the abdomen could be a sufficient indicator of sleep initiation (Fig. 6.3). However, this requires further validation through arousal threshold experiments. These behaviours may be analogous to postures seen in mammals and birds, where animals reduce their physical occupation of space by curling up or tucking their heads to preserve energy and minimise predation [385, 418].

Typically, behavioural correlates of sleep in *Drosophila* predict solely sleep. However, the "haltere switch" presented in *Keles et al.* could be an indicator of deeper sleep [185], providing temporally precise identification of sleep stages. This study was able to confirm the identity of previously described sleep postures, with the majority of flies immobile for greater than three minutes demonstrating a posture change. Simple quantification of the change in distance and position of the head, body, and abdomen was able to identify some of the described postures,

although not precisely (Fig. 6.4-6). Possibly better tracking of more relative body parts would generate better classification of the postures.

Due to the inability to classify the onset of the behaviours precisely, a precise quantification of latency is not provided. However, observationally the posture timing was seemingly random with some engaging in a posture change in the first minute to some that retained the same posture from grooming. Likewise, the few observations of the haltere switch (Fig. 6.8), were at very different time points in the sleep bout. This highlights the difficulty of any one rule or modeling of immobility to accurately predict sleep on an individual basis.

Keles et al. introduced FlyVISTA, a semi-supervised behaviour classifier that offers a software framework for identifying micro-behaviours. Like keypoint-MoSeq [364] and A-SOiD [454], FlyVISTA uses keypoint datasets from labelled videos—such as those generated by SLEAP and DeepLabCut—to train the model on user-identified behaviours. The model can then classify entire datasets or new videos, producing an ethogram. This software can be used for both post-hoc analysis and real-time perturbation, providing tailored insights into fly sleep behaviour. However, as demonstrated in this study, setups like these rely on high-resolution capture of fine details in the flies' movements, often limited to one fly at a time. While my study managed to track only three keypoints reliably, *Keles et al.* tracked 32 keypoints. This discrepancy underscores the challenge of scaling more detailed sleep metrics to broader studies and the accessibility of many of the newer machine learning behaviour classifiers. Often, these software's are built around a complex setup that will only be utilised in one group.

Attempts to integrate more detailed metrics of sleep with the accessibility of the ethoscope were largely unsuccessful (*Chapter 5*). Metrics derived from the tracking ellipse could not distinguish between rest bouts that were about to end ('light sleep') and those that would last for at least three more minutes ('deep sleep') (Fig. 5.7-8). A change in posture, such as lowering, is possibly observed in the decreasing size of the ellipse area from the start to end of the rest bout (Fig. 5.4.e). However, there is no differentiation between responding and non-responding bouts. Given the absolute difference is very small (-0.003) and the dataset very large (8199), it is plausible that this difference could be attributed to noise or slight improvements in tracking

an immobile fly overtime.

One intriguing finding was the distribution of mean velocity in immobile flies (Fig. 5.3.g). Immobile flies classified by the HMM as part of an 'active awake' sequence had a Gaussian distribution between 0.6 and 1. In contrast, the sleep states—both short and long bouts—displayed a bimodal distribution centered around 0.65 and 0.78. The 'quiet awake' distribution was in between these two. Response rates were lower in flies with mean velocities within the ranges of 0.70-0.75 and 0.80-0.85 during sleep bouts classified by the HMM (Fig. 5.5.f). It is possible the tracking may have captured subtle micro-behaviours in awake states, although this was not corroborated with any visual difference due to the low-resolution images from the ethoscope.

The limitations of this approach were clear from the outset, primarily due to the ethoscope's top-down imaging. This issue was overcome in part by using HD video setups that recorded flies in profile. A potential future application of these findings would be to develop a "flipped ethoscope", which could record multiple flies in profile. This might capture more meaningful movement during sleep, allowing for deeper analysis of behaviour during sleep stages, but still in a high throughput manner.

7.3 Conclusion

This study aimed to identify observational behavioural correlates of sleep in *Drosophila*, but its success was limited. While it was hoped that the ethoscope's ellipse tracking would reveal behaviours not detectable by eye, this was not realised, apart from possible grouping of mean velocity values, which warrant further investigation. Extending the research through HD video analysis began to uncover postures that likely correlate with sleep, as supported by previous literature, though these postures were not verified by arousal threshold measurements in this study.

Recent work by *Keles et al.* has advanced sleep research in Drosophila by using more sophisticated setups. They identified the haltere switch as a potential marker for deeper sleep and developed a closed-loop system to probe arousal thresholds [185]. While this study partially

corroborates their findings, *Keles et al.* surpasses it in the novel information it brings to the field.

Together, these findings reinforce the idea that behavioural markers can be used to score sleep in flies with greater precision than the traditional 5-minute rule or HMM-derived sleep states. However, translating these insights into a high-throughput, user-friendly system remains an unresolved challenge. The next critical steps in *Drosophila* sleep research will involve correlating behavioural markers with brain activity to confirm them as dynamic sleep stages. The ultimate goal is to develop a system capable of capturing, scoring, and storing these behavioural changes, providing a widely accessible tool for *Drosophila* sleep researchers in their everyday analyses.

Appendix A

Appendix

Transition probability matrix for *D.melanogaster* (CS and wild caught)

	Deep Sleep	Light Sleep	Quiet Awake	Active Awake
Deep Sleep	0.83462822	0.01013009	0.11524169	0.0
Light Sleep	0.11252304	0.67248921	0.21498776	0.0
Quiet Awake	0.0	0.25632002	0.73134791	0.01233207
Active Awake	0.0	0.0	0.02062261	0.97937739

Transition probability matrix for *D.simulans*

	Deep Sleep	Light Sleep	Quiet Awake	Active Awake
Deep Sleep	0.77785973	0.20578346	0.04094627	0.0
Light Sleep	0.12433228	0.63058143	0.22091449	0.0
Quiet Awake	0.0	0.46449872	0.41151333	0.12398795
Active Awake	0.0	0.0	0.09426005	0.90573995

Transition probability matrix for *D.sechellia*

	Deep Sleep	Light Sleep	Quiet Awake	Active Awake
Deep Sleep	0.77785973	0.20578346	0.01635681	0.0
Light Sleep	0.12433228	0.63213012	0.2435376	0.0
Quiet Awake	0.0	0.31141091	0.675898351	0.01269074
Active Awake	0.0	0.0	0.01514826	0.98485174

Transition probability matrix for *D.erecta*

	Deep Sleep	Light Sleep	Quiet Awake	Active Awake
Deep Sleep	0.90733131	0.08929603	0.00337265	0.0
Light Sleep	0.03079624	0.73295972	0.23624404	0.0
Quiet Awake	0.0	0.45020044	0.49015903	0.05964052
Active Awake	0.0	0.0	0.07935718	0.92064282

Transition probability matrix for *D.yakuba*

	Deep Sleep	Light Sleep	Quiet Awake	Active Awake
Deep Sleep	0.92950508	0.04951318	0.02098175	0.0
Light Sleep	0.1036084	0.62352494	0.27286666	0.0
Quiet Awake	0.0	0.3684207	0.57234612	0.05923318
Active Awake	0.0	0.0	0.02922311	0.97077689

Transition probability matrix for *D.willistoni*

	Deep Sleep	Light Sleep	Quiet Awake	Active Awake
Deep Sleep	0.94961155	0.04039581	0.00999263	0.0
Light Sleep	0.04741797	0.72146242	0.23111961	0.0
Quiet Awake	0.0	0.32728565	0.61552884	0.05708551
Active Awake	0.0	0.0	0.05707633	0.94292367

Transition probability matrix for *D.virilis*

	Deep Sleep	Light Sleep	Quiet Awake	Active Awake
Deep Sleep	0.7906379	0.19127519	0.01808691	0.0
Light Sleep	0.14862515	0.65988759	0.19148725	0.0
Quiet Awake	0.0	0.35849722	0.60039392	0.04110886
Active Awake	0.0	0.0	0.05530234	0.94469766

Table A.1: The table shows all the likelihoods of transition between behavioural stage by species as calculated by the HMM. Values are between 0 (never) and 1 (always). The pairings should be read horizontally

Emission probability matrix for *D.melanogaster* (CS and wild caught)

	Inactive	Active
Deep Sleep	1.0	0.0
Light Sleep	1.0	0.0
Quiet Awake	0.15077545	0.84922455
Active Awake	0.0144416	0.985584

Emission probability matrix for *D.simulans*

	Inactive	Active
Deep Sleep	1.0	0.0
Light Sleep	1.0	0.0
Quiet Awake	0.07451264	0.92548736
Active Awake	0.03569679	0.96430321

Emission probability matrix for *D.sechellia*

	Inactive	Active
Deep Sleep	1.0	0.0
Light Sleep	1.0	0.0
Quiet Awake	0.05570972	0.94429028
Active Awake	0.02184815	0.97815185

Emission probability matrix for *D.erecta*

	Inactive	Active
Deep Sleep	1.0	0.0
Light Sleep	1.0	0.0
Quiet Awake	0.15102444	0.84897556
Active Awake	0.06291448	0.93708552

Emission probability matrix for *D.yakuba*

	Inactive	Active
Deep Sleep	1.0	0.0
Light Sleep	1.0	0.0
Quiet Awake	0.06413117	0.93586883
Active Awake	0.02210849	0.97789151

Emission probability matrix for *D.willistoni*

	Inactive	Active
Deep Sleep	1.0	0.0
Light Sleep	1.0	0.0
Quiet Awake	0.12435357	0.87564643
Active Awake	0.04636757	0.95363243

Emission probability matrix for *D.virilis*

	Inactive	Active
Deep Sleep	1.0	0.0
Light Sleep	1.0	0.0
Quiet Awake	0.10151369	0.89848631
Active Awake	0.02722446	0.97277555

Table A.2: The table shows all the likelihoods of each state occurring per observable as calculated by the HMM. Values are between 0 (never) and 1 (always). The pairings should be read horizontally

Bibliography

[1] Cory T. Miller, David Gire, Kim Hoke, Alexander C. Huk, Darcy Kelley, David A. Leopold, Matthew C. Smear, Frederic Theunissen, Michael Yartsev, and Cristopher M. Niell. Natural behavior is the language of the brain. *Current biology: CB*, 32(10):R482–R493, May 2022.

[2] Cornelia I. Bargmann and Eve Marder. From the connectome to brain function. *Nature Methods*, 10(6):483–490, June 2013.

[3] Yael Niv. The primacy of behavioral research for understanding the brain. *Behavioral Neuroscience*, 135(5):601, 2021. ISBN: 1939-0084 Publisher: American Psychological Association.

[4] Glenn W. Most. *Hesiod: Theogony, Works and Days, Testimonia*, volume 1. Harvard University Press, 2006.

[5] Hartmut Schulz. The history of sleep research and sleep medicine in Europe. *Journal of sleep research*, 31(4):e13602, 2022. ISBN: 0962-1105 Publisher: Wiley Online Library.

[6] William C. Dement. The study of human sleep: a historical perspective. *Thorax*, 53(suppl 3):S2–S7, 1998. ISBN: 0040-6376 Publisher: BMJ Publishing Group Ltd.

[7] Ernst Otto Heinrich Kohlschütter. Messungen der Festigkeit des Schlafes. *Zeitschrift fuer rationelle Medicin, Dritte Reihe*, Dritte Reihe, 17:209 – 253, 1863.

[8] Matthias M. Weber and Wolfgang Burgmair. "The assistant's bedroom served as a laboratory": Documentation in 1888 of within sleep periodicity by the psychiatrist Eduard

Robert Michelson. *Sleep medicine*, 10(3):378–384, 2009. ISBN: 1389-9457 Publisher: Elsevier.

[9] W. H. Howell. Le problème physiologique du Sommeil. By Henri Piéron. Paris, Masson et Cie. 1913. Pp. xv+ 520, six figures in text. *Science*, 37(953):525–526, 1913. ISBN: 0036-8075 Publisher: American Association for the Advancement of Science.

[10] Scott S. Campbell and Irene Tobler. Animal sleep: a review of sleep duration across phylogeny. *Neuroscience & Biobehavioral Reviews*, 8(3):269–300, 1984. ISBN: 0149-7634 Publisher: Elsevier.

[11] Joan C. Hendricks, Amita Sehgal, and Allan I. Pack. The need for a simple animal model to understand sleep. *Progress in neurobiology*, 61(4):339–351, 2000. ISBN: 0301-0082 Publisher: Elsevier.

[12] Jerome M. Siegel. Sleep function: an evolutionary perspective. *The Lancet Neurology*, 21(10):937–946, 2022. ISBN: 1474-4422 Publisher: Elsevier.

[13] Jerome M. Siegel. Clues to the functions of mammalian sleep. *Nature*, 437(7063):1264–1271, 2005. ISBN: 0028-0836 Publisher: Nature Publishing Group UK London.

[14] Niels C. Rattenborg and Gianina Ungurean. The evolution and diversification of sleep. *Trends in Ecology & Evolution*, 38(2):156–170, 2023. ISBN: 0169-5347 Publisher: Elsevier.

[15] Tom Deboer. Behavioral and electrophysiological correlates of sleep and sleep homeostasis. *Sleep, neuronal plasticity and brain function*, pages 1–24, 2015. ISBN: 3662468778 Publisher: Springer.

[16] Alfred L. Loomis, E. Newton Harvey, and Garret Hobart. Potential rhythms of the cerebral cortex during sleep. *Science*, 81(2111):597–598, 1935. ISBN: 0036-8075 Publisher: American Association for the Advancement of Science.

[17] Alfred L. Loomis, E. Newton Harvey, and Garret A. Hobart III. Distribution of disturbance-patterns in the human electroencephalogram, with special reference to sleep. *Journal of neurophysiology*, 1(5):413–430, 1938. ISBN: 0022-3077.

[18] Eugene Aserinsky and Nathaniel Kleitman. Regularly occurring periods of eye motility, and concomitant phenomena, during sleep. *Science*, 118(3062):273–274, 1953. ISBN: 0036-8075 Publisher: American Association for the Advancement of Science.

[19] William Dement and Nathaniel Kleitman. Cyclic variations in EEG during sleep and their relation to eye movements, body motility, and dreaming. *Electroencephalography and clinical neurophysiology*, 9(4):673–690, 1957. ISBN: 0013-4694 Publisher: Elsevier.

[20] Allan Rechtschaffen. A manual of standardized terminology, techniques and scoring system for sleep stages of human subjects. , pages 1–55, 1968. Publisher: .

[21] H. Zepelin and A. Rechtschaffen. Mammalian sleep, longevity, and energy metabolism. *Brain, Behavior and Evolution*, 10(6):425–470, 1974.

[22] Greta Sokoloff, James C. Dooley, Ryan M. Glanz, Rebecca Y. Wen, Meredith M. Hickerson, Laura G. Evans, Haley M. Laughlin, Keith S. Apfelbaum, and Mark S. Blumberg. Twitches emerge postnatally during quiet sleep in human infants and are synchronized with sleep spindles. *Current biology*, 31(15):3426–3432. e4, 2021. ISBN: 0960-9822 Publisher: Elsevier.

[23] Andrew M Reiter, Gregory D Roach, Charli Sargent, and Leon Lack. Finger Twitches are More Frequent in REM Sleep Than in Non-REM Sleep. *Nature and Science of Sleep*, 12:49–56, January 2020. Publisher: Dove Medical Press _eprint: https://www.tandfonline.com/doi/pdf/10.2147/NSS.S233439.

[24] Irene Tobler. Evolution and comparative physiology of sleep in animals. In *Clinical physiology of sleep*, pages 21–30. Springer, 1988.

[25] Risa Yamazaki, Hirofumi Toda, Paul-Antoine Libourel, Yu Hayashi, Kaspar E. Vogt, and Takeshi Sakurai. Evolutionary origin of distinct NREM and REM sleep. *Frontiers in psychology*, 11:567618, 2020. ISBN: 1664-1078 Publisher: Frontiers Media SA.

[26] Shing-Tai Pan, Chih-En Kuo, Jian-Hong Zeng, and Sheng-Fu Liang. A transition-constrained discrete hidden Markov model for automatic sleep staging. *BioMedical Engineering OnLine*, 11(1):52, August 2012.

[27] Jiahui Pan, Jianhao Zhang, Fei Wang, Wuhan Liu, Haiyun Huang, Weishun Tang, Huijian Liao, Man Li, Jianhui Wu, Xueli Li, Dongming Quan, and Yuanqing Li. Automatic Sleep Staging Based on EEG-EOG Signals for Depression Detection. *Intelligent Automation & Soft Computing*, 28(1):53–71, 2021.

[28] William J. Joiner. The Neurobiological Basis of Sleep and Sleep Disorders. *Physiology (Bethesda, Md.)*, 33(5):317–327, September 2018. Place: United States.

[29] Gandhi Yetish, Hillard Kaplan, Michael Gurven, Brian Wood, Herman Pontzer, Paul R. Manger, Charles Wilson, Ronald McGregor, and Jerome M. Siegel. Natural sleep and its seasonal variations in three pre-industrial societies. *Current Biology*, 25(21):2862–2868, 2015. ISBN: 0960-9822 Publisher: Elsevier.

[30] Alexander A. Borbély. A two process model of sleep regulation. *Hum neurobiol*, 1(3):195–204, 1982. ISBN: 0721-9075.

[31] Tom Deboer. Sleep homeostasis and the circadian clock: do the circadian pacemaker and the sleep homeostat influence each other's functioning? *Neurobiology of sleep and circadian rhythms*, 5:68–77, 2018. ISBN: 2451-9944 Publisher: Elsevier.

[32] Takeshi Sakurai. Roles of orexin/hypocretin in regulation of sleep/wakefulness and energy homeostasis. *Sleep Medicine Reviews*, 9(4):231–241, August 2005.

[33] Giulio Tononi and Chiara Cirelli. Sleep function and synaptic homeostasis. *Sleep Medicine Reviews*, 10(1):49–62, February 2006.

[34] Ravi Allada, Chiara Cirelli, and Amita Sehgal. Molecular mechanisms of sleep homeostasis in flies and mammals. *Cold Spring Harbor perspectives in biology*, 9(8):a027730, 2017. ISBN: 1943-0264 Publisher: Cold Spring Harbor Lab.

[35] R. Faville, B. Kottler, G. J. Goodhill, P. J. Shaw, and B. van Swinderen. How deeply does your mutant sleep? Probing arousal to better understand sleep defects in Drosophila. *Scientific Reports*, 5(1):8454, February 2015.

[36] Martha Hotz Vitaterna, Joseph S. Takahashi, and Fred W. Turek. Overview of circadian rhythms. *Alcohol research & health*, 25(2):85, 2001. Publisher: National Institute on Alcohol Abuse and Alcoholism.

[37] Ralph E. Mistlberger. Circadian regulation of sleep in mammals: role of the suprachiasmatic nucleus. *Brain research reviews*, 49(3):429–454, 2005. ISBN: 0165-0173 Publisher: Elsevier.

[38] Shin Yamazaki, Rika Numano, Michikazu Abe, Akiko Hida, Ri-ichi Takahashi, Masatsugu Ueda, Gene D. Block, Yoshiyuki Sakaki, Michael Menaker, and Hajime Tei. Resetting central and peripheral circadian oscillators in transgenic rats. *Science*, 288(5466):682–685, 2000. ISBN: 1095-9203 Publisher: American Association for the Advancement of Science.

[39] Mirja Quante, Emily R. Kaplan, Michael Cailler, Michael Rueschman, Rui Wang, Jia Weng, Elsie M. Taveras, and Susan Redline. Actigraphy-based sleep estimation in adolescents and adults: a comparison with polysomnography using two scoring algorithms. *Nature and science of sleep*, pages 13–20, 2018. ISBN: 1179-1608 Publisher: Taylor & Francis.

[40] Alexander A. Borbély, Serge Daan, Anna Wirz-Justice, and Tom Deboer. The two-process model of sleep regulation: a reappraisal. *Journal of sleep research*, 25(2):131–143, 2016. ISBN: 0962-1105 Publisher: Wiley Online Library.

[41] Maria Sundvik, Hisaaki Kudo, Pauliina Toivonen, Stanislav Rozov, Yu-Chia Chen, and Pertti Panula. The histaminergic system regulates wakefulness and orexin/hypocretin neuron development via histamine receptor H1 in zebrafish. *The FASEB Journal*, 25(12):4338–4347, 2011. _eprint: https://faseb.onlinelibrary.wiley.com/doi/pdf/10.1096/fj.11-188268.

[42] Quan Yuan, William J. Joiner, and Amita Sehgal. A Sleep-Promoting Role for the Drosophila Serotonin Receptor 1A. *Current Biology*, 16(11):1051–1062, June 2006. Publisher: Elsevier.

[43] Ratna Chaturvedi and Patrick Emery. Fly into Tranquility: GABA's role in Drosophila Sleep. *Current Opinion in Insect Science*, page 101219, 2024. Publisher: Elsevier.

[44] Marina Bentivoglio and Gigliola Grassi-Zucconi. The pioneering experimental studies on sleep deprivation. *Sleep*, 20(7):570–576, 1997. ISBN: 1550-9109 Publisher: Oxford University Press.

[45] DE MANACEINE M. Quelques observations experimentales sur l'influence de l'insomnie absolue. *Arch Ital. Biol.*, 21:322–325, 1894.

[46] L. Daddi. Sulle alterazioni degli elementi del sistema nervoso centrale nell'insonnia sperimentale. *Rivista di Patologia Nervosa e Mentale*, 3:1–12, 1898.

[47] Giulio Tarozzi. *Sull'influenza dell'insonnio sperimentale sul ricambio materiale.* Stabilimento tipografico fiorentino, 1898.

[48] Allan Rechtschaffen, Bernard M. Bergmann, Carol A. Everson, Clete A. Kushida, and Marcia A. Gilliland. Sleep deprivation in the rat: X. Integration and discussion of the findings. *Sleep*, 12(1):68–87, 1989. ISBN: 0161-8105 Publisher: Oxford University Press.

[49] Carol A. Everson, Bernard M. Bergmann, and Allan Rechtschaffen. Sleep deprivation in the rat: III. Total sleep deprivation. *Sleep*, 12(1):13–21, 1989. ISBN: 0161-8105 Publisher: Oxford University Press.

[50] Paul J. Shaw, Giulio Tononi, Ralph J. Greenspan, and Donald F. Robinson. Stress response genes protect against lethal effects of sleep deprivation in Drosophila. *Nature*, 417(6886):287–291, 2002. ISBN: 0028-0836 Publisher: Nature Publishing Group UK London.

[51] Alexandra Vaccaro, Yosef Kaplan Dor, Keishi Nambara, Elizabeth A. Pollina, Cindy Lin, Michael E. Greenberg, and Dragana Rogulja. Sleep Loss Can Cause Death through Accumulation of Reactive Oxygen Species in the Gut. *Cell*, 181(6):1307–1328.e15, June 2020.

[52] Richard Stephenson, Karen M. Chu, and James Lee. Prolonged deprivation of sleep-like rest raises metabolic rate in the Pacific beetle cockroach, Diploptera punctata (Eschscholtz). *Journal of Experimental Biology*, 210(14):2540–2547, 2007. ISBN: 1477-9145 Publisher: Company of Biologists.

[53] Quentin Geissmann, Esteban J. Beckwith, and Giorgio F. Gilestro. Most sleep does not serve a vital function: Evidence from Drosophila melanogaster. *Science Advances*, 5(2):eaau9253, February 2019.

[54] Sarah M. Newman, Elliott M. Paletz, Niels C. Rattenborg, William H. Obermeyer, and Ruth M. Benca. Sleep deprivation in the pigeon using the Disk-Over-Water method. *Physiology & Behavior*, 93(1):50–58, January 2008.

[55] John J. Ross. Neurological findings after prolonged sleep deprivation. *Archives of neurology*, 12(4):399–403, 1965. ISBN: 0003-9942 Publisher: American Medical Association.

[56] Kurt Kräuchi, Vera Knoblauch, Anna Wirz-Justice, and Christian Cajochen. Challenging the sleep homeostat does not influence the thermoregulatory system in men: evidence from a nap vs. sleep-deprivation study. *American Journal of Physiology-Regulatory, Integrative and Comparative Physiology*, 290(4):R1052–R1061, 2006. ISBN: 0363-6119 Publisher: American Physiological Society.

[57] Pasquale Montagna. Fatal familial insomnia: a model disease in sleep physiopathology. *Sleep Medicine Reviews*, 9(5):339–353, October 2005.

[58] Vijay Kumar Chattu, Md Dilshad Manzar, Soosanna Kumary, Deepa Burman, David Warren Spence, and Seithikurippu R. Pandi-Perumal. The global problem of insufficient sleep and its serious public health implications. In *Healthcare*, volume 7, page 1. MDPI, 2018. Issue: 1.

[59] Goran Medic, Micheline Wille, and Michiel EH Hemels. Short-and long-term health consequences of sleep disruption. *Nature and science of sleep*, pages 151–161, 2017. ISBN: 1179-1608 Publisher: Taylor & Francis.

[60] Francesco P. Cappuccio, Lanfranco D'Elia, Pasquale Strazzullo, and Michelle A. Miller. Sleep Duration and All-Cause Mortality: A Systematic Review and Meta-Analysis of Prospective Studies. *Sleep*, 33(5):585–592, May 2010.

[61] Kristen L. Knutson, Karine Spiegel, Plamen Penev, and Eve Van Cauter. The metabolic consequences of sleep deprivation. *Sleep medicine reviews*, 11(3):163–178, 2007. ISBN: 1087-0792 Publisher: Elsevier.

[62] Luciana Besedovsky, Tanja Lange, and Jan Born. Sleep and immune function. *Pflügers Archiv-European Journal of Physiology*, 463(1):121–137, 2012. ISBN: 1432-2013 Publisher: Springer.

[63] Sankari Ramanathan, Jason J. Hanley, Jean-Michel Deniau, and J. Paul Bolam. Synaptic convergence of motor and somatosensory cortical afferents onto GABAergic interneurons in the rat striatum. *Journal of Neuroscience*, 22(18):8158–8169, 2002. ISBN: 0270-6474 Publisher: Soc Neuroscience.

[64] Jerrah K. Holth, Sarah K. Fritschi, Chanung Wang, Nigel P. Pedersen, John R. Cirrito, Thomas E. Mahan, Mary Beth Finn, Melissa Manis, Joel C. Geerling, and Patrick M. Fuller. The sleep-wake cycle regulates brain interstitial fluid tau in mice and CSF tau in humans. *Science*, 363(6429):880–884, 2019. ISBN: 0036-8075 Publisher: American Association for the Advancement of Science.

[65] Lulu Xie, Hongyi Kang, Qiwu Xu, Michael J. Chen, Yonghong Liao, Meenakshisundaram Thiyagarajan, John O'Donnell, Daniel J. Christensen, Charles Nicholson, and Jeffrey J. Iliff. Sleep drives metabolite clearance from the adult brain. *science*, 342(6156):373–377, 2013. ISBN: 0036-8075 Publisher: American Association for the Advancement of Science.

[66] Andawei Miao, Tianyuan Luo, Bryan Hsieh, Christopher J. Edge, Morgan Gridley, Ryan Tak Chun Wong, Timothy G. Constandinou, William Wisden, and Nicholas P. Franks. Brain clearance is reduced during sleep and anesthesia. *Nature Neuroscience*, pages 1–5, 2024. ISBN: 1097-6256 Publisher: Nature Publishing Group US New York.

[67] Adam J. Krause, Eti Ben Simon, Bryce A. Mander, Stephanie M. Greer, Jared M. Saletin, Andrea N. Goldstein-Piekarski, and Matthew P. Walker. The sleep-deprived human brain. *Nature Reviews Neuroscience*, 18(7):404–418, 2017. ISBN: 1471-0048 Publisher: Nature Publishing Group.

[68] Matthew P. Walker, Tiffany Brakefield, Joshua Seidman, Alexandra Morgan, J. Allan Hobson, and Robert Stickgold. Sleep and the time course of motor skill learning. *Learning & memory*, 10(4):275–284, 2003. ISBN: 1072-0502 Publisher: Cold Spring Harbor Lab.

[69] Matthew P. Walker, Tiffany Brakefield, Alexandra Morgan, J. Allan Hobson, and Robert Stickgold. Practice with sleep makes perfect: sleep-dependent motor skill learning. *Neuron*, 35(1):205–211, 2002. ISBN: 0896-6273 Publisher: Elsevier.

[70] Yazmin L. Serrano Negron, Nancy F. Hansen, and Susan T. Harbison. The sleep inbred panel, a collection of inbred Drosophila melanogaster with extreme long and short sleep duration. *G3: Genes, Genomes, Genetics*, 8(9):2865–2873, 2018. ISBN: 2160-1836 Publisher: Oxford University Press.

[71] Reto Huber, M. Felice Ghilardi, Marcello Massimini, and Giulio Tononi. Local sleep and learning. *Nature*, 430(6995):78–81, 2004. ISBN: 0028-0836 Publisher: Nature Publishing Group UK London.

[72] Paula Alhola and Päivi Polo-Kantola. Sleep deprivation: Impact on cognitive performance. *Neuropsychiatric disease and treatment*, 3(5):553–567, 2007. ISBN: 1178-2021 Publisher: Taylor & Francis.

[73] William DS Killgore. Effects of sleep deprivation on cognition. *Progress in brain research*, 185:105–129, 2010. ISBN: 0079-6123 Publisher: Elsevier.

[74] Ronald B. Postuma, Charles H. Adler, Brittany N. Dugger, Joseph G. Hentz, Holly A. Shill, Erika Driver-Dunckley, Marwan N. Sabbagh, Sandra A. Jacobson, Christine M. Belden, and Lucia I. Sue. REM sleep behavior disorder and neuropathology in Parkinson's disease. *Movement Disorders*, 30(10):1413–1417, 2015. ISBN: 0885-3185 Publisher: Wiley Online Library.

[75] Xinyuan Zhang, Samantha A. Molsberry, Milena Pavlova, Michael A. Schwarzschild, Alberto Ascherio, and Xiang Gao. Association of sleepwalking and REM sleep behavior disorder with Parkinson disease in men. *JAMA network open*, 4(4):e215713–e215713, 2021. Publisher: American Medical Association.

[76] Yeonsu Song, Terri Blackwell, Kristine Yaffe, Sonia Ancoli-Israel, Susan Redline, and Katie L. Stone. Relationships between sleep stages and changes in cognitive function in older men: the MrOS Sleep Study. *Sleep*, 38(3):411–421, March 2015. Place: United States.

[77] Edgar Garcia-Rill, Tiffany Wallace, and Cameron Good. Neuropharmacology of sleep and wakefulness. *Sleep: a Comprehensive Handbook*, pages 63–71, 2006. Publisher: Wiley Online Library.

[78] Danièle Jouvet-Mounier, Liliane Astic, and Daniel Lacote. Ontogenesis of the states of sleep in rat, cat, and guinea pig during the first postnatal month. *Developmental Psychobiology: The Journal of the International Society for Developmental Psychobiology*, 2(4):216–239, 1969. ISBN: 0012-1630 Publisher: Wiley Online Library.

[79] Majid Mirmiran, H. B. M. Uylings, and M. A. Corner. Pharmacological suppression of REM sleep prior to weaning counteracts the effectiveness of subsequent environmental enrichment on cortical growth in rats. *Developmental Brain Research*, 7(1):102–105, 1983. ISBN: 0165-3806 Publisher: Elsevier.

[80] Matthew S. Kayser, Zhifeng Yue, and Amita Sehgal. A critical period of sleep for development of courtship circuitry and behavior in Drosophila. *Science*, 344(6181):269–274, 2014. ISBN: 0036-8075 Publisher: American Association for the Advancement of Science.

[81] Daniel P. Brunner, Derk-Jan Dijk, and Alexander A. Borbély. Repeated partial sleep deprivation progressively changes the EEG during sleep and wakefulness. *Sleep*, 16(2):100–113, 1993. ISBN: 1550-9109 Publisher: Oxford University Press.

[82] William C. Dement and Christopher Vaughan. *The promise of sleep: A pioneer in sleep medicine explores the vital connection between health, happiness, and a good night's sleep.* Dell Publishing Co, 1999.

[83] David R. Samson and Charles L. Nunn. Sleep intensity and the evolution of human cognition. *Evolutionary Anthropology: Issues, News, and Reviews*, 24(6):225–237, 2015. ISBN: 1060-1538 Publisher: Wiley Online Library.

[84] Irene Tobler. Is sleep fundamentally different between mammalian species? *Behavioural brain research*, 69(1-2):35–41, 1995. ISBN: 0166-4328 Publisher: Elsevier.

[85] Jerome M. Siegel. Do all animals sleep? *Trends in Neurosciences*, 31(4):208–213, April 2008.

[86] John A. Lesku, Timothy C. Roth II, Niels C. Rattenborg, Charles J. Amlaner, and Steven L. Lima. History and future of comparative analyses in sleep research. *Neuroscience & Biobehavioral Reviews*, 33(7):1024–1036, 2009. ISBN: 0149-7634 Publisher: Elsevier.

[87] John A. Lesku, D. Martinez-Gonzalez, and Niels Christian Rattenborg. Sleep and sleep states: phylogeny and ontogeny. *Encyclopedia of Neuroscience*, pages 953–961, 2009. Publisher: Academic Press London, UK.

[88] William J. Joiner. Unraveling the evolutionary determinants of sleep. *Current biology*, 26(20):R1073–R1087, 2016. ISBN: 0960-9822 Publisher: Elsevier.

[89] Alex C. Keene and Erik R. Duboue. The origins and evolution of sleep. *Journal of Experimental Biology*, 221(11):jeb159533, 2018. ISBN: 1477-9145 Publisher: The Company of Biologists Ltd.

[90] Mary A. Carskadon and William C. Dement. Normal human sleep: an overview. *Principles and practice of sleep medicine*, 4(1):13–23, 2005. Publisher: Elsevier Saunders Philadelphia, PA.

[91] Erkki Kronholm, Mikko Härmä, Christer Hublin, Arja R. Aro, and Timo Partonen. Self-reported sleep duration in Finnish general population. *Journal of sleep research*, 15(3):276–290, 2006. ISBN: 0962-1105 Publisher: Wiley Online Library.

[92] Sjoerd J. Van Hasselt, Massimiliano Coscia, Giancarlo Allocca, Alexei L. Vyssotski, and Peter Meerlo. Seasonal variation in sleep time: jackdaws sleep when it is dark, but do they really need it? *Journal of Comparative Physiology B*, 194(3):335–345, 2024. ISBN: 0174-1578 Publisher: Springer.

[93] Jacqueline M. Lane, Jingjing Liang, Irma Vlasac, Simon G. Anderson, David A. Bechtold, Jack Bowden, Richard Emsley, Shubhroz Gill, Max A. Little, and Annemarie I. Luik. Genome-wide association analyses of sleep disturbance traits identify new loci and highlight shared genetics with neuropsychiatric and metabolic traits. *Nature genetics*, 49(2):274–281, 2017. ISBN: 1061-4036 Publisher: Nature Publishing Group US New York.

[94] Torbjörn Åkerstedt, Francesca Ghilotti, Alessandra Grotta, Andrea Bellavia, Ylva Trolle Lagerros, and Rino Bellocco. Sleep duration, mortality and the influence of age. *European journal of epidemiology*, 32:881–891, 2017. ISBN: 0393-2990 Publisher: Springer.

[95] Thomas A. Wehr. In short photoperiods, human sleep is biphasic. *Journal of Sleep Research*, 1(2):103–107, 1992. ISBN: 0962-1105 Publisher: Wiley Online Library.

[96] Niels C. Rattenborg, Bryson Voirin, Alexei L. Vyssotski, Roland W. Kays, Kamiel Spoelstra, Franz Kuemmeth, Wolfgang Heidrich, and Martin Wikelski. Sleeping outside the box: electroencephalographic measures of sleep in sloths inhabiting a rainforest. *Biology letters*, 4(4):402–405, 2008. ISBN: 1744-9561 Publisher: The Royal Society London.

[97] D. R. Brebbia and E. T. Pyne. Environmental hypothermia and cerebral electrical activity of little brown bat, myotis-lucifugus. *Psychophysiology*, 9(1):10011–4211, 1972.

[98] Irene Tobler and B. Schwierin. Behavioural sleep in the giraffe (Giraffa camelopardalis) in a zoological garden. *Journal of Sleep Research*, 5(1):21–32, 1996. ISBN: 0962-1105 Publisher: Wiley Online Library.

[99] Irene Tobler. Behavioral sleep in the Asian elephant in captivity. *Sleep*, 15(1):1–12, 1992. ISBN: 1550-9109 Publisher: Oxford University Press.

[100] Ravi Allada and Jerome M. Siegel. Unearthing the phylogenetic roots of sleep. *Current biology*, 18(15):R670–R679, 2008. ISBN: 0960-9822 Publisher: Elsevier.

[101] John A. Lesku, Timothy C. Roth Ii, Charles J. Amlaner, and Steven L. Lima. A Phylogenetic Analysis of Sleep Architecture in Mammals: The Integration of Anatomy, Physiology, and Ecology. *The American Naturalist*, 168(4):441–453, October 2006.

[102] Niels C. Rattenborg. Diverse sleep strategies at sea. *Science*, 381(6657):486–487, 2023. ISBN: 0036-8075 Publisher: American Association for the Advancement of Science.

[103] L. M. Mukhametov, A. I. Oleksenko, and I. G. Polyakova. The Black Sea bottlenose dolphin: the structure of sleep. *The Black Sea Bottlenose Dolphin. Nauka, Moscow*, pages 492–512, 1997.

[104] L. M. Mukhametov, A. I. Oleksenko, and I. G. Polyakova. Quantification of ECoG stages of sleep in the bottlenose dolphin. *Neurophysiology*, 20(4):398–403, 1988. ISBN: 0090-2977 Publisher: Springer.

[105] Oleg I. Lyamin, Paul R. Manger, Sam H. Ridgway, Lev M. Mukhametov, and Jerome M. Siegel. Cetacean sleep: an unusual form of mammalian sleep. *Neuroscience & Biobehavioral Reviews*, 32(8):1451–1484, 2008. ISBN: 0149-7634 Publisher: Elsevier.

[106] Lev M. Mukhametov. Unihemispheric slow-wave sleep in the Amazonian dolphin, Inia geoffrensis. *Neuroscience letters*, 79(1-2):128–132, 1987. ISBN: 0304-3940 Publisher: Elsevier.

[107] Sam Ridgway, Don Carder, James Finneran, Mandy Keogh, Tricia Kamolnick, Mark Todd, and Allen Goldblatt. Dolphin continuous auditory vigilance for five days. *Journal of Experimental Biology*, 209(18):3621–3628, 2006. ISBN: 1477-9145 Publisher: Company of Biologists.

[108] Oleg I. Lyamin and Jerome M. Siegel. Sleep in aquatic mammals. In *Handbook of behavioral neuroscience*, volume 30, pages 375–393. Elsevier, 2019.

[109] Oleg I. Lyamin, Lev M. Mukhametov, Igor S. Chetyrbok, and Alexander V. Vassiliev. Sleep and wakefulness in the southern sea lion. *Behavioural Brain Research*, 128(2):129–138, January 2002.

[110] Oleg I. Lyamin. Sleep in the harp seal (Pagophilus groenlandica). Comparison of sleep on land and in water. *Journal of Sleep Research*, 2(3):170–174, 1993. ISBN: 0962-1105 Publisher: Wiley Online Library.

[111] Oleg I. Lyamin, Vasilisa D. Borshchenko, and Jerome M. Siegel. A 108-h total sleep deprivation did not impair fur seal performance in delayed matching to sample task. *Journal of Comparative Physiology B*, 194(3):315–333, 2024. ISBN: 0174-1578 Publisher: Springer.

[112] Niels C. Rattenborg. Sleeping on the wing. *Interface Focus*, 7(1):20160082, 2017. ISBN: 2042-8898 Publisher: The Royal Society.

[113] Niels C. Rattenborg, Bryson Voirin, Sebastian M. Cruz, Ryan Tisdale, Giacomo Dell'Omo, Hans-Peter Lipp, Martin Wikelski, and Alexei L. Vyssotski. Evidence that birds sleep in mid-flight. *Nature communications*, 7(1):12468, 2016. ISBN: 2041-1723 Publisher: Nature Publishing Group UK London.

[114] Niels C. Rattenborg. Do birds sleep in flight? *Naturwissenschaften*, 93(9):413–425, 2006. ISBN: 0028-1042 Publisher: Springer.

[115] Niels C. Rattenborg, Steven L. Lima, and Charles J. Amlaner. Half-awake to the risk of predation. *Nature*, 397(6718):397–398, 1999. ISBN: 0028-0836 Publisher: Nature Publishing Group UK London.

[116] J. M. Siegel, P. R. Manger, R. Nienhuis, H. M. Fahringer, and J. D. Pettigrew. The echidna Tachyglossus aculeatus combines REM and non-REM aspects in a single sleep state: implications for the evolution of sleep. *Journal of Neuroscience*, 16(10):3500–3506, 1996. ISBN: 0270-6474 Publisher: Soc Neuroscience.

[117] Stewart C. Nicol, Niels A. Andersen, Nathan H. Phillips, and Ralph J. Berger. The echidna manifests typical characteristics of rapid eye movement sleep. *Neuroscience letters*, 283(1):49–52, 2000. ISBN: 0304-3940 Publisher: Elsevier.

[118] J. M. Siegel, P. R. Manger, R. Nienhuis, H. M. Fahringer, T. Shalita, and J. D. Pettigrew. Sleep in the platypus. *Neuroscience*, 91(1):391–400, 1999. ISBN: 0306-4522 Publisher: Elsevier.

[119] Jerome M. Siegel. REM sleep function: mythology vs. reality. *Revue neurologique*, 2023. ISBN: 0035-3787 Publisher: Elsevier.

[120] Niels C. Rattenborg, Dolores Martinez-Gonzalez, and John A. Lesku. Avian sleep homeostasis: convergent evolution of complex brains, cognition and sleep functions in mammals and birds. *Neuroscience & Biobehavioral Reviews*, 33(3):253–270, 2009. ISBN: 0149-7634 Publisher: Elsevier.

[121] Julia P. Pryaslova, Oleg I. Lyamin, Jerome M. Siegel, and Lev M. Mukhametov. Behavioral sleep in the walrus. *Behavioural brain research*, 201(1):80–87, 2009. ISBN: 0166-4328 Publisher: Elsevier.

[122] Esteban J. Beckwith, Quentin Geissmann, Alice S. French, and Giorgio F. Gilestro. Regulation of sleep homeostasis by sexual arousal. *Elife*, 6:e27445, 2017. ISBN: 2050-084X Publisher: eLife Sciences Publications, Ltd.

[123] P.-A. Libourel, W. Y. Lee, I. Achin, H. Chung, J. Kim, B. Massot, and Niels Christian Rattenborg. Nesting chinstrap penguins accrue large quantities of sleep through seconds-long microsleeps. *Science*, 382(6674):1026–1031, 2023. ISBN: 0036-8075 Publisher: American Association for the Advancement of Science.

[124] R. Elwyn Isaac, Chenxi Li, Amy E. Leedale, and Alan D. Shirras. Drosophila male sex peptide inhibits siesta sleep and promotes locomotor activity in the post-mated female. *Proceedings of the Royal Society B: Biological Sciences*, 277(1678):65–70, September 2009. Publisher: Royal Society.

[125] Erik R. Duboué, Alex C. Keene, and Richard L. Borowsky. Evolutionary convergence on sleep loss in cavefish populations. *Current biology*, 21(8):671–676, 2011. ISBN: 0960-9822 Publisher: Elsevier.

[126] Erik R. Duboué and Alex C. Keene. Investigating the evolution of sleep in the Mexican cavefish. *Biology and evolution of the Mexican cavefish*, pages 291–308, 2016. Publisher: Elsevier Amsterdam, The Netherlands.

[127] Erik R. Duboué and Richard L. Borowsky. Altered rest-activity patterns evolve via circadian independent mechanisms in cave adapted balitorid loaches. *PLoS One*, 7(2):e30868, 2012. ISBN: 1932-6203 Publisher: Public Library of Science San Francisco, USA.

[128] William R. Jeffery. Regressive evolution in Astyanax cavefish. *Annual review of genetics*, 43(1):25–47, 2009. ISBN: 0066-4197 Publisher: Annual Reviews.

[129] Chaira Cirelli and Daniel Bushey. Sleep and wakefulness in Drosophila melanogaster. *Annals of the New York Academy of Sciences*, 1129(1):323–329, 2008. ISBN: 0077-8923 Publisher: Wiley Online Library.

[130] Russell G. Foster. There is no mystery to sleep. *PsyCh journal*, 7(4):206–208, 2018. ISBN: 2046-0252 Publisher: Wiley Online Library.

[131] W. B. Webb and And HW Agnew Jr. The effects of a chronic limitation of sleep length. *Psychophysiology*, 11(3):265–274, 1974. ISBN: 0048-5772 Publisher: Wiley Online Library.

[132] Ralph J. Berger and Nathan H. Phillips. Energy conservation and sleep. *Behavioural brain research*, 69(1-2):65–73, 1995. ISBN: 0166-4328 Publisher: Elsevier.

[133] Jerome M. Siegel. Sleep viewed as a state of adaptive inactivity. *Nature Reviews Neuroscience*, 10(10):747–753, 2009. ISBN: 1471-003X Publisher: Nature Publishing Group UK London.

[134] Andrew S. Freiberg. Why we sleep: a hypothesis for an ultimate or evolutionary origin for sleep and other physiological rhythms. *Journal of circadian rhythms*, 18, 2020. Publisher: Ubiquity Press.

[135] Steven L. Lima, Niels C. Rattenborg, John A. Lesku, and Charles J. Amlaner. Sleeping under the risk of predation. *Animal Behaviour*, 70(4):723–736, 2005. ISBN: 0003-3472 Publisher: Elsevier.

[136] Kirstine Adam and Ian Oswald. Sleep helps healing. *British medical journal (Clinical research ed.)*, 289(6456):1400, 1984. Publisher: BMJ Publishing Group.

[137] Kenan Gümüstekin, Bedri Seven, Nezihe Karabulut, Ömer Aktas, Nesrin Gürsan, Sahin Aslan, Mustafa Keles, Erhan Varoglu, and Senol Dane. Effects of sleep deprivation, nicotine, and selenium on wound healing in rats. *International journal of neuroscience*, 114(11):1433–1442, 2004. ISBN: 0020-7454 Publisher: Taylor & Francis.

[138] Tzu-Hsing Kuo, Douglas H. Pike, Zahra Beizaeipour, and Julie A. Williams. Sleep triggered by an immune response in Drosophila is regulated by the circadian clock and requires the NFB Relish. *BMC neuroscience*, 11:1–12, 2010. Publisher: Springer.

[139] Mark R. Zielinski and James M. Krueger. Sleep and innate immunity. *Frontiers in bioscience (Scholar edition)*, 3:632, 2011. Publisher: NIH Public Access.

[140] Kathryn B. Renegar, Dennis Crouse, Rachael A. Floyd, and James Krueger. Progression of influenza viral infection through the murine respiratory tract: the protective role of sleep deprivation. *SLEEP-NEW YORK-*, 23(7):859–866, 2000. ISBN: 0161-8105 Publisher: American Academy of Sleep Medicine; 1999.

[141] Namni Goel, Hengyi Rao, Jeffrey S. Durmer, and David F. Dinges. Neurocognitive consequences of sleep deprivation. In *Seminars in neurology*, volume 29, pages 320–339. © Thieme Medical Publishers, 2009. Issue: 04.

[142] Hans PA Van Dongen, Greg Maislin, Janet M. Mullington, and David F. Dinges. The cumulative cost of additional wakefulness: dose-response effects on neurobehavioral func-

tions and sleep physiology from chronic sleep restriction and total sleep deprivation. *Sleep*, 26(2):117–126, 2003. ISBN: 1550-9109 Publisher: Oxford University Press.

[143] Giulio Tononi and Chiara Cirelli. Sleep and synaptic homeostasis: a hypothesis. *Brain research bulletin*, 62(2):143–150, 2003. ISBN: 0361-9230 Publisher: Elsevier.

[144] Giulio Tononi and Chiara Cirelli. Sleep and the price of plasticity: from synaptic and cellular homeostasis to memory consolidation and integration. *Neuron*, 81(1):12–34, 2014. ISBN: 0896-6273 Publisher: Elsevier.

[145] Giulio Tononi and Chiara Cirelli. Sleep and synaptic down-selection. *Micro-, meso-and macro-dynamics of the brain*, pages 99–106, 2016. ISBN: 3319288016 Publisher: Springer International Publishing.

[146] Daniel Bushey, Giulio Tononi, and Chiara Cirelli. Sleep and synaptic homeostasis: structural evidence in Drosophila. *Science*, 332(6037):1576–1581, 2011. ISBN: 0036-8075 Publisher: American Association for the Advancement of Science.

[147] Stephanie Maret, Ugo Faraguna, Aaron B. Nelson, Chiara Cirelli, and Giulio Tononi. Sleep and waking modulate spine turnover in the adolescent mouse cortex. *Nature neuroscience*, 14(11):1418–1420, 2011. ISBN: 1097-6256 Publisher: Nature Publishing Group US New York.

[148] Giorgio F. Gilestro, Giulio Tononi, and Chiara Cirelli. Widespread changes in synaptic markers as a function of sleep and wakefulness in Drosophila. *science*, 324(5923):109–112, 2009. ISBN: 0036-8075 Publisher: American Association for the Advancement of Science.

[149] Vladyslav V. Vyazovskiy, Chiara Cirelli, Martha Pfister-Genskow, Ugo Faraguna, and Giulio Tononi. Molecular and electrophysiological evidence for net synaptic potentiation in wake and depression in sleep. *Nature neuroscience*, 11(2):200–208, 2008. ISBN: 1097-6256 Publisher: Nature Publishing Group US New York.

[150] David Zada, Irina Bronshtein, Tali Lerer-Goldshtein, Yuval Garini, and Lior Appelbaum. Sleep increases chromosome dynamics to enable reduction of accumulating DNA damage

in single neurons. *Nature communications*, 10(1):895, 2019. ISBN: 2041-1723 Publisher: Nature Publishing Group UK London.

[151] Robert Stickgold. Parsing the role of sleep in memory processing. *Current opinion in neurobiology*, 23(5):847–853, 2013. ISBN: 0959-4388 Publisher: Elsevier.

[152] Graham Findlay, Giulio Tononi, and Chiara Cirelli. The evolving view of replay and its functions in wake and sleep. *Sleep Advances*, 1(1):zpab002, 2020. ISBN: 2632-5012 Publisher: Oxford University Press US.

[153] Pierre Maquet, Steven Laureys, Philippe Peigneux, Sonia Fuchs, Christophe Petiau, Christophe Phillips, Joel Aerts, Guy Del Fiore, Christian Degueldre, and Thierry Meulemans. Experience-dependent changes in cerebral activation during human REM sleep. *Nature neuroscience*, 3(8):831–836, 2000. ISBN: 1546-1726 Publisher: Nature Publishing Group.

[154] Joyce Poole and Petter Granli. Mind and movement: Meeting the interests of elephants. *An elephant in the room: the science and well being of elephants in captivity,(Forthman, DL, Kane, FL, Hancocks, D., and Waldau, PF eds.) Center for Animals and Public Policy, Cummings School of Veterinary Medicine, Tufts University*, 2009.

[155] Steven L. Lima and Niels C. Rattenborg. A behavioural shutdown can make sleeping safer: a strategic perspective on the function of sleep. *Animal Behaviour*, 74(2):189–197, 2007. ISBN: 0003-3472 Publisher: Elsevier.

[156] Howard P. Roffwarg, Joseph N. Muzio, and William C. Dement. Ontogenetic Development of the Human Sleep-Dream Cycle: The prime role of" dreaming sleep" in early life may be in the development of the central nervous system. *Science*, 152(3722):604–619, 1966. ISBN: 0036-8075 Publisher: American Association for the Advancement of Science.

[157] John A. Lesku, Alexei L. Vyssotski, Dolores Martinez-Gonzalez, Christiane Wilzeck, and Niels C. Rattenborg. Local sleep homeostasis in the avian brain: convergence of sleep function in mammals and birds? *Proceedings of the Royal Society B: Biological Sciences*, 278(1717):2419–2428, August 2011.

[158] Gianina Ungurean, John A. Lesku, and Niels C. Rattenborg. Sleep in birds. *Reference Module in Neuroscience and Biobehavioral Psychology (Elsevier)*, 2021.

[159] H. L. Payne, G. F. Lynch, and D. Aronov. Neural representations of space in the hippocampus of a food-caching bird. *Science*, 373(6552):343–348, 2021. ISBN: 0036-8075 Publisher: American Association for the Advancement of Science.

[160] Jacqueline van der Meij, Dolores Martinez-Gonzalez, Gabriël JL Beckers, and Niels C. Rattenborg. Intra-"cortical" activity during avian non-REM and REM sleep: variant and invariant traits between birds and mammals. *Sleep*, 42(2):zsy230, 2019. ISBN: 0161-8105 Publisher: Oxford University Press US.

[161] Gianina Ungurean, Dolores Martinez-Gonzalez, Bertrand Massot, Paul-Antoine Libourel, and Niels C. Rattenborg. Pupillary behavior during wakefulness, non-REM sleep, and REM sleep in birds is opposite that of mammals. *Current Biology*, 31(23):5370–5376. e4, 2021. ISBN: 0960-9822 Publisher: Elsevier.

[162] Henry Van Twyver and Truett Allison. A polygraphic and behavioral study of sleep in the pigeon (*Columba livia*). *Experimental Neurology*, 35(1):138–153, April 1972.

[163] Thomas A. Wehr. A brain-warming function for REM sleep. *Neuroscience & Biobehavioral Reviews*, 16(3):379–397, September 1992.

[164] John A. Lesku, Rebekah J. Bark, Dolores Martinez-Gonzalez, Niels C. Rattenborg, Charles J. Amlaner, and Steven L. Lima. Predator-induced plasticity in sleep architecture in wild-caught Norway rats (*Rattus norvegicus*). *Behavioural Brain Research*, 189(2):298–305, June 2008.

[165] Ryan K. Tisdale, John A. Lesku, Gabriel JL Beckers, Alexei L. Vyssotski, and Niels C. Rattenborg. The low-down on sleeping down low: pigeons shift to lighter forms of sleep when sleeping near the ground. *Journal of Experimental Biology*, 221(19):jeb182634, 2018. ISBN: 1477-9145 Publisher: The Company of Biologists Ltd.

[166] Sofija V. Canavan and Daniel Margoliash. Budgerigars have complex sleep structure similar to that of mammals. *PLoS Biology*, 18(11):e3000929, 2020. ISBN: 1544-9173 Publisher: Public Library of Science San Francisco, CA USA.

[167] Daniel T. Ksepka. Feathered dinosaurs. *Current Biology*, 30(22):R1347–R1353, November 2020.

[168] Paul-Antoine Libourel and Anthony Herrel. Sleep in amphibians and reptiles: a review and a preliminary analysis of evolutionary patterns. *Biological Reviews*, 91(3):833–866, 2016. ISBN: 1464-7931 Publisher: Wiley Online Library.

[169] Mark Shein-Idelson, Janie M. Ondracek, Hua-Peng Liaw, Sam Reiter, and Gilles Laurent. Slow waves, sharp waves, ripples, and REM in sleeping dragons. *Science*, 352(6285):590–595, 2016. ISBN: 0036-8075 Publisher: American Association for the Advancement of Science.

[170] Paul-Antoine Libourel, Baptiste Barrillot, Sébastien Arthaud, Bertrand Massot, Anne-Laure Morel, Olivier Beuf, Anthony Herrel, and Pierre-Hervé Luppi. Partial homologies between sleep states in lizards, mammals, and birds suggest a complex evolution of sleep states in amniotes. *PLoS biology*, 16(10):e2005982, 2018. ISBN: 1544-9173 Publisher: Public Library of Science San Francisco, CA USA.

[171] Michael L. Kelly, Richard A. Peters, Ryan K. Tisdale, and John A. Lesku. Unihemispheric sleep in crocodilians? *Journal of Experimental Biology*, 218(20):3175–3178, October 2015.

[172] Ryan K Tisdale, John A Lesku, Gabriel J L Beckers, and Niels C Rattenborg. Bird-like propagating brain activity in anesthetized Nile crocodiles. *Sleep*, 41(8):zsy105, August 2018.

[173] Hiroaki Norimoto, Lorenz A. Fenk, Hsing-Hsi Li, Maria Antonietta Tosches, Tatiana Gallego-Flores, David Hain, Sam Reiter, Riho Kobayashi, Angeles Macias, and Anja Arends. A claustrum in reptiles and its role in slow-wave sleep. *Nature*, 578(7795):413–418, 2020. ISBN: 0028-0836 Publisher: Nature Publishing Group UK London.

[174] Laura Domínguez, Ruth Morona, Alberto Joven, Agustín González, and Jesús M. López. Immunohistochemical localization of orexins (hypocretins) in the brain of reptiles and its relation to monoaminergic systems. *Journal of Chemical Neuroanatomy*, 39(1):20–34, 2010. ISBN: 0891-0618 Publisher: Elsevier.

[175] J. Cardot, D. Fellmann, and C. Bugnon. Melanin-concentrating hormone-producing neurons in reptiles. *General and comparative endocrinology*, 94(1):23–32, 1994. ISBN: 0016-6480 Publisher: Elsevier.

[176] Janine E. Deakin and Tariq Ezaz. Tracing the evolution of amniote chromosomes. *Chromosoma*, 123:201–216, 2014. ISBN: 0009-5915 Publisher: Springer.

[177] J. ALLAN HOBSON, OLIVE B. GOIN, and C. J. Goin. Electrographic correlates of behaviour in tree frogs. *Nature*, 220(5165):386–387, 1968. ISBN: 0028-0836 Publisher: Nature Publishing Group UK London.

[178] Louis C. Leung, Gordon X. Wang, Romain Madelaine, Gemini Skariah, Koichi Kawakami, Karl Deisseroth, Alexander E. Urban, and Philippe Mourrain. Neural signatures of sleep in zebrafish. *Nature*, 571(7764):198–204, 2019. ISBN: 0028-0836 Publisher: Nature Publishing Group UK London.

[179] Walter Kaiser and Jana Steiner-Kaiser. Neuronal correlates of sleep, wakefulness and arousal in a diurnal insect. *Nature*, 301(5902):707–709, 1983. ISBN: 0028-0836 Publisher: Nature Publishing Group UK London.

[180] Ada D. Eban-Rothschild and Guy Bloch. Differences in the sleep architecture of forager and young honeybees (Apis mellifera). *Journal of Experimental Biology*, 211(15):2408–2416, 2008. ISBN: 1477-9145 Publisher: Company of Biologists.

[181] S. Sauer, M. Kinkelin, E. Herrmann, and W. Kaiser. The dynamics of sleep-like behaviour in honey bees. *Journal of Comparative Physiology A*, 189:599–607, 2003. ISBN: 0340-7594 Publisher: Springer.

[182] Stefan Sauer, Eva Herrmann, and Walter Kaiser. Sleep deprivation in honey bees. *Journal of Sleep Research*, 13(2):145–152, 2004. _eprint: https://onlinelibrary.wiley.com/doi/pdf/10.1111/j.1365-2869.2004.00393.x.

[183] F. S. Andersen. Sleep in moths and its dependence on the frequency of stimulation in Anagasta kuehniella. *Opuscula Entomologica*, pages 15–24, 1968.

[184] Irene Tobler and Martin Neuner-Jehle. 24-h variation of vigilance in the cockroach Blaberus giganteus. *Journal of Sleep Research*, 1(4):231–239, 1992. _eprint: https://onlinelibrary.wiley.com/doi/pdf/10.1111/j.1365-2869.1992.tb00044.x.

[185] Mehmet F. Keleş, Ali Osman Berk Sapci, Casey Brody, Isabelle Palmer, Christin Le, Öznur Taştan, Sündüz Keleş, and Mark N. Wu. FlyVISTA, an Integrated Machine Learning Platform for Deep Phenotyping of Sleep in Drosophila. *bioRxiv*, 2023. Publisher: Cold Spring Harbor Laboratory Preprints.

[186] H. Schuppe. Rhythmic brain activity in sleeping bees. *Wiener Medizinische Wochenschrift (1946)*, 145(17-18):463–464, 1995. ISBN: 0043-5341.

[187] William J. Joiner, Amanda Crocker, Benjamin H. White, and Amita Sehgal. Sleep in Drosophila is regulated by adult mushroom bodies. *Nature*, 441(7094):757–760, 2006. ISBN: 0028-0836 Publisher: Nature Publishing Group UK London.

[188] Melvyn HW Yap, Martyna J. Grabowska, Chelsie Rohrscheib, Rhiannon Jeans, Michael Troup, Angelique C. Paulk, Bart Van Alphen, Paul J. Shaw, and Bruno Van Swinderen. Oscillatory brain activity in spontaneous and induced sleep stages in flies. *Nature communications*, 8(1):1815, 2017. ISBN: 2041-1723 Publisher: Nature Publishing Group UK London.

[189] Bart van Alphen, Melvyn H.W. Yap, Leonie Kirszenblat, Benjamin Kottler, and Bruno van Swinderen. A Dynamic Deep Sleep Stage in Drosophila. *The Journal of Neuroscience*, 33(16):6917, April 2013.

[190] Douglas A. Nitz, Bruno Van Swinderen, Giulio Tononi, and Ralph J. Greenspan. Electrophysiological correlates of rest and activity in Drosophila melanogaster. *Current biology*, 12(22):1934–1940, 2002. ISBN: 0960-9822 Publisher: Elsevier.

[191] Daniela C. Rößler, Massimo De Agrò, Elia Biundo, and Paul S. Shamble. Hanging by a thread: unusual nocturnal resting behaviour in a jumping spider. *Frontiers in Zoology*, 18(1):23, 2021. ISBN: 1742-9994 Publisher: Springer.

[192] Daniela C. Rößler and Marie E. Herberstein. A state with increased arousal threshold in Araneus diadematus (Araneidae) measured in the wild: new evidence for sleep in spiders. *bioRxiv*, page 2023.10. 19.563109, 2023. Publisher: Cold Spring Harbor Laboratory.

[193] Mireya Osorio-Palacios, Laura Montiel-Trejo, Iván Oliver-Domínguez, Jesús Hernández-Falcón, and Karina Mendoza-Ángeles. Sleep phases in crayfish: relationship between brain electrical activity and autonomic variables. *Frontiers in Neuroscience*, 15:694924, 2021. ISBN: 1662-453X Publisher: Frontiers Media SA.

[194] Fidel Ramón, Jesús Hernández-Falcón, Bao Nguyen, and Theodore H. Bullock. Slow wave sleep in crayfish. *Proceedings of the National Academy of Sciences*, 101(32):11857–11861, August 2004.

[195] Richard Stephenson and Vern Lewis. Behavioural evidence for a sleep-like quiescent state in a pulmonate mollusc, Lymnaea stagnalis (Linnaeus). *Journal of Experimental Biology*, 214(5):747–756, 2011. ISBN: 1477-9145 Publisher: Company of Biologists.

[196] Marcos G. Frank, Robert H. Waldrop, Michelle Dumoulin, Sara Aton, and Jean G. Boal. A preliminary analysis of sleep-like states in the cuttlefish Sepia officinalis. *PLoS One*, 7(6):e38125, 2012. ISBN: 1932-6203 Publisher: Public Library of Science San Francisco, USA.

[197] Teresa L. Iglesias, Jean G. Boal, Marcos G. Frank, Jochen Zeil, and Roger T. Hanlon. Cyclic nature of the REM sleep-like state in the cuttlefish Sepia officinalis. *Journal of Experimental Biology*, 222(1):jeb174862, 2019. ISBN: 1477-9145 Publisher: The Company of Biologists Ltd.

[198] Sylvia Lima de Souza Medeiros, Mizziara Marlen Matias de Paiva, Paulo Henrique Lopes, Wilfredo Blanco, Françoise Dantas de Lima, Jaime Bruno Cirne de Oliveira, Inácio Gomes Medeiros, Eduardo Bouth Sequerra, Sandro de Souza, and Tatiana Silva Leite. Cyclic alternation of quiet and active sleep states in the octopus. *Iscience*, 24(4), 2021. ISBN: 2589-0042 Publisher: Elsevier.

[199] Sylvain Alem, Clint J. Perry, Xingfu Zhu, Olli J. Loukola, Thomas Ingraham, Eirik Søvik, and Lars Chittka. Associative mechanisms allow for social learning and cultural transmission of string pulling in an insect. *PLoS biology*, 14(10):e1002564, 2016. ISBN: 1544-9173 Publisher: Public Library of Science San Francisco, CA USA.

[200] Daniel A. Levitis, William Z. Lidicker Jr, and Glenn Freund. Behavioural biologists do not agree on what constitutes behaviour. *Animal behaviour*, 78(1):103–110, 2009. ISBN: 0003-3472 Publisher: Elsevier.

[201] Adam J. Calhoun and Ahmed El Hady. Everyone knows what behavior is but they just don't agree on it. *Iscience*, 26(11), 2023. ISBN: 2589-0042 Publisher: Elsevier.

[202] Joshua M. Mueller, Neil Zhang, Jean M. Carlson, and Julie H. Simpson. Variation and variability in Drosophila grooming behavior. *Frontiers in behavioral neuroscience*, 15:769372, 2022. ISBN: 1662-5153 Publisher: Frontiers Media SA.

[203] John W. Krakauer, Asif A. Ghazanfar, Alex Gomez-Marin, Malcolm A. MacIver, and David Poeppel. Neuroscience needs behavior: correcting a reductionist bias. *Neuron*, 93(3):480–490, 2017. ISBN: 0896-6273 Publisher: Elsevier.

[204] Eve Marder and Jean-Marc Goaillard. Variability, compensation and homeostasis in neuron and network function. *Nature Reviews Neuroscience*, 7(7):563–574, 2006. ISBN: 1471-003X Publisher: Nature Publishing Group UK London.

[205] Paul S. Katz. Evolution of central pattern generators and rhythmic behaviours. *Philosophical Transactions of the Royal Society B: Biological Sciences*, 371(1685):20150057, 2016. ISBN: 0962-8436 Publisher: The Royal Society.

[206] Shimon Marom, Ron Meir, Erez Braun, Asaf Gal, Einat Kermany, and Danny Eytan. On the precarious path of reverse neuro-engineering. *Frontiers in Computational Neuroscience*, 3:495, 2009. ISBN: 1662-5188 Publisher: Frontiers.

[207] Eric Jonas and Konrad Paul Kording. Could a neuroscientist understand a microprocessor? *PLoS computational biology*, 13(1):e1005268, 2017. ISBN: 1553-7358 Publisher: Public Library of Science.

[208] Jonathan Green, Atsuko Adachi, Kunal K. Shah, Jonathan D. Hirokawa, Pablo S. Magani, and Gaby Maimon. A neural circuit architecture for angular integration in Drosophila. *Nature*, 546(7656):101–106, 2017. ISBN: 0028-0836 Publisher: Nature Publishing Group UK London.

[209] Cheng Lyu, L. F. Abbott, and Gaby Maimon. Building an allocentric travelling direction signal via vector computation. *Nature*, 601(7891):92–97, 2022. ISBN: 0028-0836 Publisher: Nature Publishing Group UK London.

[210] Peter Mussells Pires, Lingwei Zhang, Victoria Parache, L. F. Abbott, and Gaby Maimon. Converting an allocentric goal into an egocentric steering signal. *Nature*, 626(8000):808–818, 2024. ISBN: 0028-0836 Publisher: Nature Publishing Group UK London.

[211] Gaby Maimon, Andrew D. Straw, and Michael H. Dickinson. Active flight increases the gain of visual motion processing in Drosophila. *Nature neuroscience*, 13(3):393–399, 2010. ISBN: 1097-6256 Publisher: Nature Publishing Group US New York.

[212] Kriszat G. Uexküll von J. Streifzüge durch die Umwelt von Tieren und Menschen. *Verständliche Wissenschaft, Berlin, Wiederaufl. Rowohlt, Reinbek*, 1956.

[213] Mark G. Packard and James L. McGaugh. Inactivation of hippocampus or caudate nucleus with lidocaine differentially affects expression of place and response learning. *Neurobiology of learning and memory*, 65(1):65–72, 1996. ISBN: 1074-7427 Publisher: Elsevier.

[214] Nathaniel D. Daw, Yael Niv, and Peter Dayan. Uncertainty-based competition between prefrontal and dorsolateral striatal systems for behavioral control. *Nature neuroscience*,

8(12):1704–1711, 2005. ISBN: 1097-6256 Publisher: Nature Publishing Group US New York.

[215] Steven W. Flavell, Nadine Gogolla, Matthew Lovett-Barron, and Moriel Zelikowsky. The emergence and influence of internal states. *Neuron*, 110(16):2545–2570, 2022. ISBN: 0896-6273 Publisher: Elsevier.

[216] Nikolaas Tinbergen. *The study of instinct*. Pygmalion Press, an imprint of Plunkett Lake Press, 2020.

[217] Robert C. Bolles. The syntax of the mind. *Psychological Reports*, 21(2):493–499, 1967. ISBN: 0033-2941 Publisher: SAGE Publications Sage CA: Los Angeles, CA.

[218] Tess B. Oram and Gwyneth M. Card. Context-dependent control of behavior in Drosophila. *Current Opinion in Neurobiology*, 73:102523, 2022. ISBN: 0959-4388 Publisher: Elsevier.

[219] Floris van Breugel, Ainul Huda, and Michael H. Dickinson. Distinct activity-gated pathways mediate attraction and aversion to CO2 in Drosophila. *Nature*, 564(7736):420–424, 2018. ISBN: 0028-0836 Publisher: Nature Publishing Group UK London.

[220] Suewei Lin. Internal state-dependent modulation of olfactory responses: a tale of dopamine neurons in the adult Drosophila mushroom body. *Current Opinion in Insect Science*, page 101104, 2023. ISBN: 2214-5745 Publisher: Elsevier.

[221] Alice S. French, Quentin Geissmann, Esteban J. Beckwith, and Giorgio F. Gilestro. Sensory processing during sleep in Drosophila melanogaster. *Nature*, 598(7881):479–482, 2021. ISBN: 0028-0836 Publisher: Nature Publishing Group UK London.

[222] M. Eugenia Chiappe, Johannes D. Seelig, Michael B. Reiser, and Vivek Jayaraman. Walking modulates speed sensitivity in Drosophila motion vision. *Current Biology*, 20(16):1470–1475, 2010. ISBN: 0960-9822 Publisher: Elsevier.

[223] Adam J. Calhoun, Jonathan W. Pillow, and Mala Murthy. Unsupervised identification of the internal states that shape natural behavior. *Nature neuroscience*, 22(12):2040–2049, 2019. ISBN: 1097-6256 Publisher: Nature Publishing Group US New York.

[224] William Ernest Castle, Frederick W. Carpenter, Alonzo Howard Clark, Samuel O. Mast, and William M. Barrows. The effects of inbreeding, cross-breeding, and selection upon the fertility and variability of Drosophila. In *Proceedings of the American Academy of Arts and Sciences*, volume 41, pages 731–786. JSTOR, 1906. Issue: 33.

[225] Thomas Hunt Morgan. Sex limited inheritance in Drosophila. *Science*, 32(812):120–122, 1910. ISBN: 0036-8075 Publisher: American Association for the Advancement of Science.

[226] Barbara H. Jennings. Drosophila–a versatile model in biology & medicine. *Materials today*, 14(5):190–195, 2011. ISBN: 1369-7021 Publisher: Elsevier.

[227] Mark D. Adams, Susan E. Celniker, Robert A. Holt, Cheryl A. Evans, Jeannine D. Gocayne, Peter G. Amanatides, Steven E. Scherer, Peter W. Li, Roger A. Hoskins, and Richard F. Galle. The genome sequence of Drosophila melanogaster. *Science*, 287(5461):2185–2195, 2000. ISBN: 1095-9203 Publisher: American Association for the Advancement of Science.

[228] Steven L. Chown and Kevin J. Gaston. Body size variation in insects: a macroecological perspective. *Biological Reviews*, 85(1):139–169, 2010. ISBN: 1464-7931 Publisher: Wiley Online Library.

[229] A. H. Sturtevant. The north American species of Drosophila. *Carnegie institution of Washington*, (301), 1921.

[230] Therese A. Markow, Stephen Beall, and Sergio Castrezana. The wild side of life: Drosophila reproduction in nature. *Fly*, 6(2):98–101, 2012. ISBN: 1933-6934 Publisher: Taylor & Francis.

[231] Jean R. David and Pierre Capy. Genetic variation of Drosophila melanogaster natural populations. *Trends in Genetics*, 4(4):106–111, 1988. ISBN: 0168-9525 Publisher: Elsevier Current Trends.

[232] Therese Ann Markow. The secret lives of Drosophila flies. *eLife*, 4:e06793, June 2015.

[233] Charles William Robertson. The metamorphosis of Drosophila melanogaster, including an accurately timed account of the principal morphological changes. *Journal of morphology*, 59(2):351–399, 1936. ISBN: 0362-2525 Publisher: Wiley Online Library.

[234] Jason M. Tennessen and Carl S. Thummel. Coordinating growth and maturation—insights from Drosophila. *Current Biology*, 21(18):R750–R757, 2011. ISBN: 0960-9822 Publisher: Elsevier.

[235] Janneke Wit, Torsten Nygaard Kristensen, Pernille Sarup, Jane Frydenberg, and Volker Loeschcke. Laboratory selection for increased longevity in Drosophila melanogaster reduces field performance. *Experimental Gerontology*, 48(11):1189–1195, 2013. ISBN: 0531-5565 Publisher: Elsevier.

[236] Cory Pfeiffenberger, Bridget C. Lear, Kevin P. Keegan, and Ravi Allada. Locomotor activity level monitoring using the Drosophila Activity Monitoring (DAM) System. *Cold Spring Harbor Protocols*, 2010(11):pdb. prot5518, 2010. ISBN: 1940-3402 Publisher: Cold Spring Harbor Laboratory Press.

[237] Ravi Allada and Brian Y. Chung. Circadian organization of behavior and physiology in Drosophila. *Annual review of physiology*, 72(1):605–624, 2010. ISBN: 0066-4278 Publisher: Annual Reviews.

[238] Giorgio F. Gilestro. Video tracking and analysis of sleep in Drosophila melanogaster. *Nature protocols*, 7(5):995–1007, 2012. ISBN: 1754-2189 Publisher: Nature Publishing Group UK London.

[239] John E. Zimmerman, David M. Raizen, Matthew H. Maycock, Greg Maislin, and Allan I. Pack. A video method to study Drosophila sleep. *Sleep*, 31(11):1587–1598, 2008. ISBN: 1550-9109 Publisher: Oxford University Press.

[240] Heiko Dankert, Liming Wang, Eric D. Hoopfer, David J. Anderson, and Pietro Perona. Automated monitoring and analysis of social behavior in Drosophila. *Nature methods*, 6(4):297–303, 2009. ISBN: 1548-7091 Publisher: Nature Publishing Group US New York.

[241] Nathan Donelson, Eugene Z. Kim, Justin B. Slawson, Christopher G. Vecsey, Robert Huber, and Leslie C. Griffith. High-resolution positional tracking for long-term analysis of Drosophila sleep and locomotion using the "tracker" program. *PloS one*, 7(5):e37250, 2012. ISBN: 1932-6203 Publisher: Public Library of Science San Francisco, USA.

[242] Primoz Ravbar, Kristin Branson, and Julie H. Simpson. An automatic behavior recognition system classifies animal behaviors using movements and their temporal context. *Journal of neuroscience methods*, 326:108352, 2019. ISBN: 0165-0270 Publisher: Elsevier.

[243] Susu Qu, Qingjie Zhu, Han Zhou, Yuan Gao, Yi Wei, Yuan Ma, Zhicheng Wang, Xueting Sun, Lei Zhang, and Quanjun Yang. EasyFlyTracker: a simple video tracking python package for analyzing adult Drosophila locomotor and sleep activity to facilitate revealing the effect of psychiatric drugs. *Frontiers in Behavioral Neuroscience*, 15:809665, 2022. ISBN: 1662-5153 Publisher: Frontiers Media SA.

[244] Quentin Geissmann, Luis Garcia Rodriguez, Esteban J. Beckwith, Alice S. French, Arian R. Jamasb, and Giorgio F. Gilestro. Ethoscopes: An open platform for high-throughput ethomics. *PLOS Biology*, 15(10):e2003026, October 2017. Publisher: Public Library of Science.

[245] Kristin Branson, Alice A. Robie, John Bender, Pietro Perona, and Michael H. Dickinson. High-throughput ethomics in large groups of Drosophila. *Nature methods*, 6(6):451–457, 2009. ISBN: 1548-7091 Publisher: Nature Publishing Group US New York.

[246] Alfonso Pérez-Escudero, Julián Vicente-Page, Robert C. Hinz, Sara Arganda, and Gonzalo G. De Polavieja. idTracker: tracking individuals in a group by automatic identification of unmarked animals. *Nature methods*, 11(7):743–748, 2014. ISBN: 1548-7091 Publisher: Nature Publishing Group US New York.

[247] Reza Ardekani, Simon Tavaré, and John Tower. Assessing senescence in Drosophila using video tracking. *Cell Senescence: Methods and Protocols*, pages 501–516, 2013. ISBN: 162703238X Publisher: Springer.

[248] Semih Günel, Helge Rhodin, Daniel Morales, João Campagnolo, Pavan Ramdya, and Pascal Fua. DeepFly3D, a deep learning-based approach for 3D limb and appendage tracking in tethered, adult Drosophila. *Elife*, 8:e48571, 2019. ISBN: 2050-084X Publisher: eLife Sciences Publications, Ltd.

[249] Lili Karashchuk, Jing Shuang Lisa Li, Grant M. Chou, Sarah Walling-Bell, Steven L. Brunton, John C. Tuthill, and Bingni W. Brunton. Sensorimotor delays constrain robust locomotion in a 3D kinematic model of fly walking. *bioRxiv*, 2024. Publisher: Cold Spring Harbor Laboratory Preprints.

[250] Alexander Mathis, Pranav Mamidanna, Kevin M. Cury, Taiga Abe, Venkatesh N. Murthy, Mackenzie Weygandt Mathis, and Matthias Bethge. DeepLabCut: markerless pose estimation of user-defined body parts with deep learning. *Nature neuroscience*, 21(9):1281–1289, 2018. ISBN: 1546-1726 Publisher: Nature Publishing Group.

[251] Talmo D. Pereira, Diego E. Aldarondo, Lindsay Willmore, Mikhail Kislin, Samuel S.-H. Wang, Mala Murthy, and Joshua W. Shaevitz. Fast animal pose estimation using deep neural networks. *Nature methods*, 16(1):117–125, 2019. ISBN: 1548-7091 Publisher: Nature Publishing Group US New York.

[252] Talmo D. Pereira, Nathaniel Tabris, Arie Matsliah, David M. Turner, Junyu Li, Shruthi Ravindranath, Eleni S. Papadoyannis, Edna Normand, David S. Deutsch, and Z. Yan Wang. SLEAP: A deep learning system for multi-animal pose tracking. *Nature methods*, 19(4):486–495, 2022. ISBN: 1548-7091 Publisher: Nature Publishing Group US New York.

[253] Jacob M. Graving, Daniel Chae, Hemal Naik, Liang Li, Benjamin Koger, Blair R. Costelloe, and Iain D. Couzin. DeepPoseKit, a software toolkit for fast and robust animal pose estimation using deep learning. *Elife*, 8:e47994, 2019. ISBN: 2050-084X Publisher: eLife Sciences Publications, Ltd.

[254] Charalambos P. Kyriacou and Jeffrey C. Hall. Learning and memory mutations impair acoustic priming of mating behaviour in Drosophila. *Nature*, 308(5954):62–65, 1984. ISBN: 0028-0836 Publisher: Nature Publishing Group UK London.

[255] Beatriz Gil-Martí, Celia G. Barredo, Sara Pina-Flores, Adriana Poza-Rodriguez, Gaia Treves, Carmen Rodriguez-Navas, Lucía Camacho, Atenea Pérez-Serna, Iñaki Jimenez, and Laura Brazales. A simplified courtship conditioning protocol to test learning and memory in Drosophila. *STAR protocols*, 4(1):101572, 2023. ISBN: 2666-1667 Publisher: Elsevier.

[256] Therese A. Markow and Stephen J. Hanson. Multivariate analysis of Drosophila courtship. *Proceedings of the National Academy of Sciences*, 78(1):430–434, 1981. ISBN: 0027-8424 Publisher: National Acad Sciences.

[257] Ken-Ichi Kimura, Manabu Ote, Tatsunori Tazawa, and Daisuke Yamamoto. Fruitless specifies sexually dimorphic neural circuitry in the Drosophila brain. *Nature*, 438(7065):229–233, 2005. ISBN: 0028-0836 Publisher: Nature Publishing Group UK London.

[258] David Deutsch, Diego Pacheco, Lucas Encarnacion-Rivera, Talmo Pereira, Ramie Fathy, Jan Clemens, Cyrille Girardin, Adam Calhoun, Elise Ireland, and Austin Burke. The neural basis for a persistent internal state in Drosophila females. *Elife*, 9:e59502, 2020. ISBN: 2050-084X Publisher: eLife Sciences Publications, Ltd.

[259] Selby Chen, Ann Yeelin Lee, Nina M. Bowens, Robert Huber, and Edward A. Kravitz. Fighting fruit flies: a model system for the study of aggression. *Proceedings of the National Academy of Sciences*, 99(8):5664–5668, 2002. ISBN: 0027-8424 Publisher: National Acad Sciences.

[260] John Alcock and Randy Thornhill. The evolution of insect mating systems. *The Evolution of Insect Mating Systems. Oxford University Press, USA*, pages 275–278, 2014.

[261] Susanne C. Hoyer, Andreas Eckart, Anthony Herrel, Troy Zars, Susanne A. Fischer, Shannon L. Hardie, and Martin Heisenberg. Octopamine in male aggression of Drosophila. *Current Biology*, 18(3):159–167, 2008. ISBN: 0960-9822 Publisher: Elsevier.

[262] Olivia Schwarz, Ali Asgar Bohra, Xinyu Liu, Heinrich Reichert, Krishnaswamy Vijay-Raghavan, and Jan Pielage. Motor control of Drosophila feeding behavior. *Elife*, 6:e19892, 2017. ISBN: 2050-084X Publisher: eLife Sciences Publications, Ltd.

[263] Thomas F. Flood, Michael Gorczyca, Benjamin H. White, Kei Ito, and Motojiro Yoshihara. A large-scale behavioral screen to identify neurons controlling motor programs in the Drosophila brain. *G3: Genes, Genomes, Genetics*, 3(10):1629–1637, 2013. ISBN: 2160-1836 Publisher: Oxford University Press.

[264] Bart Van Alphen, Evan R. Semenza, Melvyn Yap, Bruno Van Swinderen, and Ravi Allada. A deep sleep stage in Drosophila with a functional role in waste clearance. *Science advances*, 7(4):eabc2999, 2021. ISBN: 2375-2548 Publisher: American Association for the Advancement of Science.

[265] Pavel M. Itskov, José-Maria Moreira, Ekaterina Vinnik, Gonçalo Lopes, Steve Safarik, Michael H. Dickinson, and Carlos Ribeiro. Automated monitoring and quantitative analysis of feeding behaviour in Drosophila. *Nature communications*, 5(1):4560, 2014. ISBN: 2041-1723 Publisher: Nature Publishing Group UK London.

[266] José-Maria Moreira, Pavel M. Itskov, Dennis Goldschmidt, Celia Baltazar, Kathrin Steck, Ibrahim Tastekin, Samuel J. Walker, and Carlos Ribeiro. optoPAD, a closed-loop optogenetics system to study the circuit basis of feeding behaviors. *Elife*, 8:e43924, 2019. ISBN: 2050-084X Publisher: eLife Sciences Publications, Ltd.

[267] Verónica María Corrales-Carvajal, Aldo A Faisal, and Carlos Ribeiro. Internal states drive nutrient homeostasis by modulating exploration-exploitation trade-off. *eLife*, 5:e19920, October 2016. Publisher: eLife Sciences Publications, Ltd.

[268] Daniel Münch, Dennis Goldschmidt, and Carlos Ribeiro. The neuronal logic of how internal states control food choice. *Nature*, 607(7920):747–755, 2022. ISBN: 0028-0836 Publisher: Nature Publishing Group UK London.

[269] Andrew L. Szebenyi. Cleaning behaviour in Drosophila melanogaster. *Animal Behaviour*, 17(4):641–651, 1969. ISBN: 0003-3472 Publisher: Elsevier.

[270] Gabriel Corfas and Yadin Dudai. Habituation and dishabituation of a cleaning reflex in normal and mutant Drosophila. *Journal of Neuroscience*, 9(1):56–62, 1989. ISBN: 0270-6474 Publisher: Soc Neuroscience.

[271] Andrew M. Seeds, Primoz Ravbar, Phuong Chung, Stefanie Hampel, Frank M. Midgley Jr, Brett D. Mensh, and Julie H. Simpson. A suppression hierarchy among competing motor programs drives sequential grooming in Drosophila. *Elife*, 3:e02951, 2014. ISBN: 2050-084X Publisher: eLife Sciences Publications, Ltd.

[272] Esteban J. Beckwith and Alice S. French. Sleep in Drosophila and its context. *Frontiers in physiology*, 10:1167, 2019. ISBN: 1664-042X Publisher: Frontiers Media SA.

[273] Orie T. Shafer and Alex C. Keene. The regulation of Drosophila sleep. *Current Biology*, 31(1):R38–R49, 2021. ISBN: 0960-9822 Publisher: Elsevier.

[274] Paul J. Shaw, Chiara Cirelli, Ralph J. Greenspan, and Giulio Tononi. Correlates of Sleep and Waking in Drosophila melanogaster. *Science*, 287(5459):1834, March 2000.

[275] Joan C Hendricks, Stefanie M Finn, Karen A Panackeri, Jessica Chavkin, Julie A Williams, Amita Sehgal, and Allan I Pack. Rest in Drosophila Is a Sleep-like State. *Cell*, 25(1):129–138, January 2000.

[276] Joe Shimizu, Takashi Kasai, Hideki Yoshida, Anh M. Huynh, Yumiko Nakao-Azuma, Makiko Shinomoto, Takahiko Tokuda, Toshiki Mizuno, and Masamitsu Yamaguchi. Novel Drosophila model for parkinsonism by targeting phosphoglycerate kinase. *Neurochemistry International*, 139:104816, 2020. Publisher: Elsevier.

[277] Xinjian Li, Feng Yu, and Aike Guo. Sleep deprivation specifically impairs short-term olfactory memory in Drosophila. *Sleep*, 32(11):1417–1424, 2009. Publisher: Oxford University Press.

[278] Lucy A L Tainton-Heap, Leonie C Kirszenblat, Eleni T Notaras, Martyna J Grabowska, Rhiannon Jeans, Kai Feng, Paul J Shaw, and Bruno van Swinderen. A Paradoxical Kind

of Sleep in Drosophila melanogaster. *Current biology : CB*, 31(3):578–590.e6, February 2021.

[279] Lei Guo and Giorgio Gilestro. Untangling stress and sleep as the cause of death in sleep deprived Drosophila. *Unpublished, ongoing work*, 2024.

[280] Aleksandra H. Nall, Iryna Shakhmantsir, Karol Cichewicz, Serge Birman, Jay Hirsh, and Amita Sehgal. Caffeine promotes wakefulness via dopamine signaling in Drosophila. *Scientific reports*, 6(1):20938, 2016. Publisher: Nature Publishing Group UK London.

[281] Elizabeth B. Brown, Kreesha D. Shah, Richard Faville, Benjamin Kottler, and Alex C. Keene. Drosophila insulin-like peptide 2 mediates dietary regulation of sleep intensity. *PLoS Genetics*, 16(3):e1008270, 2020. Publisher: Public Library of Science San Francisco, CA USA.

[282] Sami Aboudhiaf, Georges Alves, Sandrine Parrot, Mohamed Amri, Mégane M. Simonnet, Yael Grosjean, Gérard Manière, and Laurent Seugnet. LAT1-like transporters regulate dopaminergic transmission and sleep in Drosophila. *Sleep*, 41(10):zsy137, 2018. Publisher: Oxford University Press US.

[283] Rozi Andretic and Paul J. Shaw. Essentials of Sleep Recordings in Drosophila: Moving Beyond Sleep Time. In Michael W. Young, editor, *Methods in Enzymology*, volume 393, pages 759–772. Academic Press, January 2005.

[284] Joan C. Hendricks, David Kirk, Karen Panckeri, Matthew S. Miller, and Allan I. Pack. Modafinil maintains waking in the fruit fly Drosophila melanogaster. *Sleep*, 26(2):139–146, 2003. Publisher: Oxford University Press.

[285] Glen Seidner, James E. Robinson, Meilin Wu, Kurtresha Worden, Pavel Masek, Stephen W. Roberts, Alex C. Keene, and William J. Joiner. Identification of neurons with a privileged role in sleep homeostasis in Drosophila melanogaster. *Current Biology*, 25(22):2928–2938, 2015. Publisher: Elsevier.

[286] Alex C. Keene, Erik R. Duboué, Daniel M. McDonald, Monica Dus, Greg SB Suh, Scott Waddell, and Justin Blau. Clock and cycle limit starvation-induced sleep loss in Drosophila. *Current biology*, 20(13):1209–1215, 2010. Publisher: Elsevier.

[287] James H. Catterson, Mobina Khericha, Miranda C. Dyson, Alec J. Vincent, Rebecca Callard, Steven M. Haveron, Arjunan Rajasingam, Mumtaz Ahmad, and Linda Partridge. Short-term, intermittent fasting induces long-lasting gut health and TOR-independent lifespan extension. *Current Biology*, 28(11):1714–1724, 2018. Publisher: Elsevier.

[288] Matthew S. Thimgan, Yasuko Suzuki, Laurent Seugnet, Laura Gottschalk, and Paul J. Shaw. The Perilipin Homologue, Lipid Storage Droplet 2, Regulates Sleep Homeostasis and Prevents Learning Impairments Following Sleep Loss. *PLoS Biology*, 8(8):e1000466, August 2010.

[289] Fumika N. Hamada, Mark Rosenzweig, Kyeongjin Kang, Stefan R. Pulver, Alfredo Ghezzi, Timothy J. Jegla, and Paul A. Garrity. An internal thermal sensor controlling temperature preference in Drosophila. *Nature*, 454(7201):217–220, 2008. Publisher: Nature Publishing Group UK London.

[290] Diogo Pimentel, Jeffrey M. Donlea, Clifford B. Talbot, Seoho M. Song, Alexander JF Thurston, and Gero Miesenböck. Operation of a homeostatic sleep switch. *Nature*, 536(7616):333–337, 2016. Publisher: Nature Publishing Group UK London.

[291] Christine Dubowy and Amita Sehgal. Circadian rhythms and sleep in Drosophila melanogaster. *Genetics*, 205(4):1373–1397, 2017. Publisher: Oxford University Press.

[292] Ronald J. Konopka and Seymour Benzer. Clock Mutants of *Drosophila melanogaster*. *Proceedings of the National Academy of Sciences*, 68(9):2112–2116, September 1971.

[293] Amita Sehgal, Jeffrey L. Price, Bernice Man, and Michael W. Young. Loss of Circadian Behavioral Rhythms and *per* RNA Oscillations in the *Drosophila* Mutant *timeless*. *Science*, 263(5153):1603–1606, March 1994.

[294] Ravi Allada, Neal E. White, W. Venus So, Jeffrey C. Hall, and Michael Rosbash. A mutant Drosophila homolog of mammalian Clock disrupts circadian rhythms and transcription of period and timeless. *Cell*, 93(5):791–804, 1998. Publisher: Elsevier.

[295] Joan E. Rutila, Vipin Suri, Myai Le, W. Venus So, Michael Rosbash, and Jeffrey C. Hall. CYCLE is a second bHLH-PAS clock protein essential for circadian rhythmicity and transcription of Drosophila period and timeless. *Cell*, 93(5):805–814, 1998. Publisher: Elsevier.

[296] Choogon Lee, Kiho Bae, and Isaac Edery. PER and TIM Inhibit the DNA Binding Activity of a *Drosophila* CLOCK-CYC/dBMAL1 Heterodimer without Disrupting Formation of the Heterodimer: a Basis for Circadian Transcription. *Molecular and Cellular Biology*, 19(8):5316–5325, August 1999.

[297] Eun Young Kim, Hyuk Wan Ko, Wangjie Yu, Paul E. Hardin, and Isaac Edery. A DOUBLETIME Kinase Binding Domain on the *Drosophila* PERIOD Protein Is Essential for Its Hyperphosphorylation, Transcriptional Repression, and Circadian Clock Function. *Molecular and Cellular Biology*, 27(13):5014–5028, July 2007.

[298] A. Reum Jang, Katarina Moravcevic, Lino Saez, Michael W. Young, and Amita Sehgal. Drosophila TIM binds importin 1, and acts as an adapter to transport PER to the nucleus. *PLoS genetics*, 11(2):e1004974, 2015. Publisher: Public Library of Science San Francisco, CA USA.

[299] Guan Cao and Michael N. Nitabach. Circadian control of membrane excitability in Drosophila melanogaster lateral ventral clock neurons. *Journal of Neuroscience*, 28(25):6493–6501, 2008. Publisher: Soc Neuroscience.

[300] Taishi Yoshii, Margaret Ahmad, and Charlotte Helfrich-Förster. Cryptochrome mediates light-dependent magnetosensitivity of Drosophila's circadian clock. *PLoS biology*, 7(4):e1000086, 2009. Publisher: Public Library of Science San Francisco, USA.

[301] Lakshman Abhilash and Orie Thomas Shafer. A two-process model of Drosophila sleep reveals an inter-dependence between circadian clock speed and the rate of sleep pressure decay. *Sleep*, 47(2):zsad277, 2024. Publisher: Oxford University Press US.

[302] Kyunghee Koh, Joshua M. Evans, Joan C. Hendricks, and Amita Sehgal. A *Drosophila* model for age-associated changes in sleep:wake cycles. *Proceedings of the National Academy of Sciences*, 103(37):13843–13847, September 2006.

[303] Laurent Seugnet, Yasuko Suzuki, Jeff M. Donlea, Laura Gottschalk, and Paul J. Shaw. Sleep deprivation during early-adult development results in long-lasting learning deficits in adult Drosophila. *Sleep*, 34(2):137–146, 2011. Publisher: Oxford University Press.

[304] Kenta Asahina. Sex differences in Drosophila behavior: qualitative and quantitative dimorphism. *Current Opinion in Physiology*, 6:35–45, 2018. Publisher: Elsevier.

[305] Gil B. Carvalho, Pankaj Kapahi, David J. Anderson, and Seymour Benzer. Allocrine Modulation of Feeding Behavior by the Sex Peptide of Drosophila. *Current Biology*, 16(7):692–696, April 2006. Publisher: Elsevier.

[306] Yael Heifetz, Oliver Lung, Edward A. Frongillo, and Mariana F. Wolfner. The Drosophila seminal fluid protein Acp26Aa stimulates release of oocytes by the ovary. *Current Biology*, 10(2):99–102, January 2000. Publisher: Elsevier.

[307] T. Chapman, L. F. Liddle, J. M. Kalb, M. F. Wolfner, and L. Partridge. Cost of mating in Drosophila melanogaster females is mediated by male accessory gland products. *Nature*, 373(6511):241–244, January 1995. Place: England.

[308] Keith R. Murphy, Jin Hong Park, Robert Huber, and William W. Ja. Simultaneous measurement of sleep and feeding in individual Drosophila. *Nature Protocols*, 12(11):2355–2359, November 2017. Publisher: Nature Publishing Group.

[309] Iris Titos, Alen Juginović, Alexandra Vaccaro, Keishi Nambara, Pavel Gorelik, Ofer Mazor, and Dragana Rogulja. A gut-secreted peptide suppresses arousability from sleep. *Cell*, 186(7):1382–1397.e21, March 2023. Publisher: Elsevier.

[310] James H. Catterson, Seymour Knowles-Barley, Katherine James, Margarete M. S. Heck, Anthony J. Harmar, and Paul S. Hartley. Dietary Modulation of Drosophila Sleep-Wake Behaviour. *PLOS ONE*, 5(8):e12062, August 2010. Publisher: Public Library of Science.

[311] Susan T. Harbison, Yazmin L. Serrano Negron, Nancy F. Hansen, and Amanda S. Lobell. Selection for long and short sleep duration in Drosophila melanogaster reveals the complex genetic network underlying natural variation in sleep. *PLoS genetics*, 13(12):e1007098, 2017. ISBN: 1553-7404 Publisher: Public Library of Science.

[312] Chiara Cirelli, Daniel Bushey, Sean Hill, Reto Huber, Robert Kreber, Barry Ganetzky, and Giulio Tononi. Reduced sleep in Drosophila Shaker mutants. *Nature*, 434(7037):1087–1092, April 2005.

[313] Kazuhiko Kume. A Drosophila dopamine transporter mutant, fumin (fmn), is defective in arousal regulation. *Sleep and Biological Rhythms*, 4(3):263–273, October 2006.

[314] Charlotte Helfrich-Förster. Sleep in Insects. *Annual Review of Entomology*, 63(Volume 63, 2018):69–86, January 2018. Publisher: Annual Reviews.

[315] Laurence Blackhurst and Giorgio F Gilestro. Ethoscopy and ethoscope-lab: a framework for behavioural analysis to lower entrance barrier and aid reproducibility. *Bioinformatics Advances*, 3(1):vbad132, January 2023.

[316] Quentin Geissmann. *High-throughput Recording, Analysis and Manipulation of Sleep in Drosophila*. PhD thesis, Imperial College London, October 2018.

[317] hmmlearn: Hidden Markov Models in Python with scikit-learn like API, 2015.

[318] Leonard E. Baum. An inequality and associated maximization technique in statistical estimation for probabilistic functions of Markov processes. *Inequalities*, 3(1):1–8, 1972.

[319] Timothy D. Wiggin, Patricia R. Goodwin, Nathan C. Donelson, Chang Liu, Kien Trinh, Subhabrata Sanyal, and Leslie C. Griffith. Covert sleep-related biological processes are revealed by probabilistic analysis in Drosophila. *Proceedings of the National Academy of Sciences*, 117(18):10024, January 2020.

[320] Art B. Owen. Empirical likelihood ratio confidence intervals for a single functional. *Biometrika*, 75(2):237–249, 1988. Publisher: Oxford University Press.

[321] Htrotugu Akaike. Maximum likelihood identification of Gaussian autoregressive moving average models. *Biometrika*, 60(2):255–265, 1973. Publisher: Oxford University Press.

[322] Gideon Schwarz. Estimating the Dimension of a Model. *The Annals of Statistics*, 6(2):461–464, March 1978. Publisher: Institute of Mathematical Statistics.

[323] A. Viterbi. Error bounds for convolutional codes and an asymptotically optimum decoding algorithm. *IEEE Transactions on Information Theory*, 13(2):260–269, April 1967. Conference Name: IEEE Transactions on Information Theory.

[324] sequentia: Scikit-Learn compatible HMM and DTW based sequence machine learning algorithms in Python.

[325] Carl H. Lubba, Sarab S. Sethi, Philip Knaute, Simon R. Schultz, Ben D. Fulcher, and Nick S. Jones. catch22: CAnonical Time-series CHaracteristics. *Data Mining and Knowledge Discovery*, 33(6):1821–1852, November 2019.

[326] Pauli Virtanen, Ralf Gommers, Travis E. Oliphant, Matt Haberland, Tyler Reddy, David Cournapeau, Evgeni Burovski, Pearu Peterson, Warren Weckesser, Jonathan Bright, Stéfan J. Van Der Walt, Matthew Brett, Joshua Wilson, K. Jarrod Millman, Nikolay Mayorov, Andrew R. J. Nelson, Eric Jones, Robert Kern, Eric Larson, C J Carey, İlhan Polat, Yu Feng, Eric W. Moore, Jake VanderPlas, Denis Laxalde, Josef Perktold, Robert Cimrman, Ian Henriksen, E. A. Quintero, Charles R. Harris, Anne M. Archibald, Antônio H. Ribeiro, Fabian Pedregosa, Paul Van Mulbregt, SciPy 1.0 Contributors, Aditya Vijaykumar, Alessandro Pietro Bardelli, Alex Rothberg, Andreas Hilboll, Andreas Kloeckner, Anthony Scopatz, Antony Lee, Ariel Rokem, C. Nathan Woods, Chad Fulton, Charles Masson, Christian Häggström, Clark Fitzgerald, David A. Nicholson, David R. Hagen, Dmitrii V. Pasechnik, Emanuele Olivetti, Eric Martin, Eric Wieser, Fabrice Silva, Felix Lenders, Florian Wilhelm, G. Young, Gavin A. Price, Gert-Ludwig Ingold, Gregory E. Allen, Gregory R. Lee, Hervé Audren, Irvin Probst, Jörg P. Dietrich, Jacob Silterra,

James T Webber, Janko Slavič, Joel Nothman, Johannes Buchner, Johannes Kulick, Johannes L. Schönberger, José Vinícius De Miranda Cardoso, Joscha Reimer, Joseph Harrington, Juan Luis Cano Rodríguez, Juan Nunez-Iglesias, Justin Kuczynski, Kevin Tritz, Martin Thoma, Matthew Newville, Matthias Kümmerer, Maximilian Bolingbroke, Michael Tartre, Mikhail Pak, Nathaniel J. Smith, Nikolai Nowaczyk, Nikolay Shebanov, Oleksandr Pavlyk, Per A. Brodtkorb, Perry Lee, Robert T. McGibbon, Roman Feldbauer, Sam Lewis, Sam Tygier, Scott Sievert, Sebastiano Vigna, Stefan Peterson, Surhud More, Tadeusz Pudlik, Takuya Oshima, Thomas J. Pingel, Thomas P. Robitaille, Thomas Spura, Thouis R. Jones, Tim Cera, Tim Leslie, Tiziano Zito, Tom Krauss, Utkarsh Upadhyay, Yaroslav O. Halchenko, and Yoshiki Vázquez-Baeza. SciPy 1.0: fundamental algorithms for scientific computing in Python. *Nature Methods*, 17(3):261–272, March 2020.

[327] J. E. Mietus. The pNNx files: re-examining a widely used heart rate variability measure. *Heart*, 88(4):378–380, 2002.

[328] Xiaozhe Wang, Anthony Wirth, and Liang Wang. Structure-Based Statistical Features and Multivariate Time Series Clustering. In *Seventh IEEE International Conference on Data Mining (ICDM 2007)*, pages 351–360, October 2007. ISSN: 2374-8486.

[329] G. Bradski. The OpenCV Library. *Dr. Dobb's Journal of Software Tools*, 2000.

[330] Plotly Technologies Inc. Collaborative data science. *Plotly Technologies Inc.*, 2015.

[331] Michael L. Waskom. seaborn: statistical data visualization. *Journal of Open Source Software*, 6(60):3021, April 2021.

[332] John D. Hunter. Matplotlib: A 2D Graphics Environment. *Computing in Science & Engineering*, 9(3):90–95, 2007.

[333] Joses Ho, Tayfun Tumkaya, Sameer Aryal, Hyungwon Choi, and Adam Claridge-Chang. Moving beyond P values: Everyday data analysis with estimation plots. *BioRxiv*.

[334] Michaela Joyce, Federica A. Falconio, Laurence Blackhurst, Lucia Prieto-Godino, Alice S. French, and Giorgio F. Gilestro. Divergent evolution of sleep in Drosophila species. *Nature Communications*, 15(1):5091, June 2024. Publisher: Nature Publishing Group.

[335] Quentin Geissmann, Luis Garcia Rodriguez, Esteban J. Beckwith, and Giorgio F. Gilestro. Rethomics: An R framework to analyse high-throughput behavioural data. *PLOS ONE*, 14(1):e0209331, January 2019. Publisher: Public Library of Science.

[336] André EX Brown and Benjamin De Bivort. Ethology as a physical science. *Nature Physics*, 14(7):653–657, 2018. Publisher: Nature Publishing Group UK London.

[337] Jianqing Fan, Fang Han, and Han Liu. Challenges of big data analysis. *National science review*, 1(2):293–314, 2014. Publisher: Oxford University Press.

[338] Hadley Wickham. ggplot2: Elegant Graphics for Data Analysis. *Springer-Verlag New York*, 2016.

[339] Charles R. Harris, K. Jarrod Millman, Stéfan J. van der Walt, Ralf Gommers, Pauli Virtanen, David Cournapeau, Eric Wieser, Julian Taylor, Sebastian Berg, Nathaniel J. Smith, Robert Kern, Matti Picus, Stephan Hoyer, Marten H. van Kerkwijk, Matthew Brett, Allan Haldane, Jaime Fernández del Río, Mark Wiebe, Pearu Peterson, Pierre Gérard-Marchant, Kevin Sheppard, Tyler Reddy, Warren Weckesser, Hameer Abbasi, Christoph Gohlke, and Travis E. Oliphant. Array programming with NumPy. *Nature*, 585(7825):357–362, September 2020. Publisher: Nature Publishing Group.

[340] Wes McKinney. Data Structures for Statistical Computing in Python. pages 56–61, Austin, Texas, 2010.

[341] *The Grammar of Graphics*. Statistics and Computing. Springer-Verlag, New York, 2005.

[342] Martın Abadi, Ashish Agarwal, Paul Barham, Eugene Brevdo, Zhifeng Chen, Craig Citro, Greg S Corrado, Andy Davis, Jeffrey Dean, Matthieu Devin, Sanjay Ghemawat, Ian Goodfellow, Andrew Harp, Geoffrey Irving, Michael Isard, Yangqing Jia, Rafal Jozefowicz, Lukasz Kaiser, Manjunath Kudlur, Josh Levenberg, Dan Mane, Rajat Monga, Sherry

Moore, Derek Murray, Chris Olah, Mike Schuster, Jonathon Shlens, Benoit Steiner, Ilya Sutskever, Kunal Talwar, Paul Tucker, Vincent Vanhoucke, Vijay Vasudevan, Fernanda Viegas, Oriol Vinyals, Pete Warden, Martin Wattenberg, Martin Wicke, Yuan Yu, and Xiaoqiang Zheng. TensorFlow: Large-Scale Machine Learning on Heterogeneous Distributed Systems.

[343] Adam Paszke, Sam Gross, Francisco Massa, Adam Lerer, James Bradbury, Gregory Chanan, Trevor Killeen, Zeming Lin, Natalia Gimelshein, Luca Antiga, Alban Desmaison, Andreas Köpf, Edward Yang, Zach DeVito, Martin Raison, Alykhan Tejani, Sasank Chilamkurthy, Benoit Steiner, Lu Fang, Junjie Bai, and Soumith Chintala. PyTorch: An Imperative Style, High-Performance Deep Learning Library, December 2019. arXiv:1912.01703 [cs, stat].

[344] Nick Barnes. Publish your computer code: it is good enough. *Nature*, 467(7317):753–753, October 2010. Publisher: Nature Publishing Group.

[345] Carl Boettiger. An introduction to Docker for reproducible research. *ACM SIGOPS Operating Systems Review*, 49(1):71–79, January 2015.

[346] Dirk Merkel. Docker: lightweight linux containers for consistent development and deployment. *Linux j*, 239(2):2, 2014.

[347] Daniel Nüst, Vanessa Sochat, Ben Marwick, Stephen J. Eglen, Tim Head, Tony Hirst, and Benjamin D. Evans. Ten simple rules for writing Dockerfiles for reproducible data science, 2020. Issue: 11 Pages: e1008316 Publication Title: PLoS computational biology Volume: 16.

[348] Lorena A. Barba, Lecia J. Barker, Douglas S. Blank, Jed Brown, Allen B. Downey, Timothy George, Lindsey J. Heagy, Kyle T. Mandli, Jason K. Moore, and David Lippert. Teaching and learning with Jupyter. *Recuperado: https://jupyter4edu. github. io/jupyter-edu-book*, pages 1–77, 2019.

[349] Brian E. Granger and Fernando Pérez. Jupyter: Thinking and storytelling with code and data. *Computing in Science & Engineering*, 23(2):7–14, 2021. Publisher: IEEE.

[350] Jeffrey Perkel. Why Jupyter is data scientists' computational notebook of choice. *Nature*, 563:145–146, November 2018.

[351] Ezio Rosato and Charalambos P. Kyriacou. Analysis of locomotor activity rhythms in Drosophila. *Nature Protocols*, 1(2):559–568, August 2006. Publisher: Nature Publishing Group.

[352] Phillip G. Sokolove and Wayne N. Bushell. The chi square periodogram: its utility for analysis of circadian rhythms. *Journal of theoretical biology*, 72(1):131–160, 1978. Publisher: Elsevier.

[353] Peter Bloomfield. *Fourier Analysis of Time Series: An Introduction*. John Wiley & Sons, March 2004. Google-Books-ID: zQsupRg5rrAC.

[354] T. Ruf. The Lomb-Scargle Periodogram in Biological Rhythm Research: Analysis of Incomplete and Unequally Spaced Time-Series. *Biological Rhythm Research*, 30(2):178–201, April 1999.

[355] Tanya L. Leise and Mary E. Harrington. Wavelet-Based Time Series Analysis of Circadian Rhythms. *Journal of Biological Rhythms*, 26(5):454–463, October 2011.

[356] Gregory Lee, Ralf Gommers, Filip Waselewski, Kai Wohlfahrt, and Aaron O'Leary. PyWavelets: A Python package for wavelet analysis. *Journal of Open Source Software*, 4(36):1237, 2019. Publisher: The Open Journal.

[357] C Diack, O Ackaert, B A Ploeger, P H van der Graaf, R Gurrell, M Ivarsson, and D Fairman. A hidden Markov model to assess drug-induced sleep fragmentation in the telemetered rat. *Journal of pharmacokinetics and pharmacodynamics*, 38(6):697–711, December 2011. Edition: 2011/09/10 Publisher: Springer US.

[358] L. G. Doroshenkov and V. A. Konyshev. Usage of hidden Markov models for automatic sleep stages classification. In *Russian-Bavarian Conference on Bio-Medical Engineering*, volume 19. Citeseer, 2007.

[359] Brian Geuther, Mandy Chen, Raymond J. Galante, Owen Han, Jie Lian, Joshy George, Allan I. Pack, and Vivek Kumar. High-throughput visual assessment of sleep stages in mice using machine learning. *Sleep*, 45(2):zsab260, 2022. Publisher: Oxford University Press US.

[360] Richard Glennie, Timo Adam, Vianey Leos-Barajas, Théo Michelot, Theoni Photopoulou, and Brett T. McClintock. Hidden Markov models: Pitfalls and opportunities in ecology. *Methods in Ecology and Evolution*, 14(1):43–56, January 2023.

[361] Michael Reiser. The ethomics era? *Nature Methods*, 6(6):413–414, June 2009.

[362] N. Tinbergen. Ethology: The objective study of behaviour. In *The study of instinct*, pages 1–14. Clarendon Press/Oxford University Press, New York, NY, US, 1951.

[363] John Joseph Valletta, Colin Torney, Michael Kings, Alex Thornton, and Joah Madden. Applications of machine learning in animal behaviour studies. *Animal Behaviour*, 124:203–220, 2017. Publisher: Elsevier.

[364] Caleb Weinreb, Jonah E. Pearl, Sherry Lin, Mohammed Abdal Monium Osman, Libby Zhang, Sidharth Annapragada, Eli Conlin, Red Hoffmann, Sofia Makowska, and Winthrop F. Gillis. Keypoint-MoSeq: parsing behavior by linking point tracking to pose dynamics. *Nature Methods*, 21(7):1329–1339, 2024. Publisher: Nature Publishing Group US New York.

[365] Alexander B. Wiltschko, Matthew J. Johnson, Giuliano Iurilli, Ralph E. Peterson, Jesse M. Katon, Stan L. Pashkovski, Victoria E. Abraira, Ryan P. Adams, and Sandeep Robert Datta. Mapping sub-second structure in mouse behavior. *Neuron*, 88(6):1121–1135, 2015. Publisher: Elsevier.

[366] Ben D. Fulcher and Nick S. Jones. hctsa: A computational framework for automated time-series phenotyping using massive feature extraction. *Cell systems*, 5(5):527–531, 2017. Publisher: Elsevier.

[367] B. Van Swinderen, D. A. Nitz, and R. J. Greenspan. Uncoupling of brain activity from movement defines arousal states in Drosophila. *Current Biology*, 14(2):81–87, 2004. Publisher: Elsevier.

[368] Davide Raccuglia, Sheng Huang, Anatoli Ender, M.-Marcel Heim, Desiree Laber, Raquel Suárez-Grimalt, Agustin Liotta, Stephan J. Sigrist, Jörg R.P. Geiger, and David Owald. Network-Specific Synchronization of Electrical Slow-Wave Oscillations Regulates Sleep Drive in Drosophila. *Current Biology*, 29(21):3611–3621.e3, November 2019.

[369] Niki Anthoney, Lucy Tainton-Heap, Hang Luong, Eleni Notaras, Amber B Kewin, Qiongyi Zhao, Trent Perry, Philip Batterham, Paul J Shaw, and Bruno van Swinderen. Experimentally induced active and quiet sleep engage non-overlapping transcriptional programs in Drosophila. *eLife*, 12:RP88198, November 2023. Publisher: eLife Sciences Publications, Ltd.

[370] Thomas F Döring and Lars Chittka. How Human Are Insects, and Does it Matter? *Formosan Entomol*, 2011.

[371] Magnus Enquist and Stefano Ghirlanda. *Neural Networks & Animal Behaviour*. Princeton University Press, 2005.

[372] Yu Hayashi, Mitsuaki Kashiwagi, Kosuke Yasuda, Reiko Ando, Mika Kanuka, Kazuya Sakai, and Shigeyoshi Itohara. Cells of a common developmental origin regulate REM/non-REM sleep and wakefulness in mice. *Science*, 350(6263):957–961, November 2015. Publisher: American Association for the Advancement of Science.

[373] Jung-Min Lee, Wonwoo Byun, Alyssa Keill, Danae Dinkel, and Yaewon Seo. Comparison of Wearable Trackers' Ability to Estimate Sleep. *International Journal of Environmental Research and Public Health*, 15(6), 2018.

[374] Ying Chen, Xin Zhu, and Wenxi Chen. Automatic sleep staging based on ECG signals using hidden Markov models. In *2015 37th Annual International Conference of the IEEE Engineering in Medicine and Biology Society (EMBC)*, pages 530–533, August 2015. ISSN: 1558-4615.

[375] Jaehyoung Hong, Su Jung Choi, Se Ho Park, Hyukpyo Hong, Victoria Booth, Eun Yeon Joo, and Jae Kyoung Kim. Personalized sleep-wake patterns aligned with circadian rhythm relieve daytime sleepiness. *iScience*, 24(10), October 2021. Publisher: Elsevier.

[376] Cecilia G. Diniz Behn, Emery N. Brown, Thomas E. Scammell, and Nancy J. Kopell. Mathematical Model of Network Dynamics Governing Mouse Sleep–Wake Behavior. *Journal of Neurophysiology*, 97(6):3828–3840, 2007. _eprint: https://doi.org/10.1152/jn.01184.2006.

[377] Michael J. Rempe, Janet Best, and David Terman. A mathematical model of the sleep/wake cycle. *Journal of Mathematical Biology*, 60(5):615–644, May 2010.

[378] Yun Min Song, Su Jung Choi, Se Ho Park, Soo Jin Lee, Eun Yeon Joo, and Jae Kyoung Kim. A real-time, personalized sleep intervention using mathematical modeling and wearable devices. *Sleep*, 46(9):zsad179, July 2023. _eprint: https://academic.oup.com/sleep/article-pdf/46/9/zsad179/51363131/zsad179.pdf.

[379] Serge Daan, DG Beersma, and Alexander Borbely. Timing of human sleep: recovery process gated by a circadian pacemaker. *American Journal of Physiology-Regulatory, Integrative and Comparative Physiology*, 246(2):R161–R183, 1984.

[380] Daniel Jurafsky and James Martin. *Speech and Language Processing*. 2024.

[381] John Henderson, Steven Salzburg, and Kenneth H. FASMAN. Finding Genes in DNA with a Hidden Markov Model. *Journal of Computational Biology*, 4(2):127–141, January 1997. Publisher: Mary Ann Liebert, Inc., publishers.

[382] Lawrence R Rabiner. A Tutorial on Hidden Markov Models and Selected Applications in Speech Recognition. *PROCEEDINGS OF THE IEEE*, 77(2), 1989.

[383] Tingting Liu and Jan Lemeire. Efficient and Effective Learning of HMMs Based on Identification of Hidden States. *Mathematical Problems in Engineering*, 2017(1):7318940, 2017. _eprint: https://onlinelibrary.wiley.com/doi/pdf/10.1155/2017/7318940.

[384] Leonel Perez-Atencio, Nicolas Garcia-Aracil, Eduardo Fernandez, Luis C. Barrio, and Juan A. Barios. A four-state Markov model of sleep-wakefulness dynamics along light/dark cycle in mice. *PLOS ONE*, 13(1):e0189931, January 2018. Publisher: Public Library of Science.

[385] Edward C Harding, Nicholas P Franks, and William Wisden. Sleep and thermoregulation. *Current Opinion in Physiology*, 15:7–13, June 2020.

[386] N Buendía, G Sierra, M Goode, and J P Segundo. Conditioned and discriminatory responses in wakeful and in sleeping cats. *Electroencephalography and clinical neurophysiology*, pages Suppl 24:199+, January 1963.

[387] Ian Oswald, Anne M. Taylor, and Michel Treisman. Discriminative responses to stimulation during human sleep. *Brain: A Journal of Neurology*, 83:440–453, 1960. Place: United Kingdom Publisher: Oxford University Press.

[388] Henry Van Twyver and William Garrett. Arousal threshold in the rat determined by "meaningful" stimuli. *Behavioral Biology*, 7(2):205–215, April 1972.

[389] Kenneth Davis, Elizabeth Heins, and Henry Van Twyver. A study of paradoxical sleep depth in the rat. *Psychonomic Science*, 26(3):173–174, March 1972.

[390] Daniel Lachaise and Jean-François Silvain. How Two Afrotropical Endemics Made Two Cosmopolitan Human Commensals: the Drosophila Melanogaster–D. Simulans Palaeogeographic Riddle. *Genetica*, 120(1):17–39, March 2004.

[391] Jessica Yano, Ceazar Nave, Katherine Larratt, Phia Honey, Makayla Roberts, Cassandra Jingco, Melanie L. Fung, Damion Trotter, Xin He, Gazmend Elezi, Julian P. Whitelegge, Sara Wasserman, and Jeffrey M. Donlea. Elevated sleep quota in a stress-resilient Drosophila species. *Current Biology*, 34(11):2487–2501.e3, June 2024. Publisher: Elsevier.

[392] Pamela Menegazzi, Elena Dalla Benetta, Marta Beauchamp, Matthias Schlichting, Ingolf Steffan-Dewenter, and Charlotte Helfrich-Förster. Adaptation of Circadian Neuronal Network to Photoperiod in High-Latitude European Drosophilids. *Current Biology*, 27(6):833–839, March 2017.

[393] Michaela Joyce. *Homeostasis in Drosophilids: A cross-species investigation of Drosophila sleep*. PhD thesis, Imperial College London, 2023.

[394] A. H. Sturtevant. Notes on North American Drosophilidae with Descriptions of Twenty-Three New Species. *Annals of the Entomological Society of America*, 9(4):323–343, December 1916.

[395] A. H. Sturtevant. On the Subdivision of the Genus Drosophila. *Proceedings of the National Academy of Sciences*, 25(3):137–141, March 1939. Publisher: Proceedings of the National Academy of Sciences.

[396] Patrick M O'Grady and Rob DeSalle. Phylogeny of the Genus *Drosophila*. *Genetics*, 209(1):1–25, May 2018.

[397] Therese Ann Markow and Patrick M. O'Grady. Evolutionary Genetics of Reproductive Behavior in Drosophila: Connecting the Dots. *Annual Review of Genetics*, 39(Volume 39, 2005):263–291, December 2005. Publisher: Annual Reviews.

[398] Marie Louise Cariou, Daniel Lachaise, Leonidas Tsacas, John Sourdis, Costas Krimbas, and Michael Ashburner. New African species in the Drosophila obscura species group: genetic variation, differentiation and evolution. *Heredity*, 61(1):73–84, August 1988. Publisher: Nature Publishing Group.

[399] Corbin D. Jones. The genetics of adaptation in Drosophila sechellia. In Rodney Mauricio, editor, *Genetics of Adaptation*, pages 137–145. Springer Netherlands, Dordrecht, 2005.

[400] C. D. Jones. Genetics of egg production in Drosophila sechellia. *Heredity*, 92(3):235–241, March 2004. Publisher: Nature Publishing Group.

[401] Samia R'kha, Brigitte Moreteau, Jerry A. Coyne, and Jean R. David. Evolution of a lesser fitness trait: egg production in the specialist Drosophila sechellia. *Genetics Research*, 69(1):17–23, February 1997.

[402] Sofía Lavista-Llanos, Aleš Svatoš, Marco Kai, Thomas Riemensperger, Serge Birman, Marcus C Stensmyr, and Bill S Hansson. Dopamine drives Drosophila sechellia adaptation

to its toxic host. *eLife*, 3:e03785, December 2014. Publisher: eLife Sciences Publications, Ltd.

[403] Jeanine Linz, Amelie Baschwitz, Antonia Strutz, Hany K. M. Dweck, Silke Sachse, Bill S. Hansson, and Marcus C. Stensmyr. Host plant-driven sensory specialization in Drosophila erecta. *Proceedings of the Royal Society B: Biological Sciences*, 280(1760):20130626, June 2013. Publisher: Royal Society.

[404] Nadia D. Singh, Peter F. Arndt, and Dmitri A. Petrov. Minor shift in background substitutional patterns in the Drosophila saltans and willistoni lineages is insufficient to explain GC content of coding sequences. *BMC Biology*, 4(1):37, October 2006.

[405] BASHISTH N. SINGH. The genus Drosophila is characterized by a large number of sibling species showing evolutionary significance. *Journal of Genetics*, 95(4):1053–1064, December 2016.

[406] J. T. Patterson. Revision of the montana complex of the virilis species group. *Univerisity Texas Publ*, (5204):20–34, 1952.

[407] L. H. Throckmorton. The genetics and biology of Drosophila. *New York: Academic Press*, 3b, 1982.

[408] Patricia M. Mirol, Jarkko Routtu, Anneli Hoikkala, and Roger K. Butlin. Signals of demographic expansion in Drosophila virilis. *BMC Evolutionary Biology*, 8(1):59, February 2008.

[409] Mari Saarikettu, Jaana O. Liimatainen, and Anneli Hoikkala. Intraspecific variation in mating behaviour does not cause sexual isolation between *Drosophila virilis* strains. *Animal Behaviour*, 70(2):417–426, August 2005.

[410] V. Yu. Shilova, D. G. Garbuz, M. B. Evgen'ev, and O. G. Zatsepina. Small heat shock proteins and adaptation of various Drosophila species to hyperthermia. *Molecular Biology*, 40(2):235–239, March 2006.

[411] Anneli Hoikkala and Noora Poikela. Adaptation and ecological speciation in seasonally varying environments at high latitudes: Drosophila virilis group. *Fly*, 16(1):85–104, December 2022. Publisher: Taylor & Francis _eprint: https://doi.org/10.1080/19336934.2021.2016327.

[412] Jean R. David and Osamu Kitagawa. Possible similarities in ethanol tolerance and latitudinal variations between Drosophila virilis and D. melanogaster. *The Japanese Journal of Genetics*, 57(1):89–95, 1982.

[413] Daniel R Machado, Dinis JS Afonso, Alexandra R Kenny, Arzu Öztürk Çolak, Emilia H Moscato, Benjamin Mainwaring, Matthew Kayser, and Kyunghee Koh. Identification of octopaminergic neurons that modulate sleep suppression by male sex drive. *eLife*, 6:e23130, May 2017. Publisher: eLife Sciences Publications, Ltd.

[414] A. A. Borbely and I. Tobler. Endogenous sleep-promoting substances and sleep regulation. *Physiological Reviews*, 69(2):605–670, April 1989.

[415] Julien Colomb and Björn Brembs. Sub-strains of Drosophila Canton-S differ markedly in their locomotor behavior. *F1000Research*, 3, 2014. Publisher: Faculty of 1000 Ltd.

[416] Matthias Spörrle and Jennifer Stich. Sleeping in Safe Places: An Experimental Investigation of Human Sleeping Place Preferences from an Evolutionary Perspective. *Evolutionary Psychology*, 8(3):405–419, July 2010. Publisher: SAGE Publications Inc.

[417] Shahab Haghayegh, Sepideh Khoshnevis, Michael H. Smolensky, Kenneth R. Diller, and Richard J. Castriotta. Performance comparison of different interpretative algorithms utilized to derive sleep parameters from wrist actigraphy data. *Chronobiology International*, 36(12):1752–1760, December 2019. Publisher: Taylor & Francis _eprint: https://doi.org/10.1080/07420528.2019.1679826.

[418] Andrea Ferretti, Niels C. Rattenborg, Thomas Ruf, Scott R. McWilliams, Massimiliano Cardinale, and Leonida Fusani. Sleeping Unsafely Tucked in to Conserve Energy in a Nocturnal Migratory Songbird. *Current Biology*, 29(16):2766–2772.e4, August 2019.

[419] Tohei Yokogawa, Wilfredo Marin, Juliette Faraco, Guillaume Pézeron, Lior Appelbaum, Jian Zhang, Frédéric Rosa, Philippe Mourrain, and Emmanuel Mignot. Characterization of Sleep in Zebrafish and Insomnia in Hypocretin Receptor Mutants. *PLOS Biology*, 5(10):e277, October 2007. Publisher: Public Library of Science.

[420] Irina V. Zhdanova. Sleep and its regulation in zebrafish. 22(1):27–36, February 2011. Publisher: De Gruyter Section: Reviews in the Neurosciences.

[421] Matthew D Nelson and David M Raizen. A sleep state during *C. elegans* development. *Current Opinion in Neurobiology*, 23(5):824–830, October 2013.

[422] Walter Kaiser. Busy bees need rest, too. *Journal of Comparative Physiology A*, 163(5):565–584, September 1988.

[423] Chin-Lin Chen, Florian Aymanns, Ryo Minegishi, Victor D. V. Matsuda, Nicolas Talabot, Semih Günel, Barry J. Dickson, and Pavan Ramdya. Ascending neurons convey behavioral state to integrative sensory and action selection brain regions. *Nature Neuroscience*, 26(4):682–695, April 2023. Publisher: Nature Publishing Group.

[424] Fritz-Olaf Lehmann and Nicole Heymann. Unconventional mechanisms control cyclic respiratory gas release in flying Drosophila. *Journal of Experimental Biology*, 208(19):3645–3654, October 2005.

[425] H. Zepelin. Mammalian sleep. *Principles and practice of sleep medicine*, pages 69–80, 1994.

[426] Hannah Jones, Jenny A Willis, Lucy C Firth, Carlo NG Giachello, and Giorgio F Gilestro. A reductionist paradigm for high-throughput behavioural fingerprinting in Drosophila melanogaster. *eLife*, 12:RP86695, November 2023. Publisher: eLife Sciences Publications, Ltd.

[427] Chunming Xu and Scott A. Jackson. Machine learning and complex biological data. *Genome Biology*, 20(1):76, April 2019.

[428] Bing Qiao, Chiyuan Li, Victoria W Allen, Mimi Shirasu-Hiza, and Sheyum Syed. Automated analysis of long-term grooming behavior in Drosophila using a k-nearest neighbors classifier. *eLife*, 7:e34497, February 2018. Publisher: eLife Sciences Publications, Ltd.

[429] Benjamin R. Cowley, Adam J. Calhoun, Nivedita Rangarajan, Elise Ireland, Maxwell H. Turner, Jonathan W. Pillow, and Mala Murthy. Mapping model units to visual neurons reveals population code for social behaviour. *Nature*, 629(8014):1100–1108, May 2024. Publisher: Nature Publishing Group.

[430] Andrew Smith, Hardik Anand, Snezana Milosavljevic, Katherine M. Rentschler, Ana Pocivavsek, and Homayoun Valafar. Application of Machine Learning to Sleep Stage Classification. In *2021 International Conference on Computational Science and Computational Intelligence (CSCI)*, pages 349–354, December 2021.

[431] Nicholas Kuzik, John C. Spence, and Valerie Carson. Machine learning sleep duration classification in Preschoolers using waist-worn ActiGraphs. *Sleep Medicine*, 78:141–148, February 2021.

[432] Antonino Crivello, Filippo Palumbo, Paolo Barsocchi, Davide La Rosa, Franco Scarselli, and Monica Bianchini. Understanding Human Sleep Behaviour by Machine Learning. In Ryszard Klempous, Jan Nikodem, and Péter Zoltán Baranyi, editors, *Cognitive Infocommunications, Theory and Applications*, pages 227–252. Springer International Publishing, Cham, 2019.

[433] Sridhar R. Jagannathan, Travis Jeans, Matthew N. Van De Poll, and Bruno van Swinderen. Multivariate classification of multichannel long-term electrophysiology data identifies different sleep stages in fruit flies. *Science Advances*, 10(8):eadj4399, February 2024. Publisher: American Association for the Advancement of Science.

[434] Chunxiao Fu, Pengle Zhang, Jiang Jiang, Kewei Yang, and Zhihan Lv. A Bayesian approach for sleep and wake classification based on dynamic time warping method. *Multimedia Tools and Applications*, 76(17):17765–17784, September 2017.

[435] Pavel Senin. Dynamic Time Warping Algorithm Review. January 2009.

[436] Mohammad Shokoohi-Yekta, Jun Wang, and Eamonn Keogh. On the Non-Trivial Generalization of Dynamic Time Warping to the Multi-Dimensional Case. In *Proceedings of the 2015 SIAM International Conference on Data Mining (SDM)*, Proceedings, pages 289–297. Society for Industrial and Applied Mathematics, June 2015.

[437] Evelyn Fix. *Discriminatory Analysis: Nonparametric Discrimination, Consistency Properties*. USAF School of Aviation Medicine, 1985. Google-Books-ID: s85PAQAAMAAJ.

[438] JP Hailman. Comparative Methods in Behavioral Studies. In *Comparative Psychology*. Routledge, 1998. Num Pages: 11.

[439] K. Lorenz and N. Tinbergen. Taxis und Instinkthandlung in der Eirollbewegung der Graugans. [Directed and instinctive behavior in the egg rolling movements of the gray goose.]. *Zeitschrift für Tierpsychologie*, 2:1–29, 1938. Place: United Kingdom Publisher: Blackwell Publishing.

[440] I. P. Pavlov. Conditioned reflexes. *London: Oxford University Press*, 430, 1927.

[441] Colin Beer. Niko Tinbergen and questions of instinct. *Animal Behaviour*, 164:261–265, June 2020.

[442] David J. Anderson and Pietro Perona. Toward a Science of Computational Ethology. *Neuron*, 84(1):18–31, October 2014. Publisher: Elsevier.

[443] Anthony I. Dell, John A. Bender, Kristin Branson, Iain D. Couzin, Gonzalo G. de Polavieja, Lucas P. J. J. Noldus, Alfonso Pérez-Escudero, Pietro Perona, Andrew D. Straw, Martin Wikelski, and Ulrich Brose. Automated image-based tracking and its application in ecology. *Trends in Ecology & Evolution*, 29(7):417–428, July 2014. Publisher: Elsevier.

[444] Jeremy G. Todd, Jamey S. Kain, and Benjamin L. de Bivort. Systematic exploration of unsupervised methods for mapping behavior. *Physical Biology*, 14(1):015002, February 2017. Publisher: IOP Publishing.

[445] Jennifer J. Sun, Serim Ryou, Roni H. Goldshmid, Brandon Weissbourd, John O. Dabiri, David J. Anderson, Ann Kennedy, Yisong Yue, and Pietro Perona. Self-Supervised Keypoint Discovery in Behavioral Videos. pages 2171–2180, 2022.

[446] Talmo D. Pereira, Joshua W. Shaevitz, and Mala Murthy. Quantifying behavior to understand the brain. *Nature Neuroscience*, 23(12):1537–1549, December 2020. Publisher: Nature Publishing Group.

[447] Matteo Ruggero Ronchi and Pietro Perona. Benchmarking and Error Diagnosis in Multi-Instance Pose Estimation. pages 369–378, 2017.

[448] Kai J Jürgens, Maik Drechsler, and Achim Paululat. An anatomical atlas of *Drosophila melanogaster*— the wild-type. *GENETICS*, page iyae129, September 2024.

[449] J-R Martin, R Ernst, and Martin Heisenberg. Temporal pattern of locomotor activity in Drosophila melanogaster. *Journal of comparative physiology A*, 184:73–84, 1999. Publisher: Springer.

[450] Philippe Faure Jean-Rene Martin and Roman Ernst. The Power Law Distribution for Walking-Time Intervals Correlates with the Ellipsoid-Body in Drosophila. *Journal of Neurogenetics*, 15(3-4):205–219, 2001. Publisher: Taylor & Francis _eprint: https://doi.org/10.3109/01677060109167377.

[451] Jean-René Martin. A portrait of locomotor behaviour in Drosophila determined by a video-tracking paradigm. *Behavioural Processes*, 67(2):207–219, 2004.

[452] Sha Liu, Qili Liu, Masashi Tabuchi, and Mark N. Wu. Sleep Drive Is Encoded by Neural Plastic Changes in a Dedicated Circuit. *Cell*, 165(6):1347–1360, June 2016. Publisher: Elsevier.

[453] Xiaochan Xu, Wei Yang, Binghui Tian, Xiuwen Sui, Weilai Chi, Yi Rao, and Chao Tang. Quantitative investigation reveals distinct phases in Drosophila sleep. *Communications Biology*, 4(1):1–11, March 2021. Publisher: Nature Publishing Group.

[454] Jens F. Tillmann, Alexander I. Hsu, Martin K. Schwarz, and Eric A. Yttri. A-SOiD, an active-learning platform for expert-guided, data-efficient discovery of behavior. *Nature Methods*, 21(4):703–711, April 2024.